

Iron regulation in the Myxobacterium

Myxococcus xanthus DK1622

Dissertation
zur Erlangung des Grades
des Doktors der Naturwissenschaften
der Naturwissenschaftlich-Technischen Fakultät III
Chemie, Pharmazie, Bio- und Werkstoffwissenschaften
der Universität des Saarlandes

von Matthias O. Altmeyer

Saarbrücken, November 2010

Tag des Kolloquiums: 08. 02. 2011

Dekan: Prof. Dr. Stefan Diebels

Berichterstatter:
Prof. Dr. Rolf Müller
Prof. Dr. Claus Jacob

Vorsitz der Prüfungskommission:
Prof. Dr. Alexandra Kiemer
Akad. Mitarbeiter:
Dr. Carsten Volz

Vorveröffentlichungen der Dissertation

Teilergebnisse aus dieser Arbeit wurden mit Genehmigung der Naturwissenschaftlich-Technischen Fakultät, vertreten durch den Mentor, in folgenden Beiträgen vorab veröffentlicht:

Publications

1. Schley C, Altmeyer MO, Swart R, Müller R, Huber CG. Proteome analysis of *Myxococcus xanthus* by off-line two-dimensional chromatographic separation using monolithic poly-(styrene-divinylbenzene) columns combined with ion-trap tandem mass spectrometry. *J Proteome Res.* 2006 Oct;5(10):2760-8.
2. Schneiker S, Perlova O, Kaiser O, Gerth K, Alici A, Altmeyer MO, Bartels D, Bekel T, Beyer S, Bode E, Bode HB, Bolten CJ, Choudhuri JV, Doss S, Elnakady YA, Frank B, Gaigalat L, Goesmann A, Groeger C, Gross F, Jelsbak L, Jelsbak L, Kalinowski J, Kegler C, Knauber T, Konietzny S, Kopp M, Krause L, Krug D, Linke B, Mahmud T, Martinez-Arias R, McHardy AC, Merai M, Meyer F, Mormann S, Muñoz-Dorado J, Perez J, Pradella S, Rachid S, Raddatz G, Rosenau F, Rückert C, Sasse F, Scharfe M, Schuster SC, Suen G, Treuner-Lange A, Velicer GJ, Vorhölter FJ, Weissman KJ, Welch RD, Wenzel SC, Whitworth DE, Wilhelm S, Wittmann C, Blöcker H, Pühler A, Müller R. Complete genome sequence of the myxobacterium *Sorangium cellulosum*. *Nat Biotechnol.* 2007 Nov; 25(11):1281-9.
3. Bode HB, Ring MW, Schwär G, Altmeyer MO, Kegler C, Jose IR, Singer M, Müller R. Identification of Additional Players in the Alternative Biosynthesis Pathway to Isovaleryl-CoA in the Myxobacterium *Myxococcus xanthus*. *Chembiochem.* 2009 Jan;10(1):128-40
4. Hoiczyk E, Ring MW, McHugh CA, Schwär G, Bode E, Krug D, Altmeyer MO, Lu JZ, Bode HB. Lipid body formation plays a central role in cell fate determination during developmental differentiation of *Myxococcus xanthus*. *Mol Microbiol.* 2009 Sep [Epub ahead of print]
5. Altmeyer MO, Weissman KJ, Elnakady YA, Bode HB, Klefisch T and Müller R. Cellular Response of the Myxobacterium *Myxococcus xanthus* DK1622 to Iron Limitation, in preparation

Conference contribution / Tagungsbeiträge

1. Altmeyer MO, Schley C, Huber CG, Müller R. Iron regulation of protein expression and secondary metabolite production in *Myxococcus xanthus*, - a proteomics approach - (Poster), Intern. VAAM Workshop: Biology of Bacteria Producing Natural Products, Dresden 2005

2. Altmeyer MO, Perlova O, Müller R. Analysis of the phosphoproteome of the myxobacterium *Sorangium cellulosum* So ce56 (Poster), 34th Intern. Conference on the Biology of the Myxobacteria, Granada (Spain) 2007
3. Altmeyer MO, Müller R. Effects of Iron Limitation on *Myxococcus xanthus* DK1622 Growth, Proteome Profile and Secondary Metabolite Production (Short presentation and poster), Intern. VAAM Workshop: Biology of Bacteria Producing Natural Products, Nonnweiler 2007

Table of contents

List of abbreviations	5
List of figures	7
List of tables	8

1. Introduction	9
1.1 Role of iron in microbial metabolism	10
1.1.1 High-affinity iron uptake	10
1.1.2 Low-affinity iron uptake	14
1.1.3 Iron homeostasis control by the ferric uptake regulator (Fur) protein	14
1.1.4 Iron storage and overload	18
1.2 Myxobacteria	20
1.2.1 Life cycle	21
1.2.2 <i>Myxococcus xanthus</i> DK1622 as a model strain	24
1.2.3 Myxobacterial secondary metabolism	26
1.2.4 Natural products from <i>M. xanthus</i> DK1622	35
1.3 Comparative proteomics	40
1.3.1 Proteome analysis by 2D-PAGE	40
1.3.2 Proteome analysis by 2D-DIGE	41
1.3.3 Mass spectrometry based protein identification	42
1.4 Metabolite analysis by HPLC-MS	46
1.5 Protein-DNA interactions (DNA pull-down assay)	47
1.6 Target-oriented gene inactivation by homologous recombination	49
1.7 Goal of this study	53
2. Material and Methodology	55
2.1 Chemicals	55
2.2 Commercial 'kits', enzymes and markers	57
2.3 Buffers and solutions	58
2.3.1 Antibiotic solution	58
2.3.2 Buffers and solutions for 2D-gel electrophoresis	58
2.3.3 Buffers and solutions MALDI mass spectrometry	59
2.3.4 Buffers and solutions for DNA pull-down assay	60
2.3.5 Buffers and solutions for biomolecular work	62
2.4 Equipment and instrumentation	63
2.5 Bioinformatic tools and analysis	65
2.6 Bacterial strains	67
2.6.1 The strain <i>M. xanthus</i> DK1622	67
2.6.2 The strain <i>E. coli</i> DH10B	67
2.7 Cultivation media	68
2.7.1 Cultivation media for <i>M. xanthus</i> DK1622	68
Estimation of iron concentrations and iron uptake rates	68
2.7.2 Cultivation medium for <i>E. coli</i> DH10B	69
2.8 Cultivation conditions and conserving of microbial strains	70
2.8.1 Growth conditions of <i>M. xanthus</i> cultures	70
a) Application of Amberlite XAD 16 absorber resin to <i>M. xanthus</i> cultures	70
b) Growth of <i>M. xanthus</i> wild type cells on different iron concentrations	70
b) Growth of <i>M. xanthus</i> mutant cells on CTT medium	71

Table of contents

2.8.2	Growth conditions of <i>E. coli</i> cultures.....	71
2.8.3	Preparation of stock cultures and microbial conserving	72
a)	Stock cultures of <i>M. xanthus</i> strains.....	72
b)	Stock cultures of <i>E. coli</i> strains	72
2.9	Proteome analysis	73
2.9.1	Protein extraction of <i>M. xanthus</i> DK1622 samples from different iron concentrations	73
2.9.2	2D-DIGE sample preparation, running conditions and data interpretation	73
2.9.2.1	2D-DIGE sample preparation.....	73
a)	Protein precipitation and resuspension.....	73
b)	Estimation of protein concentrations.....	73
c)	2D-DIGE: CyDye protein labeling	74
d)	2D-DIGE: sample application by in-gel rehydration	75
2.9.2.2	2D-DIGE running conditions	76
a)	Isoelectric focusing (IEF).....	76
b)	Equilibration.....	76
c)	Polyacrylamide gel casting (PAGE)	77
2.9.2.3	2D-DIGE image analysis and data interpretation	77
a)	Scanning conditions	77
b)	Differential in-gel analysis (DIA)	77
c)	Biological variation analysis (BVA)	78
d)	Manual control, closing statistic.....	78
2.9.3	Protein identification (incl. protein-phosphorylation) by mass spectrometry	78
2.9.3.1	Prearrangement.....	79
a)	Spot picking and band excision.....	79
b)	Destaining and in-gel digestion.....	79
c)	Sample purification and concentrating.....	79
2.9.3.2	MALDI ToF/ToF mass spectrometry	80
a)	Sample application	80
b)	Calibration	80
c)	MS conditions (acquisition of peptide mass fingerprints)	81
d)	MS/MS conditions (acquisition of peptide fragment fingerprints)	81
e)	Protein identification using MS and MS/MS data by the MASCOT scoring algorithm.....	81
f)	Detection of protein-phosphorylation	81
2.10	DNA pull-down assay for identification of DNA interacting proteins to the promoter regions of MXAN_3702 and MXAN_6967	83
2.10.1	Loading of amplified DNA to Streptavidin-coated paramagnetic beads	83
2.10.2	Protein extraction of <i>M. xanthus</i> DK1622 samples from different iron concentrations and incubation with DNA-loaded Streptavidin beads	83
2.10.3	Washing and elution of promoter interacting proteins	83
2.10.4	Protein precipitation, PAGE, staining and protein identification, including protein-phosphorylations (MALDI-ToF/ToF).....	84
2.11	Handling and manipulation of DNA molecules	85
2.11.1	Vectors used	85
2.11.2	Designed oligonucleotides	85
2.11.3	Extraction of genomic DNA from <i>M. xanthus</i> cultures	89
2.11.4	Extraction of plasmid DNA from <i>E. coli</i>	90
a)	by 'kits'	90
b)	by alkaline lysis	90
2.11.5	Separation and purification of DNA molecules	90

Table of contents

a)	Agarose gel electrophoresis	90
b)	Clean-up of DNA molecules from agarose gels.....	91
c)	Precipitation of DNA molecules	91
2.11.6	Polymerase chain reaction (PCR)	92
a)	DNA polymerases used	92
b)	PCR composition.....	92
2.11.7	Enzymatic hydrolysis and ligation of DNA molecules.....	94
a)	Digestion/double digestion.....	94
b)	Ligation of DNA molecules	94
c)	Constructed plasmids	95
2.11.8	Transformation of bacteria via electroporation.....	96
a)	Transformation of <i>E. coli</i> DH10B.....	96
b)	Transformation of <i>M. xanthus</i> DK1622	97
2.12	Methodology of gene inactivation experiments in <i>M. xanthus</i>	97
a)	Gene inactivation by double crossover deletion	97
b)	Gene inactivation by single crossover insertion.....	98
2.13	Secondary metabolite analysis by HPLC-MS	99
2.13.1	Extraction of secondary metabolites from XAD	99
2.13.2	HPLC-MS system and conditions	99
2.13.3	Qualitative and semi-quantitative data interpretation of 7 metabolites by HPLC-MS	99
2.13.4	Generation of standard solutions.....	100
3.	Results	101
3.1	Bioinformatic analysis of iron uptake regulation in <i>M. xanthus</i>	101
3.1.1	Identification and classification of Fur homologues in <i>M. xanthus</i>	101
3.1.2	Prediction of Fur boxes in the <i>M. xanthus</i> genome.....	105
3.1.3	Metabolic background of <i>M. xanthus</i> iron regulation	110
3.2	Response of <i>M. xanthus</i> wild type to different iron availabilities	114
3.2.1	Effect of iron restriction on growth of <i>M. xanthus</i>	114
3.2.2	Effect of iron restriction on iron uptake by <i>M. xanthus</i>	115
3.2.3	Proteomic response of <i>M. xanthus</i> to iron-limitation.....	116
a)	Proteome analysis of <i>M. xanthus</i> using 2D-DIGE technology	116
b)	Identification of proteins from proteome analysis	117
c)	Analysis of phosphorylation on differentially regulated proteins.....	125
3.2.4	Profiling protein-promoter interactions at MXAN_3702 and MXAN_6967 under iron-rich and iron-limiting conditions	128
3.2.5	Effects of iron-limitation on secondary metabolome of <i>M. xanthus</i>	132
3.3	Investigation of the Fur regulon by gene inactivation	135
3.3.1	Generation of markerless in-frame deletion mutants	135
3.3.2	Generation of gene disruption mutants by single crossover	136
3.3.3	Growth analysis of the generated mutants in iron-rich environment.....	138
3.3.4	Estimation of iron uptake of generated mutant strains.....	140
3.3.5	Metabolite analysis by HCPL-MS of the generated mutants.....	141
3.3.6	Overall results from mutant analysis.....	143
4.	Discussion	145
4.1	Genetic background of <i>M. xanthus</i> iron regulation	146
4.2	Response of <i>M. xanthus</i> DK1622 to iron-limitation	154
4.2.1	Iron-limiting environment	154
4.2.2	Growth and iron uptake under iron-limiting conditions.....	156

Table of contents

4.2.3	Response of the <i>M. xanthus</i> proteome to iron-limitation	158
4.2.4	DNA binding proteins at promoter MXAN_3702 and MXAN_6967	177
4.2.5	The response of the <i>M. xanthus</i> secondary metabolome to iron-limitation	181
4.2.6	Importance of iron and Fur for <i>M. xanthus</i>	186
4.3	Probing the function of MXAN_6967 by gene inactivation.....	190
4.4	Probing the function of iron-responsive genes by site-directed mutagenesis	195
5.	Conclusion and Outlook.....	217
6.	Abstract.....	221
7.	Zusammenfassung.....	223
8.	Bibliography	225
9.	Appendix.....	255
10.	Erklärung.....	263

Table of contents

List of abbreviations

2D:	Two dimensional
A:	Adenylation domain
A:	Ampere
ACCN:	Acetonitrile
ACP:	Acyl carrier protein
AMP:	Adenosinmonophosphate
APS:	Ammonium persulfate
AT:	Acyltransferase domain
Atm:	Atmospheric pressure (= 101.325 Pa)
ATP:	Adenosintriphosphate
BLAST:	Basic Local Alignment Search Tool
bp:	Basepairs
BSA:	Bovine serum albumin
BPB:	Bromophenol blue (3',3',5',5'-tetrabromophenolsulfonphthalein)
BVA:	Biological variation analysis
C:	Condensation domain
C:	Cross-linker acrylamide monomer content
c:	Centi
CCA:	α -Cyano-4-hydroxycinnamic acid
CDD:	Conserved domain database
CHAPS:	3-[(3-Cholamidopropyl)dimethylammonio]-1-propanesulfonate
CID:	Collision induced dissociation
CM:	Cytosolic membrane
CoA:	Coenzyme A
Cy:	Condensation-cyclization domain
Da, kDa:	Atomic mass units (Dalton, kilo Dalton)
DH:	Dehydratase domain
DHB:	2,5-Dihydroxy benzoic acid
DIA:	Differential in-gel analysis
DIGE:	Differential gel electrophoresis
DMF:	N,N-Dimethylformamide
DMSO:	Dimethyl sulfoxide
DNA:	Deoxyribonucleic acid
dNTPs:	Deoxyribonucleotide triphosphate
DPS:	DNA protection during starvation protein
DTT:	Dithiothreitol
E:	Epimerization domain
EDTA:	Ethylene diamine tetraacetic acid
ER:	Enoyl-reductase domain
ESI:	Electrospray ionization
Expasy:	Expert Protein Analysis System
F:	Farad
F:	Formylation domain
Fur:	Ferric uptake regulator
g:	Gram
h:	Hour
H ₂ O:	Ultra pure water
HAC:	Hydroxylammonium chloride
HPLC:	High-performance liquid chromatography
Hz:	Hertz
I:	Sequence identity
IAA:	Iodoacetamide
IEF:	Isoelectric Focusing
IPG:	Immobilized pH gradient
K:	Kilo
KAS:	β -Ketoacyl-acyl carrier protein synthase
kb:	Kilobasepairs
K _f :	Complex formation (or stability) constant
KO:	Knockout

Table of contents

KR:	Keto-reductase domain
KS:	Keto-synthase domain
K_{sp} :	Solubility product constant
l:	Liter
m:	Meter
m:	Milli
n:	Nano
NL:	Non linear
M:	Molar
MALDI:	Matrix-assisted laser desorption/ionization
Mb:	Megabasepairs
min:	Minute
Mol:	Molarity
MS:	Mass spectrometry, mass spectrometer
MS/MS:	Tandem mass spectrometry
MTP:	Microtiter plate
NCBI:	National Center for Biotechnology Information
NMT:	<i>N</i> -Methylation domain
NRPS:	Nonribosomal peptide synthetase
O.D. ₆₀₀ :	Optical density at 600 nm
OM:	Outer membrane
Ox:	Oxidation domain
p:	Pico
PAGE:	Polyacrylamide gel electrophoresis
PBS:	Phosphate buffer saline
PCP:	Peptidyl carrier protein
PCR:	Polymerase chain reaction
PKS:	Polyketide synthase
PFF:	Peptide fragment fingerprint
PMF:	Peptide mass fingerprint
PPant:	Phosphopantetheine
ppm:	Parts per million
PSD	Post source decay
PTM	Post-translational modification
R:	Reduction domain
RE:	Restriction endonuclease
RNA:	Ribonucleic acid
rpm:	Revolutions per minute
RT:	Room temperature
S:	Sequence similarity
SDS:	Sodium dodecylsulfate
sec:	Second
SH:	Thiol
SN:	Signal-to-noise ratio
T:	Total-linker Acrylamide monomer content
TBE:	Tris-Boric acid-EDTA
TE:	Tris-EDTA
TE:	Thioesterase domain
TEMED:	<i>N,N,N',N'</i> -Tetramethylethylenediamine
TFA:	Trifluoroacetic acid
ToF:	Time of Flight
ToF/ToF:	Tandem Time of Flight MS
V:	Volt
v:	Volume
w:	Weight
WT:	Wild type
VHrs:	Volthours
x-Gal:	5-Bromo-4-chloro-3-indolyl-beta-D-galactoside
μ :	Micro
Ω :	Ohm

Table of contents

List of figures

Figure 1.1: Example molecules of the three different siderophore types.....	11
Figure 1.2: Scheme of siderophore-mediated iron uptake in Gram-negative bacteria.....	12
Figure 1.3: Model of Fur-DNA interaction.....	15
Figure 1.4: Developmental program of <i>M. xanthus</i>	22
Figure 1.5: Formation of fruiting bodies of <i>M. xanthus</i>	23
Figure 1.6: Structures of different myxobacterial fruiting bodies.....	24
Figure 1.7: Genetic map of the <i>M. xanthus</i> DK1622 chromosome.....	25
Figure 1.8: Scheme of the three PKS types (Weissman, 2009)	28
Figure 1.9: Principle of a PKS type I system.....	29
Figure 1.10: Principle of a NRPS system.....	32
Figure 1.11: Diverse secondary metabolite families, produced by <i>M. xanthus</i> DK1622	36
Figure 1.12: Chromosomal distribution of the <i>M. xanthus</i> secondary metabolite gene cluster.....	39
Figure 1.13: Diagram of DIGE workflow of single gel analysis.....	42
Figure 1.14: Workflow of DNA pull-down (promoter ligand-fishing) experiments.....	48
Figure 1.15: Diagram of in-frame gene deletion by double crossover.....	50
Figure 1.16: Gene disruption in <i>M. xanthus</i> by homologous recombination via single crossover.....	52
Figure 2.1: Workflow for DIGE system	75
Figure 3.1: Multiple sequence alignment (ClustalW) of Fur and Fur family members.....	102
Figure 3.2: Phylogenetic tree analysis by ClustalW2 of <i>M. xanthus</i> DK1622 Fur proteins and related sub-families.....	104
Figure 3.3: DNA sequence logo of the Fur box consensus sequence of <i>M. xanthus</i> DK1622	109
Figure 3.4: Effects of iron concentrations on growth of <i>M. xanthus</i> DK1622	114
Figure 3.5: Examples of the Cy3-, Cy5- and Cy2-images from a single 2D-DIGE gel	116
Figure 3.6: Distribution of average ratios of spots from 2D-DIGE analysis of <i>M. xanthus</i> DK1622	117
Figure 3.7: Analysis of peptide phosphorylation.....	126
Figure 3.8: SDS-gels of protein extracts from DNA pull down assay.....	128
Figure 3.9: Secondary metabolite production by <i>M. xanthus</i> DK1622 wild type under iron-rich and iron-limiting conditions	134
Figure 3.10: PCR results of the second crossover analysis of DEL6967.....	136
Figure 3.11: Growth profiles of the mutants in iron-rich medium	139
Figure A1: Vector map of pCR2.1-Topo (Invitrogen)	255
Figure A2: Vector map of pSWU41 (Wu et al., 1996).....	255

Table of contents

List of tables

Table 2.1: Chemicals and manufacturers.....	55
Table 2.2: Commercial 'kits', enzymes and markers.	57
Table 2.3: Buffers and solutions for 2D-gel electrophoresis.	58
Table 2.4: Buffers and solutions for mass spectrometry.....	60
Table 2.5: Buffers and solutions for protein-DNA interaction studies (DNA pull-down assay)	60
Table 2.6: Buffers and solutions for biomolecular work	62
Table 2.7: Equipment and materials.....	63
Table 2.8: Description of the used myxobacteria, wild type and generated mutants	67
Table 2.9: Description and reference to <i>E. coli</i> DH10B	67
Table 2.10: Composition of CTT medium (casitone rich).....	68
Table 2.11: Composition of LB medium.	69
Table 2.12: Applied voltages for isoelectric focusing (IEF) in IPGPhor.	76
Table 2.13: Used template-vectors.	85
Table 2.14: Primer pairs for DNA pull-down assays were used in <i>Taq</i> PCRs.....	86
Table 2.15: Primer pairs in <i>Taq</i> PCRs for single crossover gene disruption experiments.	86
Table 2.16: Primer pairs in Phusion PCRs for gene in-frame deletion.....	87
Table 2.17: Primer pairs for <i>Taq</i> PCRs to confirm mutants of <i>M. xanthus</i>	88
Table 2.18: Composition of an <i>in vitro</i> <i>Taq</i> PCR batch.....	93
Table 2.19: Composition of an <i>in vitro</i> <i>Taq</i> post-processing PCR batch.....	93
Table 2.20: Composition of an <i>in vitro</i> Phusion PCR batch.	93
Table 2.21: Composition of single and double RE digests of DNA molecules.....	94
Table 2.22: Confirmed plasmids, pCR2.1-Topo- and pSWU41-derivates.	95
 Table 3.1: Putative Fur boxes identified in the genome of <i>M. xanthus</i> DK1622.....	106
Table 3.2: Iron-uptake, transport and TonB-domain proteins of <i>M. xanthus</i> DK1622	110
Table 3.3: Rates of iron uptake by <i>M. xanthus</i> DK1622 wild type cells in CTT and CTT- Fe^{MIN}	115
Table 3.4: Proteome results of <i>M. xanthus</i> DK1622 under iron-limiting conditions.....	119
Table 3.5: Selection from proteome response: categorized proteins.....	123
Table 3.6: Selection from proteome response of <i>M. xanthus</i> DK1622: potential regulators or signal-transducing proteins.	124
Table 3.7: Protein phosphorylations of differently regulated proteins of <i>M. xanthus</i> DK1622 under iron-limitation.....	127
Table 3.8: Mass spectrometric identification of proteins from DNA pull-down assay.....	130
Table 3.9: Secondary metabolite yields of <i>M. xanthus</i> DK1622 wild type under iron-rich and iron-limiting conditions.....	133
Table 3.10: Confirmed mutants, generated by single crossover gene disruption in <i>M. xanthus</i> DK1622.	137
Table 3.11: Rates of iron uptake by mutant <i>M. xanthus</i> strains.	140
Table 3.12: Relative yields of secondary metabolites from <i>M. xanthus</i> mutant strains.	142
 Table 4.1: Annotated gene functions / BLAST results of single crossover targets.....	195
 Table A1: Classification of 131 identified proteins from 2D-DIGE.	256
Table A2: Peptides with detected phosphorylations.	260
Table A3: List of potential Fur regulated proteins from proteome experiments.....	262

Introduction

1. Introduction

Iron is probably the trace metal with the highest biological importance in comparison to others, such as zinc, manganese or nickel (Nies, 2003). Iron plays a central role for nearly all organisms, participating in diverse metabolic processes. This transition metals is an essential component of cytochrome proteins, which mediate redox reactions, of oxygen carrier proteins or of iron-sulfur clusters from many enzymes with various metabolic activities (Hantke, 2001; Krewulak and Vogel, 2008). The biological most important oxidation states of iron are the ferrous (Fe^{2+}) and the ferric (Fe^{3+}) forms (Andrews *et al.*, 2003), while iron can exist in various oxidation states (from Fe^{-2} to Fe^{+6}).

In aqueous, aerobic environment iron exist predominantly in the oxidized form of $\text{Fe}^{3+}(\text{OH})_3$ (ferric hydroxide) which exhibits extreme insolubility (K_{sp} of 10^{-18} M at pH 7.0) (Winkelmann *et al.*, 1987), but oxygen-dependend microorganisms need high amounts of iron in comparison to the low accessible concentrations. Furthermore, the accessible iron in soil can be the growth-limiting factor, in consideration to concentration below 0.1 μM (Vasil and Ochsner, 1999). Bacteria have developed different molecular strategies to support growth at such low, available iron concentrations (Andrews *et al.*, 2003).

Introduction

1.1 Role of iron in microbial metabolism

Iron is among the most critical micronutrients for bacteria (Wackett *et al.*, 1989), as it serves as a co-factor for many primary metabolic enzymes. Aerobic bacteria typically scavenge iron from the environment through the biosynthesis and secretion of high-affinity iron-chelating compounds called siderophores. Following recovery of the resulting iron-siderophore complexes by specific outer membrane receptors (Buchanan *et al.*, 1999), the iron is transported into cytoplasmatic proteins by a number of different mechanisms. These systems are grouped into high- and low-affinity acquisition.

1.1.1 High-affinity iron uptake

A wide range of species employ chelating substances for iron uptake, the so-called siderophores (*greek*: iron-carrier) (Winkelmann *et al.*, 1987; Moeck and Coulton, 1998; Stintzi *et al.*, 2000; Crosa and Walsh, 2002). These water-soluble molecules show typically high affinity to Fe^{3+} ($10^{20} \leq K_f \leq 10^{50}$) (Mahé *et al.*, 1995) and Fe^{2+} ($10^{10} \leq K_f \leq 10^{35}$) (Cornish and Page, 1998) and form very stable iron-siderophore chelate complexes.

Siderophores can be divided into three major groups, classified by the following simple structures which are used as building blocks and finally for iron ligation: a) dihydroxybenzoic acid (catecholate) molecules coupled to an amino acid, b) hydroxamate groups containing *N*'-acyl-*N*'-hydroxyornithine or *N*'-acyl-*N*'-hydroxylysine and c) hydroxycarboxylates consisting of citric acid or β -hydroxyaspartic acid (Winkelmann, 2002). An example for each of the three siderophore types is shown in figure 1.1.

Introduction

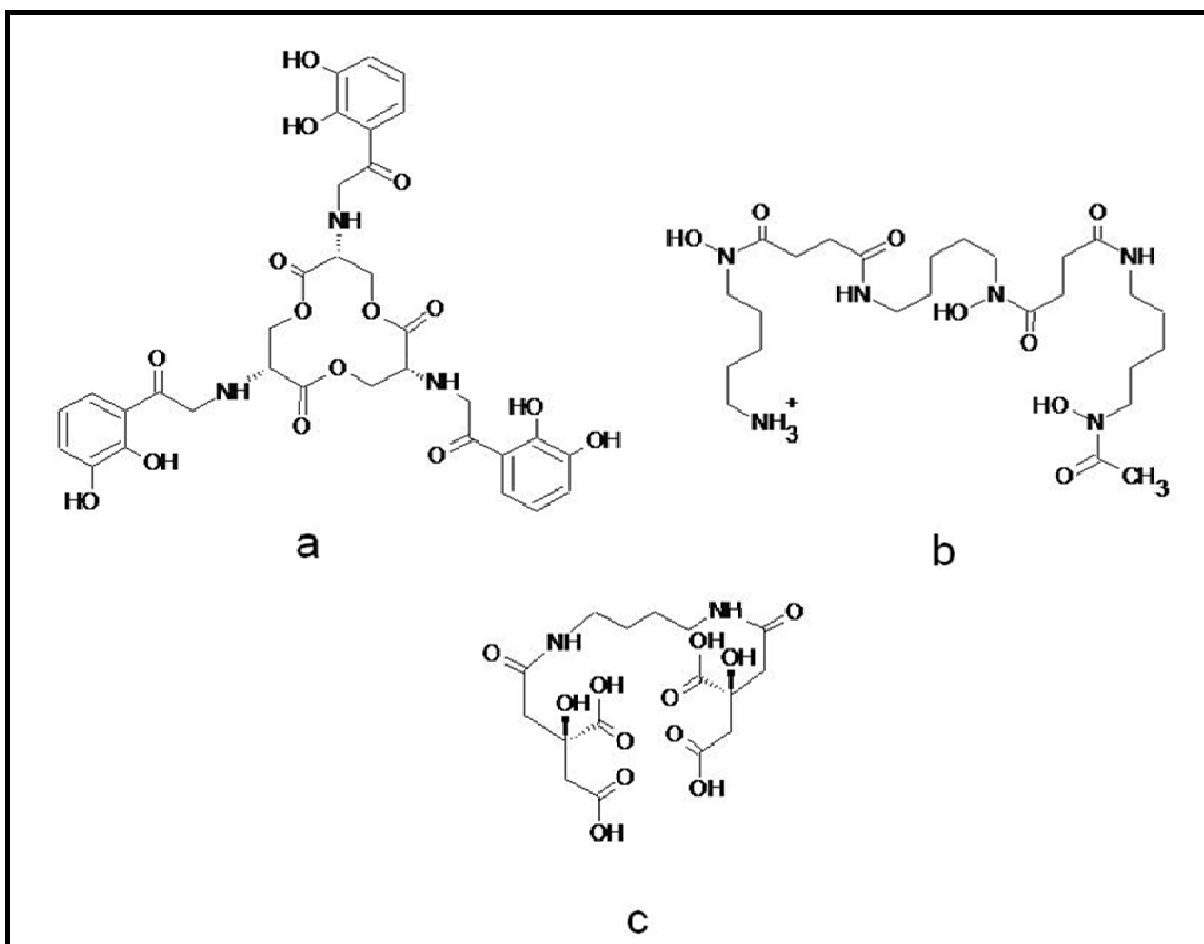


Figure 1.1: Example molecules of the three different siderophore types.

The siderophores are categorized by their basic structure (Winkelmann, 2002): **a**) catecholate type (Enterobactin), **b**) hydroxamate type (Desferrioxamine B) or **c**) hydroxycarboxylate type (Rhizoferin).

Siderophores are excreted from the producer organisms, chelate iron extracellular and iron-siderophore complexes are re-imported, subsequently. Upon receptor recognition, the iron-siderophore molecules are imported by the high-affinity TonB ExxB-ExxD iron acquisition system (figure 1.2) in an energy-consuming process (Frost and Rosenberg, 1975; Andrews *et al.*, 2003).

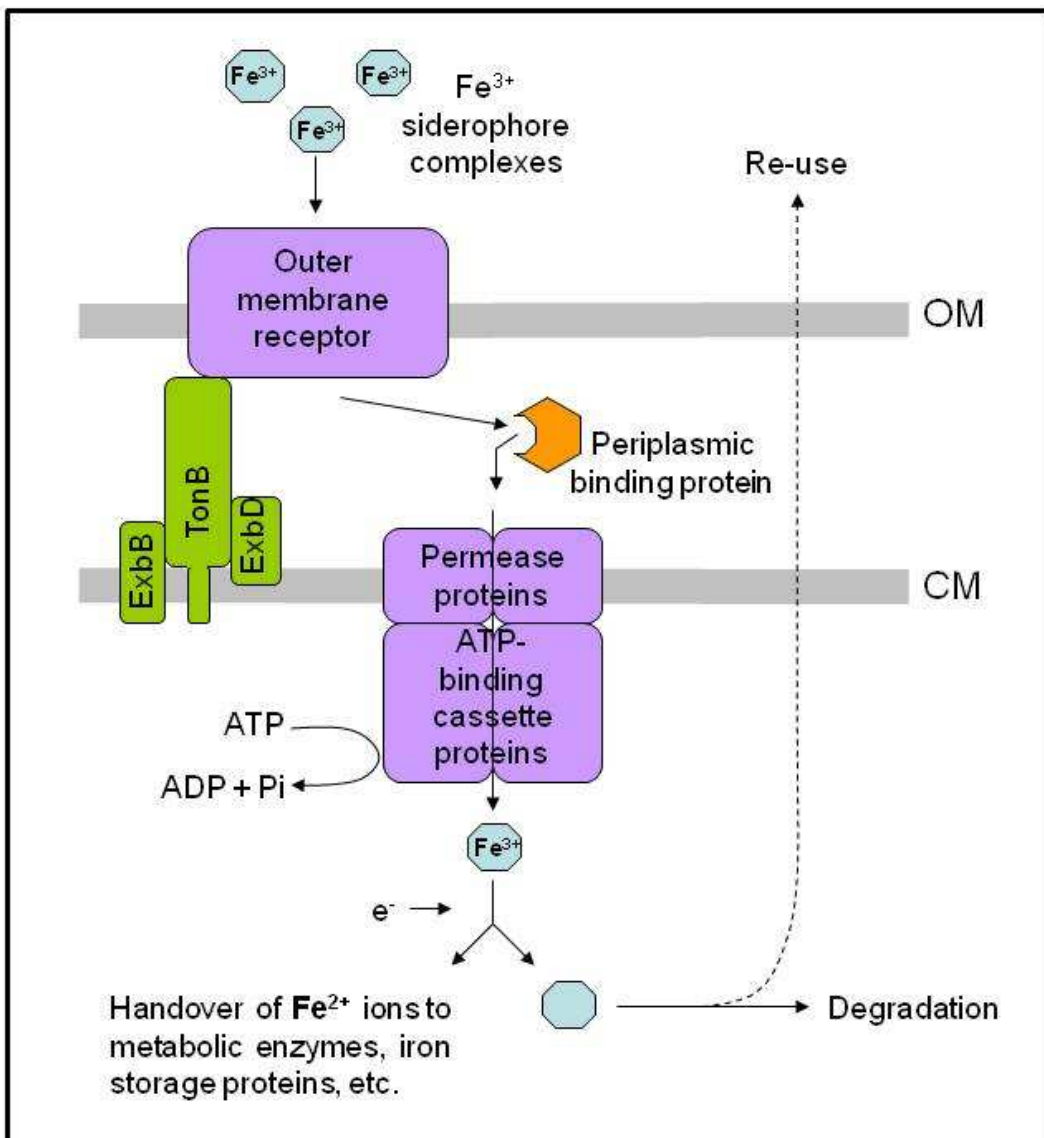


Figure 1.2: Scheme of siderophore-mediated iron uptake in Gram-negative bacteria.

Iron-loaded siderophores (blue octagon) are recognized by an outer membrane (OM) receptor, in association with a TonB ExbB/D complex. A periplasmic binding protein shuttles ferri-siderophores from the OM receptor to cytoplasm membrane (CM) ATP-dependent permease that delivers the ferri-siderophores to the cytosol. A more detailed explanation can be found elsewhere (Andrews *et al.*, 2003).

The iron-loaded siderophore complexes are recognized via highly specific outer membrane (OM) receptors (Moeck *et al.*, 1998; Andrews *et al.*, 2003), which induces a conformational change to an active transporter (Krewulak *et al.*, 2008) across the cytoplasm membrane. The TonB protein interacts with the receptor-bound ferri-siderophore complex, transducing the required energy. The receptor for iron-siderophore complexes in *Escherichia coli* (Coulton *et al.*, 1986), FhuA, is a member of a family of integral outer membrane proteins, which, together with the energy transducing protein TonB, mediate the active transport of iron-

Introduction

siderophores across the outer membrane of this Gram-negative bacterium (Ferguson *et al.*, 1998).

Subsequently, periplasmic binding proteins shuttle ferri-siderophores from the OM receptors to ATP-binding cassette (ABC) transporters that deliver the ferri-siderophores to the cytosol (Stintzi *et al.*, 2000; Crosa *et al.*, 2002; Andrews *et al.*, 2003). Typically, Fe^{3+} is reduced during the membrane transport, resulting in Fe^{2+} ions. The reaction is necessary to remove iron from iron-siderophore complexes (Andrews *et al.*, 2003). Intracellularly located, ferrous iron is complexed generally, because "free" iron would catalyze production of toxic free radicals. The mechanism of release of iron from the siderophore and the destiny of the siderophore molecules, notable degradation (Raymond *et al.*, 2003; Abergel *et al.*, 2006) or re-use (Greenwald *et al.*, 2008), seems to be structure-specific. In addition to the described function of the OM receptors, they furthermore play a role in transcriptional activation by signal transduction from iron-sensing from the outside of the bacterial cell, similar to FecA system in *E. coli* (Pressler *et al.*, 1988; Venturi *et al.*, 1995b; Marshall *et al.*, 2009). The signals are transmitted across two membranes into the cytoplasm, leading to transcriptional activation or repression of target genes (Koebnik, 2005), so metabolism can be modulated to present environmental conditions as iron concentration. In summary, different regulatory networks allow microorganisms to adjust the siderophore production and iron-uptake very precisely, avoiding intracellular iron-shortage or overload.

Moreover, some bacteria have developed additional strategies to overcome iron-deprivation and are able to steal iron-siderophore complexes by TonB dependent processes (Rabsch *et al.*, 1991; Ambrozic *et al.*, 1998). These microorganisms with capacity to growth as "iron-parasites" are well adapted to iron-limiting environments and show a much higher number of *tonB* genes than necessary for uptake of their own produced siderophores, which might also be evident for *M. xanthus* DK1622. Thus, the TonB systems were used for recognition and import of iron-loaded siderophores produced by other organisms (Venturi *et al.*, 1995b).

An additional iron resource is accessed by bacteria (often pathogenic hemolysin producers), which can degrade foreign structures like transferrin (Cornelissen and Sparling, 1994), heme, hemoglobin or hemin (Archambault *et al.*, 2003) or which employ the Feo transport system of ferrous iron (Fe^{2+}) by specific permeases (Andrews *et al.*, 2003; Cartron *et al.*, 2006). Some of these iron assimilation systems were found to be essential for colonialization of iron-limiting environments (Baltes *et al.*, 2002).

Introduction

1.1.2 Low-affinity iron uptake

Later studies have demonstrated that some microbes are able to reduce extracellular Fe^{3+} in a variety of chelate complexes (Vartivarian and Cowart, 1999). Also in yeast, a surface-localized reductase generates Fe^{2+} from Fe^{3+} . A multicopper oxidase converts Fe^{2+} back to Fe^{3+} which is immediately transported by a Fe^{3+} -permease into the cytoplasm (Kosman, 2003). Another Fe^{3+} uptake pathway was proposed in *H. pylori*. In this system, flavins reduce Fe^{3+} to Fe^{2+} which is taken up through OM porin into periplasm, and finally by an inner membrane ferrous transporter into the cytoplasm (Velayudhan *et al.*, 2000).

Such low-affinity iron transport has been measured in *E. coli* and *H. pylori*, showing 100-2000fold lower iron uptake rates than high-affinity transport systems. However, the used uptake-pathways are unclear (Velayudhan *et al.*, 2000). Low-affinity iron uptake alone does not enable normal growth even in the presence of sufficient concentrations of iron (Andrews *et al.*, 2003). These systems are negligible, used only as “emergency” system which allows the cells at least to survive without any siderophore-based iron-supply.

1.1.3 Iron homeostasis control by the ferric uptake regulator (Fur) protein

Bacteria utilize different iron management systems: (i) efficient iron uptake systems to import iron from environment, (ii) generation of intracellular iron storage pools, to provide a resource of iron also if external amounts are limited, (iii) adaptation of redox balancing systems (disarming of redox stress, repair of redox-induced damage), (iv) exact control of iron consumption (control of expression and activity of siderophore pathways or iron-containing proteins), and (v) an over-arching iron-responsive regulatory system that coordinates the expression of the above mentioned iron homeostatic machinery according to iron availability (Andrews *et al.*, 2003).

The ferric uptake regulator (Fur) protein

The balance of iron in bacteria is usually regulated by the ferric uptake regulator (Fur) protein, which plays the leading part as iron-responsive transcriptional regulator (Crosa *et al.*, 2002; Andrews *et al.*, 2003). This iron-sensing, regulatory system mediates the response to environmental conditions (figure 1.3). The iron-loaded, dimerized protein can bind to palindromic consensus DNA sequences (designated Fur boxes) (Escolar *et al.*, 1999) and

Introduction

affect selective initiation events of transcription (Mills and Marletta, 2005). Moreover, iron-free Fur proteins can have also regulatory functions (Hantke, 2001).

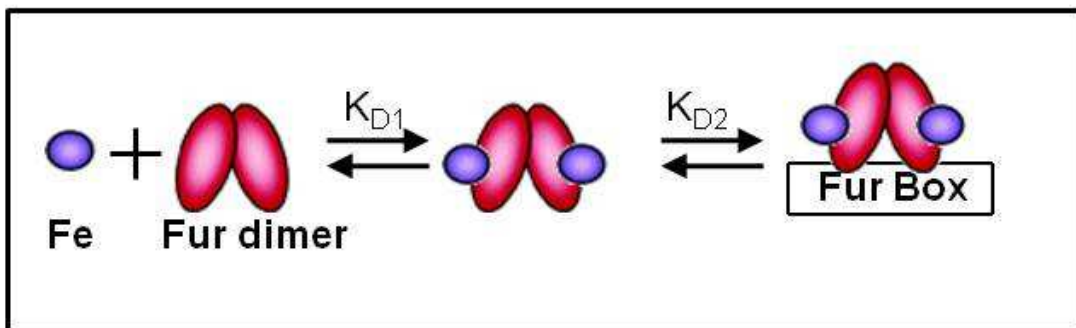


Figure 1.3: Model of Fur-DNA interaction.

The ferric uptake regulator (Fur) is a metal-dependent transcriptional repressor that is activated by divalent transition metal cations, whereas iron acts as the primary functional metal cation (Mills *et al.*, 2005). The activated dimer can bind to distinct DNA sequences, the so-called Fur boxes.

Fur boxes are normally located between the -35 and -10 sites of promoters of Fur-repressed genes, and consist of a 19 bp inverted repeat with the consensus sequence: 5'-GATAATGATwATCATTATC-3'; w = A or T (Baichoo and Helmann, 2002a). Although Fur binding causes transcriptional repression in the majority of cases, activation has also been reported (Lee and Helmann, 2007). In contrast, under iron poor conditions in which the equilibrium favors release of Fe^{2+} , Fur dissociates, and RNA polymerase can access its cognate promoters. Regulation is not always direct. For example, transcriptional repression by Fur can occur indirectly through expression of alternative sigma factors, AraC-like transcriptional regulators and two-component systems (Vasil *et al.*, 1999; Hantke, 2001), while indirect activation is often mediated via repression of small RNAs (sRNA) which function post-transcriptionally as negative regulators (Massé *et al.*, 2007).

The number of genes in bacteria regulated by Fur varies from 50 to 250, depending on the respective organism (Wandersman and Delepelaire, 2004; Rudolph *et al.*, 2006). Fur therefore serves as a global gene regulator which adjusts the state of the cell to accommodate changes in iron availability (Escolar *et al.*, 1999; Andrews *et al.*, 2003).

Fur transcriptionally regulates genes which code for proteins of diverse metabolic activities. The proteins act mainly as a negative regulator of genes from iron-metabolism like *fur* itself, or genes for either siderophore biosynthesis, iron uptake as *tonB* (Crossa *et al.*, 2002) or from primary metabolic pathways (tricarboxylic acid cycle), chemotaxis and motility, respiration, nitrogenases, hydrogenases, methane metabolism, DNA biosynthesis (ribonucleotide reductase), acid stress response, production of toxins or other virulence factors as well as

Introduction

genes from redox sensing and stress response (Escolar *et al.*, 1999; Hantke, 2001; Krewulak *et al.*, 2008).

In many Gram-negative bacteria and low GC-content Gram-positive bacteria, iron metabolism is exclusively controlled by the ferric uptake regulator (Miethke and Marahiel, 2007). Fur acts as dimeric protein, composed of two distinct domains: the dimerization is accomplished by the C-terminus containing a structural zinc binding domain, while the N-terminal portion shows iron-dependent DNA binding activity (Escolar *et al.*, 1999). When iron is abundant, Fur binds Fe²⁺ or rarely Fe³⁺ ion, both acting as co-repressor (Mills *et al.*, 2005). This induces a change of configuration which allows the dimer to bind to target DNA sequences.

Typically, bacterial genomes contain more than one *fur* gene, whereof usually at least one exhibits iron-correlated function. The preference of metal binding is coded by the highly conserved amino acids and allows the sub-grouping of Fur proteins by sequence comparison. Other members of the Fur protein family participate in sensing additional metal ions, including zinc (Zur), manganese (Mur) and nickel (Nur), as well as peroxide stress (PerR) and heme availability (Irr) (Andrews *et al.*, 2003; Yang *et al.*, 2005; Lee *et al.*, 2007), although Irr proteins have only been characterized to date from pathogens (Voyich *et al.*, 2004; Martinez *et al.*, 2005; Battisti *et al.*, 2007) or a few α -proteobacteria (Rudolph *et al.*, 2006). The crystal structures of several Fur family members have been solved as Fur of *E. coli* (Pecquer *et al.*, 2006), *P. aeruginosa* (Pohl *et al.*, 2003) and *V. cholerae* (Sheikh and Taylor, 2009); Zur of *M. tuberculosis* (Lucarelli *et al.*, 2007); PerR of *B. subtilis* (Traoré *et al.*, 2006; Jacquament *et al.*, 2009); and Nur of *S. coelicolor* (An *et al.*, 2009), allowing discovery of the residues involved in each case in metal binding. In the case of *B. japonicum* Irr, amino acids which mediate heme binding were identified by site-directed mutagenesis (Yang *et al.*, 2005). By these methods, the different binding domains in protein sequences of Fur family members have been clearly correlated to metal preferences.

The iron-responsive Fur proteins show typically an iron binding site, the so-called Zn2 site and a structural zinc site Zn1 (Sheikh *et al.*, 2009). For another Zn2 site of Zur proteins, a regulatory zinc binding motif was postulated (Lucarelli *et al.*, 2007) additionally to the structural zinc binding domain in Zur (Zn1 site), which is also present in PerR proteins; together with a regulatory non-specific common metal site in PerR (Jacquament *et al.*, 2009). In Nur proteins, a nickel/zinc specific structural site was detected and also a regulatory nickel binding site (An *et al.*, 2009). In Irr-like regulators, some amino acids involved in heme binding sites had been discovered, but the exact binding motif is unclear (Yang *et al.*, 2005;

Introduction

Sangwan *et al.*, 2008). For members of the Mur subfamily, it was published that only a single metal binding site is present, in this cases highly specific for manganese ions (Andrews *et al.*, 2003; Lee *et al.*, 2007).

As an example, primary targets of the active iron-responsive Fur proteins are genes directly involved in iron acquisition (negative regulation), or also basic metabolism, like for e.g. the aconitase (iron regulatory protein IRP1). At this juncture, the intracellular iron-concentration has direct impacts to metabolic rates, shutting down the TCA cycle in case of redox-stress by the IRP1 redox-sensitive 4Fe-4S centre, which changes the behavior of the aconitase from an enzymatic to a regulatory element (Klausner and Rouault, 1993). Also a lot of secondary effects are known, caused by a wide variety other Fur-controlled genes, responsible for transcriptional regulation of specific subsets of genes, protein phosphorylations and protein-protein interactions (Jones *et al.*, 2005), regulatory RNAs like PrrF (Vasil, 2007; Massé *et al.*, 2007) or ArrF (Wilderman *et al.*, 2004; Jung and Kwon, 2008) (*Pseudomonas* or *Azotobacter* regulatory RNA involving Fe) or like RyhB, the *E. coli* homologue (Massé and Gottesman, 2002; Vecerek *et al.*, 2007). Some of these regulators may play important roles in control of iron metabolism in *M. xanthus* DK1622.

In some organisms other strain-specific, metal-associated transcriptional regulators were described, such as DtxR in Gram-positive organisms as for e.g. *C. diphtheriae* (De Zoysa *et al.*, 2005), its homologue IdeR in *M. tuberculosis* (Dussurget *et al.*, 1999) or SirR in *S. aureus* and *S. epidermidis* (Hill *et al.*, 1998). Furthermore, the iron-dependend FeoC regulator (also a homologue of the DtxR protein) is known to rule about the *feo* gene expression, an additional transport system of bacteria to acquire environmental ferrous iron (Cartron *et al.*, 2006; Aranda *et al.*, 2009). The last regulator family, which needs to be mentioned, belongs to the IscR-like proteins, found in many Gram-negative bacteria. A small subgroup of these belong to the RirA protein family (rhizobial iron regulator), only detected in some symbiotic α -proteobacteria, namely *Rhizobium etli*, *R. leguminosarum*, *Agrobacterium radiobacter*, *Octadecabacter antarcticus* and *Liberibacter asiaticus* (Chao *et al.*, 2005; Todd *et al.*, 2005). In contrast to all other regulators, which act additionally to the Fur system(s), RirA represents the only iron-responsive transcription factor which can stand alone (Johnson *et al.*, 2007; Duan *et al.*, 2009). RirA-like regulators do not show any sequence homology to Fur proteins, but similar functions, typically repressing a set up to 100 genes from siderophore

Introduction

biosynthesis, iron transport, energy metabolism, membrane composition and flagellum control (Chao *et al.*, 2005; Todd *et al.*, 2005).

Many other genes with regulatory functions are, at least partially related to iron level, for e.g. changes in redox status causes altering in redox sensing and response (Arosio and Levi, 2002). The Fur regulon includes also ECF sigma factors (Kirby *et al.*, 2001), required for the regulation of additional subsets of genes. By this way, iron metabolism is linked to several other important organization mechanisms of the cell, as for e.g. to cell-cycle control by the carbon catabolite repressor (Miethke *et al.*, 2006). Aside from this, there are maybe several more undiscovered events in the regulatory network of cellular iron balance.

1.1.4 Iron storage and overload

Bacteria can form intracellular iron storage pools like ferritins, bactoferritins or DPS/bactoferritin proteins (Andrews *et al.*, 2003), which can accommodate up to 5000 iron atoms in a ferric hydroxide core covered by a protein shell (Arosio *et al.*, 2002), if enough iron is accessible. There are three types of iron storage molecules: The archetypal ferritins which are also found in eukaryotes, the heme-containing bacterioferritins found only in eubacteria and the smaller DPS/bactoferritin proteins present only in prokaryotes. All types can exist in the same bacterium and multiple ferritin or bacterioferritin genes are common (Andrews *et al.*, 2003). DPS/bactoferritin protein clusters (ca. 250 kDa) have a lower storage capacity with around 500 iron atoms (Zhao *et al.*, 2002), while ferritins and bacterioferritins (500 kDa) can bind between 2000-5000 iron atoms (Carrondo, 2003).

The sequestration of iron can also be managed extracellularly by selective lowering of the iron uptake via FhuA-like proteins (Neilands, 1995) or via TonB receptors (Moeck *et al.*, 1998).

At intracellular concentrations surpassing the cellular demand, iron induces by Haber-Weiss and Fenton's reaction (Goldstein *et al.*, 1993) the generation of ROS (reactive oxygen species), subsequently followed by very reactive hydroxyl and superoxide radicals (Wooldridge K.G. and Williams, 1993), which cause DNA and protein damage.

In case of extreme metal overload the usage of "emergency" efflux pumps (regulated by Fur, MerR and ArsR homologues) is described (Silver and Walderhaug, 1992; Ochsner *et al.*, 2002; Ollinger *et al.*, 2006; Vidakovics *et al.*, 2007). This transport is energy-dependent and

Introduction

can be rather non-specific with regard to metal selectivity (Nies, 2003; Cavet *et al.*, 2003; Wennerhold *et al.*, 2005; Moore and Helmann, 2005; Miethke *et al.*, 2006).

1.2 Myxobacteria

Myxobacteria are Gram-negative soil-dwelling δ -proteobacteria, which are notable for their complex life styles which culminate in the formation of multi-cellular fruiting bodies (Gerth *et al.*, 2003; 2007). The vegetative cells show a strict aerobe metabolism and are chemo-organo-heterotrophic, converting organic matter as micro-predators or scavengers. These bacteria are found worldwide; soil, rotting wood, dung pellets of herbivores are the preferred habitats (Dawid, 2000; Krug *et al.*, 2008a). Myxobacteria contain remarkable large prokaryotic genomes (e.g. *S. cellulosum* So ce56 with the largest known bacterial genome of 13.0 Mb) with a high GC content (> 70%) and a high percentage of genes coding for regulatory proteins or for secondary metabolite biosynthetic proteins (Schneiker *et al.*, 2007). Myxobacteria can move by gliding over solid surfaces, which enables them to act as coordinated swarms, providing greater metabolic access to resources than single cells (Shapiro, 1998). The term “swarming” is used in its general sense to denote a process “in which motile organisms actively spread on the surface of a suitably moist solid medium” (Goldman *et al.*, 2006).

Myxobacteria are also increasingly recognized as multi-producers of bioactive natural products, including the anti-cancer agent epothilone (Wenzel and Müller, 2009b). In many cases, however, the number of gene clusters for secondary metabolism present in myxobacterial genomes far exceeds the number of compounds produced under standard laboratory conditions (Wenzel and Müller, 2009a; Wenzel and Müller, 2009b). For example, the genome of the model myxobacterium *Myxococcus xanthus* DK1622 (Goldman *et al.*, 2006) revealed a total of 18 biosynthetic gene clusters, although only 5 compound families have been characterized from the strain to date, including the catecholate-type siderophores myxochelin A and B (Kunze *et al.*, 1989; Ambrosi *et al.*, 1998), the DKxanthenes (Meiser *et al.*, 2006b), myxalamids (Gerth *et al.*, 1983), myxochromides (Wenzel *et al.*, 2006), and myxovirescins (Gerth *et al.*, 1982).

Iron-limitation might be a potential strategy for the awaking of these silent gene clusters and subsequently to correlate those to not yet identified products, because under stress conditions a bioactive substance may provide an additional advantage to overcome this environment (Haferburg *et al.*, 2009). Under iron-limitation, carbon- and nitrate-resources are still available; the amounts of potential secondary metabolite precursors are not restricted.

While the iron response has been characterized for a number of Gram-positive and Gram-negative bacteria, as for e.g., *Bacillus subtilis* (Baichoo *et al.*, 2002b; Ollinger *et al.*, 2006),

Introduction

Bordetella pertussis (Vidakovics *et al.*, 2007), *Escherichia coli* (Hubbard *et al.*, 1986; McHugh *et al.*, 2003), *Pseudomonas aeruginosa* (Ochsner *et al.*, 2002), *Burkholderia multivorans* (Yuhara *et al.*, 2008), *Yersinia pestis* (Gao *et al.*, 2008), *Helicobacter pylori* (Lee *et al.*, 2004; Ernst *et al.*, 2005), and *Campylobacter jejuni* (Holmes *et al.*, 2005), no information is currently available how myxobacteria handle iron-limitation on transcriptional or protein level.

1.2.1 Life cycle

Myxobacteria move by gliding over solid surfaces and use two polar positioned engines to control their motility. These two engines undergo coordinated reversals, whereas changes in the reversal frequency and speed are responsible for the different patterns of movement that are observed during development. Furthermore, myxobacteria communicate with each other and coordinate their movements among others through cell-contact-dependent signals (Kaiser, 2003). Under starving conditions vegetative cells aggregate by gliding to form a multicellular fruiting body, where vegetative cells in the so-called sporangium transform into environmentally resistant myxospores (Otani *et al.*, 1995). The scheme of the myxobacterial life cycle is illustrated in figure 1.4.

The majority of myxobacteria require peptides and amino acids as nutrients. These are obtained by the degradation of proteins and/or whole cells of other bacteria and yeasts (Gerth *et al.*, 2003). The cells can secrete hydrolytic enzymes to lyse other cells and insoluble proteins to thereby obtain soluble amino acids (Berleman *et al.*, 2006).

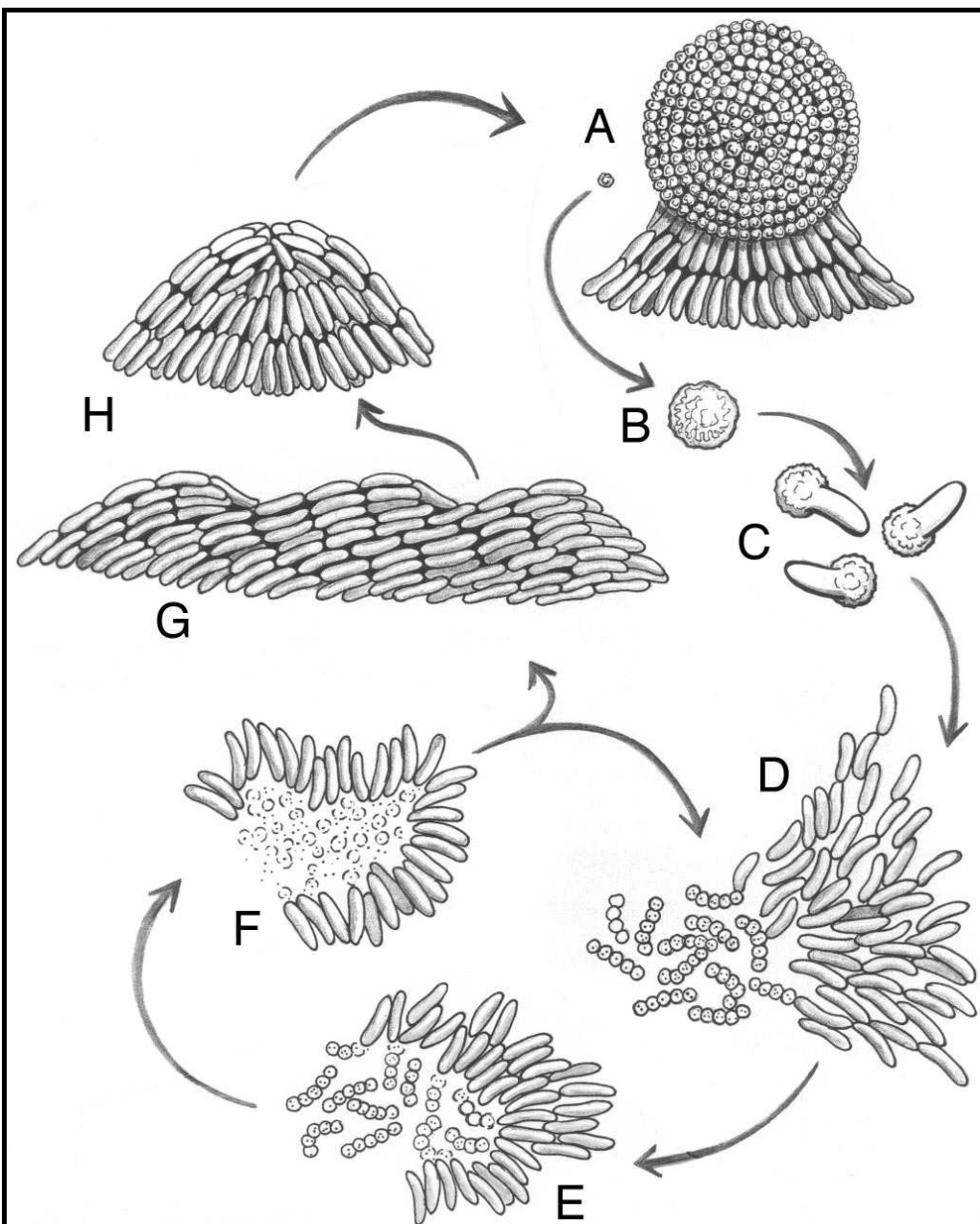


Figure 1.4: Developmental program of *M. xanthus*.

In the myxobacterial life cycle, a swarm of *M. xanthus* (a group of moving and interacting cells) can have one of two destinies depending on their environment (Goldman et al., 2006). The fruiting body (A) is a spherical structure and after morphological changes some of the cells become stress-resistant spores (B). When a fruiting body receives nutrients, the individual spores germinate (C) and thousands of *M. xanthus* cells emerge together as an “instant” swarm (D). When prey is available (*micrococci* in the figure), the swarm becomes a predatory collective that surrounds the prey. Swarm cells feed by contacting, lysing, and consuming the prey bacteria (E and F). Nutrient-poor conditions elicit a unified starvation stress response. That response initiates a self-organized program that changes cell movement behavior, leading to aggregation. The movement behavior includes wave formation (G) and streaming into mounded aggregates (H), which become spherical (A). This developmental behavior is found to be very similar in all myxobacteria (Dworkin, 1996; Plaga and Ulrich, 1999).

Introduction

Roughly 100,000 individual *M. xanthus* cells aggregate and develop to form a fruiting body over the course of several hours (figure 1.5). The fruiting body is small (0.10 mm high), sticky, and its spores are tightly packed.

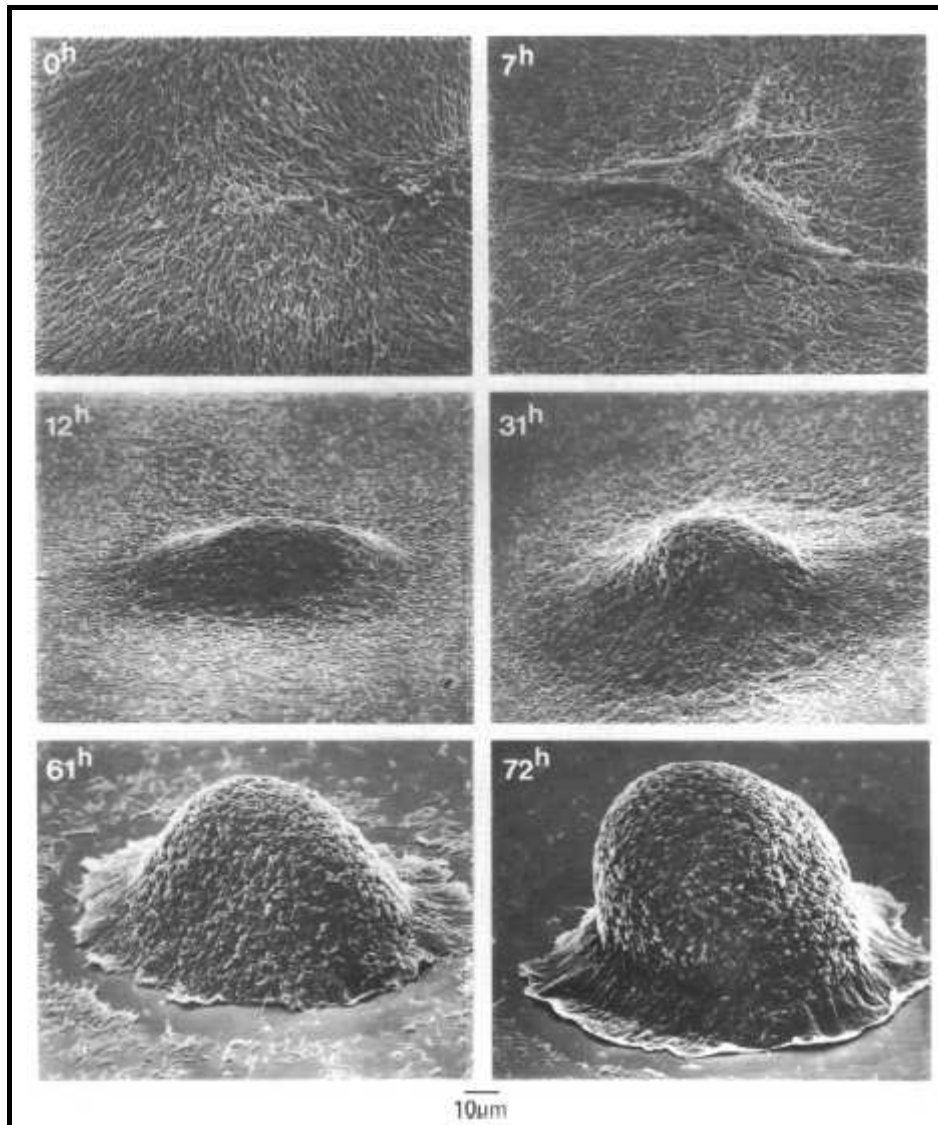


Figure 1.5: Formation of fruiting bodies of *M. xanthus*.

The cells are taken from exponentially grow phase in submerged culture, pictures are taken by field-emission scanning electron microscope (Kuner and Kaiser, 1982). The aggregated cells start a morphogenesis from flat mounds (12 h) into strain-specific fruiting bodies (72 h).

The morphology of fruiting bodies varies from simple knobs (dome shaped, e.g. genus *Myxococcus*) to more tree-like structures (e.g. genus *Chondromyces*) (figure 1.6).

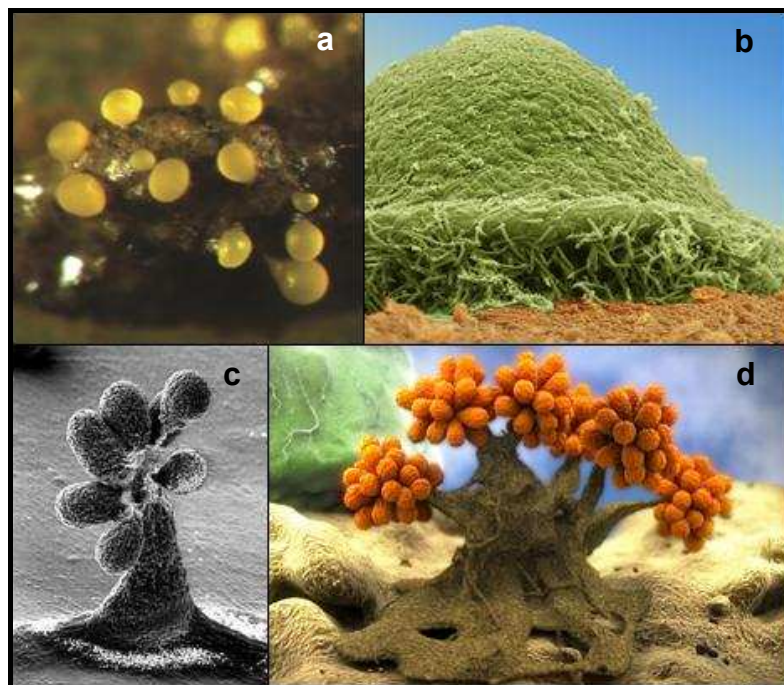


Figure 1.6: Structures of different myxobacterial fruiting bodies.

Fruiting bodies are strain-specific and can vary from simple knobs to more tree-like structure. Additionally, fruiting body morphology is an important tool for the classification of myxobacteria. The images show fruiting bodies from (and pictured by): a) *M. xanthus* (M. Vos), b) *M. xanthus* (J. Berger), c) *S. aurantiaca* (H. Lünsdorf) and d) *C. crocatus* (M. Rohde).

Enclosed in these fruiting bodies, myxospores guarantee survival of the strain while on sufficient nutrient supply, myxospores germinate again to mature cells (Shimkets *et al.*, 2006).

1.2.2 *Myxococcus xanthus* DK1622 as a model strain

The strain *M. xanthus* DK1622 belongs to the suborder Cystobacterineae and is used as a model organism for myxobacterial development (Kroos *et al.*, 1986; Downard and Kroos, 1993; Kearns *et al.*, 2001; Horiuchi *et al.*, 2002; Meiser *et al.*, 2006a; Berleman and Kirby, 2007; Kroos, 2007) and motility (Reichenbach, 1988; Spormann, 1999; Mignot *et al.*, 2005; Yu and Kaiser, 2007; Mauriello and Zusman, 2007). This organism was found to be an ideal model system for investigating of intercellular interaction and multicellular organizations in microbial communities (Pelling *et al.*, 2005). *M. xanthus* DK1622 has short doubling times and is genetically well accessible, compared to other myxobacteria, as *S. cellulosum* or *S. aurantiaca*.

The strain exists as isolated, rod-shaped cells or as aggregates. The cells interact as swarms and show a predatory, saprotrophic life style. Like other myxobacteria, the cells are capable of movement by gliding on solid surfaces. *Myxococci* use amino acids as resource of carbon,

Introduction

nitrogen, and energy while polysaccharides and simple sugars are not metabolized (Gerth *et al.*, 2003).

M. xanthus has been shown to be a potent producer of diverse secondary metabolites with unusual biosynthesis (Weissman and Müller, 2008). Several metabolites (Krug *et al.*, 2008a) are already correlated to different biosynthetic gene clusters in *M. xanthus* DK1622, while others are still silent or orphan. The *M. xanthus* DK1622 genome was sequenced in 2006 (Goldman *et al.*, 2006) and exhibited one circular chromosome with a length of 9.13 megabasepairs (Mb) with a GC-content of 68.89 %. A total of 7514 putative genes could be annotated. A scheme of the genome map is illustrated in figure 1.7, including the assigned gene functions.

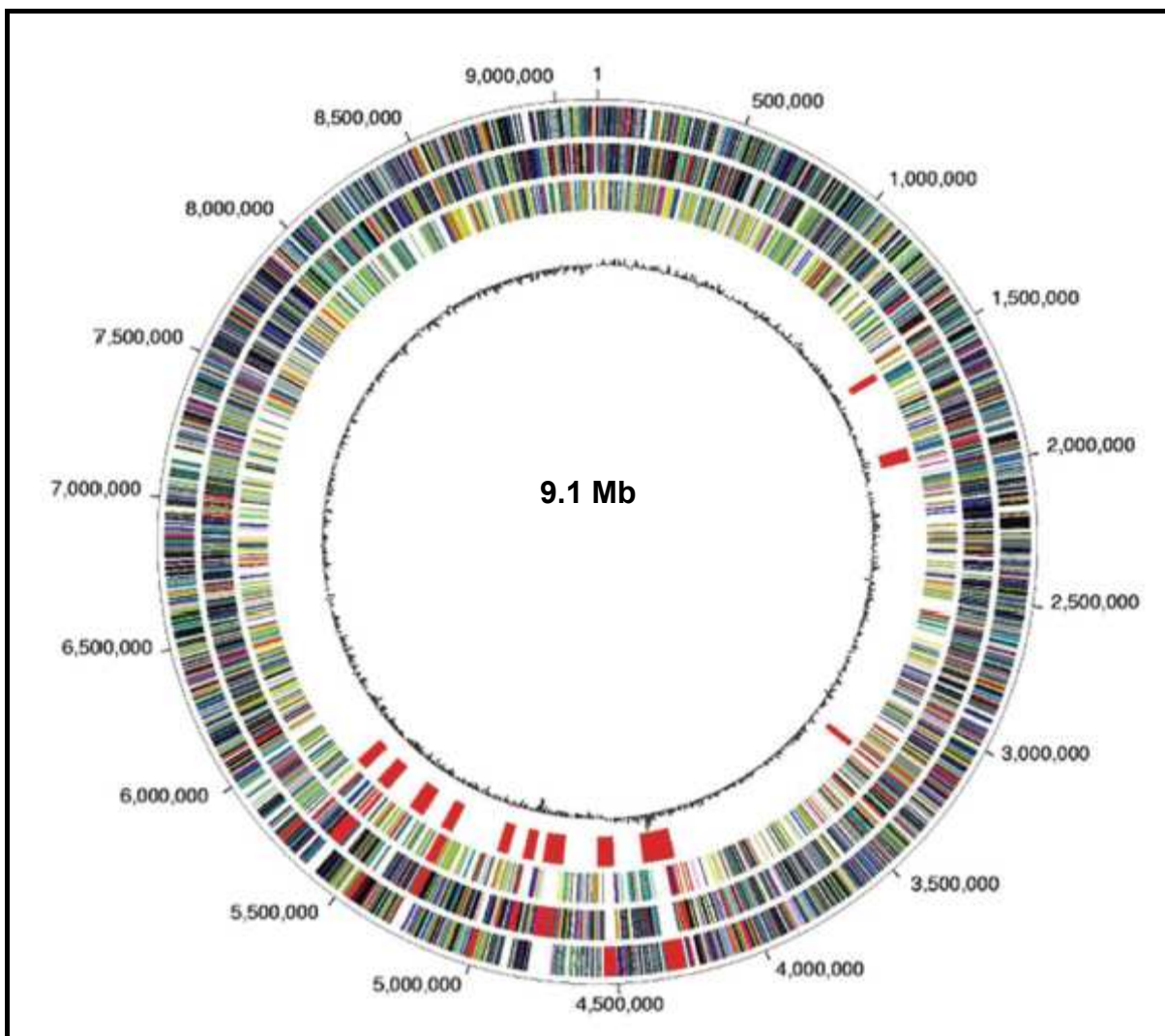


Figure 1.7: Genetic map of the *M. xanthus* DK1622 chromosome.

The scheme of the genetic map of the *M. xanthus* DK1622 chromosome was published after DNA sequencing (Goldman *et al.*, 2006). Layers (from out- to in-side): 1: ORFs (colorcoded, clockwise), 2: ORFs (colorcoded, counterclockwise), 3: lineage-specific gene duplications, 4: genes coding for

Introduction

secondary metabolite production, 5: GC skew. Base pair 1 was assigned to the predicted origin of replication.

Color code of layer 1 and 2: Purple: fatty acid, phospholipid (137) and amino acid metabolism (79), Turquoise: Co-factor, prosthetic group and carrier biosynthesis (129), Light green: Cell envelope (734), Dark blue: Transport and binding proteins (79), Yellow: DNA metabolism (125), Red brown: Mobile and extrachromosomal (116), Apricot: Protein synthesis (162) and fate (314), Red: Cellular processes (410), Orange: Purine, pyrimidine, nucleoside and nucleotide metabolism (59), Light blue: Conserved hypothetical proteins (838), Brown: Central intermediary metabolism (58), Olive: Regulatory functions (581), signal transduction (267), Light grey: Energy metabolism (343), Dark grey: Unknown function (1097). The classification of gene roles based on the publication of Goldman *et al.*, 2006, recent annotations are inserted in the online database (<http://xanthus.wikimods.org/cgi-bin/GenomeBrowser.pl>).

1.2.3 Myxobacterial secondary metabolism

In addition to the unique life style, myxobacteria are well-known and reliable producers of structurally unique and potent secondary metabolites (Weissman *et al.*, 2008; Wenzel *et al.*, 2009b). This is probably due to the constant selection pressure in their habitat to compete with other microorganisms, which is reflected by the fact that the majority of the bioactive products are active against fungi and bacteria (Gerth *et al.*, 2003). Up to now, from 7500 different myxobacterial strains which have been isolated to date, approx. 100 different basic structures and more than 500 structural variants from myxobacteria have been isolated and characterized (Reichenbach, 2001; Gerth *et al.*, 2003; Weissman *et al.*, 2008). Most of these substances are moderately lipophilic, linear, or cyclic polyketides and peptides (Reichenbach, 2001).

These products derive either from polyketide synthases (PKS), nonribosomal peptide synthetases (NRPS), or hybrid systems and show diverse bioactivities of pharmaceutical interest (Weissman *et al.*, 2008). The most prominent example is Epothilone, produced by the myxobacterium *Sorangium cellulosum* Soce 90, which has now entered the market as an anti-cancer drug (Mulzer, 2009). Research for natural products (or secondary metabolites) of pharmaceutical interest has lead to: (i) identification of novel biological molecules for therapeutic applications; (ii) elucidation of their biosynthetic pathways; (iii) analysis and modification of regulatory mechanisms of biosynthesis to increase product yields; (iv) the discovery of the mode of action, and (v) total or partial synthesis of lead-structures and derivatives.

As this work mainly deals with analysis and modification of regulatory mechanisms of biosynthesis to modify product yields, it is worth to explain the biosynthetic machinery of natural products in detail in the following section.

Polyketide synthases

Polyketide synthases (or PKS) are a family of enzymes or multienzyme complexes which assemble polyketides, a large class of secondary metabolites found in bacteria, fungi, plants, and animals. The biosynthesis of polyketides shares a high degree of similarity with animal fatty acid biosynthesis (Khosla *et al.*, 1999; Weissman, 2008).

PKS can be divided in three types (figure 1.8):

Type I PKS are large enzymes with a modular structure. Each type I PKS module consists of several domains with defined functions, separated by short spacer regions.

Type II PKS are monofunctional proteins, which aggregate to one multienzyme complex to catalyze the formation of polyketons that are cyclized resulting in aromatic moieties.

Type III PKS do not use acyl carrier domains, but single keto-synthase-like active sites to catalyze iteratively the condensations of acetate units to a CoA-derivative starter molecule (Cortes *et al.*, 2002). Bacterial type III PKS generate chalcone-like structures in a mechanism similar to plant chalcone synthase (Moore *et al.*, 2002).

Usually, in iterative systems (type II and III) one module is repeatedly used until the desired molecule length is achieved. The iteration is a programmed event. The underlying mechanism of this remarkable ability remains elusive (Wenzel and Müller, 2005b). However, today the classification is not so strict anymore, finding more and more variances from this traditional allocation (Wenzel *et al.*, 2005b; Ridley *et al.*, 2008).

Introduction

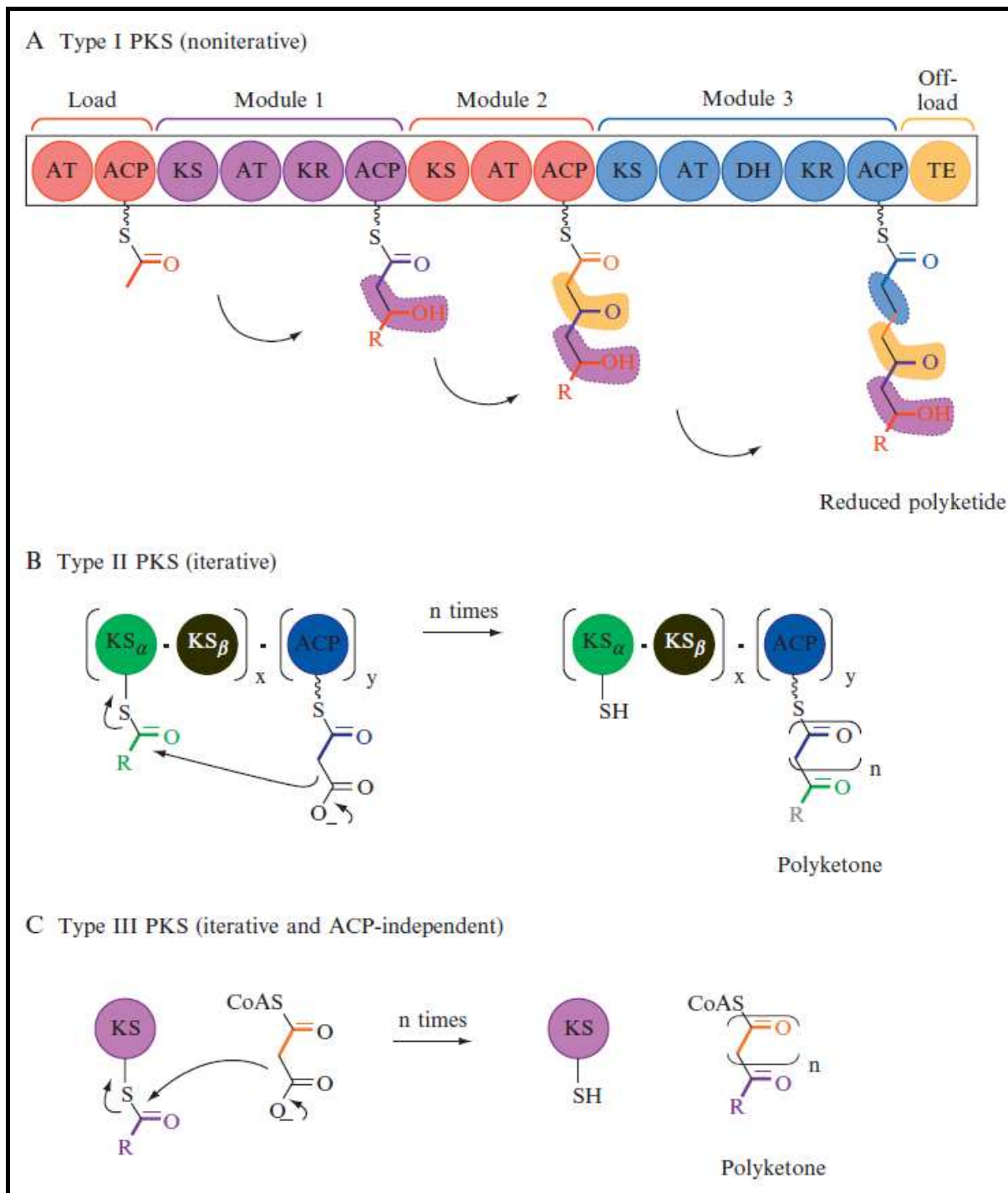


Figure 1.8: Scheme of the three PKS types (Weissman, 2009).

A) Type I PKSs consist of multifunctional polypeptides. Each subunit (or module) consists of several domains with defined functions, separated by short spacer regions. Each module typically acts once (non-iteratively) and elongates the polyketide chain by one building block, partially associated with reductive processing reactions. For each module, the added building block after modification of respective domains is indicated (by color-coded bonds, and shadings). **B)** Type II PKSs comprise discrete catalytic functions that associate into a productive complex. The “minimal PKS” includes a KS α , a KS β , and an ACP domain, which acts iteratively for a defined number of chain-extension cycles to construct a polyketone chain. **C)** Type III PKSs consist of a single multifunctional active site that, in cooperation with CoA-activated substrates, performs all the steps necessary to assemble a polyketone chain of defined length.

Introduction

The type I polyketide synthases are the most complex and the most present type in bacteria, the PKS type I mechanism is graphically more detailed explained in figure 1.9 and the following section. In such linear systems, one module corresponds to one extension-unit. This implies that the number of modules defines length and finally the structure of the resulting polyketide (colinearity rule). The loading (or starting) module and elongation module can be subdivided into their catalytic domains. A minimum set of domains for an elongation cycle is formed by a keto-synthase (KS) domain, an acyl transferase (AT) domain and an acyl carrier protein (ACP) domain.

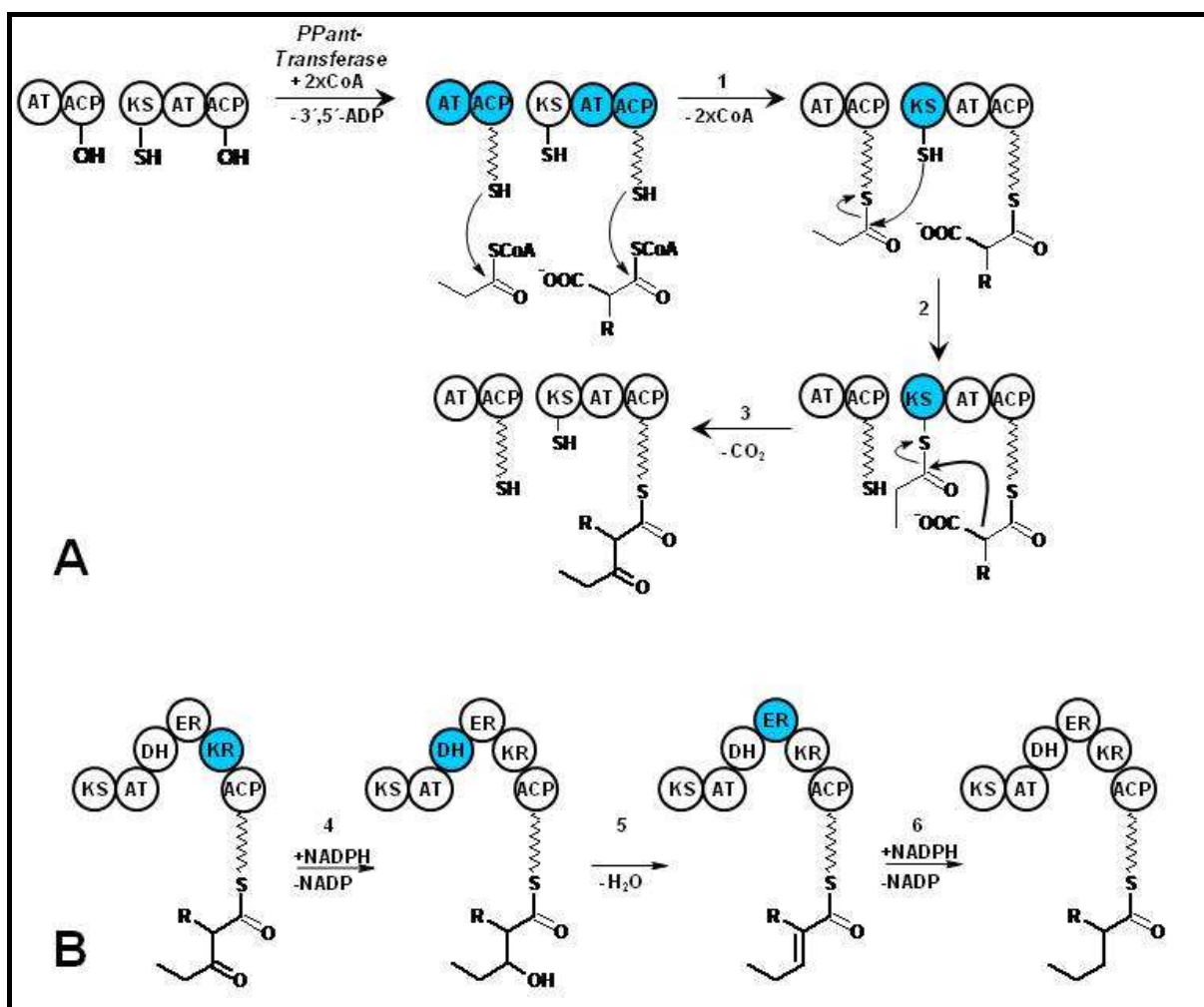


Figure 1.9: Principle of a PKS type I system.

The active domain of the intermediated step is marked in blue. The order of modules and domains of a complete polyketide-synthase is as follows (from N-terminus to C-terminus) **A)** loading and elongation: This represents an AT and an ACP domain for the loading module and a KS, an AT and an ACP domain for the elongation module. Phosphopantetheinylation activates the ACP domains first (to *holo*-form), and the starter molecule (here propionyl-CoA) is loaded to the ACP domain of the starter module, catalyzed by its AT domain. In addition, the first molecule for chain elongation (malonyl- or methylmalonyl-CoA) can be loaded to the ACP domain of the elongation module, catalyzed by its AT domain (step 1). The conserved SH group of the KS domain of the current module nucleophilic attacks the ACP-bound substrate of the previous module (step 2). The ACP-bound elongation group reacts in a Claisen condensation with the KS-bound polyketide chain under CO_2 release, resulting in a free KS domain and an ACP-bound elongated polyketide chain (step 3). Step 1-3 are repeated on the next

Introduction

module or the final module contains a TE domain for release of the polyketide chain (hydrolysis or cyclization). **B)** Optional domains of an elongation module fulfill a stepwise reduction on the β -keto group by KR, DH and ER domains. At this, the unit added in the previous module is altered, but not the component bound to the ACP domain of the current module containing the modification domain(s). The KR domain reduces the β -keto group to a β -hydroxy group (step 4), the DH domain eliminates water (step 5), resulting in the α,β -unsaturated alkene, and the ER domain reduces the α,β -double-bond to a single-bond (step 6). Taking all optional steps together (4-6), a so-called complete reductive loop is performed.

The starter molecule, the elongation units and the growing polyketide chain are bound with their carboxyl group to the thiol groups of ACP domains by a serine-attached 4'-phosphopantetheine (PPant) residue and to the KS domains by a cysteine residue via a thioester linkage. The growing chain is now handed over from one thiol group to the next and is released finally by hydrolysis or by cyclization, catalyzed by a thioesterase (TE) domain.

Biochemical reactions of PKS enzymes can be divided in three basic steps:

Starting or loading stage: The starter molecule (as CoA ester) is loaded onto the ACP domain of the starter module catalyzed by the AT domain, which is responsible for substrate activation and recognition.

Elongation or extending stages: For elongation, the molecule (as CoA ester) is relocated onto the ACP domain of the elongation module, catalyzed by the ACP-AT domain. The polyketide chain is transferred from the ACP domain of the previous module to the KS domain of the current module, catalyzed by the KS domain. The KS catalytic strategy is stepwise: first the upstream acyl group is moved onto the KS active site via nucleophilic attack by a conserved KS cysteine, thus pre-serving the thermodynamic activation of the thioester. The KS domain then decarboxylates the downstream (methyl)malonyl-S-ACP, which elongates the product and translocates it to the downstream ACP, which in turn becomes the upstream donor for the next module. Then, the growing product is linked to the current ACP domain, a reaction catalyzed by the current AT domain. In summary, the ACP-bound elongation group reacts in a Claisen condensation with the KS-bound polyketide chain under CO_2 release (driving force), leaving a free KS domain and an ACP-bound elongated polyketide chain. This cycle is repeated for each elongation module (Wenzel *et al.*, 2005b; Weissman, 2009).

Product modifications, catalyzed by additional domains inserted in the basic module, can occur during elongation cycles. The keto-reductase (KR) domain reduces β -keto groups to β -hydroxy groups, the dehydratase (DH) domain eliminates water, resulting in the α,β -unsaturated alkene, and the enoyl-reductase (ER) domain reduces the α,β double-bond to a single-bond (full reductive loop). The modification domain actually affects the previous

Introduction

addition to the chain (the group added in the previous module), not the component loaded onto the ACP domain of the module which contains the modification domain.

Termination or releasing stage: The TE domain hydrolyzes the completed polyketide chain from the ACP-domain of the previous module. After release of the polyketide chain from the PKS, post processing steps can be carried out as from glycosyl- and methyltransferases, acyltransferases, halogenases, cyclases and aminotransferases (Rix *et al.*, 2002)

Nonribosomal peptide synthetases

Nonribosomal peptides, a large class of secondary metabolites are synthesized by one or more specialized nonribosomal peptide-synthetase (NRPS) enzymes. Ribosomal peptide synthesis is normally restricted to the set of 20 amino acids from protein biosynthesis, but in NRPS several hundred substrates have been identified. The presence of additional structures, such as fatty acids, heterocyclic rings, non-proteinogenic amino acids, carboxylic acids, and modified amino acids is observed in this compound class. Thus, structural diversity is a predominant feature of non-ribosomally produced peptides (Walsh *et al.*, 1997; Crosa *et al.*, 2002; Finkin and Marahiel, 2004). The members of the NRPS family comprise large multifunctional enzymes, organized in modules, which synthesize small peptide molecules. Each module is responsible for the introduction of one additional amino acid and consists of several domains with defined functions, separated by short spacer regions. These modules carry out substrate recognition, activation, binding, modification, elongation and release. The biosynthesis of nonribosomal peptides shows similarities with the polyketide and fatty acid biosynthesis. The principles of nonribosomal peptide synthesis are shown in figure 1.10. The NRPS and PKS proteins use a very similar strategy for the biosynthesis of two distinct classes of natural products. In addition to the sharing of a modular organization, both systems use carrier proteins (PCP for NRPS and ACP for PKS) to tether the growing chain. Both PCP and ACP are post-translationally activated by a 4'-phosphopantetheine prosthetic group, and this modification is catalyzed by a family of 4'-phosphopantetheinyl-transferases. A minimum set of domains of NRPS enzymes for an elongation cycle consists of an adenylation (A) domain, peptidyl carrier protein (PCP) domain, and condensation (C) domain.

Introduction

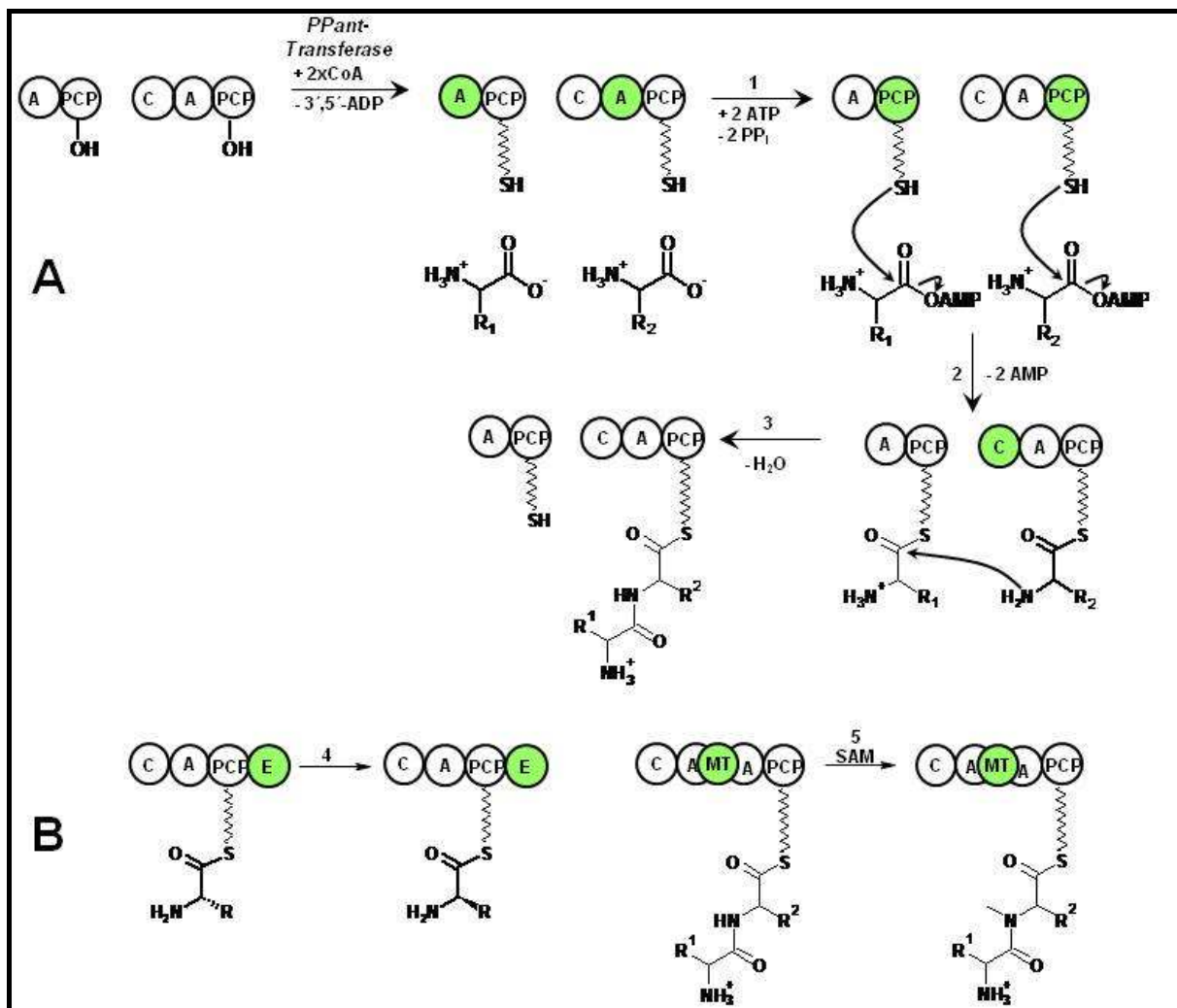


Figure 1.10: Principle of a NRPS system.

The active domain of the intermediated catalytic step is marked in green. The order of modules and domains of a complete nonribosomal peptide synthetase is as follows (from N-terminus to C-terminus)

A) Loading and elongation: The initiation-module and elongation-module can be subdivided into their catalytic domains, an A and a PCP domain for the initiation-module and a C, an A and a PCP domain for the elongation-module. The PCP domains must first be activated by phosphopantetheinylation. The initial amino acid can be loaded onto the PCP domain of the starter module, activation catalyzed by its A domain (step 1). The first activated amino acid for chain elongation can be loaded to the PCP domain of the elongation module. The C domain of the current module catalyzes the formation of an amide bound between the amino group of the current module to the thioester bound to the previous module (step 2) under the elimination of H₂O, resulting in a free PCP domain of the previous module and an PCP-bound elongated polypeptide chain (step 3) on the current module. Step 1-3 is repeated by the next module. The final module contains a TE or an R domain for release of the polypeptide chain.

B) Modifications: The growing polypeptide chain can be altered by additional E and MT domains. The E domain catalyzes the conversion of *L*-amino acids to the respective *D*-enantiomere (step 4), the MT domain adds a methyl moiety (step 5) to the amino group using S-adenosyl methionine as cofactor.

At first, the activation of the NRPS from *apo*- to *holo*-form is catalyzed by a PPant transferase. The A domain activates and selects the respective substrate for the nonribosomal peptide synthesis, consuming ATP. Then, it catalyzes the transfer of the activated acyladenylate substrate to the PCP domain. The peptide bond is formed by the C domain by

Introduction

catalyzing the nucleophilic attack of the downstream PCP-bound acceptor amino acid with the free α -amino group of the activated thioester of the upstream PCP-bound donor amino acid or peptide (Schwarzer *et al.*, 2003). Activated amino acids and the growing polypeptide chains are bound with their carboxy group to the SH (thiol) groups of the PCP domains by conserved serine-attached 4'-phosphopantetheine residues via a thioester linkage. The growing chain is handed over from one SH group to the next, and finally released by hydrolysis or by cyclization, catalyzed by a TE or reductase (R) domain, respectively.

Biochemical reactions of NRPS enzymes can be divided in three basic steps:

Initiation or Starting stage: The first amino acid is activated as AMP-derivate by the A domain, in which ATP is consumed and Mg^{2+} is used as cofactor. The activated amino acid is loaded onto the PPant arm of the PCP domain. The amino group of the bound amino acid can be further processed by a formylation (F) domain or by an N-methylation (NMT) domain (Schwarzer *et al.*, 2003).

Elongation or Extending stages: In analogy to the starting stage, each module loads its specific, activated amino acid onto its PCP domain and activation is catalyzed by the modules A domain. The C domain forms an amide bond between the thioester group of the growing peptide chain from the previous module with the amino group of the current module. The extended peptide is now attached to the current PCP domain. In some cases the C domain is replaced by a condensation-cyclization (Cy) domain. This Cy domain catalyzes the amide bond formation and additionally a sidechain reaction of the amino acids serine, threonine, and cysteine, forming oxazolidines and thiazolidine, respectively. Further peptide synthesis is carried out by stepwise condensation with amino acid building blocks bound to the PCP domain of the downstream elongation modules.

Optional modules such as epimerization (E) domains catalyze the epimerization of the incorporated amino acid of the peptide chain into the D-configuration. Further possible modules are oxidation (Ox) domains, which catalyze the oxidation of thiazolines or oxazolines to thiazoles or oxazoles or Red (reduction) domains, which catalyze the reduction of thiazolines or oxazolines to thiazolidines or oxazolidines, respectively.

Termination or Releasing stage: A final module is required to release the growing peptide chain from its phosphopantetheinyl arm. This module contains, in most cases, a thioesterase domain (TE-domain, ~ 250 aa) for releasing the product. The TE domain hydrolyzes the completed polypeptide chain from the PCP domain of the previous module, thereby often forming cyclic amides (lactams) or cyclic esters (lactones). Finally, release of the product is

Introduction

performed by the thioesterase (TE) domain by a nucleophilic attack on the PCP-peptidyl thioester. Depending on the TE domain, products can be released as linear or cyclic peptide (Schwarzer *et al.*, 2003; Sieber and Marahiel, 2005). Another way of releasing the peptide is by an R domain (reduction) that reduces the thioester bond to an aldehyde or an alcohol residue.

The great diversity of NRPS products is due to additional enzymatic processes called tailoring domains, which can be involved either during or after biosyntheses. Some represent an integral domain of the NRPS and act *in cis* (moving along in a single protein chain), and the others are distinct enzymes which act *in trans* (moving from one protein chain to another) on the way to the mature NRPS product. Some optional editing steps of the elongated peptide are for e.g. carried out by epimerization (E) domains or methyltransferase (MT) domains.

Furthermore, the released peptide can be modified in post-NRPS processing step by methylation, glycosylation, acylation, halogenation, or hydroxylation. Enzymes involved in such modification reactions are usually associated to the synthetase complex (Floss, 2006).

Hybrid systems

The structural and catalytic similarities between NRPSs and PKSs have suggested that both might exist as hybrid enzymatic systems. Such enzymatic hybrid results in the production of diverse metabolites by the incorporation of amino acids and of C2 or C3 units (derived from short chain carboxylic acids) by NRPSs and PKSs, respectively. Based on the order in which either amino acid or carboxylic acid is incorporated, the hybrid PKS-NRPSs can be divided in two classes. Those whose biosynthesis do not involve functional interaction between NRPSs and PKSs modules and those whose biosynthesis are catalyzed by hybrid PKS-NRPS systems, involving direct interactions between NRPSs and PKSs modules (Du and Shen, 2001).

In figure 1.11, example structures of the known natural products of *M. xanthus* are shown, several of these molecules were derived from PKS-NRPS hybrid systems.

Introduction

1.2.4 Natural products from *M. xanthus* DK1622

The remarkable presence of 18 gene clusters in the genome of *M. xanthus* DK1622 suggest the ability to synthesize diverse secondary metabolite products. However, only 5 of those gene clusters have assigned functions that participate in the production of specific natural products. Notably, substances which have been isolated and characterized from *M. xanthus* DK1622 (Krug *et al.*, 2008a; Kim *et al.*, 2009) are the myxalamids (Gerth *et al.*, 1983; Silakowski *et al.*, 2001b), the myxochelins (Silakowski *et al.*, 2000; Gaitatzis *et al.*, 2001; Li *et al.*, 2008), the myxochromides (Trowitzsch-Kienast *et al.*, 1993; Wenzel *et al.*, 2005a), the myxovirescins (Gerth *et al.*, 1982; Simunovic *et al.*, 2006; Simunovic and Müller, 2007a; Simunovic and Müller, 2007b) and the DKxanthenes (Meiser *et al.*, 2006a; Meiser *et al.*, 2006b; Meiser *et al.*, 2008).

A sixth compound family has been detected in *M. xanthus*, which is produced ribosomal: the ctitilins (Trowitzsch-Kienast, 1993; Krug *et al.*, 2008a)

The majority of the genes that code for PKSs and NRPSs have not yet been correlated to specific secondary metabolite end-products, while many of these proteins are demonstrably expressed (Schley *et al.*, 2006; Bode *et al.*, 2009). A structure derivative for each known family is illustrated in figure 1.11, and the biosynthesis for each known family is described briefly in the following section.

Introduction

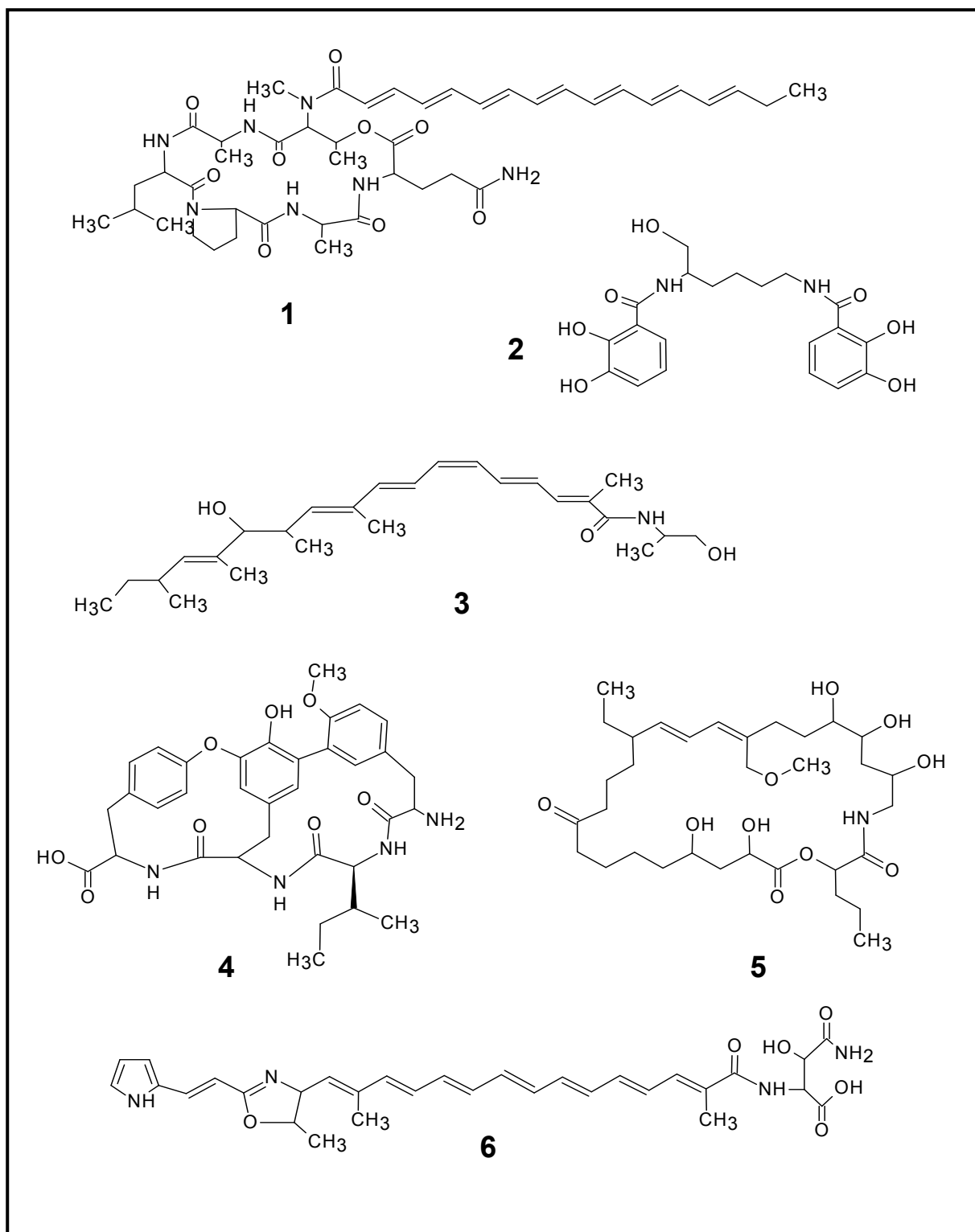


Figure 1.11: Diverse secondary metabolite families, produced by *M. xanthus* DK1622.

An example structure for each family is illustrated. 1: Myxochromide A2, 2: Myxochelin A, 3: Myxalamid A, 4: Cittilin A, 5: Myxovirescin A, 6: DKxanthene560. All structures are derived from PKS-NRPS hybrid systems, excepting for cittilin, which is produced ribosomal.

Myxochromide belongs to the category of lipo-peptide lactones and is synthesized by 3 proteins (*MchABC_A*) encoded by the *mchA* gene cluster, exclusively produced by the order

Introduction

myxococcales (Trowitzsch-Kienast *et al.*, 1993). The aliphatic side chain is generated by the PKS MchA which is capable of producing polyketide chains of different lengths (Wenzel *et al.*, 2006). The ER domain of MchA catalyzes the reduction of the polyketide chain to a polyunsaturated structure (Wenzel *et al.*, 2005a). MchBC is subdivided into 6 NRPS modules which are responsible for the formation of the hexapeptide backbone of Myxochromide A (figure 1.11). The first two modules incorporate *L*-threonine and *D*-alanine. Herein, the epimerization (E) domain of module 2 catalyse the formation to *L*-alanine. Modules 3 to 6 elongate the chain with the building blocks *L*-leucine, *L*-proline, *L*-alanine, and *L*-glutamine. Module 4 is skipped in the biosynthesis of Myxochromide S, a structural variant of Myxochromide produced by *Stigmatella aurantiaca* (Wenzel *et al.*, 2006). The exact function of myxochromide is unknown.

Myxochelins are iron-chelating compounds (siderophores) that are secreted by myxobacteria (Gaitatzis *et al.*, 2005) to acquire iron from the medium (Gaitatzis *et al.*, 2001). A conserved gene cluster, encoding for the biosynthesis machinery of myxochelin, can be found in different secondary metabolite producers, as myxobacteria or actinomycetes as *Nonomuraea pusilla* (Kunze *et al.*, 1989; Miyanaga *et al.*, 2006). For myxochelin A, an *in vitro* inhibition of tumor cell invasion could be demonstrated (Miyanaga *et al.*, 2006), but this activity might be correlated to the unspecific deprivation of iron.

The biosynthesis includes the formation of two 2,3-dihydroxybenzoic acid moieties by the MxcCDEF proteins and subsequent condensation with the amino acid *L*-lysine, bound to NRPS MxcG. First, lysine must be activated by the A domain of MxcG and loaded to its PCP domain. The C domain performs two rounds of condensation reactions to attach two 2,3-dihydroxybenzoic acid residues from MxcF to the two amino groups of lysine. The reduction domain of MxcG then reduces the PCP-bound myxochelin to the aldehyde intermediate. The MxcG Red domain and MxcL aminotransferase compete for this aldehyde intermediate, resulting in myxochelin A and B, respectively (Li *et al.*, 2008).

Myxalamid blocks electron transport chains in yeasts, molds and in some Gram-positive bacteria (Silakowski *et al.*, 2001b). This substance class is formed by a PKS-NRPS hybrid system and is produced only by *M. xanthus* species (Gerth *et al.*, 1983). The PKS complex MxaF-MxaB₁₋₂ generates the linear polyketide moiety. The elongation step is carried out by the PKS module MxaB₁₋₂, which is encoded as two separate proteins, MxaB₁ and MxaB₂.

Introduction

(Wenzel *et al.*, 2005b). Subsequently, the extension with alanine is accomplished by the NRPS MxaA (Silakowski *et al.*, 2001b).

The role of **cittilin** for myxobacteria is still unclear. The biosynthesis of the cittilins is somehow special; this cyclic tetrapeptide is not produced by an NRPS. The incorporated amino acids (three tyrosines, one isoleucine) must be coded on the genome and being attached in a ribosomal process (Grabley and Thiericke, 1999). This coding DNA region is flanked by a cytochrome p450 oxygenase gene and a methyltransferase (at MXAN_0681). Two derivates are known to be produced from *Myxococcus* species (Cittilin A, containing a methyl moiety on the first tyrosine and Cittilin B without these).

Myxovirescin shows potent inhibitory activity at the incorporation of diaminopimelic acid and uridine diphosphate-N-acetylglucosamine into *E. coli* cell walls and other Gram-negative bacteria (Gerth *et al.*, 1982; Trowitzsch *et al.*, 1982). This antibiotic is exclusively found in the genus *Myxococcus*, and is also known as antibiotic TA (Zafirri *et al.*, 1981; Rosenberg *et al.*, 1982) or as megovalicin (Takayama *et al.*, 1988). The biosynthesis is carried out by a PKS-NRPS hybrid system, utilizing 4 type I PKS (TaI, TaL, TaO, TaP), one major hybrid PKS-NRPS (Ta-1) and a number of monofunctional enzymes. All of these are encoded by the 21 ORFs of the myxovirescin biosynthetic gene cluster spanning 83 kbp (Simunovic *et al.*, 2006; Simunovic, 2007).

DKxanthene seems to play a major role in myxobacterial fruiting body development and myxospore morphogenesis (Meiser *et al.*, 2006b; Meiser *et al.*, 2008). It is maybe involved in strain communication and coordination (Meiser *et al.*, 2006a). DKxanthene assembly lines are formed by a hybrid PKS-NRPS gene cluster, exclusively found in myxobacteria. Up to now, thirteen unique structures from *M. xanthus* DK1622 were elucidated, differing in the length of their characteristic polyene functionality, as well as the extent of methyl branching (Meiser *et al.*, 2008).

The distribution of all secondary metabolite gene cluster in the chromosome of *M. xanthus* DK1622 is shown in figure 1.12, as well as the DNA template for cittilin biosynthesis.

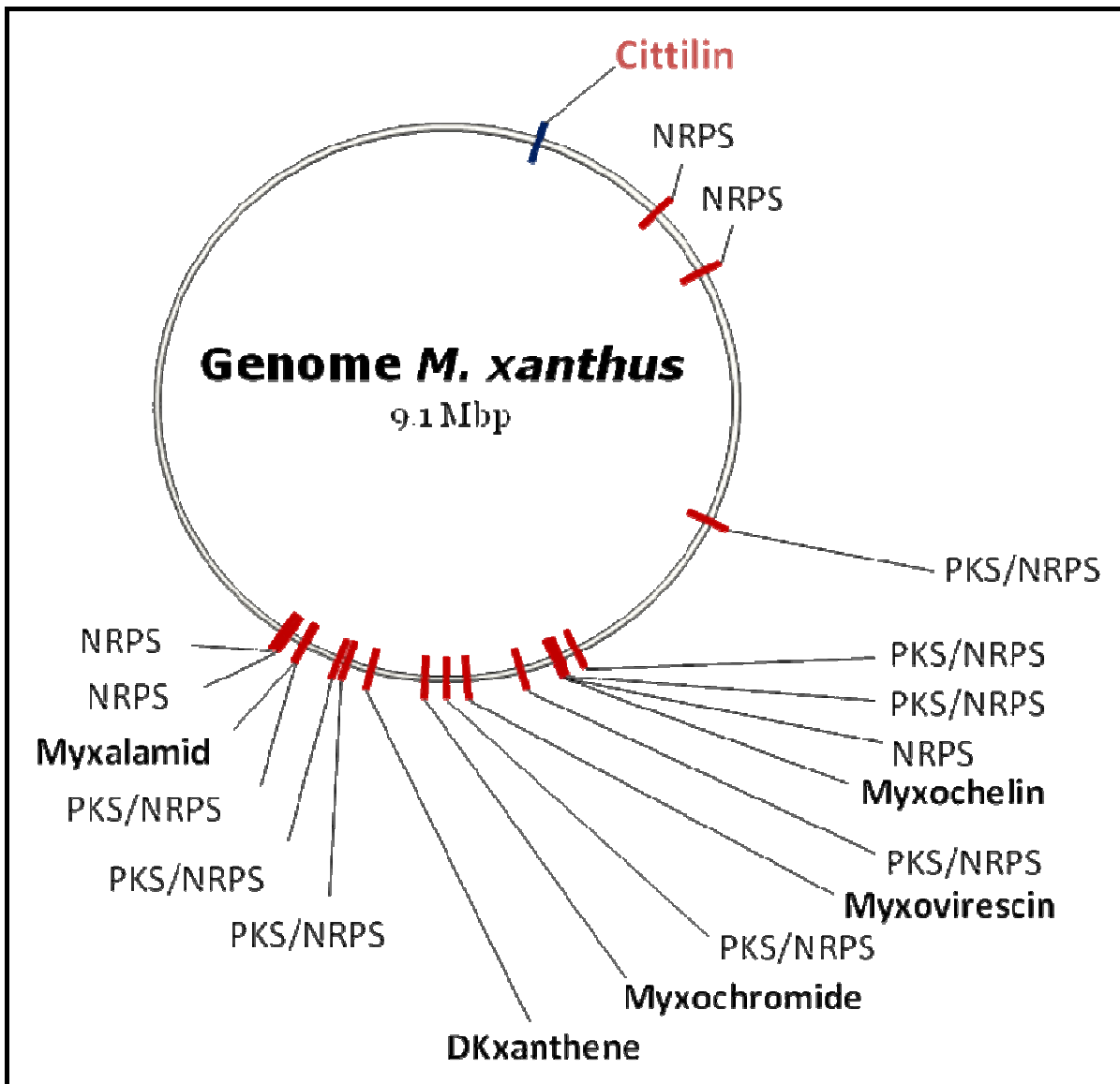


Figure 1.12: Chromosomal distribution of the *M. xanthus* secondary metabolite gene cluster.

The genome of *M. xanthus* DK1622 contains 13 PKS-NRPS hybrid clusters and 5 pure NRPS clusters. Additionally to the 18 PKS and PKS-NRPS gene clusters (red), the position of the genomic template of Cittilin is indicated (blue) in the figure. In the last years, important research contributions to regulation and/or biosynthesis of all known secondary metabolites from *M. xanthus* had been made by members from our department: Myxochromide (Wenzel et al., 2006), Myxochelin (Gaitatzis et al., 2005; Li et al., 2008), Myxalamid (Bode et al., 2007), Cittilin (Krug et al., 2008a), Myxovirescin (Simunovic et al., 2006), DKxanthene (Meiser et al., 2006b).

1.3 Comparative proteomics

Proteins are vital parts of living organisms, as they are the main components of the physiological metabolic pathways of cells. Comparative proteome analysis is the tool of choice to detect effects in the protein profile, induced by one or more certain factors.

Genome analysis provides knowledge about the stable genetic information within a cell; but allows only limited prediction about the presence of functional products. Transcription of genes, translation, post-translational modifications and protein turn-over are regulated depending on the environment, resulting in qualitative and quantitative changes on the mRNA and protein levels. The availability of fully sequenced genomes facilitated the development of methods to study such dynamic changes in the course of transcriptome or proteome analyses (Lottspeich and Engels, 2006).

A cellular proteome is defined as the protein expression profile under specific conditions as for e.g. kind of tissue, development, pH, aeration, nutrient supply, time point etc. (Wasinger *et al.*, 1995; Lottspeich *et al.*, 2006). Comparative protein pattern analysis is increasingly used in research as a tool to investigate adaptation of organisms to different environmental conditions (Heim *et al.*, 2002; Lee *et al.*, 2004; Vidakovics *et al.*, 2007). Generally, the methodological approach of proteome analyses is based on high-resolution separation of proteins from different experimental conditions and subsequent protein identification. These new techniques account in great extent for the elucidation of areal and temporal reaction- and regulation-networks, in contrast to classical protein-chemistry (Yates, 1998b).

1.3.1 Proteome analysis by 2D-PAGE

In order to analyze complex biological samples on the proteome level, high resolving separation of proteins is necessary. Two-dimensional polyacrylamide gel electrophoresis (2D-PAGE) is based on migration of proteins according to their isoelectric point (pI) by isoelectric focusing (IEF) and subsequent separation of proteins by their molecular weight via SDS-polyacrylamide gel electrophoresis (SDS-PAGE) (O'Farrell, 1975). Several developments have been introduced since then, leading to more possibilities for application of this technique in last decades (Kellner *et al.*, 1999; Görg *et al.*, 2004; Lottspeich *et al.*, 2006).

IEF is mostly performed by using immobilized pH gradients (IPG strips), whereas the migration of proteins is achieved by applying high voltage. Thus, it is important to minimize the amount of charged molecules aside from proteins (impurities like salts) (Sanchez *et al.*, 1997; Rabilloud, 2000). IEF is generally accomplished under denaturing conditions using urea and thiourea, reductants and non-ionic or zwitterionic detergents for solubilization of

Introduction

hydrophobic proteins. Highly hydrophobic proteins like integral membrane proteins are often difficult to solubilize and therefore, are rarely detectable on 2D-gels (Görg, 1999). Another problem is that very large proteins will not enter the acrylamide matrix for IEF (Görg *et al.*, 2000; Gershon, 2003).

Separation in the second dimension is performed by standard sodium dodecyl sulfate (SDS)-polyacrylamide gel electrophoresis (PAGE) on large format gels. Several thousand protein spots have been visualized on single 2D-gels (Patton, 2002; Görg *et al.*, 2004). Equilibration with a buffer containing SDS and a reducing agent is necessary to ensure strong negatively charged proteins (Lottspeich *et al.*, 2006).

Since not all proteins in a sample can be visualized on a single gel, different pH gradients in the first dimension and several acrylamide concentrations in the second dimension can be used to visualize as many of the proteins within a sample as possible, thereby multiplying time, costs and number of samples necessary for a comprehensive analysis of the proteome (Görg *et al.*, 2000).

However, 2D-PAGE is a potent protein separation method and an ideal tool to monitor cellular proteome response upon a specific factor as treatment, mutations, invasion etc.

1.3.2 Proteome analysis by 2D-DIGE

2D-DIGE (two-dimensional differential gel electrophoresis) is a technique, which combines very high sensitivity and very stable detection of parameter-induced changes in the protein profile (Minden, 2007). In DIGE technique, three different fluorescent dyes Cy2, Cy3 and Cy5 (CyDyes) are used. The reactive NHS ester group of the CyDyes binds covalently to the ε-amino group of lysine in proteins via an amide linkage.

The main advantages of 2D-DIGE compared to conventional 2D-PAGE are:

1. The ability to run multiple samples on the same gel (multiplexing by different excitation-emission wavelengths);
2. an internal standard (reference) sample which can be run on all gels; and
3. experimental designs unique to this technique (randomized, inverse labeling).

Furthermore, sensitivity and linearity about a wide dynamic range of the CyDye fluorophores provides a much higher accuracy in quantitative analysis than 2D-PAGE (Ünlü *et al.*, 1997; Yan *et al.*, 2001; Alban *et al.*, 2003; Marouga *et al.*, 2005).

Introduction

Probably most critically, this technique substantially reduces the effects of gel-to-gel variation of protein spots. Here, the usage of an internal standard allows a better (co-)detection of spots and distribution is statistical ensured, so false-positive signals can be excluded (Wu *et al.*, 2006). Therefore, the confidence that a difference in fluorescence intensity between two samples is due to biological variation rather than experimental variation has increased (Van den Bergh *et al.*, 2003). A scheme of the single working steps is shown in figure 1.13.

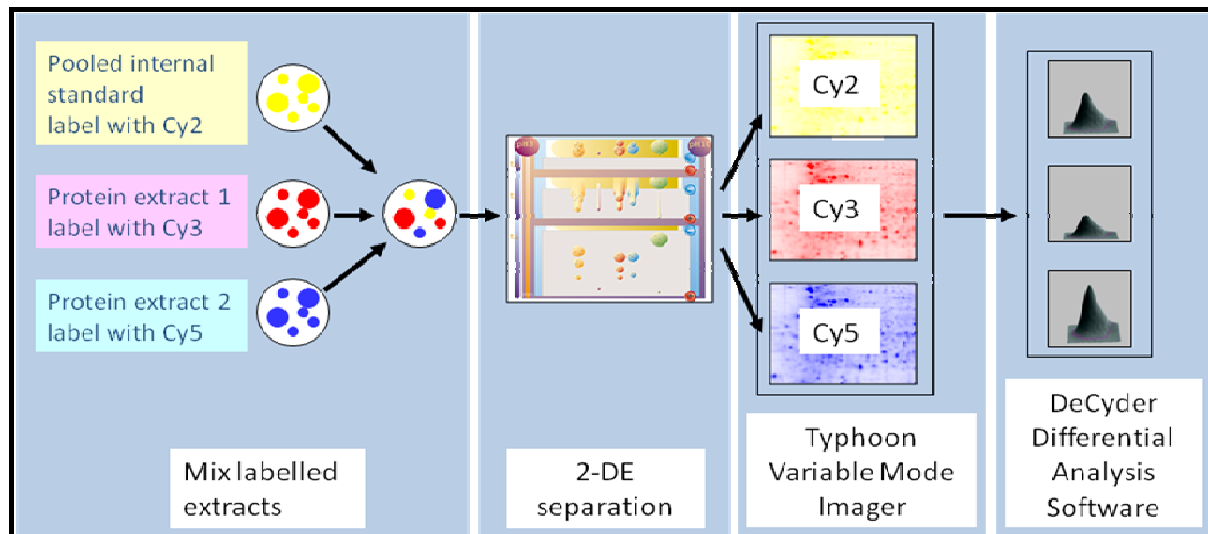


Figure 1.13: Diagram of DIGE workflow of single gel analysis.

The labeled protein samples from two different conditions (protein extracts 1 and 2) and the labeled internal standard are mixed, and separated by 2D-PAGE. Afterwards, images from all three CyDyes are obtained by scanning on a Typhoon imager. Intensity profiling of protein spots from all three samples is performed by DeCyder software analysis (GE Healthcare Bio-Sciences, 2005).

In summary, 2D-DIGE enables the analysis of experiments with different degrees of complexity from a simple control/treated experiment through to a multi-condition analysis, addressing factors such as dose and time, all performed in a single study (Patton, 2002). 2D-PAGE (and even more 2D-DIGE) provides in combination with mass spectrometric techniques a method to detect very narrow regulation events at very low detection limits and monitors protein response to certain internal or external experimental conditions.

1.3.3 Mass spectrometry based protein identification

In 1985, Karas and Hillenkamp discovered the basis for MALDI-MS, that proteins embedded in an appropriate solid organic matrix could be desorbed and ionized with a pulse of ultraviolet laser light (Karas *et al.*, 1985). Such a short pulse (5-10 ns) from a laser (nitrogen at 337 nm or Nd:YAG at 355 nm) is focused on the probe, and causes the desorption and

Introduction

ionization of the analyte molecules. All matrices share the properties of strongly absorbing ultraviolet radiation along with incorporating and isolating analyte molecules within their crystals (Chaurand *et al.*, 1999). The mechanism for MALDI is not completely understood, but it is believed that the ultraviolet radiation is absorbed by the matrix, which promptly vaporizes, carrying the embedded analyte intact into the gas phase, where ionization of analytes occurs by transfer of a proton from an excited matrix molecule (Arnott *et al.*, 1993; Braun and Neusser, 2002).

Proteins are usually identified from gels by in-gel digestions of protein spots and subsequent mass spectrometric analysis of the cleaved peptides (Yates, 1998b; Shevchenko *et al.*, 2006; Granvogl *et al.*, 2007).

In the first stage of analysis, MS scan mode is performed and generates a mass spectrum of the peptides in the sample, the so-called peptide mass fingerprint (Pappin *et al.*, 1993; Yates *et al.*, 1993; Scheler *et al.*, 1998). Since the peptide mass fingerprint is unique for an individual protein, it can be used in combination with protein databases or appropriately annotated DNA databases to identify the protein of interest (Yates, 1998a; Fenyö, 2000; Chamrad *et al.*, 2004). Doubtless protein identification from gel spots can be achieved by different techniques. One of the most frequently used methods today is tandem mass spectrometry-based peptide sequencing to obtain amino acid sequences, at least partially (Cotter *et al.*, 2007). Furthermore, for protein identification the combination of peptide mass fingerprint (PMF) and peptide fragment fingerprint (PFF) eliminates the allocation of data to false-positive identifications.

In case of tandem mass spectrometry (also called MS/MS or MS^2), operations are performed in a second MS stage to access peptide sequence information. In the MS/MS mode only a single, previously selected ion species (from the MS run) is selected to pass and used for further fragmentation reactions. The fragments are further separated and then detected by the ion detector. Since a fragment-series of a peptide differs in mass by a single amino acid, the amino acid sequence can in principle be deduced from the spectrum (peptide sequence tag or peptide fragment fingerprint, PFF) (Hunt *et al.*, 1986; Biemann, 1990; Arnott *et al.*, 1993; Shenar *et al.*, 2009). Several advantages are assured by MS/MS technologies in comparison to classical protein sequencing methods like Edman degradation, which needs higher sample amounts, and shows only a small number of N-terminal amino acids. MALDI mass spectrometry offers the possibility to generate fragment spectra in post source decay (PSD) mode (Hunt *et al.*, 1986; Dancik *et al.*, 1999; Gevaert *et al.*, 2001; Hernandez *et al.*, 2006),

Introduction

but new generation machines are also equipped with a collision induced dissociation (CID) chamber (Shenar *et al.*, 2009). Both methods are suitable for peptide fragment fingerprinting at which CID is preferential for amino acid sidechain fragmentations. In an ideal case the whole sequence from the peptide (or peptides) can be obtained. Thus, sequence information allows cross-species identification of proteins in database searches. Hence, mass spectrometry represents a powerful tool for proteome analyses of species with full sequence information (Hunt *et al.*, 1986; Yates, 1998a; Dancik *et al.*, 1999).

Here a MALDI-ToF/ToF mass spectrometer was used, which consists of a MALDI (matrix assisted laser desorption/ionization) ion source, a CID chamber, an 3 m long, electric field-free drift track for separation and an ion detector (Lottspeich *et al.*, 2006). For tandem MS experiments, a timed-ion-selector allows a very precise selection of single peptide species to enter the second MS stage.

A great advantage of protein analysis by MS methods is the detection of post-translational modifications (PTMs), like protein-phosphorylations. Analysis of protein-phosphorylation is of special importance, because it is a reversible key modification. Protein-phosphorylations occur mainly on serine, threonine and tyrosine residues that can regulate enzymatic activity, subcellular localization, complex formation and degradation of proteins (Kalume *et al.*, 2003; Peters *et al.*, 2004). In signal transduction, phospho-transfer cascades provide fast point-to-point transmission and conditional information transfer mechanisms to integrate internal and external status signals, activate regulatory molecules, and coordinate the progress of diverse asynchronous pathways (McAdams and Shapiro, 2003).

Phospho-peptides can be isolated and fragmented in MS/MS using MALDI or LTQ (linear trap quadrupole) Orbitrap measurement, which both represent latest technologies. Both MS systems provide trace analysis with high accuracy, needed for the detection and analysis of PTMs (Olsen *et al.*, 2005; Macek *et al.*, 2006; Yates *et al.*, 2006; Olsen *et al.*, 2007).

The LTQ-Orbitrap mass spectrometer is a hybrid system combining the LTQ linear ion trap mass spectrometer and the Orbitrap mass analyzer. Ions are generated in the atmospheric pressure ionization (API) ion source are trapped in the LTQ, where the ions are analyzed using the MS and MS^n scan modes. Then, the ions are axially ejected from the LTQ and collected in a C-shaped ion trap (C-trap) from which they are passed into the Orbitrap mass analyzer. The ions transferred from the C-Trap are captured by rapidly increasing the voltage on the center electrode of the Orbitrap (Olsen *et al.*, 2005). The trapped ions assume circular

Introduction

trajectories around the center electrode and their axial oscillations, along the center electrode, are detected. LTQ-Orbitrap MS was coupled to a TriVersa NanoMate microfluidics chip, which allows sample inlet miniaturization. This microchip-based technology combines the strengths of liquid chromatography, mass spectrometry, fraction collection, and chip-based infusion in one integrated system. It allows to obtain more information from complex samples than with LC/MS alone (Pereira-Medrano *et al.*, 2007). This microfluidics chip contains an array of nanoelectrospray nozzles, etched in a silicon wafer. The unique field strength created by the nanoelectrospray nozzles allows for a more efficient and stable spray with flow rates of 20 to 300 nL/min.

The system works with a very high resolving power (up to 200000), a high dynamic range (around 5000) and a very high mass accuracy (1–2 ppm) (Olsen *et al.*, 2005; Makarov *et al.*, 2006). The mass spectrometer provides high accuracy mass information of biomolecules as peptides, which is necessary for an absolutely certain analysis of potential post-translational modifications.

Introduction

1.4 Metabolite analysis by HPLC-MS

Extraction and isolation of interesting molecules from bacterial cultures is the initial stage for analyzing natural products. Most myxobacterial secondary metabolites are excreted into the medium, which allows direct access to secondary product formation. For instance, the addition of the adsorber resin XAD-16 to a myxobacterial culture allows the take-off of secondary metabolites and increases their production by shifting of the concentration balance (Gerth *et al.*, 1996). The resin binds hydrophobic compounds, and thus feedback inhibition can be prevented. This results in continuous production and accumulation of the excreted metabolites (Gerth *et al.*, 1995; Lau *et al.*, 2002).

After cultivation, XAD-16 resins are extracted and resolved as concentrated culture extracts. Finally, the samples are analyzed by HPLC-MS (Silakowski *et al.*, 2001a; Simunovic *et al.*, 2006). This system provides a good combination of analysis speed, resolution and sensitivity. The used high capacity ion trap (HCT) mass spectrometer is equipped with an electrospray ionization (ESI) ion source, which is ideal to be coupled to HPLC systems. For quantitative profiling of the single secondary metabolite families, the substances are identified via MS/MS by their characteristic fragmentation pattern. By this semi-quantitative method, production rate can be compared.

Introduction

1.5 Protein-DNA interactions (DNA pull-down assay)

Environmental and cellular changes require sophisticated responses, realized by altering gene transcription patterns. The control over gene expression is mediated by variations of DNA interaction proteins (Drewett *et al.*, 2001). A special interest in microbial research is the identification of transcriptional regulators, including the finding of the target-sequence(s) and a deeper understanding of the cellular regulatory processes (Nilsson *et al.*, 2000).

For the analysis of proteins, binding to promoter regions of interest, short immobilized DNA fragments which contain the promoter sequence are incubated with proteome samples from different cultivation conditions. The principle of DNA pull-down-assays is illustrated in figure 1.14. This method allows the capturing of proteins which were functionally active in the regulation of transcription (Nilsson *et al.*, 2000; Drewett *et al.*, 2001; Jeong *et al.*, 2004).

Introduction

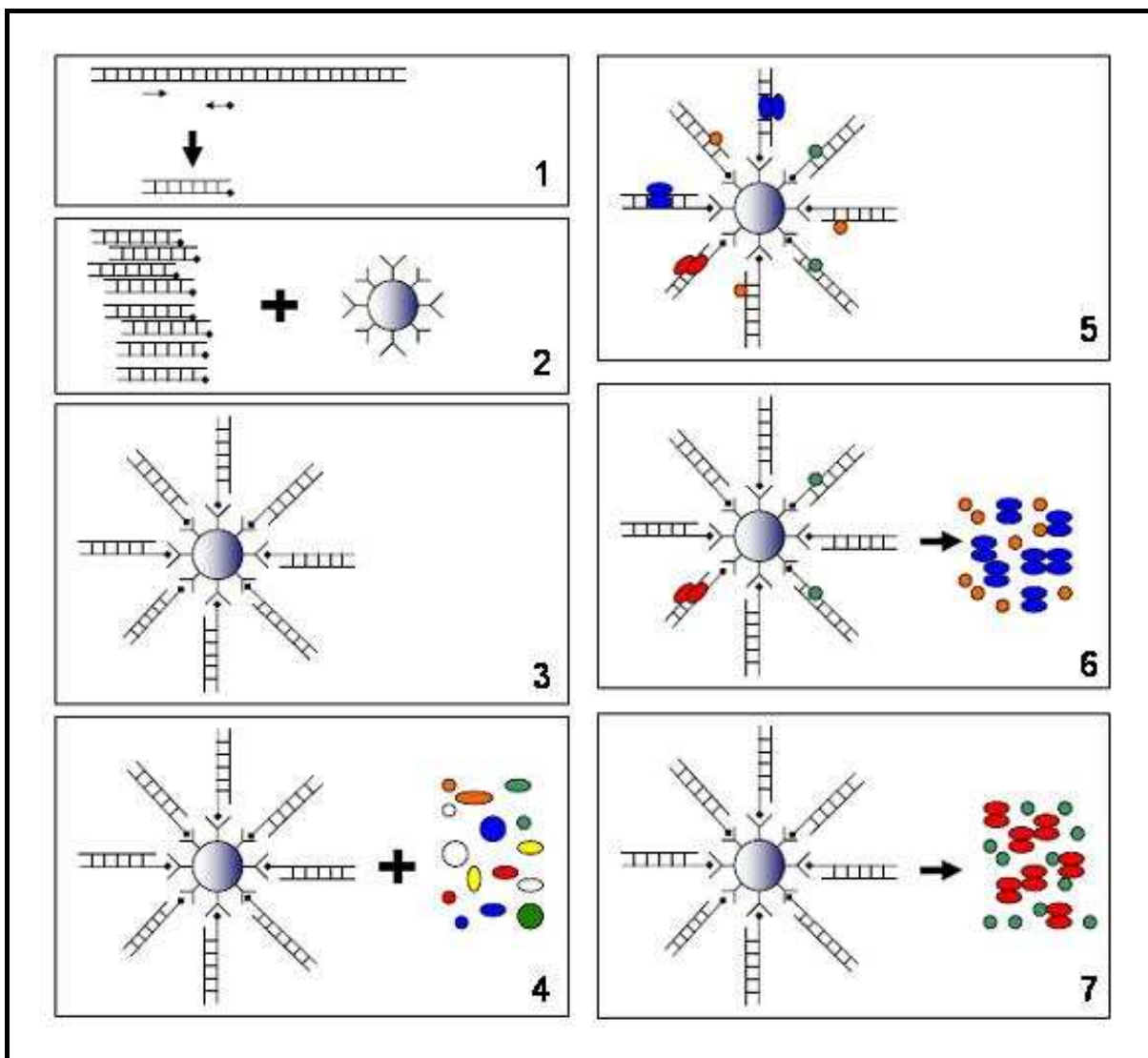


Figure 1.14: Workflow of DNA pull-down (promoter ligand-fishing) experiments.

1: Genomic DNA sequences are amplified by PCR, spanning the promoter region of the target gene, primer positions are marked by small black arrows. One primer contains a biotinylated 3'end (marked by a black diamond). 2-3: DNA is loaded to paramagnetic Streptavidin beads by biotin-tag. 4-5: DNA-loaded beads are incubated with protein extracts to load sequence-specific proteins to DNA promoter regions. 6-7: Elution of interacting proteins with increasing ionic strength; 6: Washing, 7: Proteins are eluted with high stringency, precipitated, redissolved and further analyzed by SDS-PAGE and MALDI-ToF/ToF MS.

1.6 Target-oriented gene inactivation by homologous recombination

In order to investigate the cellular role of interesting proteins, single or double crossover inactivation mutants of the corresponding genes are effective ways to get further information of protein functions. Therefore, plasmid DNA of integrative vectors, containing a gene fragment is transferred into cells. This strategy is used regularly in myxobacterial gene inactivation studies (Simunovic *et al.*, 2006; Bode *et al.*, 2006a; Meiser *et al.*, 2008; Bode *et al.*, 2009). Once the plasmid DNA is introduced into the cells, in some the DNA is inserted via homologous recombination into the chromosomal DNA, thereby switching-off the gene to non-functionality.

Gene targeting by insertion of plasmids is made possible by the high frequency of homologous recombination in *M. xanthus* (Wenzel *et al.*, 2005a; Bode *et al.*, 2006a). The mechanism of plasmid integration is found to be very similar to the well-investigated recombination/proliferation mechanism of integrative plasmids in *Streptomyces* (Hardy, 1993).

a) Gene inactivation by double crossover

The ability to delete DNA sequences in-frame from the *Myxococcus xanthus* genome, by way of the host's natural homologous recombination pathways, has started up by the detection of suitable counter-selection markers that work efficiently in different wild-type strains (Wu and Kaiser, 1996). Counter-selection markers allow for the positive selection of strains that have lost the marker and other unwanted sequences around them. In-frame deletions in *M. xanthus* are constructed by a plasmid integration-excision strategy, shown in figure 1.15. Such plasmids contain two PCR fragments (polymerase chain reaction), which are made by amplification of the genomic regions up- and down-stream from the target gene in *M. xanthus* (figure 1.15 A, shown in red and green).

Introduction

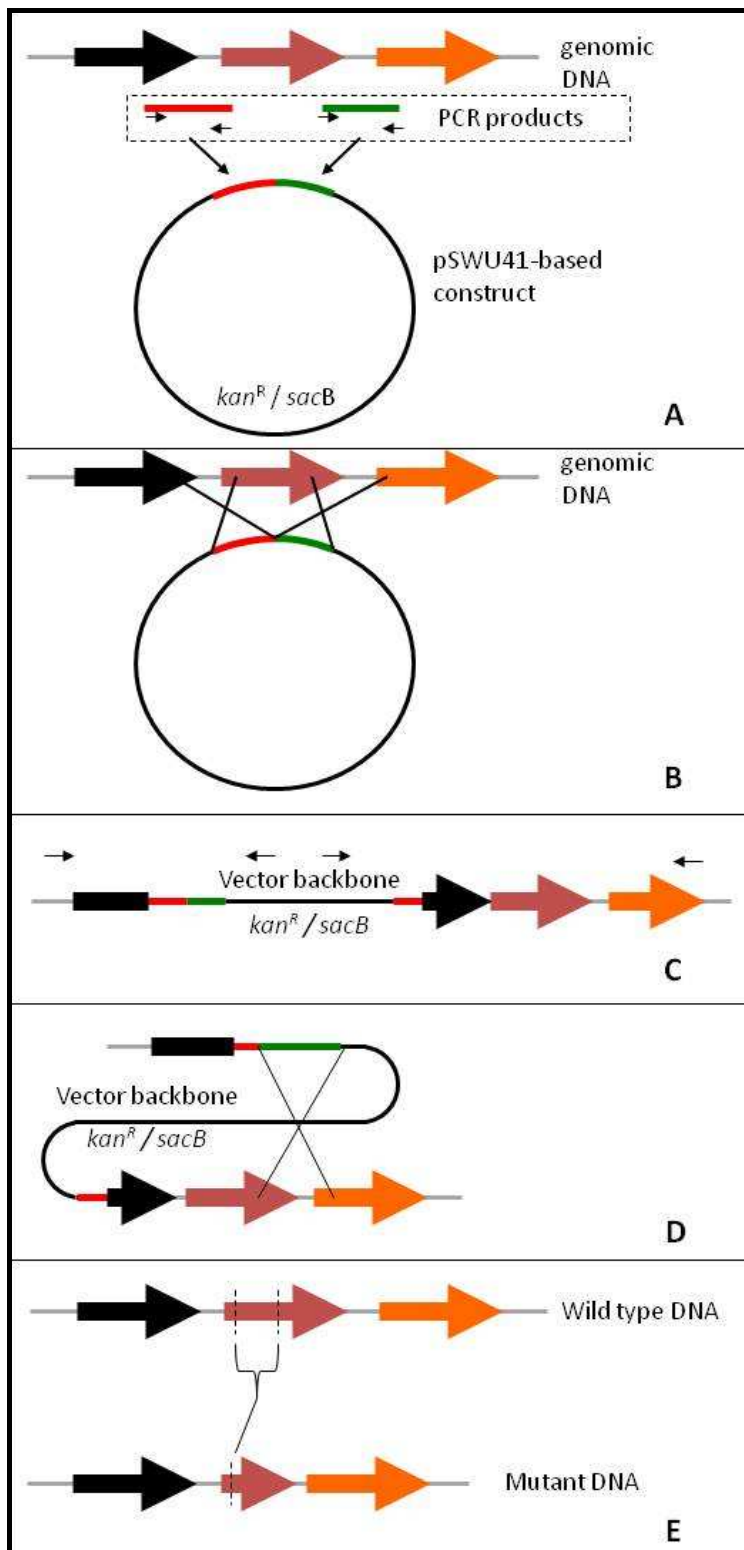


Figure 1.15: Diagram of in-frame gene deletion by double crossover.

Primer positions from PCRs are indicated by small black arrows. **A)** Vector generation for in-frame deletion: The first PCR (red) covers the start of the target gene (purple), while the second PCR (green) covers the end-sequence of the target gene. Both PCR products are combined in a digested deletion vector (here: pSWU41). **B)** First crossover by homologue recombination between homologue sequences of the black gene and first PCR fragment (red). **C)** Genomic integration of plasmid DNA: Mutants show resistance for selection marker (here: kanamycin resistance kan^R) and sensitivity to counterselection marker (here: sucrose sensitivity sacB). **D)** Induction of the second crossover: After growth for several days in exponential phase, deletion can be induced by sucrose: second crossover between homologue regions (second PCR fragment (green) and its genomic template). **E)** The

Introduction

exchange of the gene cassette after counter selection can result in truncated, inactive version of the target gene (or revert back to wild type form). The loss of the core region can be confirmed by PCR.

In-frame inactivation required the careful selection of PCR primer positions. Each PCR-product is cloned into a vector and replicated into *E. coli*. Both plasmid-derivates are extracted and purified, followed by excision using the introduced restriction sites. The purified digestion products are cloned together into a selection/counterselection vector, digested with the respective restriction endonucleases (figure 1.15 A). After replication and extraction, the purified plasmid is confirmed by hydrolysis using restriction endonucleases and by DNA-sequencing. The confirmed construct is introduced in *M. xanthus* (figure 1.15 B), resulting in a first crossover mutant, (figure 1.15 C) which leads to antibiotic-resistant clones (as here for e.g. kanamycin as selection marker). Plasmid integration into genome of *M. xanthus* can be confirmed by PCRs (primer positions can be found in figure 1.15 C, shown by the black arrows). At this, one primer harbors in the vector backbone, while the other is localized in the amplified regions, so that a signal for PCR can only be obtained upon integration at the expected position. The confirmed first crossover mutants of *M. xanthus* are then kept in exponential growth phase for several days without antibiotic, followed by plating with counter-selection marker (here: plasmid-coded *sacB* cassette, coding levansucrase which converts sucrose into a toxic levanpolymer) to introduce the second crossover (figure 1.15 D). The second crossover then occurs between homologue regions from genome and PCR fragment.

The second crossover can result in revertants (mutation back to original wild type sequence) or real in-frame deletion mutants, which miss the core region of the target gene (both kanamycin sensitive and sucrose resistant). The truncated form of the gene will not be active, but sequences in the same operon are unaffected. The two genotypes will give a very different signal by the examination via PCR (primer positions can be found in figure 1.15 E, shown by the small arrows).

b) Gene inactivation by single crossover

Plasmid constructs for single crossover gene disruption carrying a PCR fragment from the core of the targeted gene and integrate in the associated sequence. When the gene fragment in the plasmid and the chromosomal copy undergo homologous recombination, it results in two non-functional copies of the gene separated by the vector DNA. One copy is missing

Introduction

sequences upstream, while the other is missing sequences downstream (Alberts *et al.*, 2002). A diagram for the single crossover gene disruption is illustrated in figure 1.16.

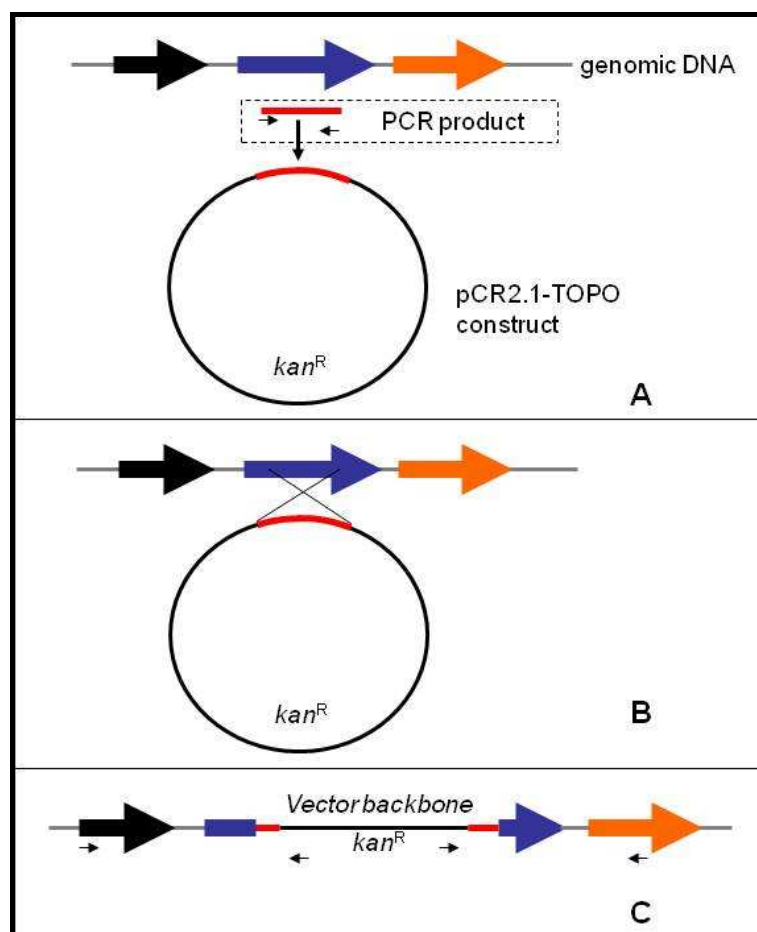


Figure 1.16: Gene disruption in *M. xanthus* by homologous recombination via single crossover.

Primer positions from PCRs are indicated by small black arrows. **A)** In order to disrupt the target gene (in blue) an internal fragment (red) of the gene lacking its transcriptional start and end sequence is cloned into an integrative vector. **B)** The plasmid can integrate via homologue recombination to disrupt the chromosomal gene. Disruption mutants are isolated using the selection marker (here: kanamycin resistance kan^R). **C)** Finally, vector integration is confirmed by PCR, spanning both incomplete copies of the gene. Further explanations to the method can be found in (Alberts *et al.*, 2002).

Clones, which have integrated the plasmid into the chromosome, can easily be isolated by antibiotic selection, using the plasmid-coded antibiotic resistance selection marker. The position of plasmid-integration in the chromosome can be confirmed by PCR.

Plasmids with homologue gene sections with less than 500 bp may be difficult to incorporate by recombination into the *M. xanthus* chromosome. For such small gene fragments (< 500 bp) it was ensured to generate inactive copies of the gene by the insertion of an additional stop-codon.

1.7 Goal of this study

Many secondary metabolite gene clusters in *Myxococcus xanthus* DK1622 are still of unknown function. Under stress conditions, a bioactive substance may provide an additional advantage to overcome a stress-inducing environment. Thus, iron limitation might be a potential strategy to awake silent gene clusters.

Because no information is currently available as how myxobacteria handle iron-limitation, the effects of iron response on secondary metabolism of the strain *M. xanthus* were evaluated. In this study, a multi-disciplinary approach was used, including proteomics, secondary metabolomics, and molecular biology (gene inactivation and protein-DNA interaction studies) also to investigate the role of those gene clusters. Hence, insight into regulation of primary and secondary *M. xanthus* metabolism could be obtained by using these techniques.

In myxobacteria, as exemplified by the model strain *M. xanthus* DK1622, the response to different environmental stress conditions, as for e.g. iron starvation, is predicted to alter growth, iron uptake, and expression of PKS-NRPS gene-clusters and subsequently the production rates of secondary metabolites. This approach may lead to the detection of new structures, derived by the orphan PKS or NRPS gene clusters without an assigned product or give an insight into the cellular response and regulatory processes of *M. xanthus* during iron starvation.

To address the question directly, how myxobacteria regulate iron-limitation, the cellular response of *M. xanthus* DK1622 to low iron conditions was investigated, using a combined bioinformatics/proteomics/metabolomics/promoter-interaction approach, coupled with gene inactivation.

Introduction

Material and Methods

2. Material and Methodology

2.1 Chemicals

The chemicals, which were used in this work, can be found in table 2.1. All chemicals were stored, as described in the data sheets.

Table 2.1: Chemicals and manufacturers

If a manufacturer is not located in Germany, it is specified.

Chemical	Manufacturer	Location
Acetone	Acros	Geel, Belgium
Agarose LE	Biozym	Oldendorf
Bacto-agar		
Casitone		
Trypton		
Yeast extract	Difco	Augsburg
Dimethylsulfoxide (DMSO)	Fischer Chemicals	Zürich, Switzerland
N,N-Dimethylformamide (DMF)	Fluka	Seelze
IPG-strip cover fluid	GE Healthcare Bio-Sciences	
Pharmalyte pH3-10		München
Potassium hydroxide	Grüssing GmbH	Filsum
Phosphate buffer saline (PBS)	Invitrogen	Karlsruhe
2,5-Dihydroxybenzoic acid (DHB)		
Ammonium acetate		
Coomassie Brilliant Blue G-250		
Ferrospectral (ferrozine)		
Ferrous chloride (FeCl_2)		
Hydroxylammonium chloride (HAC)		
Sodium perchlorate		
Trifluoroacetic acid (TFA)		
α -Cyano-4-hydroxycinnamic acid (CCA)	Merck KGaA	Darmstadt
(<i>R,R</i>)-Dithiothreitol (DTT)	MP Biomedicals	Illkirch, France
5-Bromo-4-chloro-3-indolyl-beta-D-galactoside (x-Gal)	M.P.I. international	Lansing, MI, USA
Ammonium sulfate		
Glycerol	Riedel de Haen	Seelze
Amberlite ® XAD 16	Rohm & Haas	Frankfurt
ortho-Phosphoric acid		
2-Amino-2-(hydroxymethyl)-1,3-propanediol (Tris)		
Boric acid		
Ethidium bromide		
Glycine		
<i>N,N,N',N'</i> -Tetramethylethylenediamine (TEMED)		
ROTLphorese Gel 30 (Acrylamide solution T:30.8, C: 1)		
Sodium acetate		
Sodium dodecylsulfate (SDS)		
Sodium hydroxide		
Sucrose	Carl Roth	Karlsruhe

Material and Methods

Chemical	Manufacturer	Location
Ammonium bicarbonate		
1-propanesulfonate (CHAPS)		
3-[(3-Cholamidopropyl)dimethylammonio]-ammonium hydrogenphosphate		
Ammonium hydrogenphosphate		
Ammonium persulfate		
Bromophenol blue		
Ethylene diamine tetraacetic acid (EDTA)		
Iodo acetamide		
L-Lysine		
Manganese dichloride		
Thiourea		
Urea		
Xylencyanole FF	Sigma Aldrich	Seelze
Acetic acid		
Acetonitrile (AcCN)		
Chloroform		
Dipotassium hydrogensulfate		
Ethanol		
Hydrochloric acid (HCl)		
Isopropanol		
Methanol		
Potassium dihydrogensulfate		
Sodium chloride	VWR	Darmstadt

Material and Methods

2.2 Commercial 'kits', enzymes and markers

The used 'kits' or enzymes and the respective manufacturers can be found in table 2.2. All used 'kits' or enzymes were deployed or stored, as described in the instruction.

Table 2.2: Commercial 'kits', enzymes and markers.

If a manufacturer is not located in Germany, it is specified.

Commercial 'kits', consumables, enzymes and Markers	Manufacturer	Location
4700 Calibration mixture	Applied Biosystems	Darmstadt
Bradford dye concentrate	Biorad	
CHELEX 100 resin		München
100bp Ladder		
100bp Ladder Plus		
1kb Ladder		
dNTPs		
Protein Ladder Page Ruler		
Restriction enzymes and corresponding buffers		
T4 DNA Ligase	Fermentas	St. Leon-Rot
Taq polymerase (+ buffers)	Finnzymes	Espoo, Finnland
CyDye DIGE FLUOR Cy2		
CyDye DIGE FLUOR Cy3		
CyDye DIGE FLUOR Cy5		
IPG-strips, pH 4-7	GE Healthcare Bio-Sciences	München
IPG-strips, pH 3-11 NL		
pCR®2.1 TOPO cloning Kit	Invitrogen	Karlsruhe
NucleoSpin® Extract II, MN kit	Macherey Nagel	Düren
pH Indicator sticks 5-10	Merck KGaA	Darmstadt
C ₁₈ ZipTip	Millipore	Bad Soden
Sterilization filters, 0.2 µm pore size	Nalgene	Neerijse, Belgium
Protein Ladder		
Trypsin, sequencing grade	Promega	Mannheim
Folded filters, 150 mm diameter		
Proteinase K		
Ribonuclease A (RNase)	Carl Roth	Karlsruhe
Bovine serum albumin (BSA)		
Serdolite particles		
β-Casein (bovine)	Sigma Aldrich	Seelze

2.3 Buffers and solutions

All solutions and buffers were prepared in ultrapure water (H_2O), which was pretreated by a MilliQ-ion exchange PURELAB ultra device. If necessary, water or buffers were sterilized for 20 min at 121°C (Autoclave V150). If a buffer or solution must not be autoclaved, but sterilized, this was realized by sterile filtration (pore size 0.2 μM).

The compositions and storage conditions of used buffers and solutions can be found in the following tables (table 2.3-2.6). All pH-values were estimated by a digital pH-Meter 766 Calimatic.

2.3.1 Antibiotic solution

To generate selection pressure to cells, which contain pCR®2.1-TOPO- or pSWU41-based vectors, the antibiotic kanamycin sulfate (kanamycin) was prepared in sterile H_2O (50 mg/ml). This stock solution was sterile filtrated, aliquoted and stored at – 20 °C. In media, the stock solution was diluted to a final concentration of 40 $\mu g/ml$.

2.3.2 Buffers and solutions for 2D-gel electrophoresis

The used buffers and solutions for 2D-gel electrophoresis and their compositions can be found in table 2.3. All urea- or thiourea-containing solutions prepared with sterile H_2O , followed by an incubation step with Serdolit ion exchange resin, following the manufacturers protocol. The solutions were cleared, using a folded filter and stored in sterile containers at – 20 °C.

Table 2.3: Buffers and solutions for 2D-gel electrophoresis.

Tris stock and SDS stock were autoclaved, DIGE STOP solution (in DIGE label buffer) was sterile filtrated

Appellation	Composition	Storage
Precipitation solution	90 % (v/v) acetone 10 % (v/v) methanol	- 80 °C
DIGE lysis buffer	7 M Urea 2 M Thiourea 4 % CHAPS 2 % DTT* 2 % v/v Pharmalyte 3-10 (0,5 % w/v)*	- 20 °C
DIGE labeling buffer	7 M Urea 2 M Thiourea 4 % CHAPS 30 mM Tris (pH 8.8)	- 20 °C

Material and Methods

Appellation	Composition	Storage
Rehydration buffer	8 M Urea 1 % CHAPS 0,002 % BPB 0.5 % DTT* 0.5 % v/v Pharmalyte 3-10 (0,5 % w/v)*	- 20 °C
Equilibration basis buffer	6 M Urea 2 % SDS 50 mM Tris (pH 8.8) 20 % Glycerol	- 20 °C
Equilibration buffer 1*	100 mg DTT per 10 ml Equilibration basis buffer*	-
Equilibration buffer 2*	250 mg IAA per 10 ml Equilibration basis buffer*	-
Homogeneous gel solution (12.5% T)	209 ml ROTIphorese Acrylamide solution 30.8% T 125 ml 1.5 M Tris stock solution pH 8.8 160 ml H ₂ O 5 ml 10 % SDS stock solution 2 ml 10 % APS solution** 70 µl TEMED	-
Tris stock solution	1.5 M Tris pH 8.8, adjusted with 4 M HCl	4 °C
DIGE STOP solution	10 mM L-lysine	- 20 °C
10% SDS stock solution	10 % (w/v) SDS	RT
10% APS solution**	10 % (w/v) APS	-
10xRunning buffer	1 % SDS 0.248 M Tris 1.918 M Glycine pH 8.8, adjusted with 1 M HCl	RT

*: added freshly

**: prepared freshly

2.3.3 Buffers and solutions MALDI mass spectrometry

The used buffers and solutions for mass spectrometry and their compositions can be found in table 2.4. All solutions are prepared freshly (beside the digestion buffer), only using chemicals of highest quality standard.

Material and Methods

Table 2.4: Buffers and solutions for mass spectrometry

Appellation	Composition	Storage
Ammonium bicarbonate buffer	40 mM Ammonium bicarbonate	-
Digestion buffer	40 mM Ammonium bicarbonate 5 ng/ μ l Trypsin, sequencing grade	- 20 °C
MS solution 1	0.1 % TFA in H ₂ O	-
MS solution 2	50/50 H ₂ O/AcCN	-
MS solution 3	50/50 H ₂ O/AcCN + 0.1 % TFA	-
CCA	5 mg/ml CCA in (50/50) H ₂ O/AcCN + 0.1 % TFA	-
DHB	2 mg/ml in DHB (50/50) H ₂ O/AcCN + 0.5 % phosphoric acid	-
Recrystallization solution	10 mM Ammonium hydrogenphosphate	-
Orbitrap Spray solution	50/50 H ₂ O/AcCN + 0.5 % acetic acid	-

2.3.4 Buffers and solutions for DNA pull-down assay

The used buffers and solutions for the protein-DNA interaction studies (DNA pull down assay) and their compositions can be found in table 2.5.

Table 2.5: Buffers and solutions for protein-DNA interaction studies (DNA pull-down assay)

Appellation	Composition	Storage
Cell wash buffer	10 mM Tris, pH 7.5 1 mM EDTA 40 mM NaCl	RT
Appellation	Composition	Storage
Cell lysis buffer	10 mM Tris, pH 7.5 1 mM EDTA 100 mM NaCl 1 mM DTT* 1x Complete protease Inhibitor cocktail* 0.05 % Triton-X 100	RT
DNA binding buffer	10 mM Tris, pH 7.5 100 mM NaCl 5 % Glycerol 0.05 % Triton-X 100 1 mM DTT* 2.5 mM FeCl ₂ ** 1x Complete protease Inhibitor cocktail* 10 μ g competitor DNA / mg Streptavidin beads*	RT

Material and Methods

Appellation	Composition	Storage
DNA wash buffer I	10 mM Tris, pH 7.5 100 mM NaCl 5 % Glycerol 0.05 % Triton-X 100 1 mM DTT* 2.5 mM FeCl ₂ ** 1x Complete protease Inhibitor cocktail* 10 µg/ml salmon sperm*	RT
DNA wash buffer II	10 mM Tris, pH 7.5 250 mM NaCl 5 % Glycerol 0.05 % Triton-X 100 1 mM DTT* 2.5 mM FeCl ₂ ** 1x Complete protease Inhibitor cocktail* 10 µg/ml salmon sperm*	RT
Elution buffer	10 mM Tris, pH 7.5 1000 mM NaCl 5 % Glycerol 0.05 % Triton-X 100 1 mM DTT* 2.5 mM FeCl ₂ ** 1x Complete protease Inhibitor cocktail* 10 µg/ml salmon sperm*	RT
SDS sample buffer	60 mM Tris (pH 6.8) 2 % SDS 5 % Glycerol 0.1 % (w/v) DTT 0.01 % (w/v) BPB	

*: added freshly

**: prepared freshly

Material and Methods

2.3.5 Buffers and solutions for biomolecular work

The used buffers and solutions for biomolecular work and whose compositions can be found in table 2.6.

Table 2.6: Buffers and solutions for biomolecular work

Appellation	Composition	Storage
STE-buffer (pH 7,5):	75 mM NaCl 25 mM EDTA 20 mM Tris	RT
TE-buffer (pH 8):	10 mM Tris 1 mM EDTA	RT
Cell suspension buffer (P1)	50 mM Tris-HCl, pH 8,0 10 mM EDTA 100 µg/ml RNase A	4 °C
Lysis buffer (P2)	200 mM NaOH 1 % SDS	RT
Neutralization buffer (P3)	3 M Potassium acetate, pH 5,5 pH adjusted with acetic acid	RT
dNTP solution	1.25 mM per dNTP	- 20 °C

Material and Methods

2.4 Equipment and instrumentation

The equipment used and the respective manufacturer can be found in table 2.7.

Table 2.7: Equipment and materials

If a manufacturer is not located in Germany, it is specified.

Equipment and materials	Manufacturer	Location
TriVersa NanoMate chip	Advion	NY, USA
HPLC series 1100	Agilent	Böblingen
MALDI 4800 ToF/ToF mass analyzer		
MALDI insert 384er sample plate	Applied Biosystems	Darmstadt
Centrifuge Avanti® J-E		
Rotor JA-14	Beckman Coulter	Krefeld
Microbiological incubator Serie BF	Binder	Tuttlingen
Power supply Standard PowerPack P25	Biometra	Göttingen
Agarose gel electrophoresis equipment		
Electroporation cuvettes, 0.1 cm		
Electroporator GenePulser Xcell		
SDS gel electrophoresis	Biorad	München
Photodocumentation of agarose gels Syngene	Biostep GmbH	Jahnsdorf
Microplate Reader EL 808	Bio-TEK instruments	Bad Friedrichshall
ESI ion trap MS HCT plus	Brucker Daltonics	Bremen
Rotary evaporator heating bath B-490		
Rotary evaporator Rotavapor R-200		
Rotary evaporator Vacuum controller V-800	Büchi	Essen
PURELAB lab water	Elga LabWater	Celle
Ultrasonic disintegrator USD 30	Emich Ultraschall	Berlin
Biophotometer		
Centrifugal evaporator Concentrator 5301 (SpeedVac) F-45-48-11		
Ausschwingrotor A-2-VC		
Centrifuge 5810R		
Rotor A-4-81		
MTP incubator MixMate		
PCR Mastercycler Gradient		
Thermomixer Comfort	Eppendorf	Wesseling-Berzdorf
2D-gel electrophoresis equipment		
Ettan DALTwelve		
ETTAN Spot picking robot		
Gel densitometer		
IPGphor	GE Healthcare Bio-Sciences	München
Typhoon 9410 Laser scanner		
Table shaker Unimax 2010		
Tumble shaker Polymax 1040	Heidolph Instruments	Schwabach
Centrifuge Biofuge fresco	Heraeus	Hanau
Incubator Multitron and Multitron 2	Infors	Einsbach
Sterile bench HERAsafe	Kendro	Langenselbold
pH electrode Pt 1000-Einstabmeßkette SE 100		
pH Meter 766 Calimatic	Knick	Egelsbach
HPLC column Nucleodur C18 gravity 125 x 2 mm, 3µ particle size	Macherey Nagel	Düren

Material and Methods

Equipment and materials	Manufacturer	Location
Ultrasonic bath Bandelin Sonorex	Schalltec	Mörfelden-Walldorf
Power supply Consent E835	Sigma Aldrich	Seelze
Autoclave V150	Systec GmbH	Wettenberg
LTQ-Orbitrap	Thermo Finnigan	Oberhausen
Diaphragm Vacuum pump CVC2	Vacuubrand	Wertheim
UV table Chroma43	Vetter GmbH	Wiesloch

Material and Methods

2.5 Bioinformatic tools and analysis

The software tools used and databases for *in silico* analysis and storage of DNA and protein information and sequences are listed below.

A bioinformatic screening for the presence of conserved Fur boxes in the genome of *M. xanthus* DK1622 was performed by the software tool Virtual Footprint version 3.0, hosted by the technical university of Braunschweig (<http://prodoric.tu-bs.de/vfp>) (Münch *et al.*, 2005; Klein *et al.*, 2008). The used parameters were set to: Bacterial Regulon Analysis; Position weight matrix (PWM): Fur *P. aeruginosa* (ATCC 15692/PAO1); Sensitivity-Threshold: 0.8; Core Sensitivity/Size: 0.75/6; Promoter Length (Maximum Distance to Gene): 300 bp. Hits with a PWM score higher than 9.9 were manually checked for the distance to the putative Shine-Dalgarno sequence and gene start site. If necessary, the original start sites (Goldman *et al.*, 2006) were re-annotated using protein BLAST (NCBI) (Altschul *et al.*, 1990; Altschul *et al.*, 1997) and FramePlot (<http://nocardia.nih.go.jp/fp4/>) (Ishikawa and Hotta, 1999), as well as for overall genomic context. Subsequent, these hits were used to derive a Fur box consensus sequence as sequence-logo representation (Schneider and Stephens, 1990) using WebLogo (<http://weblogo.berkeley.edu/logo.cgi>).

The putative promoter regions of all genes whose expression was found in proteomics to be altered by iron restriction, were then analyzed using ClustalW2 (<http://www.ebi.ac.uk/Tools/clustalw2/index.html>) for the presence of putative Fur boxes (Chenna *et al.*, 2003). Therefore, the derived Fur box consensus was compared to promoter regions (200 bp 5' to the translational start site and 50 bp 3' of the start site, to control for misannotations). Fur boxes were identified by the position-specific presence of at least 8 members of the consensus sequence.

Protein BLAST (NCBI) was routinely used to determine the putative functions of hypothetical proteins (Altschul *et al.*, 1990; Altschul *et al.*, 1997). Multiple sequence alignment was carried out using the ClustalW2 server for the detection of conserved residues (Thompson *et al.*, 1994; Chenna *et al.*, 2003).

For storage of DNA and protein sequences and information the VectorNTI (InforMax, USA) software package was used.

The 2D-DIGE images were analyzed by the DeCyder software 6.5 (GE Healthcare Life Sciences), including the difference-in gel analysis (DIA) and the biological variation analysis (BVA) modules.

The analysis of visibly-stained gels was accomplished by ImageMaster 2D Platinum 7.0 (GE Healthcare Life Sciences).

Material and Methods

MALDI-MS or -MS/MS measurement and spectra interpretation was performed by the 4000 series explorer and the DeNovo Explorer software (both Applied Biosystems).

The identification of proteins based on mass spectrometric analysis and was performed by MASCOT (Matrix Science). The complete *M. xanthus* protein database (FASTA format) can be obtained from ExPasy (<http://www.expasy.org/sprot/hamap/MYXXD.html>).

For verification of digest efficiencies and prediction of fragmentation of phosphor-peptides the two bioinformatics tools PeptideMass (<http://www.expasy.org/tools/peptide-mass.html>) and ProteinProspector (<http://prospector.ucsf.edu/>) were applied.

Material and Methods

2.6 Bacterial strains

2.6.1 The strain *M. xanthus* DK1622

The used *M. xanthus* DK1622 wild type strain and the mutant strains, generated in this work, can be found in table 2.8.

Table 2.8: Description of the used myxobacteria, wild type and generated mutants

Strain	Description	Reference
<i>M. xanthus</i> DK1622	Natural producer of Cittilins, DKXanthenes, Myxalamides, Myxochelins, Myxochromides and Myxovirescins Ampicilline resistant	(Kaiser, 1979)

Mutant strains	Mutagenesis	Description
MXAN_KO1044	Insertion of pKO_0144 in <i>M. xanthus</i> DK1622	MXAN_0144::pKO_0144
MXAN_KO1562	Insertion of pKO_1562 in <i>M. xanthus</i> DK1622	MXAN_1562::pKO_1562
MXAN_KO1808	Insertion of pKO_1808 in <i>M. xanthus</i> DK1622	MXAN_1808::pKO_1808
MXAN_KO1864	Insertion of pKO_1864 in <i>M. xanthus</i> DK1622	MXAN_1864::pKO_1864
MXAN_KO1893	Insertion of pKO_1893 in <i>M. xanthus</i> DK1622	MXAN_1893::pKO_1893
MXAN_KO1988	Insertion of pKO_1988 in <i>M. xanthus</i> DK1622	MXAN_1988::pKO_1988
MXAN_KO2440	Insertion of pKO_2440 in <i>M. xanthus</i> DK1622	MXAN_2440::pKO_2440
MXAN_KO3203	Insertion of pKO_3203 in <i>M. xanthus</i> DK1622	MXAN_3203::pKO_3203
MXAN_KO4189	Insertion of pKO_4189 in <i>M. xanthus</i> DK1622	MXAN_4189::pKO_4189
MXAN_KO4535	Insertion of pKO_4535 in <i>M. xanthus</i> DK1622	MXAN_4535::pKO_4535
MXAN_KO5055	Insertion of pKO_5055 in <i>M. xanthus</i> DK1622	MXAN_5055::pKO_5055
MXAN_KO5484	Insertion of pKO_5484 in <i>M. xanthus</i> DK1622	MXAN_5484::pKO_5484
MXAN_DEL3702_1CO	Insertion of pDEL3702 in <i>M. xanthus</i> DK1622	MXAN_3702::pDEL3702
MXAN_DEL6967_1CO	Insertion of pDEL6967 in <i>M. xanthus</i> DK1622	MXAN_6967::pDEL6967
MXAN_DEL6967	Markerless mutant, missing 324 bp of MXAN_6967 after elimination of the inserted vector from MXAN_D6967_1CO („double crossover“-mutant)	MXAN_6967, missing 324 bp (from 447 bases in the wild type, the nucleotides 79 to 403 were removed)

2.6.2 The strain *E. coli* DH10B

The description of the used *E. coli* strain DH10B can be found in table 2.9. The generated mutant strains were used for plasmid proliferation. After extraction, plasmids are controlled and subsequently used for plasmid insertion in *M. xanthus* DK1622.

Table 2.9: Description and reference to *E. coli* DH10B

Strain	Description	Reference
<i>E. coli</i> DH10B	F-mcrA Δ(mrr-hdsRMS-mcrBC) φ80dlacZΔM15 ΔlacZΔX74 deoR recA1 endA1 araD139 Δ(ara, leu)7697 galU galK λrpsL nupG	(Grant et al., 1990)

Material and Methods

2.7 Cultivation media

The substances for the production of solid- and liquid-media were dissolved in H₂O and sterilized by autoclaving for 20 min at 121°C (Autoclave V150). For solid media 1.5 % agar (w/v) was added, for soft-agar media only 0.75 % (w/v).

Selection pressure for genetically modified strains was applied by adding the antibiotic kanamycin (section 2.3.1) to the liquid- or solid-media (after autoclaving).

2.7.1 Cultivation media for *M. xanthus* DK1622

Growth experiments with the wild type were carried out in parallel under iron rich/limiting conditions. For the comparative growth of *M. xanthus* on different iron concentrations, a batch of CTT medium (Dworkin, 1962; Bretscher and Kaiser, 1978) was prepared as shown in table 2.10 and split, while one half was further treated by 1 % (v/v) Chelex 100 resin beads to generate CTT-Fe^{MIN} medium as iron-limiting ambiance. The Chelex-based method was found suitable for the creation of iron-limiting conditions for many bacteria (Hubbard *et al.*, 1986; Ochsner *et al.*, 2002; Ollinger *et al.*, 2006; Vidakovics *et al.*, 2007). For experiments with a defined iron concentration only plastic containers were used, as far as possible. Before usage, all glass containers and bottles were washed for 4 h at room temperature with 5 g/l Chelex 100 resin beads to ensure the absence of glass-bound iron ions.

For the cultivation of *M. xanthus* mutants, CTT medium was used.

Table 2.10: Composition of CTT medium (casitone rich).

All solutions were prepared in H₂O.

Solution	Composition
Tris stock solution	1 M Tris stock solution, pH 8.8
MgSO ₄ buffer	0.8 M MgSO ₄
1 M K-Phosphate buffer (pH 7.6)	86.6 % (v/v) 1 M K ₂ HPO ₄ 13.4 % (v/v) 1 M KH ₂ PO ₄
CTT, pH 7.6	1 % (w/v) Bacto Casitone 1 % (v/v) 1 M Tris stock solution 1 % (v/v) 0.8 M MgSO ₄ buffer 0.1 % (v/v) 1 M K-Phosphate buffer

Estimation of iron concentrations and iron uptake rates

Iron uptake rates were estimated by comparing the iron concentrations present in the culture supernatants before and after growth. By the differences, the iron uptake per time per O.D.₆₀₀

Material and Methods

(means: per $3.06 * 10^7$ cells per ml) was calculated to generate comparable values [unit: nmol * $\text{h}^{-1}\text{*O.D.}_{600}^{-1}$]. For the determination of the iron concentration a spectrophotometric method was applied, using Ferrospectral (disodium 4-[3-pyridin-2-yl-6-(4-sulfonatophenyl)-1,2,4-triazin-5-yl]benzenesulfonate, also known as Ferrozine) which generates a stable, colored complex with iron ions. This method for estimation of iron-uptake by microorganisms was described earlier (Smith *et al.*, 2006).

For implementation, 0.5 ml sample or standard solutions were mixed with 0.5 ml of a 1 mM Ferrospectral solution (prepared as per description by the company). Then, 100 μl of a 10 % (w/v) hydroxylammonium chloride solution was added slowly and incubated for 5 min at room temperature to reduce all present Fe^{3+} in the sample to Fe^{2+} . Afterwards 0.5 ml 2 M sodium acetate/2 M acetic acid buffer were admixed. Finally, 0.5 ml of a 10 % sodium perchlorate solution was added and the reaction batch was filled up to 2.5 ml with H_2O . The mixture was incubated for 5 min at room temperature. The extinction-measurement was realized in a biophotometer at 595 nm. The sample concentration could be calculated by a regression line, produced with standards with known iron concentrations.

To produce a regression line (correlation of iron concentration to extinction) a fresh 10 mM stock solution FeCl_2 in pure H_2O was generated. Based on this, different end concentrations were generated (0.1, 0.2, 0.3, 0.4, 0.5, 1, 2, 5, 10, 50 and 100 μM). H_2O was used as blank.

2.7.2 Cultivation medium for *E. coli* DH10B

For the cultivation of *E. coli* cells, LB medium (Bertani, 1951) was used. The composition of LB medium is shown in table 2.11.

Table 2.11: Composition of LB medium.

All solutions were prepared in H_2O . The pH of 7.6 was adjusted by 1 M HCl.

Medium	Composition
LB	1 % (w/v) Trypton 0.5 % (w/v) Yeast extract 0.5 % (w/v) NaCl

Material and Methods

2.8 Cultivation conditions and conserving of microbial strains

2.8.1 Growth conditions of *M. xanthus* cultures

To monitor cell concentration during cultivation, the optical density at 600 nm (O.D.₆₀₀) was checked periodical. To make sure to work in the linear range (below O.D.₆₀₀ of 0.3) of the used biophotometer, dilutions with sterile medium were generated. The dilutions were taken into account to calculate cell density in the respective flasks. Sterile Medium was also used as blank. Furthermore different dilutions were controlled under the microscope and the cells were counted.

Application of Amberlite XAD 16 absorber resin to *M. xanthus* cultures

For the analysis of secondary metabolite yields, it is necessary to extract these substances from culture broth. Therefore, application and use of Amberlite XAD 16 absorber resin for the selective take-off of hydrophobic substances was already standardized for bacteria (Sayyed and Chincholkar, 2006) and myxobacteria (Gerth *et al.*, 1996; Krug *et al.*, 2008b). First of all, the Amberlite XAD 16 absorber resin was pre-treated as described by the manufacturers. Sterilized XAD particles in pure water were added from the beginning of growth to all main cultures (25 ml) to a final concentration of 1 % (vol. /culture vol.).

When *M. xanthus* wild type or mutant strains were harvested, the XAD resin were separated from cells and media by filtration, using a metal sieve (approx. 1 mm² pore size). The XAD beads were stored at – 20 °C for HPLC-MS analysis, the flow-through was collected in new tubes.

a) Growth of *M. xanthus* wild type cells on different iron concentrations

Wild type growth experiments were carried out at 30 °C in parallel under iron rich/limiting conditions in triplicates. All glassware was pre-treated by Chelex to ensure the absence of glass-bound iron irons. *M. xanthus* wild type cells were taken from a - 80 °C stock culture and broad out on CTT agar plates by dilution streak with an inoculation loop (Brock and Madigan, 1991). Afterwards, the plates were incubated at 30 °C for several days. For the inoculation of a 10 ml pre-culture of CTT medium, a single colony of *M. xanthus* was transferred from an agar plate. After 24 h at 30 °C and 170 rpm, two 5 ml samples were removed and cell pelleting was accomplished by centrifugation (Eppendorf 5810R, Rotor: A-4-81, 4 °C, 10 min at 3250 x g). One sample was washed two times with CTT, the other with CTT-Fe^{MIN}. The samples were resuspended in the respective medium, and used to start another round of two 10 ml pre-cultures. At 30 h, the pre-cultures were pelletized and again washed twice in the

Material and Methods

appropriate medium, and used to inoculate the 25 ml growth cultures in CTT or CTT-Fe^{MIN}, the initial O.D.₆₀₀ of all cultures was 0.02. Finally, harvest was accomplished by centrifugation after 29, 40, 48 and 64 h.

b) Growth of *M. xanthus* mutant cells on CTT medium

The confirmed *M. xanthus* mutant strains (table 2.8) were taken from the - 80 °C stock culture and streaked out on CTT agar plates (containing kanamycin; section 2.3.1, but not in case of the deletion mutant of MXAN_6967) and incubated at 30 °C for several days.

A single-cell-derived colony was taken to inoculate a first pre-culture in 10 ml CTT (containing kanamycin, except MXAN_6967) in a sterile 100 ml Erlenmeyer flask, incubated at 30 °C with 170 rpm. After approx. 30-45 h, 5 ml were centrifuged and washed twice with CTT medium. The cell pellet was resuspended in 2 ml sterile medium and used to start a second pre-culture in CTT medium (without kanamycin). After further 24-30 h, 10 ml of the pre-culture was pelletized by centrifugation, washed twice (sterile medium) and used to start the main-culture in CTT (without kanamycin; 25 ml medium in sterile 250 ml Erlenmeyer flasks, containing 1 % XAD resin). Production cultures were inoculated with an O.D._{600nm} of 0.02 (except for knockout mutant of MXAN_0144 as difficult candidates had slightly higher inoculation). After growth, harvest was accomplished by centrifugation in dying phase (Eppendorf 5810R, Rotor: A-4-81, 4 °C, 10 min at 3250 x g).

2.8.2 Growth conditions of *E. coli* cultures

Plasmid proliferation and subsequent extraction was performed, using *E. coli* DH10B cells. Selection pressure for plasmid-containing strains was applied by adding kanamycin (section 2.3.1) to the liquid- or solid-media (after autoclaving).

E. coli DH10B cells or generated plasmid-containing strains (list of plasmids: table 2.22) were taken from stock cultures. To generate single-cell derived colonies, a dilution streak (Brock *et al.*, 1991) was made on LB agar plates (containing kanamycin in case of mutants, carrying plasmid-coded antibiotic resistance). The plates were incubated at 37 °C for 1 or 2 days. Single colonies were transferred by a pipette tip into a sterile 2 ml Eppendorf tube with 1.6 ml LB medium (containing kanamycin in case of mutants). The suspension was incubated for 14-16 h (overnight) in a thermomixer with 900 rpm at 37 °C. Afterwards, harvest was accomplished by centrifugation (Biofuge fresco, 4 °C, 5 min at 16060 x g).

Material and Methods

2.8.3 Preparation of stock cultures and microbial conserving

a) Stock cultures of *M. xanthus* strains

For long-time storage of *M. xanthus* strains, - 80 °C glycerol stock cultures were produced. Therefore, a previously described culture from CTT (section 2.8.1 a and b) was harvested by centrifugation (Eppendorf 5810R, Rotor: A-4-81, 4 °C, 10 min at 3250 x g) at on O.D.₆₀₀ of approx. 1.0 and resuspended in 2.5 ml CTT medium, containing 25 % glycerol (v/v). The suspension was divided into 500 µl aliquots in sterile Eppendorf tubes, quick-frozen with liquid nitrogen and stored at - 80 °C.

b) Stock cultures of *E. coli* strains

For long-time storage of *E. coli* strains, - 80 °C glycerol stock cultures were produced. Therefore, the previously described over night cultures (section 2.8.2) were centrifuged (Biofuge fresco, 4 °C, 5 min at 16060 x g) and resuspended in 500 µl sterile LB medium, containing 40 % glycerol (v/v). The suspension was quick-frozen with liquid nitrogen and stored at - 80 °C.

Material and Methods

2.9 Proteome analysis

Proteome analysis was organized as 4 individual operations: 1) protein extraction, 2) 2D-DIGE analysis, 3) MALDI-MS identification of proteins (and phosphorylations), and 4) detection of protein-phosphorylations via LTQ-Orbitrap. The methods are further specified in the following sections.

2.9.1 Protein extraction of *M. xanthus* DK1622 samples from different iron concentrations

Samples (25 ml) of *M. xanthus* DK1622 grown under iron rich and poor conditions from 29 and 40 h (see section 2.8.1) were washed with 4 °C cold PBS and centrifuged (Eppendorf 5810R, Rotor: A-4-81, 4 °C, 10 min at 3250 × g). For cell lysis, the pellets were resuspended in 1 ml DIGE lysis buffer (table 2.3) at 4 °C. The cell pellets were lysed by sonication on ice (ultrasonic disintegrator USD 30, 21 kHz, amplitude 25, 6 × 30 sec, followed each time by 2 min break). The cell debris was then pelleted by centrifugation (Beckman Coulter Avanti J-E, Rotor JA25.50, 12096 × g, 4 °C, 10 min). The supernatant was transferred into a new tube.

2.9.2 2D-DIGE sample preparation, running conditions and data interpretation

2.9.2.1 2D-DIGE sample preparation

a) Protein precipitation and resuspension

For the precipitation of protein molecules an 8/1 mixture of - 20 °C cold acetone/methanol was added to the sample until the tenfold of the sample start volume was reached. The tube was incubated at - 80 °C for 2 h. Subsequently, the proteins were pelletized by centrifugation (Eppendorf 5810R, 1000 × g, 4 °C, 10 min). The supernatant was removed quantitatively. Protein-pellets were washed three times with - 20 °C acetone, followed by centrifugation as before (Eppendorf 5810R, 1000 × g, 4 °C, 10 min). After the last washing step the pellets were dried on ice completely and finally, resuspended in 200-300 µl DIGE label buffer (table 2.3) (Elnakady *et al.*, 2007). The pH was adjusted to exact 8.5 by DIGE label buffer, containing 1 % potassium hydroxide.

b) Estimation of protein concentrations

Protein concentrations were determined by the method of Bradford (Bradford, 1976). The used Bradford protein assay is based on the detection of colored Coomassie-protein complexes at 595nm. All measurements were performed as triplicates in 96well microtiter plates in a microtiter plate reader.

Material and Methods

The measurement was accomplished by a commercial Bradford dye concentrate (table 2.2), following the manufacturers instruction. Calibration curves were generated with BSA (0.1, 0.2, 0.4, 0.6, 0.8 and 1.0 µg/µl), dissolved in DIGE label buffer (table 2.3), which was used pure as blank. Different dilutions of the samples were generated with DIGE label buffer. After measurement, samples were diluted with DIGE label buffer to adjust the protein concentration to exactly 5 µg/µl.

c) 2D-DIGE: CyDye protein labeling

The individual steps of 2D-DIGE (Van den Bergh *et al.*, 2003; Marouga *et al.*, 2005) analysis, namely sample preparation (labeling, sample pooling and in-gel rehydration), isoelectric focusing, disulfide-reduction/thiol-alkylation, PAGE running conditions, image recording and data interpretation generally based on the manuals of GE Healthcare Bio-Sciences (GE Healthcare Bio-Sciences, 2005) and (Elnakady *et al.*, 2007), modifications were detailed described in the following sections.

The protein samples were analyzed along with an internal, pooled standard containing equal amounts of proteins from all of the samples. Proteins (total of 50 µg) in DIGE labeling buffer were labeled minimally with one of three CyDye DIGE fluorophores, Cy2, Cy3 or Cy5 (GE Healthcare Bio-Sciences), the scheme is shown in figure 2.1.

For DIGE experiments, protein extracts from CTT and CTT-Fe^{MIN} were labeled by two different CyDyes (Cy3 and Cy5). Samples were taken from early (29 h) and late exponential phase (40 h). Thereby, for replicas on different gels (same biological samples) the 'inverse label' technique was used to proof non-preferential dye-interaction. The third CyDye (Cy2) was always used to label an internal standard.

Before use, DIGE CyDyes were reconstituted in DMF and were then combined with the protein samples in a ratio of 400 pmol of CyDye per 50 µg protein, following the manufacturers instruction. Labeling reaction was performed on ice in the dark for 30 min. Afterwards, the reactions were quenched by incubating with DIGE STOP solution (10 nM L-lysine) on ice in the dark for further 10 min.

The labeled protein samples (iron rich and iron poor conditions at 29 and 40 h, and the internal standard) were then loaded onto immobilized pH gradient (IPG) stripes, the scheme is shown in figure 2.1.

Material and Methods

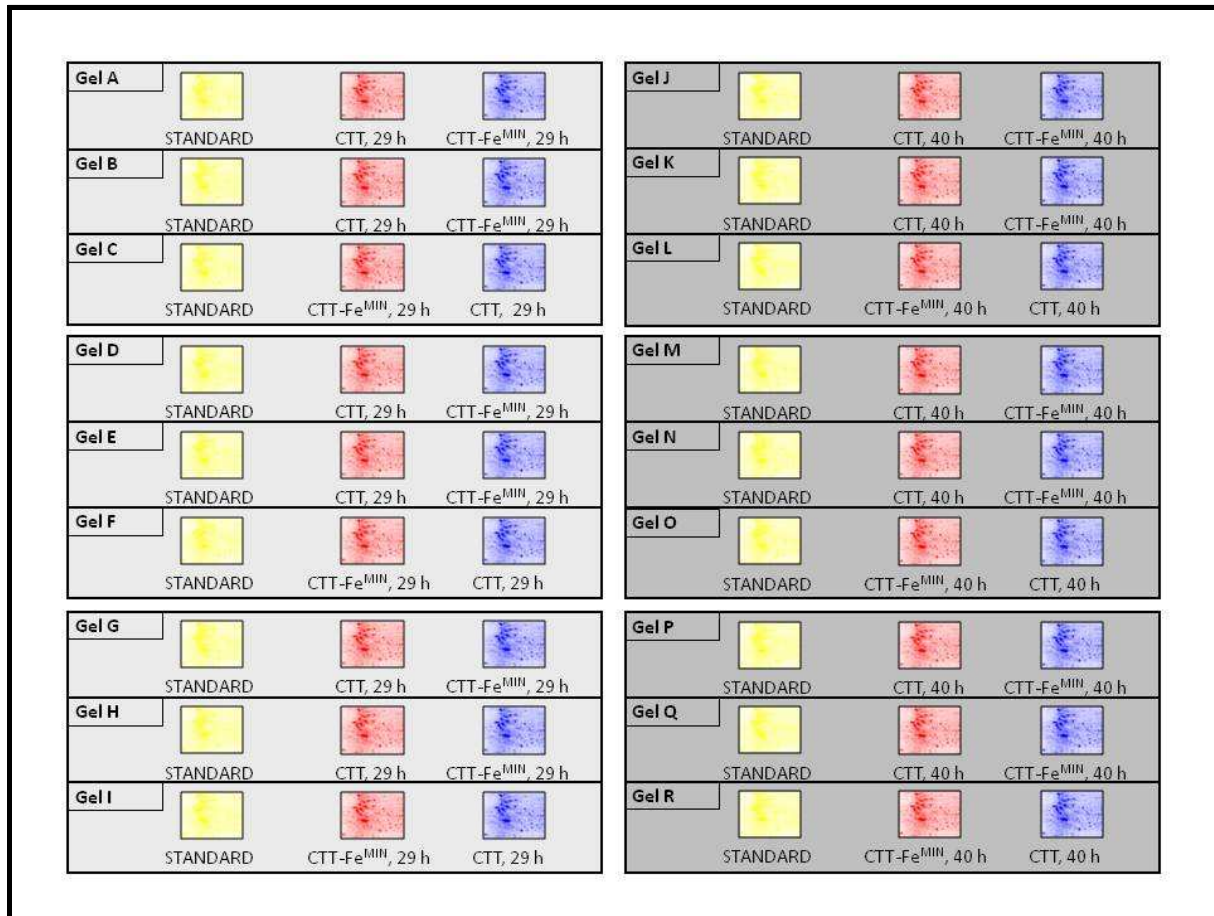


Figure 2.1: Workflow for DIGE system

The diagram shows the workflow for DIGE system. In all gels, protein extracts from two different iron concentrations (CTT and CTT-Fe^{MIN}) are compared. In detail, samples were obtained from two different time points (29 and 40 h, shown left and right). Each protein extract was analyzed in triplicates (e.g. gel A, B and C), where in one of the gels, the samples were labeled inverse (e.g. gel C). All samples were analyzed along an internal standard, always labeled with Cy2.

For the purpose of protein identification, unlabeled pooled standard sample (500 µg) was separately processed by conventional 2D gel electrophoresis. Alternatively, unlabeled pooled standard (150 µg) was spiked into each gel from 2D-DIGE.

d) 2D-DIGE: sample application by in-gel rehydration

Two corresponding samples from different iron concentrations and the internal standard were combined and give an overall volume of 36 µl. To adjust the desired amount of Pharmalytes and DTT, the same volume of DIGE lysis buffer was added. Finally, 268 µl DIGE rehydration buffer was added to reach a volume of 340 µl, which is the recommended volume for the rehydration of 18 cm IPG-strips, using an immobilized pH gradient from 4-7. The sample were brought out in lanes of the rehydration tray, IPG-strips were placed gel-side-down

Material and Methods

bubble-free in the liquid and covered carefully by IPG-strip cover fluid. The samples were incubated in the dark for 14-16 h for passive in-gel rehydration.

2.9.2.2 2D-DIGE running conditions

a) Isoelectric focusing (IEF)

After finishing the in-gel rehydration the remaining oil was removed carefully and IPG-strips were placed in IEF chamber gel-side-up. The ends of the IPG-strips were covered with water-drenched paper bridges before the electrodes were placed. All IPG-strips were covered carefully by IPG-strip cover fluid. An IPGphor focusing apparatus (table 2.7) was used for separation. The applied voltage for IEF can be found in table 2.12. By the IPGphor controlling software the actual voltage and resulting current was monitored. The temperature was kept constant at 20 °C during IEF.

Table 2.12: Applied voltages for isoelectric focusing (IEF) in IPGphor.

The current limit was set to 50 µA per IPG-strip.

Step No.	Step/Gradient	Voltage	kept for VHrs	Total applied VHrs
1	Gradient	500	2000	2000
2	Step	500	1500	3500
3	Gradient	3500	10000	13500
4	Step	3500	3500	17000
5	Gradient	8000	10000	27000
6	Step	8000	32000	59000

b) Equilibration

Following to isoelectric focusing, the IPG stripes were further treated with equilibration buffer 1 (table 2.3). After 10 min, the buffer was replaced by equilibration buffer 2 (table 2.3). Also the second equilibration step was performed for 10 min on a table shaker with 30 rpm.

Material and Methods

c) Polyacrylamide gel casting (PAGE)

Homogenous SDS-polyacrylamide gels (12.5 % T-content; table 2.3) were casted between low fluorescent glass plates. To avoid evaporation, water-saturated butanol was used for overlay.

Then, the equilibrated IPGs were washed for 10 sec with 2xRunning buffer (table 2.3), and transferred afterwards on top of SDS-polyacrylamide gels and sealed with 0.5 % agarose and 0.1 % Bromophenol blue, dissolved in 2xRunning buffer.

For separation by SDS-PAGE, the Ettan DALTwelve system was used at a constant temperature of 20 °C. The lower buffer chamber was filled with 1xRunning buffer, the upper buffer chamber with 2xRunning buffer, following the manufacturer's instruction. Protein separation was performed by the application of 2 W per gel for 1 h, followed by 17 W per gel (approx. 8 h) until the Bromophenol blue front has reached the end of the gels.

2.9.2.3 2D-DIGE image analysis and data interpretation

a) Scanning conditions

The gels were then scanned at 100 µm resolution with a Typhoon 9410 imager. The excitation/emission wavelengths for Cy2, Cy3 and Cy5 are 488/520, 532/580 and 633/670 nm, respectively. The 2D-gels containing unlabeled pooled standard sample were post-stained with colloidal Coomassie blue (Westermeier, 2006) and scanned with the same imager using an excitation wavelength of 633 nm.

Subsequently, Typhoon images were analyzed by DeCyder software. Relative protein quantification in single gels was performed using the DeCyder differential in-gel analysis (DIA) and across all samples by biological variation analysis (BVA).

b) Differential in-gel analysis (DIA)

The protein samples were analyzed along the internal, pooled standard containing equal amounts of proteins from all of the samples. DIA was used to analyze differences in individual gels by comparing protein spot intensities and distributions. Therefore, individual spots were co-detected and correlated in the three CyDye images, followed by normalization and background correction.

Material and Methods

Protein spots with non-typical dye distribution were controlled manually (and, if necessary deleted from the spot list). The protein spot intensities were compared across all three CyDye images, so the intensity ratio of the two samples (labeled by Cy3 and Cy5) was calculated.

c) Biological variation analysis (BVA)

When spot detection and quantitation of the single gels by DIA was finished, data are transferred to the BVA module for inter-gel analysis. DeCyder BVA processes multiple gel images, performs matching of multiple images from different gels for comparison to provide statistical data on different protein abundance levels between multiple groups (here two: iron-rich and iron-limitation). This module utilizes the internal standard and the experimental design to perform gel-to-gel matching on internal standard images and across sample images within the groups. This process enables comparison of protein abundance between samples on different gels.

Student's t-test and one-way analysis of variance (ANOVA) were used to proof significant differences in relative abundances of protein spot-features in cells grown under iron replete or iron-limiting conditions. This analysis was designed to identify proteins which were consistently up- or down-regulated more than 2fold at both time points, 29 and 40 h.

d) Manual control, closing statistic

Relative protein quantification across all samples was performed using DeCyder DIA and BVA. Protein spots, which show an altering of intensity, induced by other factors than iron were detected by ANOVA ($P < 0.05$) and excluded. Proteins showing constantly a change in expression levels of at least 2fold (student's t-test; $P < 0.05$), were excised directly from the gels using a semi-automated Ettan spot picker and prepared by in-gel digestion for identification with MALDI-MS (section 2.9.3).

2.9.3 Protein identification (incl. protein-phosphorylation) by mass spectrometry

The protein identification from in-gel digests by MALDI-MS for myxobacteria is already used routinely (Dahl *et al.*, 2007; Schneiker *et al.*, 2007; Bode *et al.*, 2009). Proteins of interest were subjected to trypsin in-gel digestion, following basically the protocol from (Sinha *et al.*, 2001), but reducing trypsin amount to ca. 20 ng in an end volume of approx. 25 μ l, so lowering final end-concentration and -volume. If necessary, the in-gel digests were purified by solvents (Shevchenko *et al.*, 1996) or by passages over C₁₈ ZipTips (Millipore) or

Material and Methods

stage tips (Rappsilber *et al.*, 2003; Ishihama *et al.*, 2006; Rappsilber *et al.*, 2007). The respective work steps are described in the following section.

2.9.3.1 Prearrangement

a) Spot picking and band excision

Protein spots of interest from DeCyder software analysis (section 2.9.2.3) or bands from high stringent elutions from DNA pull-down assay (section 2.10) were cut out from gels by an ETTAN spot picker. The gel plugs were transferred into the individual vials of a 96well microtiter plate (MTP).

b) Destaining and in-gel digestion

The spots were incubated for 20 min with 100 µl pure H₂O at 300 rpm on a MixMate MTP incubator. Afterwards, the liquid was replaced with 100 µl of a 50/50 solution H₂O/acetonitrile (AcCN), again incubated at 300 rpm for 20 min. In case of Coomassie staining, this step was repeated until all color had disappeared. Finally, the gel-plugs were washed with 100 µl pure AcCN at 300 rpm for 20 min. The AcCN was removed quantitatively and the gel plugs were dried completely in a SpeedVac.

After drying, 10 µl digestion buffer (table 2.4) was added per gel plug, followed by 30 min incubation at 37 °C. To cover gel pieces completely, 15 - 20 µl ammonium hydrogencarbonate buffer (table 2.4) was added. The MTP was further incubated for 14-16 h at 37 °C. Digestion was stopped by the addition of 0.5 µl 1 % TFA in H₂O. The supernatant was stored at – 20 °C.

c) Sample purification and concentrating

If necessary, peptides resulting from a tryptic in-gel digestion were purified and concentrated. Therefore, two different methods are used in this work:

The **solvent-based peptide extraction** is deduced from the procedure of (Shevchenko *et al.*, 1996). Therefore, the individual in-gel digestion supernatants were transferred into a second MTP. The gel plugs were incubated for 15 min with 30 µl of MS solution 1 (table 2.4) at 300 rpm. Afterwards, the supernatants were combined. The procedure was repeated with 30 µl MS solution 2 (table 2.4) and finally with 30 µl pure AcCN. After all supernatants from one gel plug were combined in the second MTP, then it was dried in a SpeedVac, using aqueous mode. Dried peptides were dissolved in 10 µl MS solution 1 overnight at 4 °C.

Material and Methods

For **pipette-tips based peptide extraction**, C₁₈-ZipTips (Millipore) or StageTips (Rappsilber *et al.*, 2003; Ishihama *et al.*, 2006; Rappsilber *et al.*, 2007) were used. For implementation, both kind of tips need to be pre-washed, loaded with a sample, followed by washing (pure H₂O) and subsequent elution of the formerly bound peptides.

For both kinds of tips, elution was performed with approx. 1 µl MS solution 3 (table 2.4).

2.9.3.2 MALDI ToF/ToF mass spectrometry

For protein identification by PMF and MS/MS experiments (peptide fragment fingerprinting; PFF), samples were analyzed by a 4800 MALDI ToF/ToF mass analyzerTM (Applied Biosystems) in reflective, positive ion mode, using a Neodym/YAG laser at 355 nm in a high vacuum at ca. 1.0*10⁻⁸ mbar.

a) Sample application

For the identification of proteins of interest, the digested peptides (or extracts) were spotted twice onto Opti-TOF 384 well MALDI sample plates (0.5–1 µl). Sample spots were mixed on the plate with CCA or DHB (table 2.4) as matrix, used for co-crystallization in a matrix/analyte ratio of 1/1 (*v/v*). Finally, spots were air-dried at room temperature. In cases of low ion-yields, dried spots were washed with 1 µl recrystallization solution (table 2.4), which was removed after 2 sec.

b) Calibration

Each MALDI measurement was started by calibration using the 4700 calibration peptide mixture (Applied Biosystems), to optimize sensitivity and resolution (deflector and reflector correction).

The calibration was performed in MS and MS/MS mode. In MS mode, at least 5 of 6 present peptides in the calibration mixture must be detected with a mass error smaller 20 ppm and a Signal-to-Noise (SN) ratio of 50 or more. In MS/MS calibration mode, GluFib fragment (m/z: 1572.662) from calibration mixture was fragmented (precursor selection: +/- 5 Da). MS/MS-calibration was accepted, if at least 10 peptide fragments from b- or y-series (Biemann, 1990) were detected with a mass error smaller than 0.1 Da and a SN ratio higher than 20.

Material and Methods

c) MS conditions (acquisition of peptide mass fingerprints)

In MS mode, a mass range from 800-4000 Da was covered. A spectrum was acquired by 50 shots to 20 random positions, so 1000 laser shots were accumulated. Matrix peaks were suppressed automatically. Peaks for MS based analysis must show a peptide-typical carbon-isotope distribution and have a SN ratio of 20 or higher. Peaks derived from sodium- or potassium-addition were ignored automatically in PMF analysis.

d) MS/MS conditions (acquisition of peptide fragment fingerprints)

For each measurement, the five most abundant peaks in the PMF were analyzed further by PFF (Tabb *et al.*, 2006). For MS/MS analysis of the 5 most intense peptides peaks from MS analysis, fragmentation was induced by high laser energy, causing post-source dissociation. Only in cases of inconclusive results, fragment spectra were generated, using collision induced dissociation (CID) with nitrogen as collision gas at 2.5×10^{-5} bar. In MS/MS mode, a mass range from precursor mass down to 0 Da was covered. A spectrum was acquired by 50 shots to 50 random positions, so 2500 laser shots were accumulated. Matrix peaks were suppressed automatically. Peaks for MS/MS based analysis must show a typical carbon-isotope distribution and have a Signal/Noise ratio (SN) of 15 or higher. Peaks, derived from sodium- or potassium-addition were ignored in precursor-selection, as well as known peaks from trypsin or keratin.

e) Protein identification using MS and MS/MS data by the MASCOT scoring algorithm

Protein identification was then carried out by MASOCT scoring algorithm (http://www.matrixscience.com/search_intro.html), using a combination of PMF data and the 5 PFF datasets per search using the *M. xanthus* FASTA protein database (<http://www.expasy.org/sprot/hamap/MYXXD.html>). Known trypsin- or keratin-peaks were excluded. Error tolerance was limited to 70 ppm in MS mode, and 0.1 Da in MS/MS mode. Furthermore, carboxyaminomethylation on cysteins was defined as fixed modification, oxidation of methionins as variable modification. Threshold was set to 99 % identification probability in MASCOT scoring (MOWSE score) for the identification of proteins.

f) Detection of protein-phosphorylation

The detection of protein-phosphorylations was accomplished by MALDI and LTQ-Orbitrap measurement. In both systems, the method was confirmed using a β -casein digest.

Material and Methods

With MALDI, phospho-peptide identification based on the specific induction and detection of the neutral loss of the phospho-group from the phosphorylated peptide (Kalume *et al.*, 2003; Kjellstrom and Jensen, 2004; Peters *et al.*, 2004), including sequence analysis for peptide confirmation. An exact determination of the position by this tandem MS method of the phosphate-group within the peptide was only possible, if in the respective peptide sequence only one potential phosphorylation-site occurs (table a2).

For implementation, samples from in-gel digestion or peptide extracts were spotted with CCA or phosphorous DHB as matrices (table 2.4). To analyze phosphorylations, MS and MS/MS measurements were performed as described. Also the MASCOT search was used as described, but including phosphorylation as variable modification. Potential phospho-peptides were selected for new MS/MS fragmentation runs. MS/MS spectra of a potential phospho-peptide from CCA and phosphorous DHB were combined and transferred to DeNovo Sequence Explorer software to validate the presence of a neutral loss of the phosphate group (based on a mass shift of 79.9 Da with mass tolerance of 200 ppm) and further confirmation of the sequence of the phospho-peptide (Kjellstrom *et al.*, 2004).

If necessary, phospho-peptides were further analyzed by a high-resolution LTQ-Orbitrap mass spectrometer after StageTip purification (section 2.9.3.1 c) with 20 µl Orbitrap spray solution (table 2.4) as elution solvent.

Phosphopeptides were confirmed in composite spectra from different mass ranges, covering m/z-values from 0-1000 Da (Lu *et al.*, 2007). Error tolerance was limited to 2.5 ppm.

Material and Methods

2.10 DNA pull-down assay for identification of DNA interacting proteins to the promoter regions of MXAN_3702 and MXAN_6967

In order to identify protein interaction partners from promoter regions of the genes MXAN_3702 and MXAN_6967, ligand fishing experiments (DNA pull-down assay) were performed, using Streptavidin coated paramagnetic beads. In both promoter-overarching PCR reactions, the forward primer contains a biotin tag at the 5'-end. This feature was used to connect amplified DNA molecules to Streptavidin. An overview about the individual working steps could be found in figure 1.14. The promoter region of MXAN_4899 was used as background to identify proteins from rather unspecific interactions.

2.10.1 Loading of amplified DNA to Streptavidin-coated paramagnetic beads

Copies of the promoter regions of MXAN_3702 (*fur*) and MXAN_6967 (*fur homologue*) were generated by *Taq* PCR (section 2.11.6) using the primer pairs in table 2.14. The PCR products were controlled on an agarose gel and purified (section 2.11.5 b). DNA concentration and purity was determined in a biophotometer.

Subsequently, the DNA was loaded on to 1 mg paramagnetic Streptavidin-coated beads (Dynabeads M-280, Invitrogen) via the biotin residue of one of the primers (12 pmol DNA per mg Streptavidin). The mixture was incubated for 1 h in DNA binding buffer (table 2.5).

2.10.2 Protein extraction of *M. xanthus* DK1622 samples from different iron concentrations and incubation with DNA-loaded Streptavidin beads

M. xanthus DK1622 was grown in CTT and CTT-Fe^{MIN} as described (section 2.8.1) and cells were harvested at 40 h by centrifugation (Eppendorf 5810R, 1000 × g, 4 °C, 10 min). The pellets were washed with 4 °C cold cell wash puffer (table 2.5) and centrifuged as before. Cells were resuspended in cell lysis buffer (table 2.5) and lysed using a two times a French Press with approx. 1000 atm. Cell debris were removed and protein concentration was estimated as described before (section 2.9.1).

To enable protein-promoter interaction, 2 mg of the different protein extracts were incubated with Streptavidin-bound DNA molecules on a tumble shaker (20 rpm, 21 °C, 30 min).

2.10.3 Washing and elution of promoter interacting proteins

The stringent DNA binding proteins were isolated from Streptavidin beads by increasing ionic strength using higher NaCl concentrations with each washing step (wash buffer 1 and 2, table

Material and Methods

2.5; 20 rpm, 21 °C, 20 min each). Finally, elution was performed in 250 µl elution buffer (table 2.5), applied on a rotating device (20 rpm, 21 °C, 20 min).

2.10.4 Protein precipitation, PAGE, staining and protein identification, including protein-phosphorylations (MALDI-ToF/ToF)

All supernatants from washing and elution steps were precipitated as described (Wessel and Flügge, 1984). The protein pellets were resuspended in 20 µl SDS sample buffer (table 2.5). The samples were incubated at 95 °C for 5 min and subsequently loaded on 12 % acrylamide gels. After separation, the gels were silver stained and decolorized (Sinha *et al.*, 2001), excision and in-gel digestion of protein-bands. Subsequently, bands were used for in-gel digestion prior to MS analysis or peptide purification procedures, as described before (section 2.9.3).

2.11 Handling and manipulation of DNA molecules

The working steps and materials, used for targeted gene inactivation experiments are further described in the following section.

2.11.1 Vectors used

For the purpose of gene disruption by single crossover insertion or for DNA proliferation, derivates of pCR®2.1-Topo (table 2.13) were generated. This activated vector contains a neomycin-resistance gene as selection marker and an open *lacZ* gene to detect auto-ligation. The principle of gene inactivation by single crossover insertion was already explained (section 1.6). The vector card of pCR®2.1-Topo can be found in appendix (figure a1).

For the construction of double crossover mutants, derivates of pSWU41 (table 2.13) were used. The plasmid pSWU41 contains a neomycin phosphotransferase (*nptII*) and levansucrose gene cassette (*sacB*) (Wu *et al.*, 1996). The principle of gene inactivation by double crossover deletion was already explained (section 1.6). The vector card of pSWU41 can be found in the appendix (figure a2).

Table 2.13: Template-vectors used.

Vector	Description	Referenz
pCR®2.1 Topo	LacZα, T7 promoter, f1 ori, <i>bla</i> , pUC origin	Invitrogen, USA
pSWU41	pBluescript-Derivat, <i>nptII</i> , <i>sacB</i>	(Wu <i>et al.</i> , 1996)

2.11.2 Designed oligonucleotides

Start- and end-point of PCRs are determined by the oligonucleotides used (forward- and reverse-primers). Attention was paid to similar melting temperatures (T_m) in each primer pair using the formula:

$$T_m = (69.3 + (0.41 * \text{GC content [%]})) - (650 / \text{no. binding nucleotides})$$

a) PCR Primers for DNA pull-down assay

Primers for DNA pull-down assays were used in *Taq* PCRs (table 2.14). Loading of amplified DNA molecules to Streptavidin beads was accomplished via biotin-tag carried by one of the primer in the pair.

Material and Methods

Table 2.14: Primer pairs for DNA pull-down assays were used in *Taq* PCRs.

The biotinylation is marked by [Btn]. The first primer pair covers the promoter sequence of MXAN_3702, the second the promoter of MXAN_6967.

No.	Name	Sequence
1	MA_ProMF3702F	[Btn]AGTGTCAATGAGCCAGTCCGATT
	MA_ProMF3702R	GTGGCCTCCCACCGCGAAGAA
2	MA_ProMF6967F	[Btn]GGCAGCGGTATCCCGTCAACA
	MA_ProMF6967R	CGTCCTCCAACCTCCCGCAACA

b) PCR Primers for single crossover

Primers for gene inactivations via single crossover insertion were used in *Taq* PCRs (table 2.15). The amplified DNA molecules were cloned into pCR®2.1-Topo and used after verification for gene disruption by homologue recombination.

Table 2.15: Primer pairs in *Taq* PCRs for single crossover gene disruption experiments.

To create stringent insertion into small genes (< 500 bp), additional in-frame stop codons were generated. These are marked by underlining; these codons were created by insertion of nucleotides.

No.	Name	Sequence
1	KO_MXAN0142for	GACGGCGTCGTGCGCGCCTGG
	KO_MXAN0142rev	GAGCCATCCGCCCGAGGCCG
2	KO_MXAN0144for	CAGCCCAGCAGACGCCGGAG
	KO_MXAN0144rev	CAGGCGCATCAGCGCGTCCGG
3	KO_MXAN1562for	CGCGCACT <u>GAAACATCAAGGGTC</u>
	KO_MXAN1562rev	TTCGATGCGCT <u>AGGCCAGGAG</u>
4	KO_MXAN1619for	CGGTGG <u>CTAGGC</u> TTGGATCGC
	KO_MXAN1619rev	CTGCTGCT <u>TAACCACGCC</u> CG
5	KO_MXAN1808for	GACCACTGCCCGACGAATCG
	KO_MXAN1808rev	CGAGAGAAGTGC <u>GAGGCTCG</u>
6	KO_MXAN1864for	GGCAAGAAC <u>GGCCTGGCGAAG</u>
	KO_MXAN1864rev	GGAGCC <u>CTTCAGCATCCCAGG</u>
7	KO_MXAN1893for	CATTCTGACGT <u>GAGTGC</u> CCGC
	KO_MXAN1893rev	GCGTCT <u>CTCCTACGGAGGGTC</u>
8	KO_MXAN1988for	GCTCGCTGCC <u>ACTTCAATC</u>
	KO_MXAN1988rev	CAGGTGG <u>TTGTCCACCTGGTC</u>
9	KO_MXAN2094for	GGAAACAC <u>CTAGGGGCC</u> CTA
	KO_MXAN2094rev	CTGC <u>GTTCCACACTACAGCCC</u>
10	KO_MXAN2347for	GGGGAA <u>CTGGAGGTGC</u> GGTCG
	KO_MXAN2347rev	GCGCG <u>GAAGTGGCGGCCATT</u>
11	KO_MXAN2440for	GCTGCC <u>GGGCACGCTGGCGGAG</u>
	KO_MXAN2440rev	TCCGGG <u>CTCCGGAGGCCGGAGG</u>
12	KO_MXAN2520for	CGTGCTGGCGCC <u>GGCC</u> TTCC
	KO_MXAN2520rev	CCTCGCG <u>CTCGCGCTTCTCCG</u>
13	KO_MXAN3203for	CCGCCGCC <u>ACGTAGCC</u> CCCC
	KO_MXAN3203rev	TGGGG <u>CTCCAGGCCGGCCGTG</u>
14	KO_MXAN4189for	GTCCGGG <u>CTTAACCCGCGT</u> GGG
	KO_MXAN4189rev	GACTGGCC <u>GGCTAGAAGCCTCG</u>

Material and Methods

No.	Name	Sequence
15	KO_MXAN4535for KO_MXAN4535rev	GCCCGAGGAT <u>GAACCCACGAA</u> GAACCGCTAGGTCGACCGTTC
16	KO_MXAN5055for KO_MXAN5055rev	GGAGGTGGCCACGCAGTCCC GGACTGCTCCACGGCGCGCTC
17	KO_MXAN5484for KO_MXAN5484rev	ACGCCGGGG <u>TAGCCCCGCCGTC</u> CGCGGTCCCGCTACGGCAGCAC

c) PCR Primers for double crossover

Two pSWU41-based constructs were created for in-frame deletion of core-regions from the genes MXAN_3702 and MXAN_6967, respectively. For both constructs, the up- and downstream sequences of the genes were amplified via PCR, missing the core region of the gene. Each of these two fragments were combined with a digested vector and subsequently used for first and second crossover in *M. xanthus*. Primers for the amplification for the fragments (table 2.16) are used in Phusion PCRs.

Table 2.16: Primer pairs in Phusion PCRs for gene in-frame deletion.

Primer pairs were used in Phusion PCRs for double crossover gene in-frame deletion experiments of MXAN_3702 and MXAN_6967. To create restriction nuclease cutting sites, additional nucleotides were introduced by primer sequence, leaving sequence in-frame. These nucleotides are marked in bold, the cutting sites by underlining.

No.	Primer	Sequence
1	D3702_F1forw	CAGAAGTCCGAG <u>CTC</u> ACGGCAACCG
	D3702_F1rev	GTGCT <u>GCGGCCGC</u> ATGTAGCGG
2	D3702_F2forw	CGTGGC <u>GCGGCCG</u> CAAGCACGGCTTCAA
	D3702_F2rev	GT <u>GGGATC</u> CTCCACGCCATGCCAGCCGG
3	D6967_F1forw	CGGCTTCCGGAG <u>CTCCAG</u> CTTCCC
	D6967_F1rev	CGGGG <u>CGCGGCCG</u> CTGCTGCGCAG
No.	Primer	Sequence
4	D6967_F2forw	CCCCG <u>CGCGGCCG</u> ATGTCCCAGCG
	D6967_F2rev	GCACGGGG <u>GATCC</u> CGGGTGAAGCTC

d) PCR primers for verification of mutants

Verification of single crossover insertion into the chromosome of *M. xanthus* was accomplished by *Taq* PCRs, using the primers in table 2.17 on genomic DNA of the corresponding mutant. Always, one gene-specific primer and one standard primer (M13 forward or M13 reverse) were selected, following the scheme in figure 1.16 c.

Verification of first crossover mutants for in-frame deletion follows the same principle, but using pSWU41-backbone specific primers (table 2.17) instead of M13 primers (Invitrogen). Second crossover mutants were confirmed by *Taq* PCRs, using only the gene specific primers CONF_D3702 and CONF_D6967.

Material and Methods

Table 2.17: Primer pairs for *Taq* PCRs to confirm mutants of *M. xanthus*

The primers were used for *Taq* PCRs to confirm mutants of *M. xanthus*, created by gene disruption using pCR2.1®TOPO insertion, pWSU41 first crossover insertions and second crossover in-frame deletion. The standard primer M13 forward and reverse were obtained from Invitrogen.

No.	Name	Sequence
1	M13 forward M13 reverse	GTAAAACGACGGCCAGT CAGGAAACAGCTATGAC
2	CONF_0142F CONF_0142R	GCGGCAGGGACGGCCG CGCGTGGCCTCCAGC
3	CONF_0144F CONF_0144R	CTGTCGACCGCGTTGA CACCAAGAAGTCGTGC
4	CONF_1562F CONF_1562R	CTGGAGTCTTAAGCCCC CAGCCTCGAGCGAAGC
5	CONF_1619F CONF_1619R	GTTCGGCGTCACGGTGC CTCGTGCCGGTTCATGA
6	CONF_1808F CONF_1808R	GAGGAGTTGTGTGATCC GAGTGGTAGGTCGCGTA
7	CONF_1864F CONF_1864R	GAGTCGACCTCCATGG GCATCTGGTGCATGAGG
8	CONF_1893F CONF_1893R	GTAGAGTTCGGCGAGG CCAGCTCTTCATTACA
9	CONF_1988F CONF_1988R	GCTCCGTGGTGCCTCA ACCACGGTGTGAAAGC
10	CONF_2094F CONF_2094R	CAGAACCCCTAGGCGAT CACCTGGACCGAGGCCAC
11	CONF_2347F CONF_2347R	CCCGAGTTGTACGAGAA GGCCGGCGAGGGCGTGT
12	CONF_2440F CONF_2440R	GCCCCTCACGGTGGGCTT CCCGGAGGCACAGGACGGT
13	CONF_2520F CONF_2520R	CGCTCTAACGATGTCCGG GATCCACCTCGCTGCCA
14	CONF_3203F CONF_3203R	GGAGGGGCAACGTTGCC GCCAGCGTCTCCACCTGAC
No.	Name	Sequence
15	CONF_4189F CONF_4189R	CGATATCTGCACGGTCA GTGAAGACGATGGCGA
16	CONF_4535F CONF_4535R	CGAACTCACCAGTGGC CGCAGTCTCAAGCCAA
17	CONF_5055F CONF_5055R	CCCAGCGAGCTGCTGCCCCGC GCCCGCTCGTCCTCCAGCTCGC
18	CONF_5484F CONF_5484R	CAAGGATGCGACGCATT GGTGCATGTTGATGCTC
19	CONF_pSWU41F CONF_pSWU41R	CTGGCGAAAGGGGGATGTGCTGCA GACATTGATCCGGGGTCAGCACCGT
20	CONF_D3702F CONF_D3702R	AGTGTCAATGAGCCAGTCCGATT GTGGCCTCCCACCGCGAAGAA
21	CONF_D6967F CONF_D6967R	GGCAGCGGTATCCCGTCAACA CGTCCTCCAATCCCGCAACA

Material and Methods

2.11.3 Extraction of genomic DNA from *M. xanthus* cultures

For the extraction of genomic DNA from *M. xanthus*, wild type or mutants strains were incubated till an O.D.₆₀₀ of approx. 1.0, as described before (section 2.8.1). The cells were then harvested by centrifugation (Eppendorf 5810R, Rotor: A-4-81, 4 °C, 10 min, 3250 x g) and resuspended in 3 ml STE buffer (table 2.6). Furthermore, 300 µl of a 10 % SDS solution and 300 µl proteinase K (1 mg/ml) were added and gently mixed. The tube was incubated at 55 °C for 2 h, and periodically inverted. Then, 1.2 ml 5 M sodium chloride solution was added slowly. After the mixing with 5 ml Chloroform the tube was put on a tumble shaker with 10 rpm for 45 min. Subsequently, the tubes were centrifuged (4 °C, 10 min, 3250 x g) for the separation of the aqueous and the organic phase. The upper (water) phase was transferred carefully into a new tube. The same volume of isopropanol was added. The tube was mixed gently and incubated at room temperature for 10 min, followed by another centrifugation step (4 °C, 10 min, 3250 x g). The supernatant was removed and the pellet was washed 3 times with 4 °C cold 70 % ethanol, each time followed by centrifugation as before. After the last centrifugation all liquid was removed quantitatively. The tubes were air-dried completely at room temperature. The pellet was resuspended in 200 µl TE buffer (table 2.6) and stored at -20 °C.

Material and Methods

2.11.4 Extraction of plasmid DNA from *E. coli*

a) by 'kits'

Isolation of plasmid DNA (table 2.22) from *E. coli* strains was performed by NucleoSpin®Extract II kit, following the manufacturer's instruction. The cells were grown as described before (section 2.8.2). For elution of plasmid DNA, always the minimal volume was used (20 µl H₂O) and flow-though was stored at - 20 °C.

b) by alkaline lysis

To isolate plasmid DNA, a modified protocol of alkaline lysis (Birnboim and Doly, 1979) was used. The *E. coli* cells were grown as described before (section 2.8.2), the cell pellets were resuspended in 250 µl buffer P1 (table 2.6). For cell lysis, 250 µl buffer P2 was added and the tube was inverted 10 times. To neutralize pH again 250 µl buffer P3 was added and the tube was inverted 10 times, followed by 5 min incubation on ice. Cell debris and precipitated proteins were removed by centrifugation (Biofuge fresco, 4 °C, 10 min at 16060 x g). The supernatant was transferred into a new tube and mixed with 600 µl isopropanol. Then, the tube was inverted 10 times, again followed by centrifugation (4 °C, 10 min at 16060 x g). After washing the DNA pellet with 500 µl 70 % ethanol, all liquid was removed quantitatively. The tubes were dried completely at room temperature. The pellet was resuspended in 40 µl pure H₂O and stored at - 20 °C.

2.11.5 Separation and purification of DNA molecules

a) Agarose gel electrophoresis

For the separation of DNA molecules by size, 0.8 % (w/v) agarose gels were used. The agarose was mixed in TBE-buffer (table 2.6) and boiled until the agarose was dissolved completely. Gels were casted at ca. 40 °C after mixing with ethidium bromide solution (2.5 µl ethidium bromide to 35 ml agarose solution). After solidification the gels were put into the electrophoresis chamber, and overlaid with TBE buffer. The samples were mixed with sample loading buffer (table 2.6), before application. DNA electrophoresis was performed with 50 – 70 V for approx. 2 h. Migration distance of DNA molecules was correlated to an applied DNA ladder as size marker (table 2.2).

Material and Methods

b) Clean-up of DNA molecules from agarose gels

For the extraction of DNA molecules from agarose gels (PCR products or DNA restrictions), the area of interest was cut out and transferred into a new tube (exposure time on UV table as short as possible). The single working steps of the NucleoSpin®Extract II kit (lysis of agarose and purification) were performed as described in the manufactures protocol. For elution, always the minimal volume was used (20 µl H₂O) and flow-through was stored at - 20 °C.

c) Precipitation of DNA molecules

For the precipitation of DNA molecules from 100 µl solution, 10 µl 3 M sodium acetate solution was added. Then, the 300 µl pure ethanol was admixed. The tube was incubated at - 20 °C for 1 h. Subsequently, the DNA was pelletized by centrifugation (4 °C, 10 min at 16060 x g). The supernatant was removed quantitatively. The pellet was washed three times with 70 % ethanol, followed by centrifugation as before. After the last washing step the pellet was dried at room temperature completely. Finally, the pellet was resuspended in 20 µl pure H₂O and stored at - 20 °C.

Material and Methods

2.11.6 Polymerase chain reaction (PCR)

Selected genomic DNA regions from *M. xanthus* were amplified *in vitro* by polymerase chain reaction. The start- and end-points were defined by oligonucleotides, homologue to genomic DNA of *M. xanthus* (primers, table 2.14-2.17). A single reaction cycle is divided into three parts:

- 1) Denaturation (98 °C). Double-stranded DNA melted to build 2 separate single strands.
- 2) Annealing (the annealing temperature was calculated by the primer sequence). The oligonucleotides can bind to homologue DNA sequences.
- 3) Elongation (72 °C). Starting from the primer sequence the complementary strand can be synthesized by a heat stable DNA polymerase in 5'-3' direction. The elongation time was correlated to the size of the amplified region.

The cycle was repeated 35 times.

a) DNA polymerases used

Amplification of selected genomic DNA regions from *M. xanthus* for single cross gene inactivation was performed by *Taq* polymerase. *Taq* polymerases add template-free characteristic poly-adenine tails ('sticky ends') to newly synthesized DNA sequences, which are necessary for an efficient pCR®2.1-TOPO cloning.

Error-free DNA amplicates were produced by high-fidelity DNA Phusion polymerase with proof-reading function. This enzyme was used for the amplicates to create markerless in-frame deletions of MXAN_3702 and MXAN_6967. Phusion generated DNA molecules were precipitated, resuspended and subsequently post-processed by *Taq* polymerase to build the poly-adenine tail for pCR®2.1-TOPO cloning.

b) PCR composition

For a PCR batch, all chemicals were mixed together (table 2.18-2.20), but not the polymerase. Before the first PCR cycle starts the tubes were initially heated for 3 min to 98 °C to ensure single-stranded, genomic DNA. Subsequently, the polymerase was added and the first cycle was started immediately.

Material and Methods

Table 2.18: Composition of an *in vitro* *Taq* PCR batch.

The polymerase-corresponding buffers are shown by underlining. The used *Taq* polymerase builds template-free poly A tails on the 3' end of the PCR product, which are required for pCR®2.1-TOPO cloning.

Chemical, buffer	Volume
<u>10x KCl buffer</u>	2.5 µl
<u>25 mM MgCl₂</u>	2.5 µl
dNTP's (1.25 mM)	4.0 µl
DMSO	0.6 µl
Forward primer (50 pM)	0.2 µl
Reverse primer (50 pM)	0.2 µl
Template DNA	0.2 µl
H ₂ O	14.6 µl
<i>Taq</i> polymerase	0.2 µl

Table 2.19: Composition of an *in vitro* *Taq* post-processing PCR batch.

The polymerase-corresponding buffers are shown by underlining. The used *Taq* polymerase builds template-free poly A tails on the 3' end of the PCR product, which are required for pCR®2.1-TOPO cloning.

Chemical, buffer	Volume
<u>10x KCl buffer</u>	1.5 µl
<u>25 mM MgCl₂</u>	1.5 µl
dATP (1.25 mM)	3.8 µl
DMSO	0.4 µl
Target DNA	5 µl
H ₂ O	2.7 µl
<i>Taq</i> polymerase	0.1 µl

Table 2.20: Composition of an *in vitro* Phusion PCR batch.

The polymerase-corresponding buffers are shown by underlining.

Chemical, buffer	Volume
<u>5x "GC" buffer</u>	2.5 µl
dNTP's (1.25 mM)	4.0 µl
DMSO	0.6 µl
Template DNA	0.2 µl
H ₂ O	14.6 µl
Phusion polymerase	0.2 µl
Forward primer (50 pM)	0.2 µl
Reverse primer (50 pM)	0.2 µl

Material and Methods

2.11.7 Enzymatic hydrolysis and ligation of DNA molecules

a) Digestion/double digestion

PCR amplificates were cut-out or their internal sequences were confirmed by digestion of plasmids with highly sequence-specific restriction-endonucleases (REs). The reaction batches for digests or double digests are shown in table 2.21.

Table 2.21: Composition of single and double RE digests of DNA molecules.

The RE-corresponding buffers were obtained from the company and are shown by underlining. The volume of the second REs for double digests could be varied, depending on manufacturer's recommendation and the buffer used. The DNA concentration was estimated as before using a biophotometer, 1 µg usually was equal to approx. 4 µl.

Digest	
Target DNA	0.5-1.0 µg (ca. 4 µl)
<u>RE-buffer</u>	2 µl
RE	0.2 µl
H ₂ O	13.8 µl
Total volume	20 µl

Double digest	
Target DNA	0.5-1.0 µg (ca. 4 µl)
<u>RE-buffer</u>	2 µl
RE 1	0.2 µl
RE 2	x µl
H ₂ O	y µl
Total volume	20 µl

The restriction was performed for ca. 3 h at the optional temperature (usually 37 °C), followed by an agarose gel electrophoresis for band-detection and to control hydrolysis efficiency. If necessary, another 0.1 µl of the restriction enzyme(s) was added and the mixture was incubated for another hour. In case of further cloning steps (ligation of DNA molecules), the restriction batch was heat-inactivated, loaded on a quantitative agarose gel and the band of interest was extracted as described before (section 2.11.5).

b) Ligation of DNA molecules

Vector-Insert ligation by the Topo-cloning kit

Direct cloning of *Taq*-derived or *Taq* post-treated DNA fragments was performed by the pCR2.1-Topo cloning kit (Invitrogen). All steps of Topo-cloning were performed, following the manufacturers instruction, but with reduced volume. In PCR reactions, the *Taq* polymerase synthesizes template-free poly-adenine tails at the 5'-ends of new synthesized DNA molecules. These cohesive-ended fragments ('sticky end') utilizing the free 3'-thymine overhangs at pCR2.1-Topo vectors to bind a PCR product (insert) in a topoisomerase-

Material and Methods

catalyzed reaction, an enzyme covalently attached to both of the free 3' ends of the linear vector.

Ligation of digested DNA molecules by T4-DNA ligase

For the ligation of digested vector- and insert-molecules, T4-DNA ligase was used. The ligase connects 5'-phosphate groups to 3'-hydroxy groups of DNA molecule(s) with ATP and Mg²⁺ ions as co-factors. At first, vector and insert DNA molecules were digested by the respective REs, controlled on agarose gels and subsequently purified from these. DNA concentrations were checked by a biophotometer to ensure a molar ratio of vector/insert of 1/3. The required amounts of DNA were mixed with 10x ligation buffer and one unit T4-DNA ligase, following the manufacturer's instruction. Then, ligation was performed by incubation overnight at 16 °C in a Comfort thermomixer. Ligation batches were used either directly for transformation of *E. coli* cells (section 2.11.8) or after purification by precipitation (section 2.11.5 c).

c) Constructed plasmids

Plasmids (table 2.22) were isolated from *E. coli* strains and confirmed via RE-hydrolysis or, in case of in-frame deletion constructs (table 2.22; no. 17 and 18) via DNA sequencing by the company Eurofins MWG. After subsequent insertion of the respective construct into the *M. xanthus* chromosome, plasmid integration was controlled by PCR (section 2.11.2).

Table 2.22: Confirmed plasmids, pCR2.1-Topo- and pSWU41-derivates.

No.	Name	Plasmid description
1	pKO_0144	681 bp amplicate (Taq) Primer KO_MXAN0144for/rev with gDNA <i>M. xanthus</i> DK1622 in pCR2.1Topo
2	pKO_1562	291 bp amplicate (Taq) Primer KO_MXAN1562for/rev with gDNA <i>M. xanthus</i> DK1622 in pCR2.1Topo
3	pKO_1808	643 bp amplicate (Taq) Primer KO_MXAN1808for/rev with gDNA <i>M. xanthus</i> DK1622 in pCR2.1Topo
4	pKO_1864	462 bp amplicate (Taq) Primer KO_MXAN1864for/rev with gDNA <i>M. xanthus</i> DK1622 in pCR2.1Topo
5	pKO_1893	294 bp amplicate (Taq) Primer KO_MXAN1893for/rev with gDNA <i>M. xanthus</i> DK1622 in pCR2.1Topo
6	pKO_1988	595 bp amplicate (Taq) Primer KO_MXAN1988for/rev with gDNA <i>M. xanthus</i> DK1622 in pCR2.1Topo
7	pKO_2440	700 bp amplicate (Taq) Primer KO_MXAN2440for/rev with gDNA <i>M. xanthus</i> DK1622 in pCR2.1Topo
8	pKO_3203	654 bp amplicate (Taq) Primer KO_MXAN3203for/rev with gDNA <i>M. xanthus</i> DK1622 in pCR2.1Topo
9	pKO_4189	432 bp amplicate (Taq) Primer KO_MXAN4189for/rev with gDNA <i>M. xanthus</i> DK1622 in pCR2.1Topo
10	pKO_4535	360 bp amplicate (Taq) Primer KO_MXAN4535for/rev with gDNA <i>M. xanthus</i> DK1622 in pCR2.1Topo
11	pKO_5055	744 bp amplicate (Taq) Primer KO_MXAN5055for/rev with gDNA <i>M. xanthus</i> DK1622 in pCR2.1Topo

Material and Methods

No.	Name	Plasmid description
12	pKO_5484	426 bp amplicate (Taq) Primer KO_MXAN5484for/rev with gDNA <i>M. xanthus</i> DK1622 in pCR2.1Topo
13	pD3702_F1	521 bp amplicate (Phusion) Primer D3702_F1for/rev with gDNA <i>M. xanthus</i> DK1622 in pCR2.1Topo
14	pD3702_F2	544 bp amplicate (Phusion) Primer D3702_F2for/rev with gDNA <i>M. xanthus</i> DK1622 in pCR2.1Topo
15	pD6967_F1	372 bp amplicate (Phusion) Primer D6967_F1for/rev with gDNA <i>M. xanthus</i> DK1622 in pCR2.1Topo
16	pD6967_F2	501 bp amplicate (Phusion) Primer D6967_F2for/rev with gDNA <i>M. xanthus</i> DK1622 in pCR2.1Topo
17	pDEL3702	521 bp fragment from \perp SacI/NotI of pD3702_F1 and 544 bp fragment from \perp NotI/BamHI of pD3702_F2 in pSWU41 \perp SacI/BamHI
18	pDEL6967	372 bp fragment from \perp SacI/NotI of pD6967_F1 and 501 bp fragment from \perp NotI/BamHI of pD6967_F2 in pSWU41 \perp SacI/BamHI

2.11.8 Transformation of bacteria via electroporation

a) Transformation of *E. coli* DH10B

For the preparation of electro-competent *E. coli* DH10B cells, the strain was grown to an O.D.₆₀₀ of 0.6 – 0.8. Aliquots of 1.5 ml were harvested by centrifugation (Biofuge fresco, 4 °C, 5 min at 16060 x g). Then, cell pellets were washed three times with ice-cold 10 % glycerol and finally resuspended in 40 µl sterile H₂O.

Insertion of DNA molecules was accomplished by electroporation. Electro-competent *E. coli* cells were mixed with different volumes (1, 2, 4 µl) of ligation batches from pCR2.1-Topo cloning or pSWU41-based ligations (section 2.11.7 b) and transferred into pre-cooled 1 mm electro-cuvettes. Thus, electroporation was performed in a GenePulser electroporator (table 2.7), using a voltage of 1.25 kV, a capacitance of 25 µF and a resistance of 200 Ω.

Directly after electroporation, phenotypic expression was realized in 1 ml LB medium (table 2.11) at 37 °C with 900 rpm (thermomixer Comfort) for 1 h.

Subsequently, cells were transferred to LB-agar plates, containing kanamycin with an end-concentration of 40 µg/ml. In case of conventional pCR2.1-Topo cloning, 40 µl of (20 mg/ml) x-Gal solution (in dimethylformamide) was distributed on the surface on the agar plates, which allows differentiation of clones, containing auto-ligated vectors or vector-insert constructs. After 16-24 h incubation, clones were isolated on new LB-agar plates (40 µg/ml kanamycin) and finally used to inoculate new liquid growth cultures (section 2.8.2) for plasmid isolation and verification. Inserts were controlled by digestion with RE(s) to prove internal PCR-derived sequences. In case of pSWU41-based in-frame deletion constructs, plasmids were finally confirmed by DNA sequencing.

Material and Methods

b) Transformation of *M. xanthus* DK1622

For the preparation of electro-competent *M. xanthus* DK1622 cells, the strain was grown to an O.D.₆₀₀ of 0.6 – 0.8. Aliquots of 1.5 ml were harvested by centrifugation (Biofuge fresco, 4 °C, 5 min at 16060 x g). Then, cell pellets were washed three times with sterile, ice-cold H₂O and finally resuspended in 40 µl sterile H₂O.

Insertion of DNA molecules was accomplished by electroporation. Electro-competent *M. xanthus* cells were mixed with different volumes (1, 2, 4 µl) of confirmed pCR2.1-Topo constructs or pSWU41-based constructs after extraction from *E. coli* (section 2.11.4), partially followed by purification (section 2.11.5). The mixture was transferred into pre-cooled 1 mm electro-cuvettes. Thus, electroporation was performed in a GenePulser electroporator (table 2.7), using a voltages between 0.85 – 1.25 kV, a capacitance of 25 µF and a resistance of 400 Ω.

Directly after electroporation, phenotypic expression was realized in 1.5 ml CTT medium (table 2.10) at 30 °C with 300 rpm (thermomixer Comfort) for 6 h.

Subsequently, cells were mixed with CTT-soft-agar and transferred to CTT-agar plates, both containing kanamycin with an end-concentration of 40 µg/ml. After a few days incubation, clones were isolated on new CTT-agar plates (40 µg/ml kanamycin) and used to cross-check sucrose sensitivity in case of pSWU41-based single crossover mutants.

Furthermore, *M. xanthus* clones were used to inoculate new growth cultures (section 2.8.1) for isolation of genomic DNA and final verification of plasmid-insertion in the *M. xanthus* genomic DNA by PCR.

2.12 Methodology of gene inactivation experiments in *M. xanthus*

Targeted gene inactivation experiments had become already standard procedures for myxobacteria (Bode *et al.*, 2006b; Simunovic *et al.*, 2007a; Meiser *et al.*, 2008). Briefly, two different strategies were used: a) in-frame gene deletion by double crossover and b) gene disruption by single crossover insertion

a) Gene inactivation by double crossover deletion

In the attempt to delete in-frame the putative Fur genes MXAN_3702 and 6967 by double crossover (figure 1.15), the two terminal fragments of both genes were amplified by Phusion PCR, and each cloned into plasmid pCR2.1-Topo in *E. coli*. The used primer pairs for the in-

Material and Methods

frame deletion can be found in table 2.16. The products were then excised as *SacI/BamHI* or *BamHI/XbaI* fragments, and cloned into plasmid pSWU41 which had been digested previously with both *SacI/XbaI* (section 2.11.7). Ligated plasmids were transferred into *E. coli*. Re-isolated plasmids were controlled by RE digestion and DNA-sequencing. The final deletion-constructs were introduced into *M. xanthus* by electroporation, and clones were selected for kanamycin resistance and sucrose sensitivity. Finally, correct integration was confirmed by PCR (primer: table 2.17).

To induce double homologous recombination (second crossover), single crossover mutants were grown in CTT medium without kanamycin and were repeatedly recultured in fresh medium. Aliquots were regularly drawn from the culture broth, mixed with CTT soft agar containing 5 % sucrose, and plated onto CTT agar containing 5 % sucrose. After a few days, single clones were transferred onto fresh CTT agar plates containing either sucrose or kanamycin.

For verification of double crossover mutants, colonies of *M. xanthus* which grew only on sucrose agar were analyzed genetically using PCR after counter selection (section 2.12). Both primers (table 2.17) harbor in the surrounding regions of the deleted sequence (Weinig *et al.*, 2003; Simunovic *et al.*, 2006). Wild type and positive markerless in-frame deletion mutants show significant differences in length (321 nt less in deletion mutant of MXAN_3702 and 324 nt in deletion mutant of MXAN_6967; figure 1.15 E) of the specific PCR amplificate.

The PCR amplificates of confirmed in-frame deletion mutants were finally sequenced to prove an intact genomic context without frame-shift.

b) Gene inactivation by single crossover insertion

The genes MXAN_0142, 0144, 1562, 1619, 1808, 1864, 1893, 1988, 2094, 2347, 2440, 2520, 3203, 4189, 4535, 5055 and 5484 were targets to be disrupted by insertional mutagenesis (single crossover). In all cases, internal gene fragments were amplified by *Taq* PCR using primers in the table 2.15. The PCR constructs were cloned into pCR2.1-Topo vectors (section 2.12), and the resulting plasmids were purified from *E. coli* DH10B and introduced into *M. xanthus* DK1622 via electroporation as described (section 2.11.8) (Bode *et al.*, 2006b), leading to kanamycin-resistant mutants, respectively. For detection of single crossover insertion mutants of *M. xanthus* (Meiser *et al.*, 2006a), PCR on genomic DNA was run, using one primer from the pair harboring in the vector backbone (table 2.17), giving a specific signal only if insertions occur at the expected position (figure 1.16 c).

Material and Methods

2.13 Secondary metabolite analysis by HPLC-MS

2.13.1 Extraction of secondary metabolites from XAD

All chemicals used for secondary metabolite analysis were obtained in highest quality standard.

Samples were obtained from *M. xanthus* cultures from CTT and CTT-Fe^{MIN}, as well as from mutant cultures, each time as triplicates (section 2.8.1). The XAD resin was separated from the culture medium by sieving, and washed twice with methanol (double of the culture volume), each time for 25 min. The extracts were pooled in roundbottom-flasks and then concentrated *in vacuo* and resuspended in methanol (10 % of the original culture volume).

2.13.2 HPLC-MS system and conditions

HPLC-MS analysis of secondary metabolite extracts was performed by an Agilent 1100 system (125 × 2 mm Nucleodur C₁₈/3 µm RP-column, Macherey Nagel) using a mixture of solvents A (H₂O + 0.1 % formic acid) and B (acetonitrile + 0.1 % formic acid) with a flow rate of 0.4 ml/min (Meiser *et al.*, 2008). The gradient starts with 5 % solvent B and a linear increase to 40 % within 30 min, followed by an increase to 95 % solvent B within 40 min. Mass detection was carried out using a Bruker Daltonics HCT Plus mass spectrometer operating in positive and negative ionization modes (mass range, *m/z* = 100–1000). An aliquot of 5 µl of different dilutions (1 % and 10 % in pure methanol) of the culture extracts were injected. The 7 compounds (DKxanthene 560, myxalamid A, myxovirescin A and myxochromide A2, Cittilin A, Myxochelin A and B) were detected semi-quantitative by MS² fragmentation in positive ionization mode.

Screening for novel metabolites was performed by detailed analysis of extracts grown under iron-poor conditions (CTT-Fe^{MIN}) using both UV/Vis (DAD-detector) and mass spectrometry in comparison to data obtained following growth in iron-repleted medium (CTT).

2.13.3 Qualitative and semi-quantitative data interpretation of 7 metabolites by HPLC-MS

Relative quantification was carried out on a representative member of each of the metabolite families DKxanthene 560, cittilin A, myxovirescin A (antibiotic TA), myxalamid A, myxochromide A2, and myxochelins A and B as previously described (Krug *et al.*, 2008a), based on peak integration from extracted ion chromatograms, and compared to yields from the wild type sample. Here, production rates were calculated as function of peak area O.D.⁻¹ h⁻¹

Material and Methods

¹, to account for minor differences in growth. All samples were compared along standard solutions.

2.13.4 Generation of standard solutions

Data from HPLC-MS of all samples were compared to standard solutions. These solutions were generated from independently grown wild type cultures (as triplicates) from *M. xanthus* under iron-rich conditions (CTT) as described (section 2.8.1). XAD extraction and HPLC-MS analysis was performed as before (section 2.13). To generate comparable values, production rates were calculated as function per time per O.D.₆₀₀ (as peak area O.D.⁻¹ h⁻¹).

3. Results

3.1 Bioinformatic analysis of iron uptake regulation in *M. xanthus*

As a starting point, the genome of *M. xanthus* was examined by bioinformatic methods to elucidate the biochemical background of iron-regulation. Therefore, amino acid sequence comparison with members of each Fur homologue family was performed (section 3.1.1) to identify potential candidates in the genome of *M. xanthus*. Further analysis of these proteins exhibit residues involved in metal-binding, including the preferred interaction partner, which allows the classification of the *M. xanthus* Fur proteins into known Fur sub-families (see introduction, section 1.1.2). In addition, Fur boxes in the genome of *M. xanthus* were detected (section 3.1.2), which allows the postulation of a Fur consensus sequence of *M. xanthus* (figure 3.3). Furthermore, the entirety of all proteins from *M. xanthus*, which are putatively involved in iron-uptake and transport could be determined (section 3.1.3).

3.1.1 Identification and classification of Fur homologues in *M. xanthus*

For the identification of Fur homologues in *M. xanthus*, BLAST analysis against the translated *M. xanthus* DK1622 genome was performed, using a sequence representative of each Fur sub-family: Fur, Zur, PerR, Mur, Nur and Irr. The result revealed clearly two Fur family members (MXAN_3702 and MXAN_6967), which show only 26 % mutual sequence identity.

In order to classify the two *M. xanthus* Fur homologues, important residues involved in selective metal binding (see introduction 1.1.2) were compared. These amino acids were originally discovered in crystal structures of Fur homologues, which have been solved or by site-directed mutagenesis of Fur proteins, as for e.g. Fur from *E. coli*, *P. aeruginosa* and *V. cholerae*; Zur from *M. tuberculosis*; Irr from *B. japonicum*, PerR from *B. subtilis*; and Nur from *S. coelicolor*.

In order to identify the equivalent residues in MXAN_3702 and MXAN_6967, a multiple sequence of Fur homologues were aligned by ClustalW2 algorithm, employing verified members of each Fur sub-type (figure 3.1). To identify Fur sub-types in this analysis, searches were carried out with the three additionally selected, closest homologues of MXAN_3702 and MXAN_6967 (detailed analysis set up, see section 2.5).

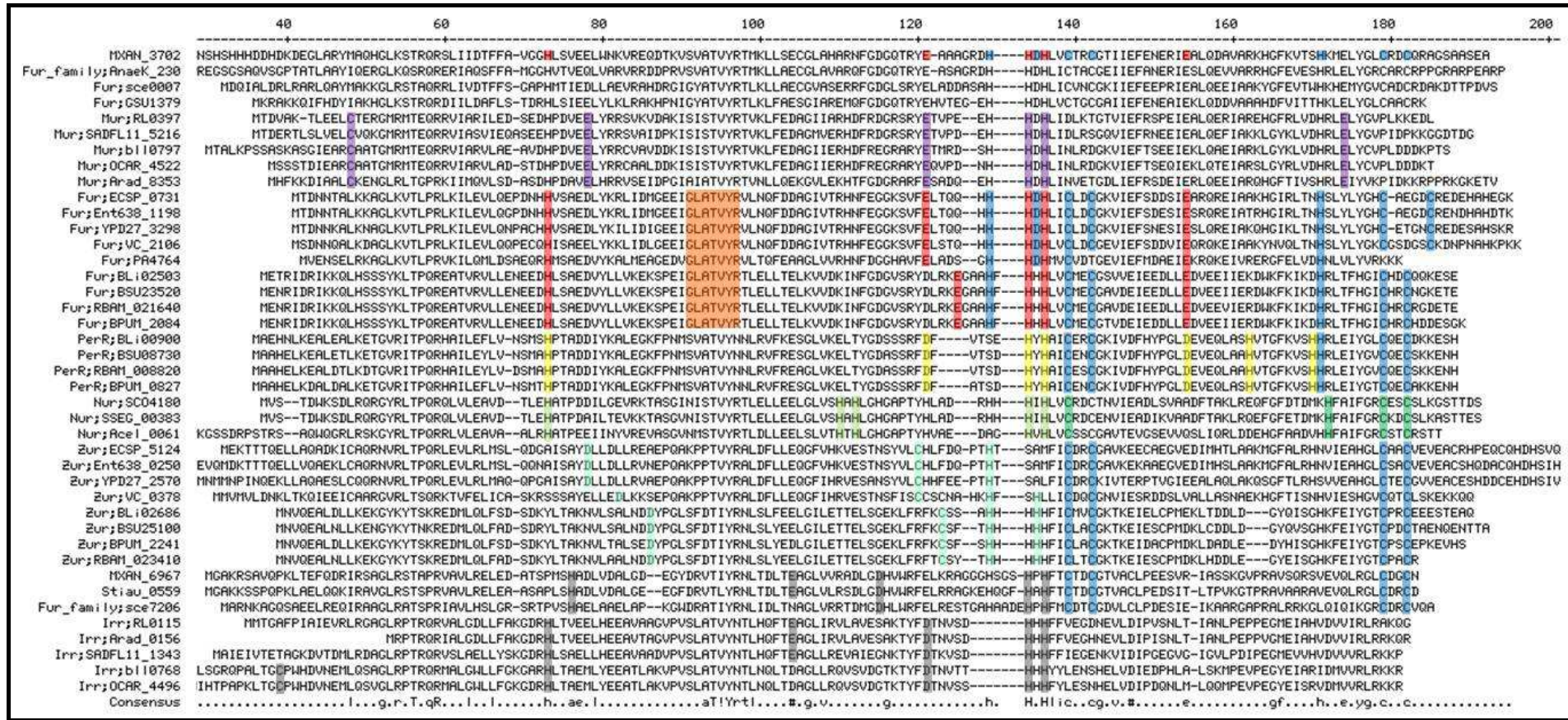


Figure 3.1: Multiple sequence alignment (ClustalW) of Fur and Fur family members.

Metal binding residues in the *M. xanthus* DK1622 sequences of MXAN_3702 and MXAN_6967 were detected by alignment with Fur sub-types (Fur, Nur, Mur, Zur, Per and Irr) from *A. cellulolyticus* 11B (Acel), *Anaeromyxobacter* sp. K (AnaEK), *A. radiobacter* K84 (Arad), *B. licheniformis* ATCC14580 (BLi), *B. japonicum* (bli), *B. pumilus* SAFR-032 (BPUM), *B. subtilis* str. 168 (BSU), *E. coli* O157:H7 (ECSP), *Enterobacter* sp. 638 (Ent638), *G. sulfurreducens* PCA (GSU), *M. xanthus* DK1622 (MXAN), *O. carboxidovorans* OM5 (OCAR), *P. aeruginosa* PAO1 (PA), *B. amyloliquefaciens* FZB42 (RBAM), *R. leguminosarum* (RL), *L. alexandrii* DFL-11 (SADFL11), *S. cellulosum* So ce56 (sce), *S. coelicolor* A3(2) (SCO), *S. sviceus* ATCC 29083 (SSEG), *S. aurantiaca* DW4/3-1 (Stiau), *V. cholerae* (VC) and *Y. pestis* D27 (YPD27).

The key residues are indicated by colors as follows: Red: Fe binding sites in Fur (Zn2 site); Blue: Zn structural site (Zn1 site); Purple: Mn binding site; Orange: DNA-binding motif of Fur; Yellow: regulatory site in PerR; Green: Ni regulatory site in Nur; Dark green Ni/Zn structural site in Nur; Light blue: Zn binding residues in Zur (Zn2 site); Grey: heme-binding motif in Irr.

Results

The proteins Fur, Zur, PerR and Nur contain two metal-binding sites, a proposed structural and a regulatory (see introduction, section 1.1.2). Both of these sites show variations in site compositions, which account for metal selectivity. The character and location of these motifs are shown in figure 3.1.

The analysis revealed that MXAN_3702 incorporates both metal binding motifs (a structural Zn- and a Fe-binding site) of iron-responsive Fur proteins, suggesting that it be functional in *M. xanthus* iron sensing. In contrast, the second Fur protein MXAN_6967 contains only a single structural Zn-binding motif, which is noted only in Irr and Mur proteins (see introduction, section 1.1.2). Two of the five residues which comprise the iron-binding site were found absent in MXAN_6967, clearly eliminating a possible function in iron sensing. To determine the sub-family relationship of MXAN_6967 more detailed, a phylogenetic tree analysis was performed using ClustalW2 algorithm (figure 3.2).

Results

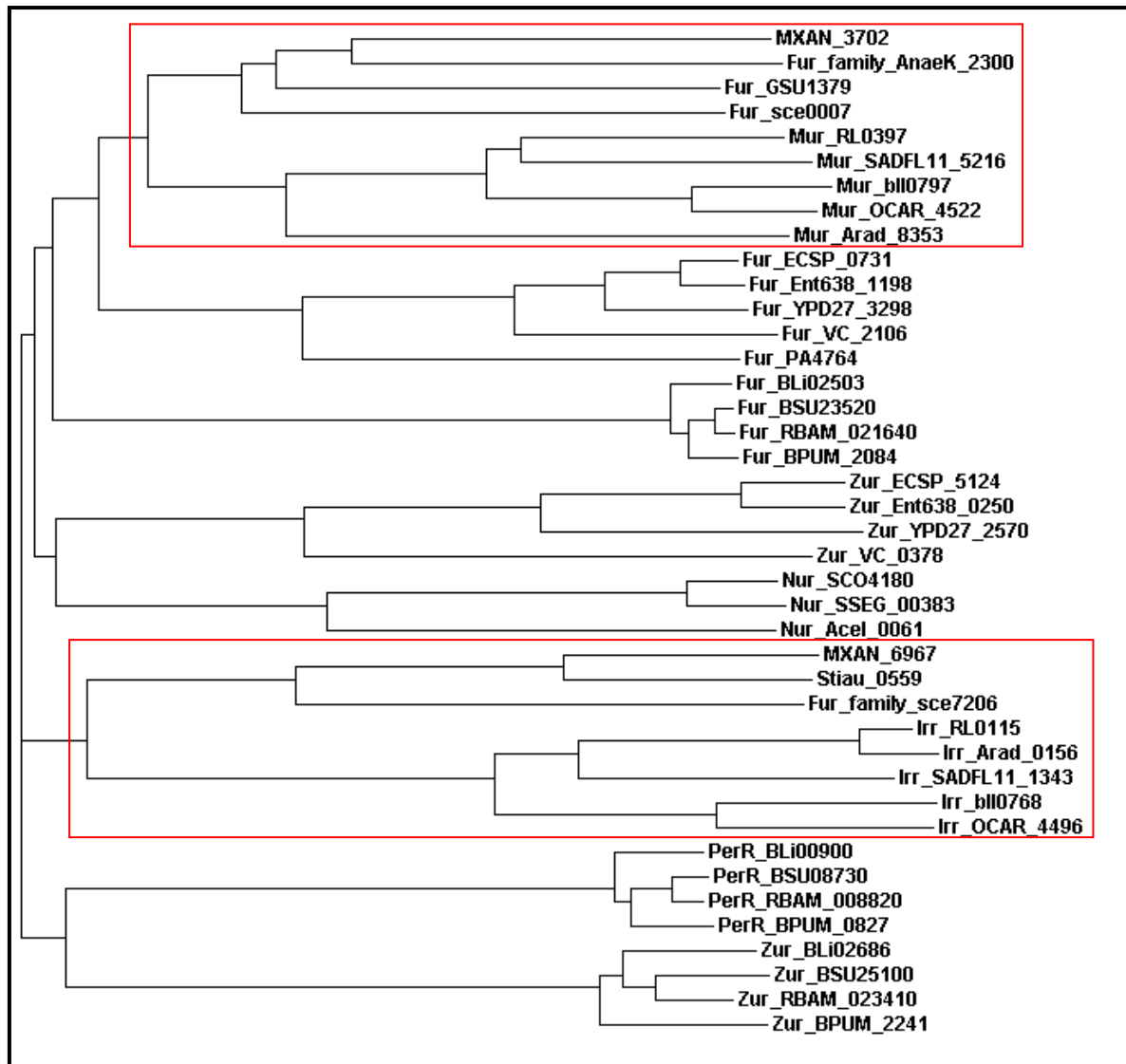


Figure 3.2: Phylogenetic tree analysis by ClustalW2 of *M. xanthus* DK1622 Fur proteins and related sub-families.

The two proteins from *M. xanthus* MXAN_3702 and MXAN_6967 can be found in the red boxes. The three each closest homologues of MXAN_3702 and MXAN_6967 and representatives of each type of Fur sub-family members (Fur, Zur, PerR, Mur, Nur, and Irr) were used in the classification of Fur sub-group belonging, employing sequences from *A. cellulolyticus* 11B (Acel), *Anaeromyxobacter* sp. K (Anaek), *A. radiobacter* K84 (Arad), *B. licheniformis* ATCC14580 (BLi), *B. japonicum* (bli), *B. pumilus* SAFR-032 (BPUM), *B. subtilis* str. 168 (BSU), *E. coli* O157:H7 (ECSP), *Enterobacter* sp. 638 (Ent638), *G. sulfurreducens* PCA (GSU), *M. xanthus* DK1622 (MXAN), *O. carboxidovorans* OM5 (OCAR), *P. aeruginosa* PAO1 (PA), *B. amyloliquefaciens* FZB42 (RBAM), *R. leguminosarum* (RL), *L. alexandrii* DFL-11 (SADFL11), *S. cellulosum* So ce56 (sce), *S. coelicolor* A3(2) (SCO), *S. sviceus* ATCC 29083 (SSEG), *S. aurantiaca* DW4/3-1 (Stiau), *V. cholerae* (VC) and *Y. pestis* D27 (YPD27).

The phylogenetic tree analysis discovered that MXAN_3702 and its closest homologues are only distantly related to the majority of iron-responsive Fur proteins from both Gram-positive and Gram-negative bacteria, consistent with convergent evolution of regulatory functions (figure 3.2). On the other hand, the phylogenetic analysis suggests that MXAN_6967 shows closest relationship to the heme-responsive Irr proteins, since MXAN_6967 is localized in this

Results

sub-group (figure 3.2). Albeit MXAN_6967 and other Fur homologues from myxobacteria (*S. aurantiaca* DW 4/-1 and *S. celluloseum* So ce56) show all high sequence homology among themselves, indicated in figure 3.2 by clustering in an additional branch from Irr proteins. In any case, the exact function of MXAN_6967 in *M. xanthus* remains uncertain.

3.1.2 Prediction of Fur boxes in the *M. xanthus* genome

Given the putative function of MXAN_3702 as an authentic (iron-responsive) Fur protein, the genome was scanned for the presence of Fur boxes using the software tool Virtual Footprint 3.0 (detailed description in section 2.5). Fur boxes are mostly located between the – 50 and – 10 sites of promoters of Fur-repressed genes (relative to transcriptional start sites), and consist of a 9-1-9 bp inverted repeat with a strain-specific consensus sequence (see introduction 1.1.2).

Here, Fur-binding sites match was limited to sequences with high similarities to the *P. aeruginosa* Fur model consensus sequence by position weight matrix (PWM) score higher than 9.9. Hits were checked manually for the distance to the putative Shine-Dalgarno sequence and gene start site, as well as for overall genomic context. Overall, 40 putative Fur boxes could be identified using this method (table 3.1).

Results

Table 3.1: Putative Fur boxes identified in the genome of *M. xanthus* DK1622.

Hits from Virtual Footprint version 3.0 with a position weight matrix (PWM) score higher than 9.9 were manually checked for the distance to the putative Shine-Dalgarno sequence and gene start site (max. 300 bp distance to start), as well as for overall genomic context. Uncharacterized proteins were further checked by BLAST analysis, positive results are shown in squared brackets. Genes in bold indicate possible operon structures (see text).

No.	PWM Score	Gene	Fur box sequence	Distance to translational start site	Description of proposed function
1	10.17	MXAN_0085	GATAAAAGTAATCATCAAC	35	Uncharacterized protein
2	9.91	MXAN_0122	GAAAAAGAATCTCAATCAC	8	Metal-dependent GTP cyclohydrolase II
3	11.15	MXAN_0501	GAAATTCTGATTATTTT	48	D-fructose-6-phosphate amidotransferase GlmS
4	10.71	MXAN_0502	TCAAATTCTTATTATTTAT	2	Transcriptional regulator AsnC
5	9.91	MXAN_0612	CATATTGGGTCTCAATAAC	115	Sensory box histidine kinase
6	9.95	MXAN_0675	GCGAATCATCATCATCGCC	10	Aha1 domain protein
7	12.24	MXAN_1314	GAAAATCAGTATCAATATC	27	Uncharacterized protein
8	10.67	MXAN_1559	GAAAACCACCATCATTGC	66	Uncharacterized protein [putative RNA methylase]
9	12.2	MXAN_1688	GAGAATGAGTATCAATATC	62	TonB family protein (MxcH homologue)
10	10.15	MXAN_1873	GACAAGACAAGTCATTAAC	47	Site-specific recombinase, integrase family
11	10.37	MXAN_1984	GACAATGCCCTCATTCC	274	Uncharacterized protein
12	9.95	MXAN_2884	GGAATTGTTGTCATTGTG	91	Tetratricopeptide repeat protein
13	9.96	MXAN_2974	CACAATGAACGTCAGTCG	36	Uncharacterized protein [endopeptidase inhibitor activity]
14	10.42	MXAN_3603	CCCAATAAACATTATTGAC	14	Uncharacterized protein
15	12.16	MXAN_3639	GAAAATGATATTCAATATC	16	Iron-chelator utilization protein (MxcB homologue)
16	12.66	MXAN_3647	GAAAATCATTCTCATTATC	51	2,3-Dihydro-2,3-dihydroxybenzoate dehydrogenase MxcC
17	10.65	MXAN_3915	GAGAACGATTCTCAATTTC	37	TonB family protein
18	10.2	MXAN_3974	GAAAAATACTATGATTCTG	37	Sensory box histidine kinase
19	11.58 or MXAN_4533	MXAN_4532 or MXAN_4533	GATAATAACGATTATTACA	216	Non-ribosomal peptide synthase
				124	Major facilitator family transporter
20	10.87	MXAN_4784	TAAAATCGTTTCATATTC	120	Sulfate permease SulP family
21	10.03	MXAN_5024	GTAAATGACAATCAACTTC	32	Delta-60 repeat domain protein
22	11.64	MXAN_5025	GATAATCGTTATCAGTTTC	50	Uncharacterized protein [putative iron-regulated protein A precursor]
23	10.08	MXAN_5047	AGCAATCCTCTCATTGCC	27	Uncharacterized protein

Results

No.	PWM Score	Gene	Fur box sequence	Distance to translational start site	Description of proposed function
24	10.28	MXAN_5098	CTCAATCGCAATCATTCCC	88	Ig domain protein
25	9.96	MXAN_5348	CGGAATCACCATCAGTGTG	7	M23 zinc metallopeptidase domain protein
26	10.07	MXAN_5416	CACAAGAAGATTCAATTCA	7	Uncharacterized protein
27	10.34	MXAN_5422	CCCACTGGTAATCATTCTG	85	Ankyrin repeat protein-protein interaction motifs
28	10.2	MXAN_5524	TTCAATCGTCATCATCATC	53	Uncharacterized protein [Glutathione-dependent formaldehyde-activating enzyme]
29	10.17	MXAN_5535	GACAATCACCTCGTTAGC	98	Uncharacterized protein [P-loop containing Nucleoside triphosphate hydrolase]
30	10.13	MXAN_5682	AAAAAAACCAAATCAGTAGC	18	Metal cation ZIP family transporter, Zn ²⁺ -Fe ²⁺ permease
31	9.99	MXAN_5919	CCAAATGCCTATCGTTCTC	4	Electron transfer flavoprotein, EtfA
32	11.02	MXAN_6068	AAGAATAACAATAAAATAAG	61	Uncharacterized protein
33	10.18	MXAN_6265	AAAAAACAAATGTCATTCA	132	Monooxygenase, FAD-dependent
34	10.57	MXAN_6607	GAGAACCGCTTCATTGC	4	Adventurous gliding motility protein AgmT
35	10.54	MXAN_6641	GATAACGATTCTCATATT	4	Uncharacterized protein [Hemin-binding protein HmuY]
36	11.04	MXAN_6642	GAGAACGTTATCAATTAT	113	Iron utilization domain protein
37	11.92	MXAN_6805	GATAATCAGTATCAATTTC	44	30S Ribosomal protein S4 RpsD
38	10.6	MXAN_6911	GCAAATCAATATCAATTGA	14	TonB-dependent receptor
39	10.05	MXAN_6998	TGCAATGTGCATCATTACG	297	Helix-turn-helix DNA-binding protein
40	10.06	MXAN_7353	GACATTGGGTGTCATTAA	4	Putative β-ketoacyl-acyl carrier protein synthase KASIII

Results

The genes with putative Fur boxes (table 3.1) belong to various parts of metabolism (as from siderophore biosynthesis, redox response or from iron uptake systems), while other genes with regulatory functions (as transcriptional regulator or sensory box histidine kinase) had not been connected before to the regulatory network, which maintains iron homeostasis. Some of the genes from table 3.1 may represent only the first genes of a polycistronic mRNAs, in detail:

- 1) **MXAN_1314** (to MXAN_1321): putative uncharacterized protein (MXAN_1315), TonB receptor (MXAN_1316), putative lipoprotein (MXAN_1317), hemin transport protein HemS (MXAN_1318), hemin ABC transporter (periplasmic hemin-binding protein) (MXAN_1319), hemin ABC transporter (permease protein) (MXAN_1320), and hemin ABC transporter, (ATP-binding protein) (MXAN_1321),
- 2) **MXAN_3647** (to MXAN_3640): Myxochelin-operon: isochorismate synthase MxcD (MXAN_3646), 2,3-dihydroxybenzoate-AMP ligase MxcE (MXAN_3645), isochorismatase MxcF (MXAN_3644), non-ribosomal peptide synthase MxcG (MXAN_3643), 3-deoxy-7-phosphoheptulonate synthase (MXAN_3642), major facilitator superfamily protein MxcK homologue (MXAN_3641), and the siderophore biosynthesis aminotransferase MxcL (MXAN_3640),
- 3) **MXAN_6641** (to MXAN_6635): putative uncharacterized protein [TonB-dependent receptor] (MXAN_6640), Chalcone/stilbene synthase family protein [naringenin-chalcone synthase homologue from *S. aurantiaca* DW4/3-1] (MXAN_6639), putative uncharacterized protein [isoprenylcysteine carboxyl methyltransferase ICMT) family] (MXAN_6638), acyl carrier protein (MXAN_6637), AMP-binding protein (MXAN_6636) and a FAD-binding monooxygenase (MXAN_6635),
- 4) **MXAN_6998** (to MXAN_6994): TonB domain protein (MXAN_6997), sensor protein asgD (two-component regulator required for A-signaling and nutrient sensing) (MXAN_6996), and a putative uncharacterized protein (MXAN_6995) and sensor signal transduction histidine kinase-related protein (MXAN_6994).

The detected Fur box sequences (table 3.1) were used to generate an initial consensus motif for *M. xanthus* Fur boxes (figure 3.3).

Results

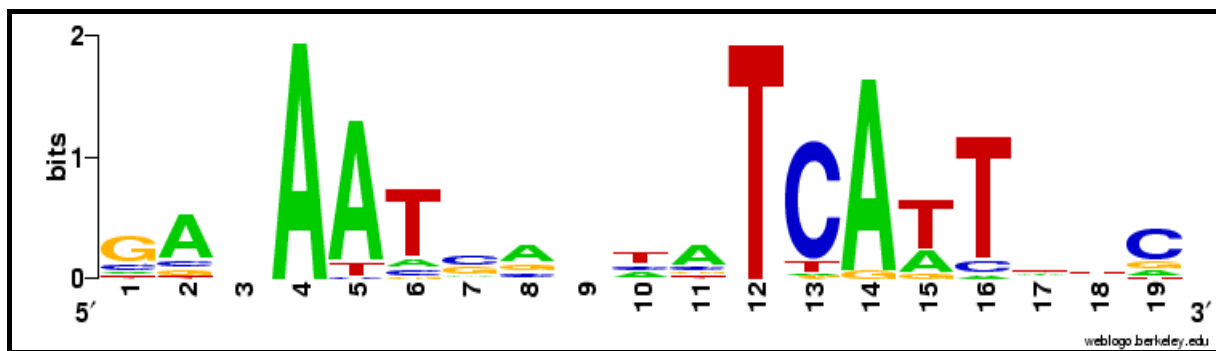


Figure 3.3: DNA sequence logo of the Fur box consensus sequence of *M. xanthus* DK1622.

The DNA sequence logo of the Fur-binding sites was derived by a bioinformatics approach. The sequence-logo representation shows the most conserved bases in the putative Fur box elements of *M. xanthus*.

According to the current bacterial model, a 19 bp sequence suggests to be organized as 9-1-9 palyndromic motif. These sequence motifs are recognized by iron-loaded Fur dimers (see introduction, section 1.1.2), each of the two sub-units interacts with one of two 9-1-9 palyndromic sequences of the inverted repeats of Fur boxes (figure 3.3).

No indication for the presence of a Fur box was found at the promoter regions of *M. xanthus* Fur homologues, neither for the *fur* gene (MXAN_3702), nor for the *fur* homologue (MXAN_6967). Nonetheless, it was expected that iron-limiting conditions would produce a significant change in *M. xanthus* phenotype as iron availability represents a very important nutrient-factor for cells generally. This implicates the analysis of the proteome as next consequent step to elucidate the response of *M. xanthus* to iron-limitation.

Results

3.1.3 Metabolic background of *M. xanthus* iron regulation

An important control point of iron-uptake marks the import-management via Fhu proteins or via TonB receptor-dependent processes (see introduction 1.1.1). In the process of screening the genome of *M. xanthus*, various TonB-dependent iron import systems and Fhu homologues were found to be present, much more than expected for Gram-negative bacteria. Furthermore, several evidences were made that *M. xanthus* is capable to use heme as iron source, accomplished by diverse proteins of heme import and degradation.

Table 3.2: Iron-uptake, transport and TonB-domain proteins of *M. xanthus* DK1622

No.	Gene number	Putative function
1	MXAN_0272	Carboxypeptidase/TonB domain protein
2	MXAN_0273	TonB-system transport protein ExbD
3	MXAN_0274	Biopolymer transport protein, ExbD/TolR family
4	MXAN_0275	TonB domain protein/TolQ proton channel
5	MXAN_0276	TonB domain protein
6	MXAN_0518	TRP/TonB domain protein
7	MXAN_0578	TonB domain protein
8	MXAN_0684	Ferric siderophore ABC transporter, ATP-binding protein; Fhu homologue
9	MXAN_0685	Ferric siderophore ABC transporter, permease protein
10	MXAN_0686	Ferric siderophore ABC transporter, permease protein
11	MXAN_0687	Ferric siderophore ABC transporter, periplasmic ferric siderophore-binding protein
12	MXAN_0770	Iron ABC transporter, periplasmic iron-binding protein
13	MXAN_0771	Iron ABC transporter, permease protein
14	MXAN_0772	Iron ABC transporter, ATP-binding protein
15	MXAN_0819	Transport energizing protein, ExbD/TolR family
16	MXAN_0820	TonB domain protein
17	MXAN_0821	TonB-dependent receptor
18	MXAN_0856	TonB family protein
19	MXAN_0983	Heavy metal efflux pump, CzcA family
20	MXAN_0985	Putative heavy metal resistance protein
21	MXAN_1316	TonB-dependent receptor
22	MXAN_1318	Hemin transport protein HemS
23	MXAN_1319	Hemin ABC transporter, periplasmic hemin-binding protein
24	MXAN_1320	Hemin ABC transporter, permease protein HemU
25	MXAN_1321	Hemin import ATP-binding protein HmuV
26	MXAN_1446	Biopolymer transport protein, ExbD/TolR family
27	MXAN_1447	Biopolymer transport protein, ExbD/TolR family
28	MXAN_1449	TonB domain protein
29	MXAN_1450	TonB-dependent receptor
30	MXAN_1688	TonB family protein
31	MXAN_2305	Putative TonB domain protein
32	MXAN_2680	Phosphotransferases of the serine or threonine-specific kinase subfamily/TonB domain protein

Results

No.	Gene number	Putative function
33	MXAN_2777	TonB domain protein
34	MXAN_2878	Putative bacterioferritin
35	MXAN_3044	TonB domain protein
36	MXAN_3256	Heme exporter protein CcmC
37	MXAN_3257	Heme exporter protein CcmB
38	MXAN_3279	Metal ion transporter family CorA
39	MXAN_3377	FHA/TonB domain protein
40	MXAN_3449	Heavy metal efflux pump, CzcA family
41	MXAN_3671	Heavy metal efflux pump, CzcA family
42	MXAN_3915	TonB domain protein
43	MXAN_4365	TonB-dependent receptor
44	MXAN_4559	TonB-dependent receptor
45	MXAN_4670	Biopolymer transport protein, ExbD/TolR family
46	MXAN_4746	TonB domain protein CirA
47	MXAN_4867	FHA domain/TonB domain protein
48	MXAN_5023	TonB domain protein FecA
49	MXAN_5682	Metal cation transporter, zinc (Zn^{2+})-iron (Fe^{2+}) permease (ZIP) family
50	MXAN_5754	Transport energizing protein TolR
51	MXAN_5755	TonB domain protein
52	MXAN_6000	Iron compound ABC transporter, periplasmic iron compound-binding protein
53	MXAN_6042	Putative ABC transporter, periplasmic substrate-binding protein
54	MXAN_6044	TonB-dependent receptor plug
55	MXAN_6484	Transport energizing protein, ExbD/TolR family
56	MXAN_6485	Ferric siderophore transporter, periplasmic energy transduction protein TonB
57	MXAN_6547	TonB-dependent receptor
58	MXAN_6568	Ferrichrome ABC transporter, permease protein
59	MXAN_6569	Ferrichrome ABC transporter, ATP-binding protein; Fhu homologue
60	MXAN_6575	FecCD transport family protein
61	MXAN_6576	Periplasmic iron-binding protein
62	MXAN_6579	TonB domain protein FepA
63	MXAN_6716	TonB-dependent receptor domain protein
64	MXAN_6737	TonB-dependent receptor
65	MXAN_6845	TonB-dependent receptor
66	MXAN_6861	Biopolymer transport protein, ExbD/TolR family
67	MXAN_6911	TonB-dependent receptor
68	MXAN_6920	Protozoan/cyanobacterial globin family protein
69	MXAN_6997	TonB domain protein
70	MXAN_7331	TonB-dependent receptor
71	MXAN_7437	Heavy metal efflux pump, CzcA family

Protein names and functions: CcmB/C: heme exporter protein; CirA: outer membrane receptor proteins, mostly iron transport; CorA: metal transporter gene family (mostly Mg^{2+}); CzcA: H^+ /heavy metal cation antiporter; ExbD: membrane bound transport proteins essential for ferric ion uptake in bacteria; FecA: outer membrane receptor for Fe^{3+} -dicitrate; FecCD: periplasmic-binding-protein-independent transport mechanism for Fe^{3+} -dicitrate; FepA: siderophore-iron transmembrane transporter activity; Fhu homologues: ferric hydroxymate binding/uptake protein; HemS: hemin storage and degradation protein; HemU: hemin permease protein; HmuV: involved in hemin import; TolQ: powers transport of siderophores across the bacterial outer membrane; TolR: TonB-dependent transport energizing protein.

Results

Searching the genome of *M. xanthus* for the presence of significant homologies to known regulatory RNAs as PrrF, ArrF or RyhB (see introduction 1.1.2) did not reveal any related sequence. This suggests *M. xanthus* can use other alternative strategies to control iron balance as for e.g. iron-correlated transcriptional regulators, which were detected in the chromosome of *M. xanthus*.

Some AraC-type regulators as for e.g. RipA (regulator of iron proteins A) are known to be involved in iron-balancing, acting as both positive and negative transcriptional factors (see introduction, section 1.1.2). In *M. xanthus* DK1622, 15 AraC-type regulatory proteins were found to be present (MXAN_0387, 0445, 0631, 0707, 1137, 1667, 1719, 2213, 2216, 3142, 3429, 4060, 6206, 6479 and 7078), but their role in metabolism is unclear, as long as the subset of genes which is controlled by the single regulators remains unknown.

Furthermore, three iron-associated, oxygen-sensitive Rrf2-like regulators (transcriptional main regulators of cytochromes) were identified in the genome of *M. xanthus* (MXAN_1152, MXAN_1643 and MXAN_6918).

As over-arching control over further heavy metal (arsenic/mercury) resistance operons, ArsR- or MerR-like repressors regulate expression of metal efflux systems with rather low metal selectivity. Several homologue genes of ArsR-like repressors were detected in *M. xanthus*: MXAN_1970, 2835, 3679, 5617, 6215, 6233, 6275, and 7501. Also MerR-like transcriptional regulators were found in the genome of *M. xanthus* (MXAN_0777, 0903, 0904, 1093, and 6983). Proteome experiments will give ultimate insight, if some of these transcriptional regulators could be involved in iron balancing in *M. xanthus*.

In order to analyze the *M. xanthus* genome by bioinformatic methods to precast response to iron-limitation, MXAN_3450 was found to be misannotated automatically as DNA-binding heavy metal response regulator (Goldman *et al.*, 2006), but BLAST results detect only high similarities to two-component transcriptional regulators (winged helix family), composed of three single domains: a phosphorylation site, a dimerization site, and a DNA binding site (60 % sequence identity I, and 76 % sequence similarity S). No evidence for any metal binding amino acids was detected in the protein sequence of MXAN_3450, showing also significant differences to Fur homologues or any other known heavy metal-associated transcriptional regulators in length, domain organization and sequences with special attention to metal binding domain architecture, which had been expected for a DNA-binding heavy

Results

metal response regulator. The result from BLAST analysis, that no homologies to any metal-associated regulators could be found, proves that MXAN_3450 was misannotated.

Results

3.2 Response of *M. xanthus* wild type to different iron availabilities

In order to evaluate response of *M. xanthus* to iron-limiting conditions, effects concerning growth (section 3.2.1), iron uptake (section 3.2.2), proteome response (section 3.2.3), and secondary metabolite production (section 3.2.5) were analyzed. Furthermore, protein-extracts from iron-rich and iron-low conditions were used to detect protein-interactions to the promoters regions of both Fur homologues; MXAN_3702 and MXAN_6967 (section 3.2.4).

3.2.1 Effect of iron restriction on growth of *M. xanthus*

Iron-limiting conditions are typically created by treating bacterial complex growth media with iron chelators. Here, the complex growth medium CTT (rich Casitone) was pre-treated with the transition metal chelating agent Chelex (see section 2.7.1). Analysis of the untreated (CTT) and treated (CTT-Fe^{MIN}) media by colorimetric assay using Ferrospectral revealed iron concentrations of 4.8 ± 0.6 and ca. $0.5 \pm 0.12 \mu\text{M}$, respectively. A more precise determination of the iron concentration of CTT-Fe^{MIN} was not possible, reaching the detection limit (at ca. $0.3 \mu\text{M}$) of the used photospectrometric method. The declared concentration of ca. $0.5 \mu\text{M}$ of CTT-Fe^{MIN} was estimated by extrapolation of the regression-line. The growth conditions are explained in detail in section 2.8, the growth curves of *M. xanthus* DK1622 on CTT and CTT-Fe^{MIN} are shown in figure 3.4.

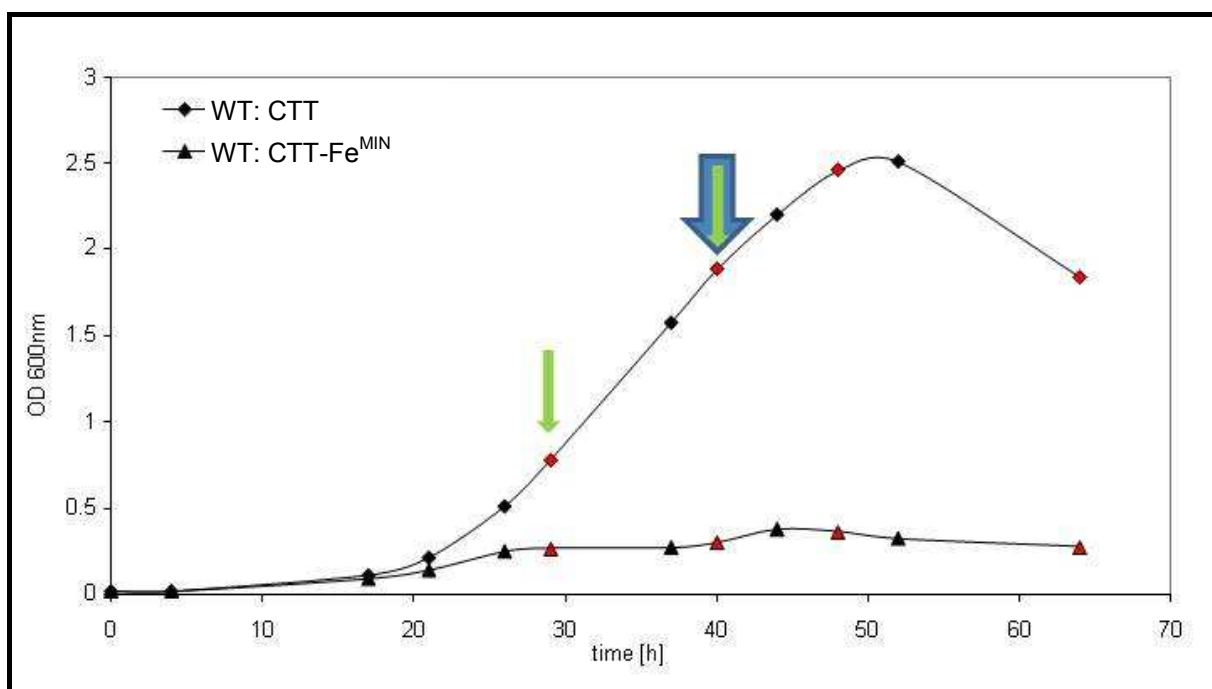


Figure 3.4: Effects of iron concentrations on growth of *M. xanthus* DK1622.

Growth profiles of *M. xanthus*, obtained from iron-rich (diamonds, CTT medium containing $4.8 \mu\text{M}$ iron) or from iron-poor condition (triangles, CTT-Fe^{MIN} medium containing ca. $0.5 \mu\text{M}$ iron). Comparative

Results

samples for iron-uptake measurement and HPLC-MS analysis were taken after 29, 40, 48 and 64 h (red). Further sampling for DNA pull-down assays was accomplished after 40 h of growth (blue arrow), for proteome analysis after 29 and 40 h (green arrows).

The strain *M. xanthus* exhibited a characteristic growth pattern in untreated CTT medium with an exponential phase between ca. 25 and 50 h and after reaching the maximum O.D.₆₀₀ of ca. 2.5 immediately entering death phase (figure 3.4). In contrast, in CTT-Fe^{MIN} growth entered stationary phase after approximately 25 h and the O.D.₆₀₀ never exceeded 0.4.

3.2.2 Effect of iron restriction on iron uptake by *M. xanthus*

Iron uptake rates of *M. xanthus* samples were quantified in both CTT and CTT-Fe^{MIN}, by measuring the concentration of iron present before and after growth for 29, 40, 48 or 64 h, respectively. The rates were calculated as function with the unit nmol h⁻¹ O.D.⁻¹ to account for differences in growth rates in the iron-rich and iron-poor media (table 3.3).

Table 3.3: Rates of iron uptake by *M. xanthus* DK1622 wild type cells in CTT and CTT-Fe^{MIN}.

Wild type (WT) cells of *M. xanthus* were grown in liquid cultures under iron-rich (CTT medium containing 4.8 µM iron) or under iron-poor condition (CTT-Fe^{MIN} medium containing ca. 0.5 µM iron). The uptake rate from CTT at time point 64 h was set to 100 % (marked by ^X) for comparison with uptake rates from iron-limiting conditions and mutant strains (table 3.11).

Wild type samples	O.D. ₆₀₀	Time (h)	Iron uptake rate (nmol O.D. ⁻¹ h ⁻¹)	% of WT iron uptake
CTT (1)	0.78	29	43.6 ± 0.6	
CTT (2)	1.88	40	16.9 ± 1.4	
CTT (3)	2.46	48	31.6 ± 0.2	
CTT (4)	1.84	64	37.1 ± 0.4	100.0 ^X
CTT-Fe ^{MIN} (1)	0.27	29	12.6 ± 0.5	
CTT-Fe ^{MIN} (2)	0.30	40	13.8 ± 0.1	
CTT-Fe ^{MIN} (3)	0.37	48	12.4 ± 0.1	
CTT-Fe ^{MIN} (4)	0.31	64	16.0 ± 0.1	

In iron-replete medium, uptake was highest in the period preceding exponential growth (0–29 h; 43.6 nmol h⁻¹ O.D.⁻¹), lowest during the exponential phase (29–40 h; 16.9 nmol h⁻¹ O.D.⁻¹), and then rose again once growth leveled off (48–64 h; 37.0 nmol h⁻¹ O.D.⁻¹). The rate of iron influx was lower (ca. 30-50 % of iron-uptake under iron-rich conditions) and essentially constant under iron-poor conditions (average over all time points, 13.7 nmol h⁻¹ O.D.⁻¹).

Results

However, as the concentration of iron in the CTT-Fe^{MIN} medium was only 10 % of that in standard CTT, the uptake efficiency had increased by 3-5fold. This clearly shows that the triggering effect of low iron concentrations had activated iron uptake systems as responds in *M. xanthus*.

3.2.3 Proteomic response of *M. xanthus* to iron-limitation

To obtain deeper insight into the cellular response of iron-limitation in *M. xanthus*, the proteome profiles of *M. xanthus* grown under iron-rich and iron-poor conditions were compared using 2D-DIGE (section 3.2.3 a), inclusive MS/MS-based protein identification (section 3.2.3 b) and analysis of phosphorylation of differently expressed protein spots (section 3.2.3 c). A detailed description of analysis can be found in section 2.9.

a) Proteome analysis of *M. xanthus* using 2D-DIGE technology

For 2D-DIGE analysis, samples in triplicate were obtained from both cultures (CTT or CTT-Fe^{MIN}) after 29 and 40 h of growth (detailed description, see figure 2.1). An example of the three images, obtained from a single 2D-DIGE gel is shown in figure 3.5.

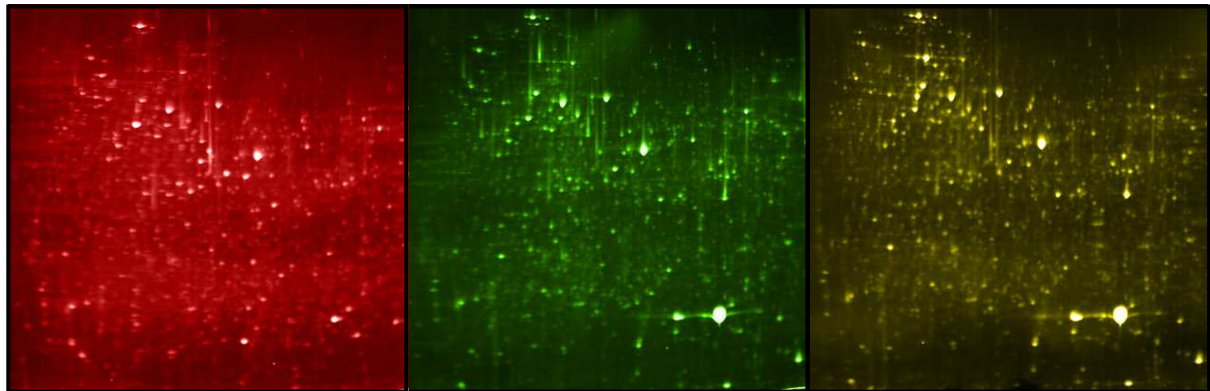


Figure 3.5: Examples of the Cy3-, Cy5- and Cy2-images from a single 2D-DIGE gel.

Protein patterns of *M. xanthus* DK1622, grown on different iron-concentrations, were compared by 2D-DIGE technology. Here, samples from 29 h were taken as an example, iron-rich sample labeled with Cy5 (red), iron-poor with Cy3 (green) and the internal standard with Cy2.

In average, 1979 protein spots were detected per image with a deviation of less than 1.9 % between all 2D-DIGE gels. In order to minimize the detection of non-specific variation between samples, statistical analysis was carried out to determine proteins which were

Results

consistently up-regulated or down-regulated at both time points for at least 2fold. By this criterion, a total of 172 differently expressed protein spots could be detected. From these, 74 protein spots were detected with lower expression under iron starvation, and 98 with higher expression. The intensity distribution of the average ratios of the 1979 individual spots can be found in figure 3.6.

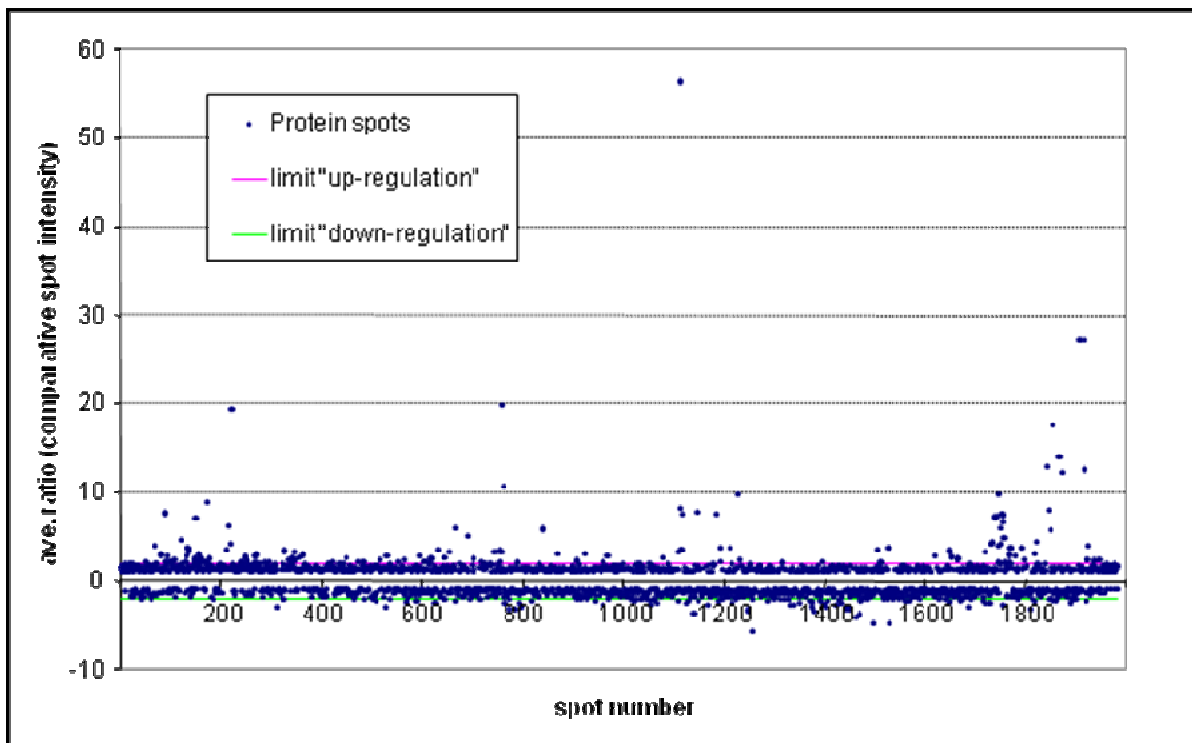


Figure 3.6: Distribution of average ratios of spots from 2D-DIGE analysis of *M. xanthus* DK1622.

1979 individual spots were detected in average on all 2D-DIGE gels. Protein spots of interest have to show a change in intensity higher than 2fold (marked by purple and green line). The spot number is correlated to spot detection, so low numbers represent very large, high number very small proteins.

b) Identification of proteins from proteome analysis

Subsequently, all 172 protein spots, which show an altering in spot intensity were excised, in-gel digested with trypsin and further analyzed by matrix-assisted-laser desorption ionization/tandem time-of-flight mass spectrometry (MALDI-ToF/ToF). The resulting peptide profiles (MS) and sequence analysis (MS/MS) were used for protein database searches (detailed description, see section 2.9.3). All proteins from proteome response, including the ratio of up- or down-regulations and putative protein functions are summarized in table 3.4. By the analysis, 169 protein spots could be identified as 131 distinct proteins. Subsequently, the amino acid sequences of proteins with unknown functions were employed for protein

Results

BLAST analysis.

Results

Table 3.4: Proteome results of *M. xanthus* DK1622 under iron-limiting conditions.

All identified *M. xanthus* proteins, which were found to be down- or up-regulated under iron-restricted conditions, were here ordered by gene number. The table includes the extent of up- or down-regulation, T-test ($P < 0.05$) and protein functions (putative protein functions from BLAST are shown in square brackets).

No.	Av. ratio	T-test	Gene no.	Description of proposed function
Proteins with reduced expression under iron-limited conditions				
1	-2.64	0.008	MXAN_0264	DNA topoisomerase activity GyrB
2	-2.27	0.012	MXAN_0350	Membrane protein
3	-2.53	0.013	MXAN_0365	Hypothetical protein [DUF 82]
4	-2.29	0.012	MXAN_0405	GTP-binding protein (2Fe-2S ferredoxin) YchF
5	-2.12	0.013	MXAN_0463	Xaa-Pro aminopeptidase PepP
6	-2.84	0.023	MXAN_0498	Lipoprotein
7	-2.8	0.006	MXAN_0559	ABC transporter ATP-binding protein Mac1
8	-2.1	0.081	MXAN_0599	Hypothetical protein [DUF 262/1524]
9	-2.74	0.032	MXAN_0720	Sensor histidine kinase
10	-2.98	0.008	MXAN_1073	Hsp33 family protein
11	-2.39	0.012	MXAN_1158	Hypothetical protein [Fe-S assembly protein Suft]
12	-3.56	0.012	MXAN_1539	Lipoprotein
13	-2.62	0.012	MXAN_1619	Hypothetical protein [Helix-turn-helix type 11 domain protein]
14	-2.46	0.011	MXAN_1892	Serine/threonine protein kinase
15	-3.76	0.011	MXAN_2016	Prolyl endopeptidase Pep
16	-3.4	0.014	MXAN_2318	Glutathione-disulfide reductase Gor
17	-2.61	0.015	MXAN_2408	Translation elongation factor G FusA
18	-2.1	0.039	MXAN_2408	Translation elongation factor G FusA
19	-2.04	0.012	MXAN_2609	Exonuclease ABC subunit A UvrA
20	-2.02	0.008	MXAN_2640	Hypothetical protein
21	-2.22	0.012	MXAN_2822	Hypothetical protein
22	-2.15	0.042	MXAN_3068	Elongation factor Tuf1
23	-2.05	0.027	MXAN_3068	Elongation factor Tuf1
24	-2.14	0.022	MXAN_3079	Hypothetical protein
25	-2.05	0.043	MXAN_3080	Hypothetical protein
26	-2.03	0.009	MXAN_3297	Elongation factor G 2 FusA
27	-3.23	0.011	MXAN_3298	Translation elongation factor Tuf2
28	-2.67	0.005	MXAN_3307	50S Ribosomal protein L29 RpmC
29	-2.25	0.032	MXAN_3326	RNA polymerase subunit A RpoA
30	-2.04	0.028	MXAN_3326	RNA polymerase subunit A RpoA
31	-2.03	0.011	MXAN_3326	RNA polymerase subunit A RpoA
32	-2.17	0.011	MXAN_3537	NADP-dependent isocitrate dehydrogenase Icd
33	-2.17	0.015	MXAN_3540	Succinate dehydrogenase SdhB (Fe-S protein)
34	-2.85	0.013	MXAN_3542	Succinyl-CoA synthetase subunit A SucD
35	-2.88	0.011	MXAN_3556	Hypothetical protein [M18 bacteriocin protein]
36	-2.07	0.036	MXAN_3571	Hypothetical protein [band 7 protein]
37	-4.85	0.034	MXAN_3617	Hypothetical protein
38	-2.09	0.011	MXAN_3633	Hypothetical protein [DUF407]
39	-2.14	0.016	MXAN_3777	Inosine-5'-monophosphate dehydrogenase GuaB
40	-2.57	0.012	MXAN_3793	Ribosomal protein S1 RpsA
41	-2.58	0.008	MXAN_4137	Hypothetical protein
42	-2.31	0.010	MXAN_4242	Transcriptional regulator
43	-2.32	0.015	MXAN_4467	60 kDa chaperonin GroEL1
44	-2.3	0.049	MXAN_4467	60 kDa chaperonin GroEL1
45	-2.22	0.037	MXAN_4467	60 kDa chaperonin GroEL1
46	-2.13	0.036	MXAN_4467	60 kDa chaperonin GroEL1
47	-2.12	0.024	MXAN_4467	60 kDa chaperonin GroEL1

Results

No.	Av. ratio	T-test	Gene no.	Description of proposed function
48	-3.06	0.023	MXAN_4535	ECF sigma factor
49	-2.12	0.025	MXAN_4802	Hypothetical protein [DUF876]
50	-2.92	0.028	MXAN_4895	60 kDa chaperonin GroEL2
51	-2.6	0.041	MXAN_4895	60 kDa chaperonin GroEL2
52	-2.33	0.055	MXAN_4895	60 kDa chaperonin GroEL2
53	-2.32	0.038	MXAN_4895	60 kDa chaperonin GroEL2
54	-2.31	0.039	MXAN_4895	60 kDa chaperonin GroEL2
55	-2.3	0.032	MXAN_4895	60 kDa chaperonin GroEL2
56	-2.12	0.043	MXAN_4895	60 kDa chaperonin GroEL2
57	-2.1	0.011	MXAN_4895	60 kDa chaperonin GroEL2
58	-2.08	0.068	MXAN_4895	60 kDa chaperonin GroEL2
59	-3.23	0.037	MXAN_5055	Hypothetical protein [methyltransferase/chromosome segregation protein SMC domain]
60	-2.08	0.031	MXAN_5168	ABC Transporter (ATP-binding) protein
61	-2.11	0.028	MXAN_5484	Hypothetical protein [putative serine/threonine protein kinase]
62	-3.24	0.041	MXAN_5511	Hypothetical protein
63	-2.47	0.007	MXAN_5588	Hypothetical protein
64	-2.66	0.010	MXAN_5846	Hypothetical protein [M14-like metallo-carboxypeptidase]
65	-2.28	0.010	MXAN_6032	Response regulator/chemotaxis protein CheW
66	-2.51	0.009	MXAN_6496	Thioredoxin peroxidase Tpx
67	-2.22	0.009	MXAN_7020	CRISPR-associated helicase Cas3
68	-2.41	0.011	MXAN_7040	Outer membrane protein P1
69	-2.2	0.015	MXAN_7393	Hypothetical protein [sigma-54 transcriptional regulator, Fis family]
70	-2.15	0.011	MXAN_7446	Hypothetical protein
71	-2.15	0.044	MXAN_7492	Hypothetical protein
72	-2.41	0.008	MXAN_7497	Signal-peptide processing peptidase (M16B)
73	-5.8	0.001		Not identified
74	-3.11	0.012		Not identified

Proteins with increased expression under iron-limited conditions

No.	Av. ratio	T-test	Gene no.	Description of proposed function
75	3.75	0.017	MXAN_0142	WD domain G-beta repeat protein
76	2.9	0.008	MXAN_0144	Hypothetical protein [WGR domain protein]
77	3.16	0.018	MXAN_0144	Hypothetical protein [WGR domain protein]
78	2.05	0.028	MXAN_0236	DNA polymerase III subunit B DnaN
79	2.18	0.014	MXAN_0237	Hypothetical protein
80	7.78	0.043	MXAN_0303	Oxidoreductase aldo/keto reductase family
81	2.23	0.010	MXAN_0351	Thioredoxin domain protein
82	6.06	0.009	MXAN_0498	Lipoprotein
83	2.08	0.039	MXAN_0543	Peptidase M20 (glutamate carboxypeptidase) family
84	3.71	0.027	MXAN_0548	Glutathione-S-transferase domain protein
85	2.51	0.049	MXAN_0599	Hypothetical protein [DUF262/1524]
86	4.39	0.024	MXAN_0790	Hypothetical protein
87	5.75	0.028	MXAN_0791	Peptidase M16 (pitrilysin) family
88	3.97	0.002	MXAN_0831	Saccharopine dehydrogenase Lys1
89	27.16	0.047	MXAN_0866	DPS protein TpF2
90	3.34	0.029	MXAN_0959	Nuclease SbcC
91	2.81	0.045	MXAN_1024	Hypothetical protein
92	7.49	0.022	MXAN_1069	Hypothetical protein
93	2.23	0.010	MXAN_1141	Peptidase M16 (pitrilysin) family
94	2.17	0.010	MXAN_1264	Phosphoenolpyruvate carboxykinase (GTP) PckG

Results

No.	Av. ratio	T-test	Gene no.	Description of proposed function
95	2.99	0.038	MXAN_1318	Hemin transport protein HemS
96	27.14	0.039	MXAN_1562	DPS protein TpF1
97	12.83	0.033	MXAN_1563	Alkyl hydroperoxide reductase D AhpD
98	13.96	0.021	MXAN_1563	Alkyl hydroperoxide reductase D AhpD
99	2.09	0.042	MXAN_1564	Alkyl hydroperoxide reductase C AhpC
100	3.13	0.041	MXAN_1564	Alkyl hydroperoxide reductase C AhpC
101	3.69	0.046	MXAN_1564	Alkyl hydroperoxide reductase C AhpC
102	2.44	0.013	MXAN_1591	Hypothetical protein [Sigma-54 factor/ AAA ATPase]
103	3.85	0.011	MXAN_1808	Restriction/modification enzyme (N6-adenine DNA methylase)
104	2.04	0.017	MXAN_1815	Hypothetical protein [DUF 2169]
105	3.33	0.035	MXAN_1864	N6-adenine DNA methyltransferase
106	12.24	0.013	MXAN_1893	Hypothetical protein [ClpX protease]
107	8.16	0.039	MXAN_1954	Thioredoxin-disulfide reductase TrxB
108	4.59	0.008	MXAN_1988	Hypothetical protein [SAM-dependent methyltransferases]
109	2.74	0.032	MXAN_2073	Polyribonucleotide nucleotidyltransferase PnpA
110	2.34	0.051	MXAN_2094	Hypothetical protein [TPR-domain protein]
111	2.91	0.001	MXAN_2347	Hypothetical protein [Protamine P1 homologue]
112	4.75	0.025	MXAN_2410	Hypothetical protein
113	2.69	0.098	MXAN_2440	Hypothetical protein [Provisional transcription termination Rho domain]
114	3.2	0.039	MXAN_2440	Hypothetical protein [Provisional transcription termination Rho domain]
115	2.69	0.043	MXAN_2513	General secretory pathway protein E GspE
116	2.57	0.013	MXAN_2520	FHA domain/tetratricopeptide repeat protein
117	2.04	0.019	MXAN_2539	Hypothetical protein
118	2.45	0.023	MXAN_2675	Glutamyl-tRNA synthetase GltX
119	2.55	0.044	MXAN_2685	Chemotaxis protein CheW
120	3.72	0.025	MXAN_2729	NADH dehydrogenase I subunit D
121	5.78	0.012	MXAN_2940	Hypothetical protein
122	2.19	0.011	MXAN_2952	Hypothetical protein
123	2.9	0.013	MXAN_3068	Translation elongation factor EF-Tu1
124	5.95	0.045	MXAN_3307	50S Ribosomal protein L29 RpmC
125	3.53	0.025	MXAN_3379	GTP-binding protein TypA
126	2.13	0.030	MXAN_3388	Carbamoyl-phosphate synthetase CarB
127	2.72	0.029	MXAN_3571	Hypothetical protein [band 7 protein]
128	9.62	0.036	MXAN_3617	Hypothetical protein
129	10.62	0.044	MXAN_3640	Aminotransferase MxcL
130	19.74	0.037	MXAN_3640	Aminotransferase MxcL
131	7.54	0.012	MXAN_3644	Isochorismatase MxcF
132	3.39	0.027	MXAN_3647	2,3-Dihydro-2,3-dihydroxybenzoate dehydrogenase MxcC
133	2.48	0.012	MXAN_3679	Hypothetical protein [ArsR-like regulator]
134	2.07	0.046	MXAN_4003	Oxidoreductase
135	19.25	0.036	MXAN_4003	Oxidoreductase
136	12.5	0.013	MXAN_4067	Ferredoxin-like protein ThiS
137	2.17	0.013	MXAN_4149	Response regulator FrzS
138	3.42	0.014	MXAN_4189	Tetratricopeptide repeat protein
139	7.18	0.041	MXAN_4863	Adventerous gliding motility protein AgmK
140	7.61	0.007	MXAN_5023	TonB-dependent receptor; outer membrane receptor
141	2.82	0.029	MXAN_5055	Hypothetical protein [methyltransferase/ chromosome segregation protein SMC domain]

Results

No.	Av. ratio	T-test	Gene no.	Description of proposed function
142	7.06	0.047	MXAN_5055	Hypothetical protein [methyltransferase/chromosome segregation protein SMC domain]
143	2.76	0.049	MXAN_5070	Hypoxanthine phosphoribosyltransferase Hpt
144	7.91	0.041	MXAN_5108	Argininosuccinate synthase ArgG
145	4.14	0.025	MXAN_5180	Hypothetical protein
146	3.26	0.037	MXAN_5401	Hypothetical protein
147	8.74	0.044	MXAN_5484	Hypothetical protein [putative serine/threonine protein kinase]
148	3.3	0.020	MXAN_5588	Hypothetical protein
149	3.07	0.035	MXAN_5597	Cell division protein FtsZ
150	6.68	0.027	MXAN_5650	Hypothetical protein
151	2.31	0.035	MXAN_5670	Thioredoxin TrxB2
152	56.33	0.049	MXAN_5670	Thioredoxin TrxB2
153	2.12	0.016	MXAN_5743	Hypothetical protein [PEGA domain protein]
154	2.04	0.013	MXAN_5795	Exonuclease
155	3.17	0.044	MXAN_5806	Glutamate-cysteine ligase
156	2.35	0.010	MXAN_5855	Hypothetical protein [Phosphate-selective porin superfamily]
157	17.48	0.031	MXAN_6434	Hypothetical protein
158	2.68	0.010	MXAN_6438	ATP-dependent protease ClpP2
159	3.6	0.041	MXAN_6450	β -lactamase-related protein
160	3.22	0.041	MXAN_6482	Oxidoreductase aldo/keto reductase family
161	7.44	0.046	MXAN_6482	Oxidoreductase aldo/keto reductase family
162	2.06	0.039	MXAN_6502	Hypothetical protein [SGNH-hydrolase]
163	5.83	0.008	MXAN_6524	CobW/P47K family protein
164	4.07	0.014	MXAN_6536	Antioxidant/oxidoreductase, thioredoxin family AhpC/Tsa
165	7.37	0.047	MXAN_6536	Antioxidant/oxidoreductase, thioredoxin family AhpC/Tsa
166	2.68	0.010	MXAN_6911	TonB-dependent receptor
167	4.09	0.024	MXAN_6911	TonB-dependent receptor
168	4.97	0.025	MXAN_7028	ATP Synthase F1 subunit A AtpA
169	2.86	0.044	MXAN_7090	Glutathione peroxidase family protein
170	3.73	0.013	MXAN_7380	CBS domain protein
171	4.35	0.013	MXAN_7492	Hypothetical protein
172	9.61	0.038		Not identified

To provide a better overview, all proteins were categorized by metabolic function (table a1). A selection of *M. xanthus* iron-metabolism proteins, identified in proteome experiments, is shown in table 3.5. The selection of the respective proteins based on biochemical context and a similar change in expression under iron-limitation, typically observed for this sub-group of proteins. Many of the proteins can be correlated to iron-uptake system, siderophore biosynthesis, or iron-induced changes of redox status (table 3.5).

Results

Table 3.5: Selection from proteome response: categorized proteins.

Differentially regulated proteins of *M. xanthus* DK1622 under iron-limiting conditions were categorized by their biochemical function. The ratio of relative expression levels under iron-rich and iron-limited conditions for the selected proteins is shown column 2 ("Fold change")

Biochemical context / Gene no.	Fold change	Description of proposed function
Proteins with increased expression under iron-limited conditions		
Iron acquisition		
MXAN_1318	3.0	HemS (heme binding protein)
MXAN_3640	10.6, 19.7 ^a	MxCL (myxochelin biosynthesis)
MXAN_3644	7.5	MxCF (myxochelin biosynthesis)
MXAN_3647	3.4	MxCC (myxochelin biosynthesis)
MXAN_5023	7.6	TonB-dependent receptor
MXAN_6911	4.1 ^a , 2.7 ^b	TonB-dependent receptor
Redox stress resistance		
MXAN_0303	7.8	Oxidoreductase, aldo/keto reductase family
MXAN_0351	2.2	Thioredoxin domain protein
MXAN_0866	27.2	Ferritin/ DPS family protein (TpF2)
MXAN_1562	27.1	Ferritin/ DPS family protein (TpF1)
MXAN_1563	12.8, 14.0 ^a	AhpD (Alkyl hydroperoxide reductase D)
MXAN_1564	2.1, 3.1, 3.7 ^a	AhpC (Alkyl hydroperoxide reductase C)
MXAN_1954	8.2	TrxB1 (Thioredoxin disulfide reductase)
MXAN_4003	2.0, 19.5 ^a	Oxidoreductase
MXAN_5670	2.3, 56.3 ^a	TrxB2 (Thioredoxin)
MXAN_6482	3.2, 7.4 ^a	Oxidoreductase
MXAN_6536	4.1, 7.4 ^a	Antioxidant, AhpC/Tsa family
Motility/chemotaxis		
MXAN_2513	2.7	GspE (General secretory pathway protein E)
MXAN_2685	2.6	CheW (Chemotaxis protein)
MXAN_4149	2.2	FrzS (Response regulator)
MXAN_4863	7.2 ^b	AgmK (Adventerous gliding motility)
Biochemical context / Gene no.	Fold change	Description of proposed function
Proteins with decreased expression under iron-limited conditions		
DNA metabolism/transcription		
MXAN_0264	-2.6	GyrB (DNA topoisomerase activity)
MXAN_2609	-2.0	UvrA (Exonuclease ABC, A subunit)
MXAN_3326	-2.0, -2.2 ^a	RpoA (RNA polymerase subunit A)
MXAN_3777	-2.1	Inosine-5'-monophosphate dehydrogenase
MXAN_4242	-2.3	Transcriptional regulator
MXAN_7020	-2.2	Cas3 (CRISPR-associated helicase)
Translation		
MXAN_0405	-2.3	YchF (GTP-binding protein)
MXAN_2408	-2.1, -2.6 ^a	FusA (Translation elongation factor G1)
MXAN_3068	-2.1	Tu1 (Translation elongation factor)
MXAN_3297	-2.0	FusA (Translation elongation factor G2)
MXAN_3298	-3.2	Tu2 (Translation elongation factor)
MXAN_3307	-2.7 ^b	RpmC (50S ribosomal protein L29)
MXAN_3793	-2.6	RpsA (Ribosomal protein S1)

^a These proteins were present in more than one spot.

^b Found to be phosphorylated.

A high number (29) of the categorized proteins (table a1) exhibit interesting activity in signal-transduction or as regulators, a few with potentially global effects on DNA, RNA or protein

Results

metabolism. The selection of these proteins, hypothetically involved in iron regulation is shown in table 3.6.

Table 3.6: Selection from proteome response of *M. xanthus* DK1622: potential regulators or signal-transducing proteins.

The hypothetical regulators or signal-transducing proteins were found with altered expression profiles under iron-limitation (putative functions from BLAST are shown in square brackets).

No.	Gene no.	Description of proposed function
Proteins with increased expression under iron-limited conditions		
1	MXAN_0142	WD domain G-beta repeat protein
2	MXAN_0144	Hypothetical protein [WGR domain protein] ^a
3	MXAN_0866	Ferritin/ DPS (DNA protection during starvation protein) family protein TpF2
4	MXAN_0959	Nuclease SbcC (DNA nuclease, mediates DNA-protein interactions)
5	MXAN_1562	Ferritin/ DPS (DNA protection during starvation protein) family protein TpF1
6	MXAN_1591	Hypothetical protein [sigma-54 factor/ AAA ATPase]
7	MXAN_1808	Restriction/modification enzyme (N6-adenine DNA methyltransferase)
8	MXAN_1864	N6-adenine DNA methyltransferase
9	MXAN_1988	Hypothetical protein [PUA domain/ SAM-dependent methyltransferases]
10	MXAN_2094	Hypothetical protein [tetratricopeptide repeat domain protein]
11	MXAN_2347	Hypothetical protein [Protamine P1, interacts selectively with DNA]
12	MXAN_2440	Hypothetical protein [provisional transcription termination Rho domain] ^{a, b}
13	MXAN_2520	FHA domain/tetratricopeptide repeat protein
14	MXAN_2685	Chemotaxis protein CheW
15	MXAN_3679	Hypothetical protein [ArsR-like regulator]
16	MXAN_4149	Response regulator FrzS
17	MXAN_4189	Tetratricopeptide repeat protein
18	MXAN_5055	Hypothetical protein [methyltransferase domain/chromosome segregation protein SMC domain] ^{a, b}
19	MXAN_5795	Exonuclease (tRNA turnover)
20	MXAN_7380	CBS domain protein (cystathione-beta-synthase; plays a regulatory role making proteins sensitive to adenosyl carrying ligands)
No.	Gene no.	Description of proposed function
Proteins with decreased expression under iron-limited conditions		
21	MXAN_0720	Sensor histidine kinase
22	MXAN_1619	Hypothetical protein [helix-turn-helix type 11 domain protein]
23	MXAN_1892	Serine/threonine protein kinase
24	MXAN_4242	Transcriptional regulator
25	MXAN_4535	ECF sigma factor
26	MXAN_5055	Hypothetical protein [methyltransferase domain/ chromosome segregation protein SMC domain] ^{a, b}
27	MXAN_5484	Hypothetical protein [putative serine/threonine protein kinase] ^a
28	MXAN_6032	Response regulator/chemotaxis protein CheW
29	MXAN_7020	CRISPR-associated helicase Cas3
30	MXAN_7393	Hypothetical protein [sigma-54 transcriptional regulator, Fis family]

^a These proteins were present in more than one spot.

^b Found to be phosphorylated.

Results

Perhaps most importantly, the Fur regulon of *M. xanthus* includes 8 putative ECF sigma factors and other regulatory proteins, some with receiver domains of sensor protein kinases, also described for other bacteria (see introduction, section 1.1.2). In addition to these results, several proteins with putative phospho-transferase activity were detected, acting as counterpart of some helix-turn-helix transcriptional regulators (table 3.6): Members of these two-component regulatory systems contain a response regulator receiver domain and an associated transcriptional regulatory region. These results motivate a direct analysis of protein-phosphorylations.

c) Analysis of phosphorylation on differentially regulated proteins

In order to detect protein-phosphorylations, a MS screening of all proteins was performed, which were found to be differently regulated in 2D-DIGE. A detailed explanation of analysis conditions is shown in the methods part (section 2.9.3.2). In principle, the detection of protein-phosphorylations by mass spectrometric methods is based on induction and identification of the specific neutral loss of the phosphate group. An example spectrum is shown in figure 3.7.

Results

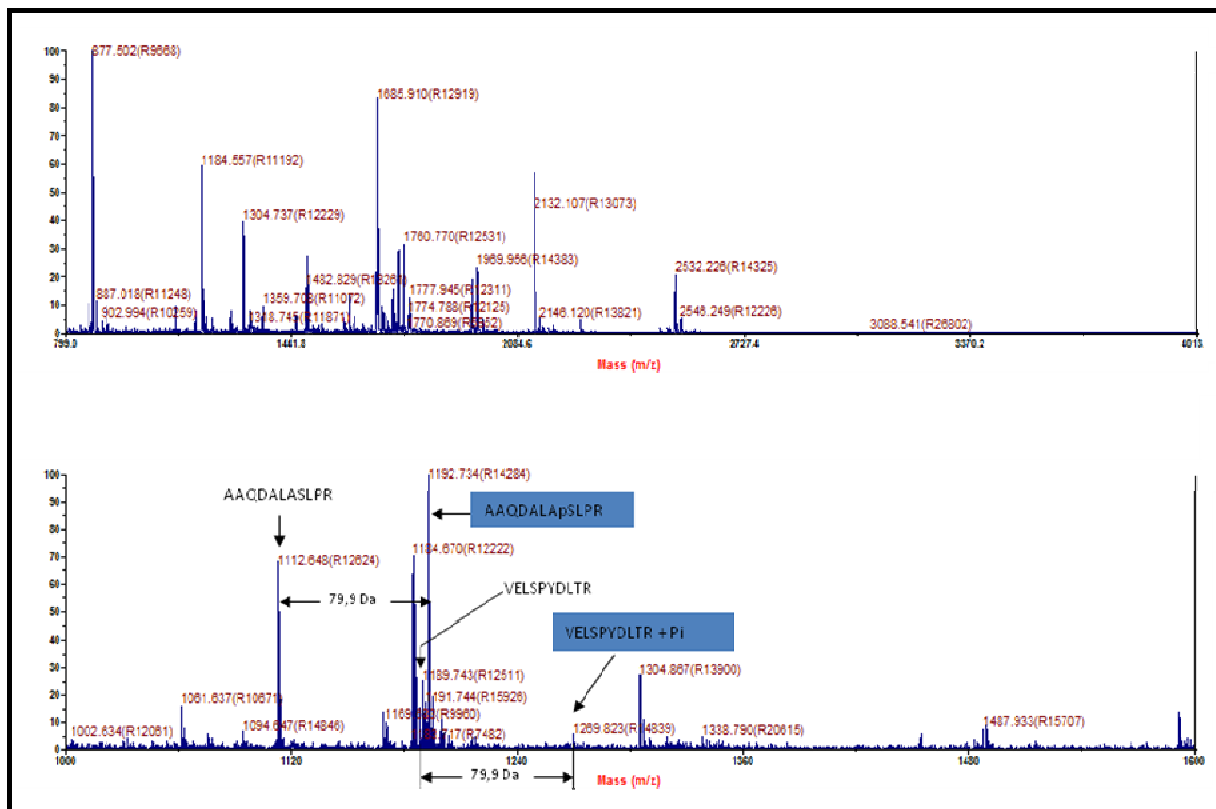


Figure 3.7: Analysis of peptide phosphorylation.

The MALDI spectra show an example of an in-gel digest, using the matrices CCA (Top) or DHB/phosphoric acid (Bottom) to analyze peptide phosphorylation by neutral loss. The digest contains two phospho-peptides, both intact (in blue boxes: AAQDALApSLPR at 1192.7; and VELSPYDLTR[p(STY)] at 1269.8) and after neutral loss (1112.6 or 1189.7, respectively). For the peptide VELSPYDLTR three phosphorylation sites are possible, so the exact position could not be determined (STY).

Remaining doubts could be cleared out by LTQ-Orbitrap measurement of in-gel digests containing potential phospho-peptides, based on highly precise measurement (error < 1 ppm). Among the 169 identified protein spots, overall 15 protein spots (12 individual proteins) were detected with one or more phosphorylations (table 3.7). Thereof 10 proteins were detected with 1 phosphorylation, 4 protein spots carrying 2 and 1 protein containing 3 detectable phospho-residues.

Results

Table 3.7: Protein phosphorylation analysis of differently regulated proteins of *M. xanthus* DK1622 under iron-limitation.

The table shows the protein phosphorylations of differently regulated proteins of *M. xanthus* DK1622 under iron-limitation, detected by MALDI-MS/MS using 2,5-dihydroxybenzoic acid (DHB) supplemented with phosphoric acid (1 %). If the protein was detected several times in proteome response with different phosphorylation patterns, more than one number is shown in column 3 ("no. of phosphorylations"). Hypothetical proteins were further analyzed by BLAST, results are shown in squared brackets. Peptide phosphorylation positions are shown in detail in table a2.

Gene no.	Description of proposed function	No. of phosphorylations
MXAN_2440	Hypothetical protein [Provisional Rho domain protein]	1, 2
MXAN_3079	Hypothetical protein	1
MXAN_3307	50S ribosomal protein L29 RpmC	1
MXAN_3326	RNA polymerase subunit A RpoA	0, 1, 2
MXAN_3571	Hypothetical protein [Flotillin/band 7 protein]	0, 1
MXAN_4137	Hypothetical protein	1
MXAN_4467	GroEL1	0, 1
MXAN_4863	Adventurous gliding motility protein AmgK	2
MXAN_5055	Hypothetical protein [methyltransferase/SMC domain protein]	0, 1, 2
MXAN_5401	Hypothetical protein	1
MXAN_6911	TonB-dependent receptor	0, 3
MXAN_7497	Signal-peptide processing peptidase M16B	1

For a high content (76 %) of protein-phosphorylations the exact positions within the respective protein were clarified (table a2). However, the analysis was performed on the mixture of 2D-DIGE typical in-gel digestion of all samples. Therefore, it was not possible in the case of MXAN_5055 by this method to determine if the phosphorylated protein was more dominant under the iron-rich or iron-poor conditions.

Results

3.2.4 Profiling protein-promoter interactions at MXAN_3702 and MXAN_6967 under iron-rich and iron-limiting conditions

The promoter sequences of the two *fur* genes MXAN_3702 and MXAN_6967 were screened for highly stringent interacting proteins, using extracts from iron-rich and iron-limiting conditions. In order to detect such potential regulator proteins, a ca. 450 bp sequence of the *M. xanthus fur* promoters, either MXAN_3702 or MXAN_6967, was linked via biotinylation to streptavidin beads. Then, the beads were incubated with protein extracts from iron-rich and iron-limiting conditions. After removing by washing of unspecific-bound proteins, DNA binding proteins were eluted with increasing stringency, precipitated, and separated by SDS-PAGE, followed by silver staining (figure 3.8). Preliminary experiments, binding of proteins was found to be more reliable, when manganese was used instead of iron to generate a stable, non-oxidative environment for metal-dependent protein binding conditions.

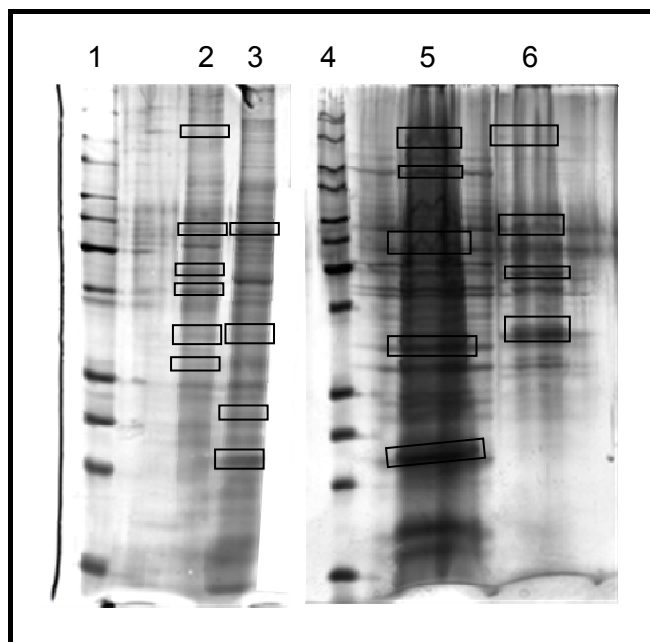


Figure 3.8: SDS-gels of protein extracts from DNA pull down assay.

The protein extracts of *M. xanthus* DK1622 were used to identify highly stringent protein interactions to promoter regions of MXAN_3702 (lanes 2 and 3) and MXAN_6967 (lanes 5 and 6). The protein extracts were obtained from iron-rich (lanes 2 and 6) or iron-limiting conditions (lanes 3 and 5). A Protein Ladder (table 2.2) was used as protein size standard (lane 1 and 4). The gels were stained by silver (Sinha *et al.*, 2001).

All bands, detected in final elution steps were further in-gel digested with trypsin and subsequently identified by mass spectrometry, followed by the screening of phosphorylated proteins (section 2.9.3). Identified proteins, which were detected to bind to the promoter

Results

regions of MXAN_3702 and/or MXAN_6967, are listed in table 3.8. For the identification of specific protein-promoter interactions on *fur* (MXAN_3702) or the *fur* homologue (MXAN_6967), the promoter of MXAN_4899 was used as a background to determine proteins which bind unspecific to promoter regions generally.

Results

Table 3.8: Mass spectrometric identification of proteins from DNA pull-down assay.

Marked protein bands from DNA pull-down polyacrylamide gel (figure 3.8) were cut out, digested with trypsin and identified by mass spectrometry. The sample lanes of the gel were loaded with proteins, bound to the promoter of MXAN_3702 (lane 2 and 3) or MXAN_6967 (lane 5 and 6), whereas the proteins were obtained from iron-rich (lane 2 and 6) or iron-limiting conditions (lane 3 and 5). The order of the identified proteins from the single lanes corresponds to their position in figure 3.8, from high- to low-molecular weight. Unspecific binding proteins were present in all samples and MXAN_4899 which was used as control. Hypothetical proteins were further analyzed by BLAST, results are shown in squared brackets.

Sample	Gene-no.	putative function [BLAST]
Lane 2: MXAN_3702; iron-rich conditions		
Band 1	MXAN_5055	Hypothetical protein [methyltransferase domain/ chromosome segregation protein SMC]
Band 2	MXAN_0959	Nuclease SbcC (DNA nuclease, mediates DNA-protein interactions)
Band 3	MXAN_0144	Hypothetical protein [WGR domain protein; motive of polyA polymerases and molybdate metabolism regulators]
Band 4	MXAN_2347	Hypothetical protein [Protamine P1, interacts selectively with DNA]
Band 5	MXAN_1359	Hypothetical protein [DeoR-family transcriptional regulator]
Band 6	MXAN_3626	Transcription factor Jumonji JmjC
Lane 3: MXAN_3702; iron-poor conditions		
Band 1	MXAN_0959	Nuclease SbcC (DNA nuclease, mediates DNA-protein interactions)
Band 2	MXAN_1359	Hypothetical protein [DeoR-family transcriptional regulator]
Band 3	MXAN_4116	Transposase IS66 family (DNA transposition)
Band 4	MXAN_1562*	DPS/bactoferritin family protein TpF1
Lane 5: MXAN_6967; iron-poor conditions		
Band 1	MXAN_5055	Hypothetical protein [methyltransferase domain/ chromosome segregation protein SMC]
Band 2	MXAN_1808	Restriction/modification enzyme (N6-adenine DNA methyltransferase)
Band 3	MXAN_3897	DNA mismatch repair protein MutS
Band 4	MXAN_5271	DNA binding domain protein LuxR-like
Band 5	MXAN_5872	DNA binding protein [HTH XRE-family like proteins]
Band 5	MXAN_1562	DPS/bactoferritin family protein TpF1
Lane 6: MXAN_6967; iron-rich conditions		
Band 1	MXAN_5055	Hypothetical protein [methyltransferase domain/ chromosome segregation protein SMC]
Band 2	MXAN_0959	Nuclease SbcC (DNA nuclease, mediates DNA-protein interactions)
Band 3	MXAN_2609	Excision repair protein UvrA domain II; Nucleotide excision repair / ABC component of the metal-type transporters
Band 4	MXAN_3203	FHA domain protein; (signaling domain found in protein kinases and transcription factors)
Unspecific bound proteins		
	MXAN_1922	TPR domain protein (mediates protein-protein interactions)
	MXAN_2800	DNA polymerase III, delta subunit HolB
	MXAN_3982	DNA polymerase III, DnaE

Only one protein (MXAN_1562 at promoter of MXAN_3702 under iron-poor conditions) was found to carry a phosphorylation (peptide: LADGLDLhpSQIK).

Results

At both analyzed promoters (MXAN_3702 and MXAN_6967) neither the Fur protein nor the Fur homologue were detected to bind to the DNA sequences. This finding is consistent with the missing of potential Fur boxes in their respective promoter regions (see table 3.1).

The combination of different transcriptional regulators (MXAN_1359 and MXAN_3626 at promoter of MXAN_3702 or MXAN_5271 and MXAN_5872 at promoter of MXAN_6967) indicates a heterogeneous and large set of regulators, involved in transcriptional control of Fur family members in *M. xanthus*.

The DPS/bactoferritin protein TpF1 (MXAN_1562) was found to bind only under iron-limiting conditions to the promoters of MXAN_3702 (protein contains a phosphorylation) and 6967 (protein without any phosphorylation). This finding indicates another, more important biological role of DPS/bactoferritin proteins, rather than only protecting DNA, but may have also regulatory functions for genes of iron metabolism.

Furthermore, MXAN_3203 (FHA protein, forkhead associated domain) was detected to bind to MXAN_6967 only under iron-rich conditions. This protein operates as putative phosphopeptide recognition site, involved in signal transduction, found in a wide range of protein kinases and transcription factors.

In addition, MXAN_1808 was detected to interact only to the promoter of MXAN_6967 in iron-poor environment, and its function as DNA methyltransferase might indicate the gene-silencing of MXAN_6967 under these conditions.

In contrast, MXAN_5055 (methyltransferase domain / chromosome segregation protein SMC) binds to the promoter of MXAN_6967 in both; however, MXAN_5055 only binds to the promoter of MXAN_3702 only under iron-rich conditions.

The found composition of regulators, methyltransferases and nucleases suggests a very heterogeneous and dynamic control of expression, more complicated than the proposed model of Fur auto-regulation, at least in *M. xanthus*. To investigate the cellular functions of MXAN_0144, 1562, 1808, 3203, 2347 and 5055, the corresponding genes were selected as target for single crossover inactivation.

Some proteins were detected across all samples, including the control sample (promoter of MXAN_4899). The binding of these proteins was declared as unspecific (table 3.8).

Results

3.2.5 Effects of iron-limitation on secondary metabolome of *M. xanthus*

To investigate the effects of iron restriction on the secondary metabolism of *M. xanthus*, the relative yields of the known natural products myxochromide, myxochelin, myxalamid, cittilin, DKxanthene, and myxovirescin were quantified from cultures grown under high- and low-iron conditions. As these compounds all represent metabolite families, quantification was performed on the most abundant metabolite in each family. Samples were obtained at four different time points (29, 40, 48 and 64 h).

Secondary metabolite analysis was accomplished by HPLC-MS of culture-extracts (section 2.13.1) from the wild type, grown at different iron concentrations (section 2.8.1). A detailed description of the calculation of the secondary metabolite yields was already given (section 2.13.3). The relative yields of secondary metabolite production are shown in table 3.9.

Results

Table 3.9: Secondary metabolite yields of *M. xanthus* DK1622 wild type under iron-rich and iron-limiting conditions.

Relative yields of secondary metabolites in quantitative comparison of production by *M. xanthus* under iron-rich (CTT, 4.8 µM Fe) and iron-limiting conditions (CTT-Fe^{MIN}, ca. 0.5 µM Fe). The relative standard deviations (mean of three cultures) are shown behind the respective value.

Sample	Relative secondary metabolite yields (peak area O.D. ⁻¹ h ⁻¹) ^{a,b}						
	MchrA2	McheA	McheB	MxaA	Cittilin	DKx	MyvA
WT^x; 64 h	100	100	100	100	100	100	100
CTT							
29 h	28 ± 2	N.D.	22.1 ± 0.7	116 ± 1	N.D.	9 ± 5	74 ± 11
40 h	42 ± 4	24 ± 3	50 ± 9	125 ± 10	85 ± 5.2	9 ± 5	130 ± 12
48 h	51 ± 8	101 ± 6	99 ± 11	105 ± 3	87 ± 3.9	27 ± 9	104 ± 10
64 h	100 ± 7	100 ± 6	100 ± 2	100 ± 3	100 ± 5.1	100 ± 3	100 ± 6.9
CTT-Fe ^{MIN}							
29 h	61 ± 9	943 ± 52	731 ± 33	100 ± 4	N.D.	N.D.	3 ± 2
40 h	382 ± 41	2075 ± 192	3705 ± 14	156 ± 1	0.04 ± 0.01	3.5 ± 0.2	82 ± 4
48 h	658 ± 62	4690 ± 197	13955 ± 48	117 ± 1	0.5 ± 0.1	32 ± 7	71 ± 9
64 h	2325 ± 127	8131 ± 367	67822 ± 70	131 ± 3	1.3 ± 0.2	61 ± 11	86 ± 3

^a All calculated production rates were normalized to an independently grown wild type culture (WT^x, 64 h = 100 %).

^b Abbreviations: MchrA2: Myxochromide A2; McheA and McheB: Myxochelin A and B; MxaA: Myxalamid A; DKx: DKxanthene560; MyvA: Myxovirescin A; N.D.: not detected

Results

This analysis demonstrated that biosynthesis of the siderophores myxochelins A and B was very significantly increased at every examined time point (table 3.9). At 64 h, the yield of myxochelin A and B from the iron-depleted cultures was approximately 81 and 678fold higher than that observed under iron-rich conditions, respectively. Additionally, the biosynthesis of myxochromide A was also substantially up-regulated (23fold) at this time point, while citterlin production was reduced by the factor 75. In contrast, the production rates of the DKxanthenes, myxalamids and myxovirescin were not substantially affected (< 2fold change), although the onset of myxovirescin production was somewhat delayed. In figure 3.9, examples of extracted ion chromatograms from three compound classes (myxochromide, myxochelin and citterlin) can be found.

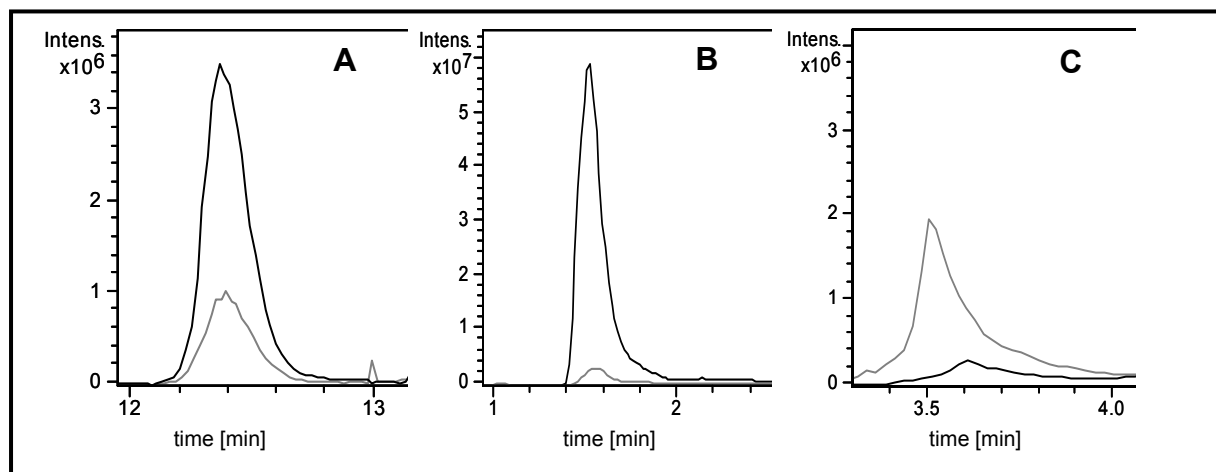


Figure 3.9: Secondary metabolite production by *M. xanthus* DK1622 wild type under iron-rich and iron-limiting conditions

The illustration shows the HPLC-MS profiles of secondary metabolite of *M. xanthus* DK1622 wild type under iron-rich (grey line, CTT; 4.8 μ M Fe) and iron-limiting conditions (black line, CTT- Fe^{MIN} ; ca. 0.5 μ M Fe). The extracted ion chromatograms display: **A**) Myxochromide A2 ($[M+\text{H}]^+ = 833.9$), **B**) Myxochelin B ($[M+\text{H}]^+ = 404.4$) and **C**) Citterlin A ($[M+\text{H}]^+ = 631.7$).

Furthermore, the extracts from the iron-limiting growth were screened for the presence of novel compounds by comparing the MS and UV/Vis spectra (section 2.13) to that of the wild type under standard conditions. The detection of previously unknown secondary metabolite products was complicated by many media compounds and primary metabolic end-products, which show partially large variations in response of *M. xanthus* to iron-limitation. However, this analysis did not reveal any candidates for new metabolites.

Results

3.3 Investigation of the Fur regulon by gene inactivation

Gene knockouts were generated by single crossover disruption or double crossover in-frame deletion in order to understand the biological roles of the predicted protein functions. Selected gene targets were those which encode for proteins; found in promoter-interaction studies or detected in proteomics to be differently regulated in response to iron-limiting conditions. Mutants were analyzed in iron-rich medium (section 2.8.1), concerning effects to growth, iron-uptake rates and secondary metabolism (including siderophore production).

3.3.1 Generation of markerless in-frame deletion mutants

For the investigation of the roles of the putative iron-responsive Fur protein MXAN_3702 and a Fur homologue MXAN_6967 in iron homeostasis, both genes were attempted to delete by double crossover. However, no in-frame deletion of MXAN_3702 could be generated. Therefore, several different vectors and constructs (pSWU41-, pBJ113- and pBJ114-derived vectors (Wu *et al.*, 1996; Black and Yang, 2004) were employed, containing several different inactivation regions), additionally to the application of different iron-concentrations to selection plates.

In contrast, MXAN_6967 could be inactivated successfully, whereas double crossover mutants contain only a truncated, non-functional form of the gene, verified by the PCR result, shown in figure 3.10.

Results

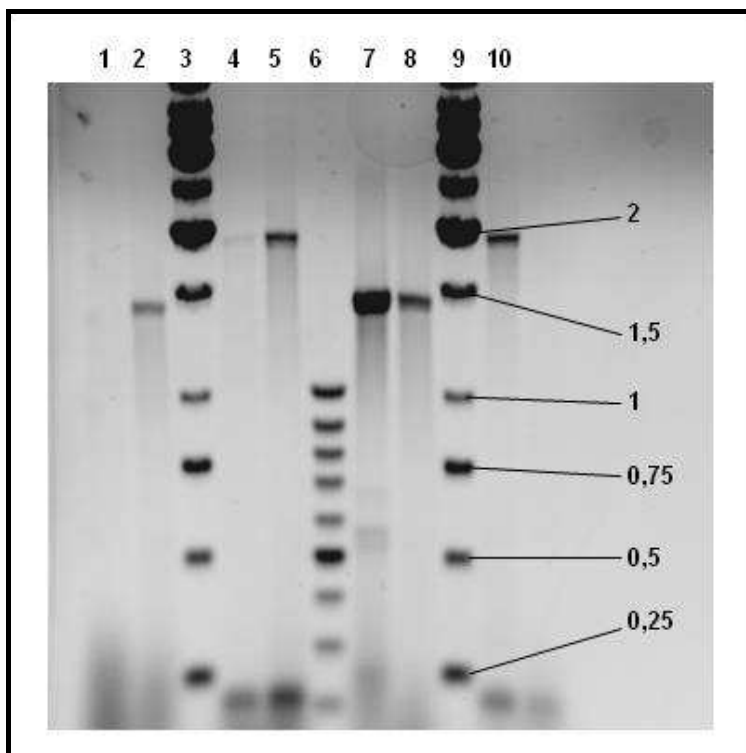


Figure 3.10: PCR results of the second crossover analysis of DEL6967.

The agarose gel shows the PCR results of the second crossover analysis. PCR was run on genomic DNA from *M. xanthus* wild type (lane 10) and second crossover mutants of MXAN_6967 (DEL6967), where PCR products should miss 324 nt. Revertants and wild type genotype yield a product of 1.79 kbp with primer pair CONF_D6967F/CONF_D6967R from table 2.17 (lanes 4, 5 and 10), while analysis of successfully generated double crossover mutants yielded in a truncated PCR product of 1.47 kbp (lanes 2, 7 and 8). Lane 3 and 9 contain 1 kb ladder and lane 6 contains 100 bp ladder (table 2.2), for some bands the DNA size is denoted (in kb).

The PCR results, shown in figure 3.10, clearly proof the generated in-frame deletion in MXAN_6967. When comparing genotypes of wild type (lane 10) and DEL6967 (lane 2, 7 and 8), 324 bp of MXAN_6967 were eliminated. The strategy, how to generate a truncated form of the wild type gene is shown in figure 1.16, the PCR results from figure 3.10 correspond to figure 1.16 E. Finally, selected clones (lane 2, 7 and 8) were sequenced to confirm the truncated form of MXAN_6967 stays in the former reading frame.

3.3.2 Generation of gene disruption mutants by single crossover

Deeper insight into the putative functions of genes whose regulation was altered by iron availability was achieved by a series of single gene inactivation experiments, targeting the following genes: MXAN_0142, MXAN_0144, MXAN_1562, MXAN_1619, MXAN_1808, MXAN_1864, MXAN_1893, MXAN_1988, MXAN_2094, MXAN_2347, MXAN_2440, MXAN_2520, MXAN_3203, MXAN_4189, MXAN_4535, MXAN_5055 and MXAN_5484 (see table 2.15).

Results

Some genes, which were selected as target for single crossover disruption, could not be inactivated successfully (MXAN_0142, 1619, 2094, 2347, 2520).

Briefly, the following genes whose expression was up-regulated under iron-limiting conditions were inactivated successfully: MXAN_0144, 1562, 1808, 1864, 1893, 1988, 2440, 4189 and 5055, as well as MXAN_4535 which was down-regulated. Additionally, MXAN_5484 was inactivated, because the gene product was detected as two spots, whereas one was up-, to other down regulated (table 3.10). Some of the genes might be more important in iron response, indicated by the detected phosphorylation(s) at the encoded proteins of MXAN_2440 and MXAN_5055 (table a2).

Several genes (MXAN_0144, MXAN_1562, MXAN_1808 and MXAN_3203) were chosen for inactivation because of the binding of the encoded proteins to the promoter regions of MXAN_3702 and/or MXAN_6967 (table 3.8). A more detailed explanation about motivation of selection for knockout experiments can be found in the discussion part of the respective clones (section 4.4).

Table 3.10: Confirmed mutants, generated by single crossover gene disruption in *M. xanthus* DK1622.

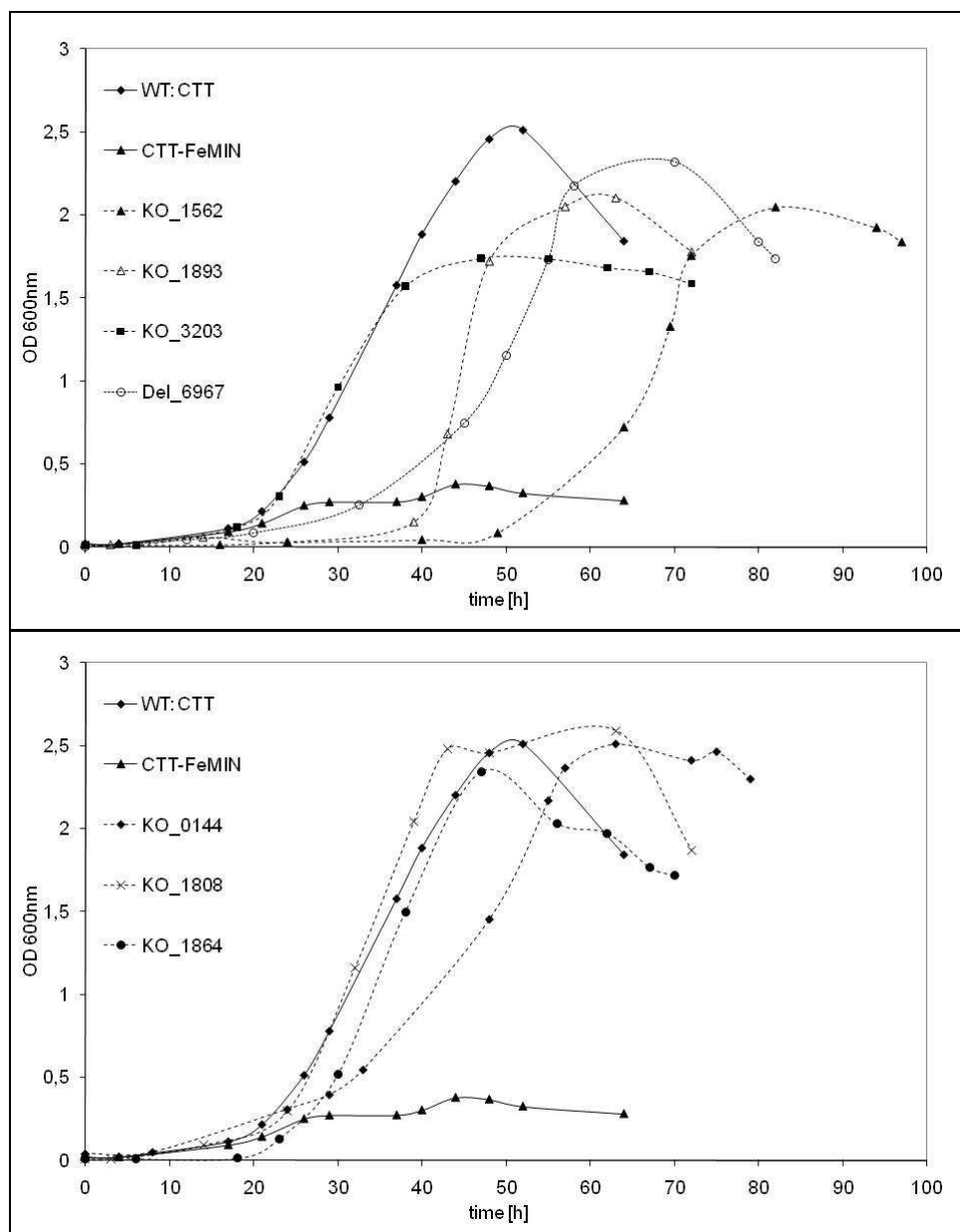
No.	Gene number	Gene size (nt)	Size PCR fragment for homol. recombination	Stop-Codon introduced
1	MXAN_0144	2733	681	
2	MXAN_1562	477	291	yes
3	MXAN_1808	4971	643	
4	MXAN_1864	1284	462	
5	MXAN_1893	438	294	yes
6	MXAN_1988	1197	595	
7	MXAN_2440	2223	700	
8	MXAN_3203	1167	654	
9	MXAN_4189	729	432	yes
10	MXAN_4535	600	360	yes
11	MXAN_5055	6045	744	
12	MXAN_5484	732	426	yes

Growth, iron uptake rates as well as secondary metabolite production of the mutant strains were monitored in iron rich medium, along the deletion mutant DEL6967 (section 3.3.3).

Results

3.3.3 Growth analysis of the generated mutants in iron-rich environment

Strains were cultured in CTT medium and growth rates were monitored by measuring the optical cell density (O.D._{600}) at different time points (figure 3.11). Comparison of the growth rates of the mutants showed that they differ in each case from the wild type, and thus allowance was made for cell density when estimating both iron uptake rates and secondary metabolite yields.



Results

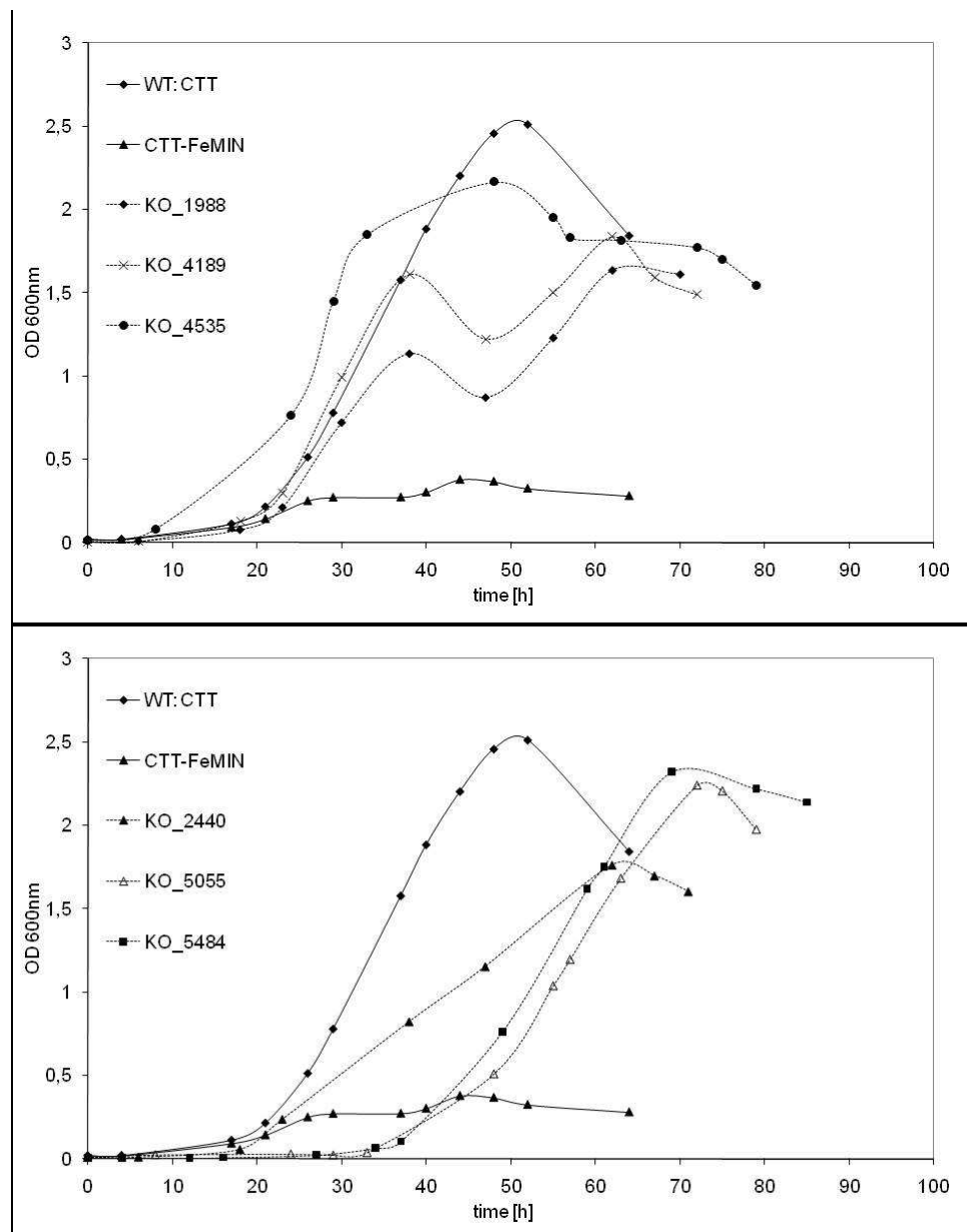


Figure 3.11: Growth profiles of the mutants in iron-rich medium.

The illustration display the O.D.₆₀₀ growth curves of the generated mutant strains (dashed and dotted lines) in iron-rich medium (CTT medium, containing 4.8 µM iron). Additionally, the growth profiles of *M. xanthus* DK1622 wild type strain (WT; solid lines) under iron-rich (diamonds, CTT medium) or under iron-poor condition (triangles, CTT-Fe^{MIN} medium containing ca. 0.5 µM iron) are shown. The mutants were generated by single crossover (indicated as **KO**) or by in-frame deletion (indicated as **DEL**) of the corresponding gene in *M. xanthus* DK1622.

All mutations had defects in growth; therefore correlation to growth stage was made when iron uptake (section 3.3.4) and metabolite production (section 3.3.5) of the respective strains were judged as functions of O.D.₆₀₀.

As an example, the detailed comparison of the wild type to mutant DEL6967, the mutant strain shows a larger lag-phase (30 h) in growth, and larger doubling times, but reaches almost the same maximum O.D._{600nm} (93 %) as the wild type under the same iron rich conditions.

Results

The maximum O.D._{600nm} (approx. 2.33) was achieved after 65 h, ca. 15 h later than the wild type. The growth rate was found to be very similar at the knockout mutants of MXAN_1562 and 1893. A more detailed discussion of the single mutants can be found in section 4.4.

3.3.4 Estimation of iron uptake of generated mutant strains

The relative iron uptake rates for each mutant (table 3.11) was calculated by subtracting the iron concentration at a single time point during growth (at which there was sufficient cell mass) from initial concentration, and then normalized the result to O.D.₆₀₀ and time. Finally, rates were compared to the rate measured for the wild type strain (analyzed at t = 64 h with 37.1 nmol h⁻¹ O.D.⁻¹).

Table 3.11: Rates of iron uptake by mutant *M. xanthus* strains.

Iron uptake rates were determined as end point measurement of triplicates. The standard deviation is shown behind the respective value (unit: nmol h⁻¹ O.D.⁻¹). Additionally, the ratio to wild type (WT) iron uptake (analyzed at t = 64 h with 37.1 nmol h⁻¹ O.D.⁻¹) is shown as %-value.

Sample	O.D. ₆₀₀	Time [h]	Iron uptake rate [nmol h ⁻¹ O.D. ⁻¹]	% of WT iron uptake
KO0144	2.3	79	8.2 ± 0.6	22.1
KO1562	1.84	97	0.5 ± 0.3	1.3
KO1808	1.87	72	15.5 ± 2.8	41.8
KO1864	1.97	67	2.6 ± 0.9	7.1
KO1893	1.78	72	32.8 ± 0.2	88.4
KO1988	1.61	67	29.0 ± 0.8	78.2
KO2440	1.7	67	24.3 ± 0.8	65.5
KO3203	1.66	67	9.8 ± 0.5	26.4
KO4189	1.59	67	0.8 ± 0.3	2.2
KO4535	1.55	79	10.0 ± 0.9	27.0
KO5055	2.0	79	23.1 ± 0.8	62.3
KO5484	2.14	86	0.7 ± 0.2	1.9
DEL6967	1.74	82	15.9 ± 0.5	43.9

Not one of the mutants showed an increase of the iron-uptake, compared to the wild type. Thus, the deletion mutant does not show the typical behavior of mutants of iron-responsive Fur genes, resulting in characteristic deregulation and constitutive iron uptake, which contradicts for an iron-monitoring function of MXAN_6967.

Results

3.3.5 Metabolite analysis by HCPL-MS of the generated mutants

Secondary metabolite analysis was accomplished by HPLC-MS (section 2.13) of culture-extracts from the mutant strains, grown in CTT (section 2.8.1).

Final relative metabolite yields were calculated by comparing compound amounts observed in the mutant strains (expressed as peak area $\text{h}^{-1} \text{O.D.}^{-1}$) to those of the wild type. The results of the secondary metabolite analysis of the mutants, generated under iron-rich conditions can be found in table 3.12 (production relative to the wild type as a function of O.D._{600}).

Results

Table 3.12: Relative yields of secondary metabolites from *M. xanthus* mutant strains.

Relative yields of secondary metabolites in quantitative comparison to production of *M. xanthus* mutants under iron-rich (CTT, 4.8 µM Fe). The relative standard deviations (mean of three cultures) are shown behind the respective value. Triplicates with very large variations in detected concentrations of the respective substance were marked in red.

Sample	Time [h]	Relative secondary metabolite yields (peak area O.D. ⁻¹ h ⁻¹) ^{a,b}						
		MchrA2	McheA	McheB	MxaA	Cittilin	DKx	MyvA
WT ^x , 64 h	64	100	100	100	100	100	100	100
KO_0144	79	98 ± 38	ND	0.4 ± 0.3	26 ± 5	26 ± 11	47 ± 5	0.6 ± 0.3
KO_1562	97	30 ± 4	0.5 ± 0.2	0.05 ± 0.03	4 ± 4	4.2 ± 1.8	4.9 ± 0.7	2 ± 1
KO_1808	72	107 ± 9	20 ± 20	23 ± 23	831 ± 73	93 ± 66	1839 ± 178	1182 ± 571
KO_1864	67	57 ± 19	14 ± 7	14 ± 2	16 ± 12	4.9 ± 3.7	8 ± 8	2.9 ± 0.3
KO_1893	72	1.0 ± 0.2	0.16 ± 0.04	0.2 ± 0.0	22.3 ± 0.3	0.2 ± 0.03	14 ± 2	0.15 ± 0.04
KO_1988	67	122 ± 50	2 ± 1	176 ± 49	18 ± 18	102 ± 74	2243 ± 430	545 ± 182
KO_2440	67	78 ± 13	12 ± 4	20 ± 8	74 ± 12	2.8 ± 2.1	1241 ± 762	404 ± 114
KO_3203	67	92 ± 6.5	56 ± 18	65 ± 12	128 ± 20	80 ± 14.8	1926 ± 497	493 ± 54
KO_4189	67	57 ± 11	36 ± 14	34 ± 34	11 ± 4	15 ± 15	59 ± 59	92 ± 22
KO_4535	79	129 ± 70	0.8 ± 0.8	0.13 ± 0.08	56 ± 12	55 ± 5.7	104 ± 31	16 ± 1
KO_5055	79	77.7 ± 0.4	25 ± 12	12 ± 8	44 ± 4	5.9 ± 3.4	81 ± 13	12 ± 4
KO_5484	86	377 ± 118	6.4 ± 2.4	1.1 ± 0.5	212 ± 9	3.2 ± 2.1	43 ± 6	114 ± 4.5
DEL6967	82	50 ± 12	0.3 ± 0.2	0.5 ± 0.3	2 ± 2	4.6 ± 4.6	6 ± 2	3 ± 2

^a All calculated production rates were normalized to an independently grown wild type culture (**WT^x, 64 h = 100%**).

^b Abbreviations: MchrA2, Myxochromide A2; McheA and McheB; Myxochelin A and B; MxaA, Myxalamid A; DKx, DKxanthene560; MyvA, Myxovirescin A; ND = not detected.

Results

Not one of the mutants showed a significant increase in myxochelin production, which corresponds well to the iron uptake rates of the mutants, found at wild type levels or below. Some mutants exhibit a drastic decrease (more than 90 %) in iron uptake (MXAN_1562, 1864, 4189 and 5484). Additionally, some exhibit a strong decrease in myxochelin production (detected for DEL6967, MXAN_0144, 1562, 1893, 4535). Only for the knockout mutant of MXAN_1562 a correlation could be made between production of less siderophores, subsequently followed by reduction of iron uptake. This may indicate alternative mechanisms of iron acquisition (see introduction, section 1.1.1-1.1.3), at least active in a subset of mutants. The deletion mutant DEL6967 and the knockout mutants of MXAN_1562 and 1893 showed an extensive reduction of all monitored metabolites.

To give a detailed example, the mutant DEL6967 shows that the efficient iron uptake was found in contrast to the strong reduction of the amounts of produced myxochelins. This observation (a strong reduction of myxochelin amounts, in contrast to an only slightly reduced iron uptake rate) was also evident for the knockout mutant of MXAN_1893. In detail, in DEL6967 the myxochelin A production was reduced by the factor 377.2, while B was reduced by 195.5. In contrast, the strain was able to take up iron with ca. 50 % of wild type rates .The cells produce 16.6fold less of DKxanthenes and 39.4fold less myxovirescin. Also myxalamid production decreased by the factor 59.6, but effects on myxochromide production were relatively small (2.0fold less). The production of citterlin was reduced by the factor 21.7. All secondary metabolite production rates show a decrease in this mutant, compared to wild type under iron rich conditions.

However, in many mutants also secondary metabolites were found to be effected, which did not show any response in the wild type under iron-limiting conditions. A detailed discussion of the single mutants can be found in section 4.4.

3.3.6 Overall results from mutant analysis

The most common consequence of the mutations was to retard (5–30 h) the onset of exponential growth (figure 3.11), as well as to lower the overall growth maximum. While the iron uptake rate of several mutants was not substantially altered (MXAN_1893, 1988, 2440 and 5055), the predominant effect was a substantial reduction in the efficiency of iron acquisition such as in the knockout mutants of MXAN_1562, 1864, 4189 and 5484.

None of the mutants showed an increased ability to take up iron or a significant increase in

Results

myxochelin production.

Frequently, the result of the mutations was to reduce secondary metabolite yields across multiple metabolite classes (table 3.12). In fact, in mutants of MXAN_1562 and MXAN_1893, production of all compounds was significantly reduced, while in mutant MXAN_0144, the production of all metabolites with the exception of the myxochromides, were lower. In some cases (mutants of MXAN_4189, MXAN_4535 and MXAN_5055), the effects were limited to a subset of metabolite classes (myxovirescin, myxalamid and the myxochelins).

In contrast, in mutants of MXAN_1808, MXAN_1988 and MXAN_2440, there was a drastic increase in production of specific compounds, including the DKxanthenes and myxovirescin, and in the case of MXAN_1808, biosynthesis of the myxalamids was also up-regulated.

A detailed discussion of the single mutants can be found in section 4.4.

Because of the limited time frame, the mutants were not grown and examined in separate experiments under iron-limiting conditions. Furthermore, it might be interesting to evaluate effects of iron-overfeeding of these mutants.

Discussion

4. Discussion

In this study, the response of the genome-sequenced strain *M. xanthus* DK1622 to low iron concentration was evaluated. In parallel, iron-limitation was a potential strategy for awakening silent biosynthetic gene clusters in myxobacteria.

Reflecting the vital role of iron as enzymatic cofactor, studies in both transcriptomics and proteomics of a range of bacteria have been performed. Thereby, it could be experimentally probed that the extensive restructuring of bacterial metabolism, which occurs is based on iron availability (Escolar *et al.*, 1999; Andrews *et al.*, 2003; Massé and Arguin, 2005). Many of the iron-induced changes of transcriptomes and/or proteomes are directly or indirectly mediated by Fur (ferric uptake regulator) proteins, but although Fur-independent, iron-dependent changes, have been reported for some bacteria (Lee *et al.*, 2004; Holmes *et al.*, 2005; Ernst *et al.*, 2005). The Fur regulon has been shown to encompass proteins with obvious roles in maintaining iron homeostasis (siderophore biosynthesis, uptake systems for iron-loaded siderophores and other iron-containing compounds, iron storage and redox stress and in some cases also subordinated regulators of such systems), also to include less clearly related functions such as acid shock response, flagellum assembly, chemotaxis/swarming or production of toxins and virulence factors (Escolar *et al.*, 1999). Because only little is known about how myxobacteria handle iron-limitation, the response of the myxobacterial model-strain *M. xanthus* DK1622 to iron-limitation was investigated.

Discussion

4.1 Genetic background of *M. xanthus* iron regulation

As a starting point, *in silico* analysis of the *M. xanthus* genome was carried out to determine whether the iron response in *M. xanthus* may be mediated by Fur, and to predict members of the Fur sub-families and the Fur regulon. This investigation includes amino acid sequence alignment by **BLAST** (section 3.1) and **ClustalW2** analysis (figure 3.1), which was further used to generate the **phylogenetic tree** (figure 3.2). The character of the detected two Fur proteins from *M. xanthus* were then compared to the genome of **two other members from the group of myxobacteria** (*Sorangium cellulosum* So ce56 and *Stigmatella aurantiaca* DW4/3-1). Furthermore, members of the Fur regulon in *M. xanthus* were identified by the **prediction of Fur boxes**, which were a part of promoter elements of various genes using the Virtual footprint analysis software (table 3.1).

Protein BLAST analysis, using representative members of the Fur family against the translated *M. xanthus* genome revealed two candidate proteins, MXAN_3702 and MXAN_6967 (figure 3.1), which share only little similarities among each other (29 % I, 42 % S). Further hits could be clearly delimited, showing only homologies to very small sequence parts (less than 50 bp). Thus, *M. xanthus* contains more than one Fur sub-family member like the majority of bacteria characterized to date (Lee *et al.*, 2007) as for example the model strain. *Escherichia coli* (contains a iron-responsive Fur protein and a homologue with zinc-sensing function Zur) (Hantke, 2002) or *Bacillus subtilis* (contains a Fur and Zur, and an additional peroxide sensing regulator, PerR) (Fuangthong and Helmann, 2003).

Although a lot of bacteria contain multiple Fur homologues, many such putative Fur proteins do not function as regulators of iron homeostasis (Moore *et al.*, 2005). Structure-guided sequence analysis by the **ClustalW2** algorithm (figure 3.1) of the *M. xanthus* Fur proteins coupled to **phylogenetics** (figure 3.2), strongly suggested that MXAN_3702 is likely to be a true (iron-responsive) Fur protein, indicated by the presence of important residues in the amino acid sequence as the two highly conserved motifs for DNA-binding (ATVYR) at position 78-82 and for iron-binding (HHDH) at position 113-116 (figure 3.1). The important amino acids were detected in the crystal structures of other bacterial Fur proteins to complex iron, suggesting the same function of MXAN_3702 in *M. xanthus*. In agreement to this, no evidence was found for binding sites of manganese ions, characteristically for Mur proteins, despite of the close clustering of MXAN_3702 with other members of the Mur sub-group (figure 3.2), which may argue for the convergent evolution of this branch of iron-sensing Fur

Discussion

proteins.

The function of MXAN_6967 is less clear, however, it contains the structural Zn-binding motif noted for iron-responsive Fur proteins, PerR and Zur family members (Sheikh *et al.*, 2009), but clades with heme-responsive Irr proteins in the phylogenetic tree (figure 3.2), which typically miss the zinc-binding residues. The heme-binding motif is not completely understood (Stojiljkovic and Hantke, 1994; Yang *et al.*, 2005), but important residues (e.g. histidine at position 84, 101 and 103) were found to be present in the sequence of MXAN_6967. Taking this fact together with the finding of several heme-uptake-correlated genes in the genome of *M. xanthus* (table 3.2) and the detection of the heme-binding/degradation protein HemS in proteomics (table 3.4) to be differently regulated, indicates that heme may be used as iron-resource by *M. xanthus*.

In order to get deeper insight into the function of both Fur genes of *M. xanthus* DK1622, a search for Fur homologues was performed with **two other sequenced myxobacterial genomes**, that of *Sorangium cellulosum* So ce56, a member of the suborder Sorangiineae and *Stigmatella aurantiaca* DW4/3-1, a member of the suborder Cystobacterineae. The genome of *S. cellulosum* contains homologues of both MXAN_3702 (Sce0007 with 56 % I, and 72 % S) and MXAN_6967 (Sce7206 with 52 % I, 75 % S), but additionally two other putative Fur family members which are more distantly related to the *M. xanthus* sequences (Sce1132 and Sce1752). Surprisingly, *S. aurantiaca* DW4/3-1 contains only a single Fur-family member, a homologue of MXAN_6967 (STIAU_0559), which misses the iron-binding motif. In this case, homology is exceptionally high (74 % I, 87 % S). This result was unexpected, as MXAN_6967 clearly lacks the iron-binding residues, typically observed in Fur crystal structure, so MXAN_6967 is unlikely to be an iron-responsive Fur regulator. Apparently, additional strain-specific control systems must function to maintain iron homeostasis in *S. aurantiaca*, which has been reported for only a few bacteria as for example in *E. coli*, *Vibrio anguillarum*, and *Staphylococcus aureus* (Escolar *et al.*, 1999; Crosa *et al.*, 2002; Chao *et al.*, 2005), which employ iron-responsive transcriptional regulators beside Fur family members as DtxR, SirA and/or IdeR proteins (see introduction section 1.1.2). Because all of the mentioned organisms contain also iron-responsive Fur proteins (and sometimes several other Fur homologues), the importance of alternative control-mechanisms in iron-regulation might have been underestimated, at least for myxobacteria. Newer findings indicate that some

Discussion

microorganisms, such as several α -proteobacteria live without any Fur homologue, corroborating the hypothesis of alternative regulators of iron-metabolism (Johnson *et al.*, 2007) which may also play a key role in regulatory network of myxobacterial iron metabolism additionally to Fur proteins.

As the data from BLAST and phylogenetics (section 3.1.1) strongly suggested that MXAN_3702 is a classical Fur protein, the genome was further screened for putative **Fur recognition sites (Fur boxes)** using the bioinformatic tool Virtual Footprint version 3.0 (Münch *et al.*, 2005; Klein *et al.*, 2008). It has been shown previously that Fur proteins interact also to 19 bp sequences with less than 50 % match to the consensus sequence in both, *Bacillus subtilis* and *Neisseria meningitidis* (Lee *et al.*, 2007). Hence, the analysis was refined by manual evaluation of candidate Fur boxes, specifically addressing positioning with respect to promoter elements and presumed translational start sites. This method revealed putative Fur boxes upstream of 40 genes of diverse putative functions (table 3.1). To avoid overestimation of the numbers of Fur boxes, the distance to translational start-sites was limited to maximum 300 bp, because only a few exceptions up to distances of 500 bp were described (Gao *et al.*, 2008).

The Fur boxes of *M. xanthus* seem to be organized as two inverted repeats (figure 3.3), conform to the model of bacterial Fur boxes (Lee *et al.*, 2007). As expected, Fur box consensus sequences (table 3.1) were identified within the promoter regions of genes typically involved in iron acquisition as tonB-family genes (MXAN_3915 and MXAN_6911), a putative ZIP family metal cation transporter (MXAN_5682) and genes from myxochelin biosynthetic cluster as MxcB (MXAN_3639), MxcH (MXAN_1688) and the main myxochelin operon (MXAN_3647-3640). Additionally, Fur boxes were found in proximity to genes, mediating a wide range of functions including primary metabolism, redox-reaction, translation, motility and probably most important, regulation. A large number of genes (13), coding for hypothetical proteins with unknown functions were also detected, but 6 could be correlated by BLAST analysis to putative activities. However, the overall findings are consistent with the size and diverse membership of Fur regulons observed in other bacteria, in which typically genes were included from siderophore biosynthesis, redox response, tonB-dependent uptake systems, primary metabolism, transcriptional regulators and several other, often iron-correlated functions (Ochsner *et al.*, 2002; Holmes *et al.*, 2005; Massé *et al.*, 2005; Ollinger *et al.*, 2006; Vidakovics *et al.*, 2007; Lee *et al.*, 2007).

Interestingly, the gene MXAN_7353 (putative β -ketoacyl-acyl carrier protein synthase KAS

Discussion

III, a FabH homologue) was detected to be putatively regulated by a Fur box in the promoter region. The coded enzyme is thought to catalyze the first elongation reaction of the fatty acid synthase in plants and bacteria and allows the organism to modulate fatty-acid composition according to changes in environmental conditions (Li *et al.*, 2005). That iron has, at least partially, an influence on the fatty acid profile was already published for *E. coli* (Zhang *et al.*, 2005b) and seems to be also the case for *M. xanthus*.

Another gene under Fur box control was MXAN_1873, which exhibits high homologies to integrase/recombinase proteins. These proteins are site-specific tyrosine recombinases, which catalyze the cutting and rejoicing of the recombining DNA molecules. Many are associated with mobile DNA elements, including phage, transposons, and phase variation loci (Yates *et al.*, 2003). The sequence shared highest homology to integrases/recombinases, whereof some were already found in association with metal-uptake and -regulation in bacteria (Ambrozic *et al.*, 1998; Bach *et al.*, 1999; Sonoda *et al.*, 2002; Segall and Craig, 2005). This protein family was already included to the Fur regulon since detection in the response of *Shewanella oneidensis* to iron-starvation (Wan *et al.*, 2004). Furthermore, it was published that this protein family is required for the genome-integration of plasmid-coded siderophore biosynthetic genes as postulated for the aerobactin cluster in *Shigella* strains (Vokes *et al.*, 1999). Another known recombinase activity, in interplay with sequence-specific methyltransferase restriction-modification systems, is to modify or even invert parts of promoter sequences, perhaps to generate Fur box sequences.

No prediction of Fur boxes was made in promoter regions of genes, coding for ArsR- or MerR-like transcriptional regulator proteins (Nies, 2003), indicating separate regulatory networks for the distinct trace metals in *M. xanthus*.

The genome of *M. xanthus* is known to be highly dynamic, indicated by the fact of the spontaneous mutation to TAN phase-locked phenotype (Laue and Gill, 1995). This convertibility may be associated to integrases/recombinases, for which it makes sense to be induced in hostile environment to overcome iron stress conditions in order to utilize plasmids, which contain genes of iron acquisition, commonly found in nature (Ambrozic *et al.*, 1998; Vokes *et al.*, 1999; Sonoda *et al.*, 2002).

Four of the genes from table 3.1 may represent only the first genes of polycistronic mRNAs:

1) The possible operon MXAN_1314 to MXAN_1321 contains a TonB receptor and 4 hemin transport proteins besides 3 uncharacterized proteins. This potential operon supports the hypothesis that heme and heme-derivates may be taken up and be metabolized by *M. xanthus*.

Discussion

- 2) A Fur box was determined to regulate the myxochelin biosynthetic gene cluster (MXAN_3647 to MXAN_3640), which was already known from other myxobacteria to be transcribed as single operon, containing the genes *mxcCDEFGKL* (Silakowski *et al.*, 2000). Another gene in this cluster codes for a 3-deoxy-7-phosphoheptulonate synthase (MXAN_3642), which catalyzes the first step of the shikimate/chorismate/tryptophan synthesis. Chorismate molecules and derived structures (as for e.g. catecholate) from this pathway are known from other organisms to be provided for siderophore biosynthesis (Neilands, 1995; Kerbarh *et al.*, 2005). Furthermore, the gene MXAN_3641 was found with high similarities to the major facilitator superfamily protein MxcK, which acts as transporter of small solutes. For the variation of the ratio between the two myxochelin derivates A and B, the responsible aminotransferase MxcL (MXAN_3640) must have an additional regulatory site besides the Fur box of the whole operon that its expression can be adjusted more individually, if necessary. An additional way to vary the ratio of myxochelin A and B could be performed by modulation of the enzymatic activities of MxcG and/or MxcL, which compete for the substrate, namely the myxochelin aldehyde intermediate (Li *et al.*, 2008). The Fur-control of siderophore biosynthesis is detected most frequently in bacteria (Crosa, 1997), here taken as positive control in *M. xanthus*, arguing for the correctness of the used bioinformatic method.
- 3) The operon structure from MXAN_6641 to MXAN_6635 would include a RppA-like chalcone/stilbene synthase family protein with very high homology (76 % I, 84 % S) to the chalcone synthase STIAU_8629 from *S. aurantiaca* DW4/3-1, an acyl carrier protein, an AMP-binding protein and a FAD-binding monooxygenase. Further two of the three uncharacterized proteins (BLAST homologies to: hemin-binding protein HmuY and tonB-dependent receptor) of the potential polycistronic mRNA seem to be associated to iron-uptake. Finally the metallo-enzyme isoprenylcysteine carboxyl methyltransferase ICMT was predicted to be part of the operon. This protein family carries out carboxyl methylation of target molecules, whose modification could have important function during iron-starvation.
- 4) The potential operon from MXAN_6998 to MXAN_6994 would include a helix-turn-helix DNA-binding protein, a TonB domain protein, a sensor protein asgD (two-component regulator required for A-signaling and nutrient sensing), a putative uncharacterized protein and sensor signal transduction histidine kinase-related protein. Most of the proteins have regulatory functions, considering that phosphorylation status of some target molecules may be correlated in *M. xanthus* to iron-response. However, the large number of eukaryotic protein

Discussion

kinase-like kinases in the genome of *M. xanthus* DK1622 (Perez *et al.*, 2008) suggests that some of these play important roles in regulatory processes, as for e.g. iron-balancing.

However, no indication for the existence of a Fur box was found for both Fur homologue promoters in *M. xanthus*, neither for the *fur* gene (MXAN_3702), nor for the *fur* homologue (MXAN_6967), fitting to the used Fur box prediction model from *P. aeruginosa* (Vasil *et al.*, 1999), which was found to be the only applicable model for *M. xanthus* to generate convincing results, in contrast to both other available Fur models (*H. pylori* and *E. coli*) from Virtual Footprint analysis.

In the model organism *E. coli*, Fur negatively auto-regulates its own transcription via a Fur box (Wandersman *et al.*, 2004). However, this mode of repression was not observed in *P. aeruginosa* (Vasil *et al.*, 1999), *Bradyrhizobium japonicum* (Rudolph *et al.*, 2006) or *Campylobacter jejuni* (Holmes *et al.*, 2005) and does obviously also not appear to operate in *M. xanthus*, as a Fur box was not identified upstream of MXAN_3702. Anyway, transcriptional control of Fur family members can depend on alternative transcriptional regulators (see introduction 1.1.2). Several genes coding for such transcriptional regulators were found to be present in the genome of *M. xanthus* (section 3.1.3). Furthermore, some of the transcriptional regulator genes were predicted to be Fur-controlled, as MXAN_0502 and MXAN_6998 (table 3.1).

To gain experimental evidence for proteins interacting with high specificity to the promoters of MXAN_3702 and MXAN_6967, both promoter regions were further examined by DNA pull-down assays (section 3.2.4). By this experiment, it was observed that both *M. xanthus* Fur proteins neither bind to the promoter of MXAN_3702 nor to MXAN_6967, while several other transcriptional regulators were identified to interact with these promoter sequences (table 3.8). The promoter of MXAN_4899 was used as control to identify at least unspecific binding of proteins to promoter sequences. Up to now, no promoter in *M. xanthus* had been detected experimentally, to which Fur proteins bind to.

As mentioned, a potential limitation of the bioinformatic prediction of Fur boxes is that some genes associated with Fur boxes are not regulated by Fur, while other genes which are under Fur control are regulated from sites with little similarity to conventional Fur box consensus sequences (Baichoo *et al.*, 2002a). A further issue is that it is not possible on the basis of sequence information alone to distinguish sites which would be bound by MXAN_3702 or

Discussion

MXAN_6967, because Fur sub-family recognition motifs (as from Fur, Mur, Nur, Zur, Irr and PerR) are quite similar (Fuangthong *et al.*, 2003; Lee *et al.*, 2007). A heterologous expression of the two *M. xanthus* Fur proteins, followed by *in vitro* DNA footprint experiments could elucidate sequence specificity of the DNA binding regions of both and clarify which genes underlie Fur-mediated expression control.

The small overlapping of Fur box-controlled genes (table 3.1) and genes from iron-uptake, -transport as TonB domain proteins (table 3.2) suggests that *M. xanthus* can use other, alternative strategies to control iron balance. The genome contained much more TonB-depending systems than necessary for the uptake of iron-myxochelin complexes, indicating for a potential import of competitor siderophore structures as found for *Escherichia* and *Salmonella* strain (Rabsch *et al.*, 1991; Ambrozic *et al.*, 1998), also if the activation of the uptake mechanism is not understood yet. The organism-foreign siderophores must be taken up somehow after iron-complexation, which argues for the expression of such formerly inactivation TonB-dependend import-systems, which might be accomplished by integrases/recombinases, a protein family which is known to modify and subsequently activate promoter sequences (Hall and Collis, 1995; Koenig *et al.*, 2008). As mentioned before, the integrase/recombinase MXAN_1873 was detected to be Fur-controlled (table 3.1).

To summarize the results from bioinformatic analysis: The iron-regulation in the order of myxobacteria seems to be very strain-specific, suggested by the finding of different numbers of Fur proteins and functions encoded in the genomes of *M. xanthus* DK1622, *S. aurantiaca* DW4/3-1 and *S. cellulosum* Soce 56 (Quatrini *et al.*, 2007). Diverse control-systems enable *M. xanthus* to use various possibilities to respond to iron-limitation.

The overall response of *M. xanthus* shares a high degree of similarities with results from other bacteria (Wan *et al.*, 2004; Ernst *et al.*, 2005; Quatrini *et al.*, 2007). More precisely, *M. xanthus* shows some features, typically found in Gram-negative bacteria, as in the genome several Fur proteins were coded, whereof one is iron-responsive (MXAN_3702), or as the existence and structure of Fur boxes of many iron-uptake and -transport genes. On the other hand, *M. xanthus* might be able to use several uncommon strategies such as iron-responsive putative integrase/recombinase proteins or as the import and degradation system for heme derivates, only known from a few other bacteria.

Discussion

Two genes of *M. xanthus* (MXAN_4532 and MXAN_6639; a NRPS and a chalcone/stilbene synthase), each putatively controlled by Fur boxes substantiate the hypothesis that it may be possible to bring hidden metabolites into the range of detection during iron starvation. Surprisingly, with the β -ketoacyl-acyl carrier protein synthase MXAN_7353, a protein of the initial step of fatty acid biosynthesis was predicted to be iron-responsive.

In any case, the bioinformatic prediction of Fur homologues in *M. xanthus* DK1622 provides some interesting information about how the strain might respond to iron-limitation in advance of any practical experiments.

4.2 Response of *M. xanthus* DK1622 to iron-limitation

After *in silico* analysis, the response of *M. xanthus* to iron-limitation concerning growth, iron-uptake, proteome and secondary metabolite production was analyzed. To ensure statistical relevance of detected events, all experiments were carried out as triplicates. Additionally, protein interactions with the promoters of the two *fur* genes (MXAN_3702 and MXAN_6967) were evaluated via DNA pull-down assays, using protein samples from iron-rich or iron-limiting conditions.

4.2.1 Iron-limiting environment

Iron concentration was determined in growth media before (CTT) and after (CTT-Fe^{MIN}) treatment with Chelex. Iron concentrations were thereby measured photometrically using Ferrospectral, as used routinely for bacterial iron-limiting environments (Cinkaya, 2002; Smith *et al.*, 2006; Hamann, 2007; Ilg, 2007). To provide a defined amount of iron, it must be ensured that glass-bound iron was removed quantitatively from all containers used in advance of any practical experiments. This was accomplished by pre-treatment of all glass-containers with Chelex resin beads (see section 2.7.1).

The iron concentration of CTT medium was 4.8 µM, with a standard deviation of approximately 0.6. Iron-rich conditions for other bacteria (growth without obvious limitation) are described to be in the range between 2 and 20 µM in the respective growth media (Hubbard *et al.*, 1986; Winkelmann *et al.*, 1987; Basler *et al.*, 2006), which was also correct for CTT. Some exemptions have to be made as for several bacterial species, which use ferric iron as final electron acceptor, such as *Geobacter* strains (Mahadevan *et al.*, 2006) or organisms, which do not need any iron at all, such as *Lactobacilli* (Archibald, 1983).

The iron concentration of CTT-Fe^{MIN} was ca. 0.5 µM, with a standard deviation of ca. 0.12. In previous approaches of other groups, the used concentrations of iron-limiting conditions were found to be in the same range, i.e. between 0.2 and 2 µM (Hubbard *et al.*, 1986; Lodge *et al.*, 1986; Wennerhold *et al.*, 2005; Najimi *et al.*, 2008). A second round of reduction of the iron concentration below 0.3 µM by re-treating the CTT-Fe^{MIN} with Chelex leads to a significant growth deficit, making this medium not feasible for follow-up studies.

As all measurements, the here used spectrophotometric system is defective. Remaining doubts could be cleared out by the usage of orthogonal detections mechanisms, as for e.g. by Atomic Absorption Spectrophotometry, which determines the total amount of iron, independent from change.

Discussion

In the laboratory, bacteria are grown in culture media which are designed to provide all the essential nutrients in solution for bacterial growth and for maintaining cellular biosynthesis and energy metabolism. In principle, there are different ways to create iron-limiting bacterial growth media: When using complete **synthetic (or minimal) media**, iron-concentrations can be easily adjusted by adding the respective amount of iron to medium. Such approaches have been performed with e.g. *Brucella* (Anderson *et al.*, 2008) or *Corynebacterium* (Wennerhold *et al.*, 2005) strains.

An alternative strategy to create iron-limiting media is the **complexation of present iron**. This can be accomplished by commercial available siderophores, which then remain in the media. As an example, desferrioxamine B (Desferal) was added to media of *Neisseria meningitidis*, (Basler *et al.*, 2006) or *H. pylori* (Lee *et al.*, 2004) to generate iron-limiting conditions. Furthermore, the iron chelators ethylenediamine-di-*o*-hydroxyphenylacetic acid (EDDA) and 2,2'-dipyridyl were used to create iron-limiting conditions for *Aeromonas salmonicida* (Najimi *et al.*, 2008). It cannot be completely excluded for *M. xanthus* that some of the various TonB-related import systems may potentially take up competitor ferric-siderophore complexes which finally would then be metabolized, since some bacterial strains are able to import foreign siderophore molecules (Rabsch *et al.*, 1991; Ambrozic *et al.*, 1998), as mentioned before.

Alternative setups include the **removal of iron** from media before inoculation, e.g. with the transition metal chelating agent Chelex. The approach of bacterial growth in Chelex-pretreated media as iron-limiting environment was reported previously for many bacterial strains, such as *E. coli* (Hubbard *et al.*, 1986), *Pseudomonas* (Ochsner *et al.*, 2002), *Bacillus* (Ollinger *et al.*, 2006), *Bordetella* (Vidakovics *et al.*, 2007) as well as *Klebsiella pneumoniae* (Lodge *et al.*, 1986).

Also here, for the preparation of CTT-Fe^{MIN}, the complex medium CTT was treated with Chelex resin beads. However, iron is the preferred binding target with the highest affinity from all potential interacting metals (see Chelex-manual). Effects on other trace metal should be negligible (Vidakovics *et al.*, 2007), indicated by the fact that there was still 10 % of the initial iron (the preferred interaction partner) left in CTT-Fe^{MIN}, i.e. Chelex treatment was not performed exceedingly.

There might be the possibility that divalent metal ions other than iron were affected by the Chelex-based method; ongoing experiments (iron supplementation of CTT-Fe^{MIN} back to the untreated level of CTT; R. Müller, T. Klefisch) will ultimately provide the evidence that

Discussion

Chelex has created iron-limitation with a very high specificity. Again, these facts would argue for an additional determination method of total iron in both media, using techniques with higher accuracy and specificity, as e.g. Atomic Absorption Spectrophotometry.

Accordingly, it has been expected that an approximately 10fold reduction of iron concentration in CTT generates an iron-limiting environment. In order to discover response of *M. xanthus* to iron-limitation, comparative studies were made using CTT or CTT-Fe^{MIN}. The effects on growth, proteome and secondary metabolite level, as well as protein interactions with promoters of the putative *fur* genes MXAN_3702 and MXAN_6967 were monitored. The results from *M. xanthus* (growth limitation, iron-uptake rates, proteome and secondary metabolites) show the fundamental characteristic response of Gram-negative bacteria to iron-limitation. A detailed discussion will be given in the following sections.

4.2.2 Growth and iron uptake under iron-limiting conditions

To evaluate the direct consequence of iron, *M. xanthus* DK1622 was grown under both iron-rich and iron-poor conditions. Resulting **growth profiles** (section 3.2.1), **iron uptake rates** (section 3.2.2), **proteomes** (section 3.2.3), **DNA pull-down assays** (*fur* promoter-protein interaction; section 3.2.4) and **secondary metabolomes** (section 3.2.5) were then compared. The results are discussed in detail in the following sections.

Under conditions of iron sufficiency (CTT), wild type *M. xanthus* reproducibly exhibited a characteristic tri-phasic **growth** pattern (figure 3.4), with exponential growth commencing at 20 h (after lag-phase), continuing for 30 h (log-phase), and then dropping off (dying phase). The maximum cell density was achieved after 50 h at an O.D.₆₀₀ of ca. 2.5.

Under iron-limiting conditions (CTT-Fe^{MIN}), the growth rate was drastically repressed. Growth of *M. xanthus* did not exceed an O.D._{600nm} of 0.4 upon iron-limitation (figure 3.4). A significant reduction in growth rate is characteristically observed in iron-poor medium, reflecting the essential requirement of iron in basic bacterial metabolism (Ochsner *et al.*, 2002; Lee *et al.*, 2004; Holmes *et al.*, 2005), demonstrating that the used Chelex-based method produced iron-restricted conditions.

For the **determination of iron uptake rates**, iron-concentrations were determined by absorbance before and after growth using the iron reagent Ferrospectral (ferrozine) (Stookey, 1970; Carter, 1971), as applied for many microorganisms, such as e.g. *Rhodospirillaceae* (Smith *et al.*, 2006), *Archaea* (Hamann, 2007) or *Clostridium* strains (Cinkaya, 2002). Iron

Discussion

uptake rates were calculated by subtracting the remaining iron concentration in used media from the initial iron concentration in fresh media and normalized to the optical density of cells (Smith *et al.*, 2006).

The **iron uptake** (table 3.3) was highest in the period preceding exponential growth ($43.6 \text{ nmol h}^{-1} \text{ O.D.}^{-1}$), lowest during the exponential phase ($16.9 \text{ nmol h}^{-1} \text{ O.D.}^{-1}$), and then rose again once growth leveled off ($37.0 \text{ nmol h}^{-1} \text{ O.D.}^{-1}$). These observations indicate that iron transport and growth are decoupled in *M. xanthus* DK1622 as found for *E. coli*, in which intracellular iron storage pools are deposited pre- and post-exponentially (Abdul-Tehrani *et al.*, 1999). In fact, there was a significant reduction in the iron uptake of *M. xanthus* under iron-rich conditions at the exponential phase.

The results from iron-uptake rates (section 3.2.2) clearly indicate that *M. xanthus* had activated its iron uptake systems in order to respond to the low iron conditions. Accordingly, the relative increase of iron uptake was reported earlier (Touati *et al.*, 1995), correlated to enhanced protein expression of siderophore biosynthesis and ferri-siderophore re-import.

Correspondingly, the proportion of iron influx was significantly higher than under iron-rich conditions (ca. 5fold; calculated to total present iron), and essentially constant through the whole culture period (table 3.3). In fact, a very strong increase of both iron storage DPS/bactoferritin proteins MXAN_0866 and MXAN_1562 (both 27fold) was observed in the response of proteomes from *M. xanthus* to iron-deprivation. However, such a strong induction was unexpected; therefore gene MXAN_1562 was selected as a target for inactivation via single crossover (see section 4.4).

Anyway, the highest rate of iron import was determined in the dying phase, which was also the fact under iron-limitation.

Discussion

4.2.3 Response of the *M. xanthus* proteome to iron-limitation

The search for proteins and protein networks involved in iron-dependent processes was attempted by comprehensive proteomic experiments. Monitoring of the protein profiles from iron-rich and iron-limiting conditions and subsequent screening for differentially expressed proteins allows to pinpoint key changes in the *M. xanthus* proteome, and additionally may help to discover crosstalks between secondary metabolic pathways, in response to changed iron supply.

In *Helicobacter pylori* (Lee *et al.*, 2004) and *Campylobacter jejuni* (Holmes *et al.*, 2005), regulation by Fur and iron of selected genes was observed to differ at the transcriptional and protein levels, reflecting the existence of post-transcriptional/translational control mechanisms. This observation argues for direct analysis of cellular proteins, including post-translational modifications.

For implementation, three protein samples labeled with different CyDye DIGE fluorophores were run per 2D-gel. One of these samples, the internal standard, results from the pooling of aliquots of all biological samples in the experiment. Thereby, 2D-DIGE system brings statistical confidence and reliability to 2D-electrophoresis (see section 1.3.2).

2D-DIGE experiments to identify iron-correlated, up- or down-regulation of proteins from samples of two different time points (29 and 40 h) were designed in a way that non-specific variations in the protein profiles were minimized (see figure 1.13/figure 2.1).

Analysis by 2D-DIGE revealed in average 1979 protein spots per gel (standard deviation: 1.86 %) and a total of 172 spots whose expression levels differed constantly at least 2fold under the two culture conditions (table 3.4). By the MALDI-MS analysis, 169 of these 172 spots could be identified, resulting in 131 individual proteins (table a1). The detection of a single protein as several protein spots occurs frequently in proteome analysis. Such proteins are thought to be more important than single-spot proteins in the response to a certain factor, even more notable, if the regulation of the different spots show the same direction (all up- or all down-regulated). From the 131 identified proteins, 53 were analyzed as down-regulated in the presence of iron-limitation and 78 which were up-regulated (in case of protein, present as multiple spots, the not-modified protein species was taken into account). The occurrence of a higher number of up- than down-regulated proteins during iron-starvation is a characteristically result from bacteria under these conditions (Heim *et al.*, 2002; Basler *et al.*, 2006; Vidakovics *et al.*, 2007).

Discussion

To get a better overview about proteome response of *M. xanthus* to iron-limitation, the 131 identified proteins were categorized by their biological functions (table a1): **Central metabolism (12), protein regulation (13), chaperone and GST domain proteins (6), membrane-associated (4), iron acquisition (6), redox stress resistance (15), motility/chemotaxis (4), DNA metabolism/transcription (13), translation (10), hypothetical proteins or unknown function (48)**. Many of the identified proteins from general metabolism, peptidases or proteins with DNA interaction activities could be further connected to iron metabolism, because of the usage of iron as cofactor. Strikingly, 48 (37 %) of the identified proteins do not have an annotated function and thereof 25 did not exhibit any high homology to proteins with annotated functions in the NCBI database (table a1), an observation which may ultimately provide insight into their potential functions.

To elucidate the underlying metabolic changes responsible for the iron-starvation phenotype of *M. xanthus* DK1622, the following section will give a detailed view to the protein categories, found to be differently regulated (table a1).

Iron-limitation has significant effects on **central metabolism** in *M. xanthus*. As observed for other bacteria (Ochsner *et al.*, 2002; Holmes *et al.*, 2005), lower levels of tricarboxylic acid (TCA) cycle enzymes were detected, including the Fe-S protein succinate dehydrogenase (MXAN_3540, - 2.2fold). As an iron dependent protein, the succinate dehydrogenase is typically down-regulated by bacteria in the absence of iron (Wilderman *et al.*, 2004); its additional role in the electron transport chain makes the detection of this protein even more important, because it serves a key function in energy metabolism. Furthermore, the NADP-dependent isocitrate dehydrogenase Icd (MXAN_3537, - 2.2fold) participates in the TCA cycle. It catalyzes the third step of the cycle: the oxidative decarboxylation of isocitrate, producing α -ketoglutarate and CO₂ while converting NAD⁺ to NADH. Another protein from the TCA cycle, the succinyl-CoA synthetase, SucD (MXAN_3542, - 2.9fold), catalyzes a reversible step, which involves the substrate-level phosphorylation of GDP. All detected proteins from the TCA cycle were down-regulated and many of them use iron as cofactor. This strategy avoids the wasteful generation of iron-requiring proteins when there is no iron to combine with them, and increases the availability of this transition metal for more essential processes (Andrews *et al.*, 2003).

Another important protein, which was found to be differently regulated (MXAN_1264, 2.2fold) was the PckG (phosphoenolpyruvate carboxykinase), the reaction-rate determining enzyme in the metabolic pathway of gluconeogenesis. Plants and bacteria can generate

Discussion

glucoses from acetyl-CoA monomers by the glyoxylate cycle, which might give a hint for the enhanced consumption of acetyl-CoA units for the process of glyoxylate-gluconeogenesis in *M. xanthus* and simultaneously increase NADH formation to balance energetically the reduced TCA cycle (Kwon *et al.*, 2008). The energy-rich, reduced form of NADH is used in oxidative metabolism as energy-delivering coenzyme from the respiratory chain, which generates ATP. However, higher expression levels of PckG increase ATP formation (Kwon *et al.*, 2008). The switch from citrate-cycle to glyoxylate-cycle is performed by the isocitrate dehydrogenase Icd (- 2.2fold decreased). The difference in the energy status is also confirmed by induction of an ATP synthase (MXAN_7028; 5.0fold) and a CBS protein (sensor of cellular energy status; MXAN_7380, 3.7fold) under iron-limitation.

On the other hand, the lower availability of iron is also important for the heme-containing cytochrome P450 proteins, a central energy-providing protein family. From the 7 present P450 proteins (MXAN_0683, 1743, 2304, 3943, 4127, 4919 and 7298), none was detected as differently regulated. This indicates their importance for the cell, so available iron is used in the central processes of energy metabolism, coupled P450-catalyzed reactions of *M. xanthus*. Accordingly, the Rrf2 proteins (known to act as transcriptional main regulators for cytochromes) MXAN_1152, 1643 and 6918 of *M. xanthus* were not detected as differently regulated under iron-limitation. That no proteins from P450 cytochromes or Rrf2-like regulators were found as differently regulated could be reasoned by the general low abundance of these families or variations of 2D-DIGE spots were too small to be detected (Heim *et al.*, 2002; Lee *et al.*, 2004).

The argininosuccinate synthase ArgG (MXAN_5108, 7.9fold) and the carbamoyl-phosphate synthetase CarB (MXAN_3388, 2.1fold) were found induced under iron-limitation. Both proteins are correlated to the biosynthesis of the amino acid *L*-arginine, possibly involved in further synthesis of the non-proteinogenic amino acid ornithine, a precursor molecule of hydroxyornithine siderophores (Winkelmann, 2002). Anyway, housekeeping activities such as **amino acid biosynthesis** are typically found modulated during iron-starvation in other bacteria (Ochsner *et al.*, 2002; Baichoo *et al.*, 2002b; Ernst *et al.*, 2005).

However, no prove was found for an enhanced pathway of lysine biosyntheses, so this amino acid seems to be provided in sufficient amounts for the increased myxochelin production (table 3.3), which requires lysine as educt. Additionally, no evidence was found in the genome-screening or the proteome experiments of *M. xanthus* to excrete and subsequent re-

Discussion

import the amino acid cysteine, which is known to be used for iron utilization, as for e.g. by *L. pneumophila* (Jiang *et al.*, 1997).

Furthermore, 3 up-regulated proteins from the proteome studies could be correlated to glutamate metabolism (MXAN_0543, 2675, 5806), which was expected to be effected during iron starvation. Glutamate is the most abundant amino acid in both Gram-positive and Gram-negative bacteria. Organisms can produce large intracellular glutamate pools, up to 100 mM for vegetative growth and adaptational processes. Previously, iron-starving conditions had also indicated the aconitase as the iron-dependent bottleneck of glutamate synthesis in *B. subtilis* (Miethke *et al.*, 2006). In *M. xanthus* some proteins from this pathway were found to be up-regulated very similar, arguing for the accumulation of the important metabolite glutamate, as long as enough iron is available for the biosynthetic proteins. Additionally, glutamate is the start point for the biosynthesis of heme derivates by the C5 or Beale-pathway (Panek and O'Brian, 2002).

On the other hand, the heme-degradation function of HemS may perform a fast acquiring of iron from foreign heme structures without *de novo* synthesis of required proteins. The ability to use heme as an iron resource was thought for many years to be restricted to pathogenic bacteria, but there is increasing evidence that many soil bacteria can also acquire iron from heme (Noya *et al.*, 1997; Yang *et al.*, 2005). Thus, *M. xanthus* might be able to degrade foreign heme derivates from other organisms, as performed for e.g. by *S. aureus*, which can metabolize human heme-molecules (Zhu *et al.*, 2008).

Significantly, the up-regulation of a HemS binding protein (MXAN_1318) was observed under iron-limiting conditions in *M. xanthus* (3.0fold) as found in some pathogens, such as *P. aeruginosa*, *S. oneidensis* or *C. jejuni* (Ochsner *et al.*, 2002; Wan *et al.*, 2004; Holmes *et al.*, 2005). Additionally, the two proteins HemU and HmuV from heme uptake (MXAN_1320: hemin permease protein and MXAN_1321: involved in hemin import) could be detected to be present in *M. xanthus* (table 3.2).

Worth mentioning, proteins from heme degradation as for e.g. MXAN_1318 (HemS protein) were detected to be induced (3.0fold) during iron starvation. This was unexpected, because up to now, these proteins were only found in pathogen microorganisms and a few α -proteobacteria (Panek *et al.*, 2002; Todd *et al.*, 2005). The detected protein HemS is required for heme-storage and -degradation, the exact function is correlated to the current state of conformation (Schneider *et al.*, 2006). Additionally, a Fur box was detected in the promoter of MXAN_6641, a HmuY homologue, which is a hemophore that scavenges heme from

Discussion

infected hosts and delivers it to outer membrane receptors (Olczak *et al.*, 2008). The iron-storage function of heme and hemin molecules may be required in face of an increase of iron-influx, also indicated by the fact that the iron-depending rate limiting step of the glutamate synthesis, the aconitase, was not found down-regulated, which is the starting point for synthesis of heme derivates.

These findings were quite unusual, because heme was not expected to be an iron-resource in the natural environment of myxobacteria. This might be an oddment of a heme-degradation pathway, or the utilization of heme may be generally underestimated for soil-living organisms. Because *M. xanthus* can lyse prey-organisms, it is logical that iron-containing structures of these could be utilized as iron-resource (e.g. prey P450 cytochromes). The addition of heme as only iron resource in an iron-limiting environment as for e.g. CTT-Fe^{MIN} could clarify this possibility.

Anyway, myxobacterial iron metabolism and its regulation seem to be more complex than in other bacteria.

Among the differently regulated proteins were 14 categorized as **protein-regulation, -modification and -metabolism**. Seven hereof are predicted to possess proteolytic functions, three are peptidases of the M16 (pitrilysin) metallopeptidase family (MXAN_0791, 5.8fold; MXAN_1141, 2.2fold; and MXAN_7497, - 2.1fold), one is a M20 peptidase family member (MXAN_0543, 2.1fold), and one is an ATP-dependent Clp2 protease (MXAN_6483, 2.7fold). As most of these proteins were found to exhibit a higher expression under iron-limiting conditions in *M. xanthus*, the proteases may be involved in dismantling native, iron-incorporating proteins in the cell in order to increase the intracellular availability of iron for more essential proteins. Furthermore, peptidases are known to have fundamental roles in the activation of pre-proteins or to acquire particular metabolite storage pools without *de novo* synthesis by hydrolysis, for example from extracellular matrices (Clemans *et al.*, 1991; Kearns *et al.*, 2002; Curtis *et al.*, 2007).

Clearly significant for regulatory events, two protein-phosphorylation-correlated sensor kinases (MXAN_0720, - 2.7fold and MXAN_1892, - 2.5fold) were down-regulated, and a FHA (forkhead associated) receiver domain protein (MXAN_2520, 2.6fold) was induced in *M. xanthus* during iron starvation. Because these proteins can represent important key regulators of diverse functions, including secondary metabolism, the gene of MXAN_2520 was selected for gene inactivation. That more than 10 % of the identified proteins (14 from 131) belong to protein-regulation, -modification and -metabolism is an unusual result for

Discussion

bacterial response to iron-limitation (Ochsner *et al.*, 2002; Baichoo *et al.*, 2002b; Ernst *et al.*, 2005), which may be contributed by the complex life cycle of myxobacteria.

All three identified **chaperones** from proteome experiments were analyzed with a reduced expression (MXAN_1073, - 3.0fold; MXAN_4467, all 5 detected spots between - 2.1 and - 2.3fold; and MXAN_4895, all 9 detected spots between - 2.1 and - 2.9fold). This might be correlated to an unspecific reduction of protein biosynthesis and lower metabolic rates generally. Anyway, chaperones were typically down-regulated in bacteria under low-iron conditions as postulated for *N. meningitidis* (Basler *et al.*, 2006), *C. jejuni* (Holmes *et al.*, 2005) and *H. pylori* (Ernst *et al.*, 2005), to give only a few examples. Further proteins from this group, such as **GST domain proteins** (disarming of potentially harmful substances) or WD40 domain proteins (mediation of protein-protein interactions), did not show a clear trend.

Massive rearrangement in the composition of the **membrane proteins** of pathogenic bacteria is known, if grown *in-vivo* in the iron-limiting environment of body fluids (Griffiths, 1990).

In *M. xanthus*, several efflux pumps of the ABC type were also down-regulated (MXAN_0559, MXAN_5168), as well as an outer membrane protein P1 (MXAN_7040), a putative membrane- (MXAN_0350) and a putative lipo-protein (MXAN_0498), suggesting some remodeling of the outer membrane and cell surface structures, which takes place in response to low iron as detected in proteome analysis of *H. pylori* (Ernst *et al.*, 2005).

Anticipatory, to increase the number of identified membrane-proteins, sub-cellular fractionation could be performed. By this way, separate data could be attained for the sub-proteomes of hardly-soluble and periplasmic fraction from the plasma membrane (Görg, 1999; De la Cerda *et al.*, 2007). Such an approach would provide a deeper insight into the membrane-adaptation of *M. xanthus* in response to iron-deprivation.

Among the six proteins predicted to be involved in **iron acquisition**, all were detected with a higher expression during iron-starvation, partially with very strong increases of almost 20fold. This observation is consistent with a strong increase of iron-responsive genes dedicated to siderophore biosynthesis and iron-uptake in other bacteria, as for e.g. *E. coli*, *P. aeruginosa*, and *B. subtilis* (Ochsner *et al.*, 2002; Baichoo *et al.*, 2002b; McHugh *et al.*, 2003).

As expected from the increase of iron-uptake rates (table 3.3), a significant up-regulation was detected for all three identified proteins from the biosynthetic pathway of the siderophore myxochelin: the aminotransferase MxcL (MXAN_3640), the isochorismatase MxcF (2,3-

Discussion

dihydro-2,3-dihydroxybenzoate synthase, MXAN_3644), and the 2,3-dihydro-2,3-didhydroxybenzoate dehydrogenase MxcC (MXAN_3647) (Silakowski *et al.*, 2000). Surprisingly, MxcL was found as two protein spots in the 2D-DIGE experiment, both with a strong induction under iron-poor conditions (19.7fold and 10.6fold). This indicates a significant shift of the ratio of the myxochelins, to enhance rather the amino-derivate, which might have the higher affinity to iron. Indeed, HPLC-MS analysis exhibits a much more drastic increase of myxochelin B (678fold) than A (81fold), compared to iron-rich conditions (table 3.9).

For some proteins, which had been expected to be differently expressed under iron-limiting conditions as for e.g. the iron-chelator utilization protein (MXAN_3639, MxcB), no up-regulation was found. It can be speculated that at least some of the differences in expression may be too small to be detected by proteome experiments.

In accordance with iron acquiring proteins, an increase in the level of several iron transport proteins was observed, including three TonB-dependent receptors, all of which were found constantly up-regulated (MXAN5023, 7.6fold and MXAN_6911 as two spots, 2.7 and 4.1fold) as postulated for other microorganisms under iron-limitation (Ochsner *et al.*, 2002; Wan *et al.*, 2004). The TonB-ExbB-ExbD (see introduction; section 1.1.1) is an energy consuming system required for uptake of ferri-siderophore complexes by outer membrane receptors (Krewulak *et al.*, 2008), a mechanism which furthermore allows bacteria to pirate siderophores from their competitors.

The genome of *M. xanthus* contains other numerous TonB-dependent uptake systems (table 3.2); but proteome analysis exhibits only three TonB domain proteins with a difference in expression. As mentioned before, activation of the various TonB-depending receptor, -binding and -shuttling proteins may require a genomic modification by integrase-based DNA shuffling for the uptake of iron, connected to unknown structures. Furthermore, it might be possible that other undiscovered regulatory mechanisms were used in *M. xanthus* to control expression of some TonB-correlated import proteins.

In the group of proteins which alter redox state and/or provide **redox stress resistance**, a high content of up-regulated enzymes (14 of the 15 proteins) was detected. This highlights the adaption of the redox-status, in anticipation of an increased relative influx of iron which potentiates the formation of reactive oxygen species. Additionally, this observation is consistent with high proportions of iron-induced changes, dedicated to maintain redox-homeostasis in other bacteria during iron-starvation, as for e.g. *E. coli*, *P. aeruginosa*, *C.*

Discussion

jejuni and *B. subtilis* (Ochsner *et al.*, 2002; Baichoo *et al.*, 2002b; McHugh *et al.*, 2003; Holmes *et al.*, 2005).

Likewise, the main response of *M. xanthus* to iron-limitation based on the increase of the uptake of iron while simultaneously preparing a protection for the cell from any toxic effects, caused by the stronger influx of iron. The importance of these shielding effects is evident from the identification of the three most up-regulated proteins: thioredoxin TrxB2 (MXAN_5670; 56fold), a partner thioredoxin disulfide reductase, TrxB_1 (MXAN_1954; 8.3fold), and two iron detoxification/iron storage proteins (DPS/bactoferritin; DNA protection during starvation) TpF1 and TpF2 (MXAN_1562 and MXAN_0866; both 27fold), which are supposed to protect the chromosome from iron-induced free radical damage by sequestering intracellular iron (Escolar *et al.*, 1999; Holmes *et al.*, 2005), which is correlated to the additional function of both proteins as bactoferritins.

The remaining stress response proteins include the thioredoxin domain protein MXAN_0351, the antioxidant alkyl hydroperoxide reductases AphC (MXAN_1564, as three spots 2.1, 3.1 and 3.7fold induced and MXAN_6536, as two spots 4.1 and 7.4fold) and AphD (MXAN_1563, 14fold), a glutathione peroxidase family protein (MXAN_7090, 2.9fold), and three oxidoreductases (MXAN_0303, MXAN_4003, MXAN_6482), which are all typically involved in redox-balancing of bacteria (Vasil *et al.*, 1999; Ochsner *et al.*, 2002; Lee *et al.*, 2004).

Almost all detected proteins from this group were found induced, several at very high levels (as ca. 56fold for the thioredoxin protein TrxB2; MXAN_5670), which can be explained by the increase of the relative iron-influx. The only protein in this group, which was with reduced expression under iron-limiting conditions (- 2.5fold), was the thioredoxin peroxidase Tpx (MXAN_6496). This reduction may be reasoned by a function of these proteins in cell-to-cell communication, as antioxidant or as regulators in biomechanical signal transduction, as postulated for other organisms (Yu *et al.*, 2007).

The detection of significant increases of all proteins with predicted roles in **motility** and/or **chemotaxis** was found in *M. xanthus* (table 3.5), also reported for *B. subtilis* (Ollinger *et al.*, 2006), *C. jejuni* (Holmes *et al.*, 2005) or *H. pylori* (Ernst *et al.*, 2005). In contrast to other bacteria, myxobacteria as *M. xanthus* are able of coordinated movement in which cells move cooperatively (or ‘glide’) over solid surfaces (see introduction, section 1.2), as required for developmental aggregation processes in the formation of myxospores. This behavior is driven by two genetically-separable locomotive systems, the adventurous (A) and the social (S)

Discussion

motility systems. Social gliding motility is powered by the retraction of Type-IV pili (a sort of bacterial ‘grappling hook’), while the more controversial, adventurous gliding motility involves mucus secretion and fixed focal adhesion sites (Mignot and Kirby, 2008). In proteomic experiments, the key player in controlling both the A and S motility systems, the response regulator FrzS (MXAN_4149; 2.2fold) was found with a higher expression level, as well as specific components of both movement mechanisms: a CheW-like chemotaxis protein (MXAN_2685; 2.5fold) and the GspE protein (MXAN_2513; 2.7fold, involved in type IV pilus biosynthesis), both required for S motility, and AgmK (MXAN_4683; 7.1fold), a tetratricopeptide repeat protein involved in A motility. Activation of the motility apparatus under iron starvation conditions enhance gliding of *M. xanthus* over surfaces, probably in search for additional resources of iron, including prey organisms.

From 13 potential **DNA interacting proteins** from proteomic experiments (table a1), only 5 were detected with a higher expression under iron-depleted conditions. The RNA polymerase α -subunit (MXAN_3326) was down-regulated, as well as four proteins with possible regulatory functions (MXAN_4149, MXAN_4242, MXAN_4535 and MXAN_6032).

The gene MXAN_4535, coding for an ECF sigma factor was selected for single crossover disruption (section 4.4), because of the significant reduction during iron starvation (- 3.1fold). The majority of the proteins, involved in DNA metabolism and transcription appears down-regulated (2–3fold lower). Typically, proteins from **transcriptional regulation/DNA metabolism** had been found with the same response in other bacteria (Ochsner *et al.*, 2002; Baichoo *et al.*, 2002b; Ernst *et al.*, 2005). This result may be derived from the significantly slower growth rate and a reduction of metabolism generally observed in bacteria during iron insufficiency (Baichoo *et al.*, 2002b). Therefore, it can be concluded that up-regulated proteins from the group may have important roles in the regulation of iron-metabolism.

Remarkably, the Fur regulon of *M. xanthus* also includes several putative transcription factors, such as ECF sigma factors (MXAN_1591, 1619, 4242, 4535 and 7393), which are important for the regulation of specific subsets of genes with broad ranges of function, as described for example for *Pseudomonas*, *Campylobacter* or *Bordetella* strains (Ochsner *et al.*, 2002; Holmes *et al.*, 2005; Vidakovics *et al.*, 2007). Furthermore, it must be noticed that both N6-adenine DNA methyltransferases (MXAN_1808 and MXAN_1864) were found with a higher expression under iron-limiting conditions (3.9 and 3.3fold). This protein family was already associated to gene regulation in bacteria (Jeltsch, 2002), which was taken as a reason to generate knockout mutants of the genes MXAN_1808 and MXAN_1864 in further studies.

Discussion

A more detailed explanation of the function of these proteins and the phenotypes of the clones can be found in the discussion parts of the respective mutants (section 4.4). In a few organisms, further strain-specific, metal-associated regulators (see introduction 1.1.3), such as DtxR (De Zoysa *et al.*, 2005), IdeR (Dussurget *et al.*, 1999), SirR (Hill *et al.*, 1998). FeoC (Cartron *et al.*, 2006; Aranda *et al.*, 2009), RirA or IscR-like proteins (Chao *et al.*, 2005; Todd *et al.*, 2005) had been identified, which did not share homologies to proteins from the Fur family (Rudolph *et al.*, 2006). Also here, several transcriptional regulators had been identified to be influenced by iron. As mentioned before, the importance of iron-responsive transcriptional regulators instead of Fur proteins might have been underestimated, indicated by newer findings that some α -proteobacteria did not contain any Fur homologue, but employ alternative regulator proteins for iron-management (Johnson *et al.*, 2007). Such alternative regulators might be also present in *M. xanthus*, in addition to the two Fur proteins.

Surprisingly, a high content of DNA interacting proteins with possible global regulatory functions has been detected during proteome analysis (13 of 131; table 3.6). This was not expected, because other results from bacterial iron-limiting response contain typically only a few proteins with DNA binding character (Ochsner *et al.*, 2002; Baichoo *et al.*, 2002b; Ernst *et al.*, 2005). Hypothetically, *M. xanthus* could have developed several DNA-interaction-based response strategies in order to overcome iron shortage, which can occur easily in soil (Vasil *et al.*, 1999), the habitat of myxobacteria. However, the enormous modulation on the level of many DNA interacting proteins may also be reasoned by the complex life cycle and the extraordinary large genomes of myxobacteria.

The group of **translation-associated** proteins contained 10 different proteins, hereof only 3 up-regulated. The down-regulation of all four translation elongation factors (MXAN_2408, 3068, 3297 and 3298) and two ribosomal proteins (MXAN_3307 and 3793) may be attributable to the significantly lower growth rate of bacteria, typically found under iron insufficiency (Ochsner *et al.*, 2002; Baichoo *et al.*, 2002b; Ernst *et al.*, 2005), which accords to the reduction of the majority of proteins from transcription.

Finally, 27 of the 48 **hypothetical proteins** were activated, several at very high levels as MXAN_6434 (17.5fold), MXAN_1893 (12.2fold) or MXAN_3617 (9.6fold). 25 of the 48 hypothetical proteins show no strong homologies in public databases or share only similarities with other hypothetical proteins. Thus, no information about putative functions of these is currently available (table a1).

Discussion

Convincing homologies by BLAST analysis (E-value < 10^{-20} , high sequence coverage) could be detected for 23 of the 48 hypothetical proteins. Probably most important, 9 proteins were found with potentially regulatory functions. These proteins include 2 hypothetical peptidases (MXAN_1893, 12.2fold and MXAN_5846, - 2.7fold), 2 hypothetical DNA methyltransferases (MXAN_1988, 4.6fold and MXAN_5055, 2.8/7.1fold) and 5 hypothetical transcriptional regulators (MXAN_1591, 2.4fold; MXAN_1619, - 2.6fold; MXAN_2440, 2.7/3.2fold; MXAN_3679, 2.5fold and MXAN_7393, - 2.2fold). Only the function of MXAN_3679 (hypothetical protein; 2.5fold) could be specified as ArsR-like regulator, required for repressing the expression of heavy metal efflux pumps, which are usually down-regulated during iron-starvation. Induction of those repressors seems to be the logical consequence in *M. xanthus* during iron-starvation.

Furthermore, it must be mentioned that MXAN_5484 shares high homology to the HasB protein (heme acquisition system) from pathogen strains of *Serratia marcescens* (Benevides-Matos *et al.*, 2008). This protein family is involved in shuttling heme molecules across to cell membranes into cytoplasm in analogy to iron-siderophore complex import by TonB-dependent systems (Letoffe *et al.*, 1994).

However, some of the hypothetical proteins (MXAN_2440, 5055 and 5484) were detected as several proteins spots partially with phosphorylations, indicating a central function under iron-limiting conditions. As the exact cellular role of these proteins in *M. xanthus* is unknown, some genes were selected (MXAN_1619, 2440, 1988, 5055 and 5484) as target for gene inactivation experiments by single crossover knockout. A more detailed explanation of the function of these proteins, the motivation of selection for knockout clones and the single phenotypes can be found in the discussion parts of the respective mutants (section 4.4).

However, only two of the 40 genes from **Virtual Footprint analysis** Fur box prediction could be correlated to identified proteins from the **proteome experiment** (MXAN_3647 and MXAN_6911). This significant discrepancy may be explained by the inability of a simple proteome experiment to reveal all changes in protein expression, but may also reflect that many iron-responsive changes in *M. xanthus* are not only mediated by Fur, as in *P. aeruginosa* for example, only 27 of 78 iron-regulated genes contain a Fur box (Ochsner *et al.*, 2002). Another possibility was that the *P. aeruginosa* Fur box model used in the bioinformatic Fingerprint analysis was only a poor match for the *M. xanthus* recognition sequence. Therefore, it was aimed to correlate the proteomic response to the initial analysis of genes, regulated by Fur boxes. To address this concern, the promoter regions of all genes

Discussion

whose expression was affected by iron-limitation were **re-analyzed** for the presence of putative Fur boxes (table a3). The analysis was refined by manual control of candidate Fur boxes, specifically addressing positioning with respect to promoter elements and presumed translational start sites. Previously, it has been shown that Fur interacts in both *B. subtilis* and *Neisseria meningitidis* (Lee *et al.*, 2007) to sequences which match only 11 of the 19 bp consensus Fur box. In *M. xanthus*, localization and characterization of only 10 nucleotides from the designated 19 bp Fur box (figure 3.3) was possible, so these data were compared in the sequence alignment with promoter regions of proteins, which show altered expression in iron-limitation proteome response. For positive hits, it was required that the sequence of such proteome-responsive genes, the Fur boxes matches exactly to 8 or more of the 10 defined positions, in order to identify possible weaker-binding sites (Lee *et al.*, 2007). Exact match to only 8 from the 19 bp consensus sequence (42 %) had been shown to be an acceptable criterion for binding of Fur proteins to Fur boxes in other bacteria (Baichoo *et al.*, 2002a; Quatrini *et al.*, 2007), therefore the threshold for the discovering of Fur boxes in promoters of iron-responsive genes in *M. xanthus* was set to 8 or more nucleotides as well. This analysis revealed putative Fur boxes upstream of 29 additional genes whose expression was up- or down-regulated in *M. xanthus* proteome response to low iron conditions (table a3).

Interestingly, the alternative approach to re-analyze iron-responsive genes from proteome-response for the presence of Fur boxes was highlighted by MxCL, an additional member of the myxochelin biosynthetic pathway (MXAN_3640; 10.6 and 19.7fold) and the highly up-regulated proteins MXAN_0866 (DPS/bactoferritin protein TpF2; 27fold) and MXAN_5023 (tonB-dependent receptor; 7.6fold). Surprisingly, the second DPS/bactoferritin protein MXAN_1562, which was also detected in proteome experiments with a 27fold higher expression, was neither predicted to contain a Fur box (table 3.1), nor the manual sequence-check of its promoter region revealed any convincing sequence homology to the designated Fur box sequence of *M. xanthus*.

However, ultimate determination of the Fur box sequences would require direct investigation of Fur protein binding (Baichoo *et al.*, 2002a; Baichoo *et al.*, 2002b; Holmes *et al.*, 2005), as by heterologous expression of the Fur proteins followed by *in vitro* DNA footprint experiments.

Discussion

Even small differences in protein expression levels can be discovered using the 2D-DIGE system by comparing protein spot intensity obtained from one fluorescently labeled sample directly with another. Here, differences in protein abundance of at least 2fold between *M. xanthus* DK1622 samples from iron-rich and iron-poor conditions were detected, with statistical confidence greater than 95 % (t-test; $P < 0.05$) (Lee *et al.*, 2004).

To recapitulate and compare the overall 2D-DIGE results of *M. xanthus* under iron-limiting conditions, it was shown that the main part of the proteome was not affected, while only a minority was detected to be changed or modified. This is found in accordance to characteristic proteome results, obtained from other bacteria under iron-limitation: in *Neisseria meningitidis* ca. 10 % of the proteome was found to be influenced by iron-limitations (70 spots with different expression from ca. 700 detected spots) (Basler *et al.*, 2006); in *Bordetella pertussis* ca. 20 % (181 spots with different expression from ca. 900 detected spots) (Vidakovics *et al.*, 2007), and ca. 13 % in *Campylobacter jejuni* (Holmes *et al.*, 2005) (67 spots with changed expression from ca. 500 in total). All these approaches use higher detection limits in comparison to the 2D-DIGE technology, here applied to samples of *M. xanthus* (1979 detected protein spots per gel in average). Additionally, 2D-DIGE provides a much lower threshold (smaller range of changed expression) for protein spots to be defined as “differently expressed”.

Furthermore, all three mentioned publications are based on data from conventional 2D-electrophoresis. Therefore, it can be speculated that at least some of the detected changes could be caused by gel-to-gel variations, which were the major source of errors in a classical 2D-PAGE experiment (Wu *et al.*, 2006), minimized in 2D-DIGE based approaches by the application of an internal standard.

Here, samples from *M. xanthus* in 2D-DIGE exhibited 2-3 times more spots than the three mentioned bacterial strains. Though, under iron-limiting conditions the number of differently expressed spots was only marginally higher (172 spots; ca. 8.7 % of the total), in face of a very tight threshold for the definition of proteins as differently expressed (2fold). Taking these facts together, the 2D-DIGE-based proteome analysis of *M. xanthus* was performed with higher specificity and lower detection limits than the three mentioned similar approaches (Holmes *et al.*, 2005; Basler *et al.*, 2006; Vidakovics *et al.*, 2007).

Nonetheless, a limitation of gel-based techniques is that some cellular proteins can only be detected with difficulties or not at all, typically caused by low solubility and/or extremely low abundance, or proteins at the boundary of the isoelectric or mass range (including the huge

Discussion

polyketide synthases and non-ribosomal peptide synthetases of myxobacterial secondary metabolism). To overcome the problem that several of the PKS- or NRPS-proteins are far too large to be analyzed, proteome analysis needs to be set up in another way, such as multidimensional chromatographic separation approaches, which was already applied to *M. xanthus* samples (Schley *et al.*, 2006).

However, changes in regulation of at least some of the differently expressed proteins may be Fur-independent, a hypothesis in agreement with the much smaller number of detected Fur boxes in *M. xanthus*, which was also postulated for other bacteria (Ochsner *et al.*, 2002; Baichoo *et al.*, 2002b).

The overall proteome response of *M. xanthus* to iron-limiting conditions (table a1) consists mainly in changed expression of proteins from iron metabolism/acquisition, central metabolism, redox stress resistance, motility/chemotaxis, DNA metabolism/transcription, translation and proteins with regulatory functions. Iron-concentration-based effects to these protein groups was discovered frequently in proteome or microarray analysis, e.g. in *B. subtilis* (Hoffmann *et al.*, 2002; Baichoo *et al.*, 2002b), *B. pertussis* (Vidakovics *et al.*, 2007), *E. coli* (McHugh *et al.*, 2003), *S. oneidensis* (Thompson *et al.*, 2002; Wan *et al.*, 2004), *P. aeruginosa* (Ochsner *et al.*, 2002), *C. jejuni* (Holmes *et al.*, 2005), or *H. pylori* (Lee *et al.*, 2004; Ernst *et al.*, 2005).

Furthermore, it could be demonstrated for *M. xanthus* that fewer proteins are negatively- (74) than positively-regulated (98) by iron-deficiency. This result is characteristic for bacteria, in which Fur acts in the classical role as an iron-responsive repressor with iron as co-repressor. This might argue again for an iron-responsive function of at least one of the two Fur proteins of *M. xanthus*.

Additionally, when comparing the proteome results from *M. xanthus* to other bacteria during iron-limiting conditions, a very high agreement was also found for the direction of regulation (induction or repression of the respective protein groups), shown in table 3.5.

Unexpectedly, for 4 of the 7 metal-depending proteases an up-regulation was detected under iron-starvation. This may indicate the importance of these proteins in protein-processing or protein-turnover events, perhaps with a key role in restructuring of the protein profile to free iron for more important processes or in highly specific processing or degradation reactions. Furthermore, the proteome experiments of iron-response of *M. xanthus* exhibited some very unusual features, as the potential to take-up and metabolize heme-derivates or the detection of

Discussion

a array of iron-regulated transcriptional regulators (much more than in other microorganisms, table 3.6) and a extensive rearrangement of proteins, functional in protein-metabolism, - regulation and -modification (table a1).

That many of these proteins from protein-regulation (such as protein kinases) were influenced by iron availability in *M. xanthus* is a remarkable result for bacteria (Deutscher and Saier, Jr., 2006b; Perez *et al.*, 2008). Additionally, the detection of numerous protein-phosphorylations (table a2) is also an atypical effect for prokaryotes (Deutscher *et al.*, 2006b), indicating miscellaneous possibilities for *M. xanthus* to respond and adapt to new life situations besides the complex life cycle of myxobacteria generally. These facts suggest significant modification of some proteins, which was found in contrast to the typical response of bacteria to changes in environment, usually varying protein profile rather in a quantitative and qualitative manner than to modify it. The common strategy of prokaryotes to control enzymatic activity (besides feedback inhibition or end product inhibition) mainly operates in regulation of biosynthetic pathways; and control or regulation of enzyme synthesis (Brock *et al.*, 1991). However, in the genome of *M. xanthus*, 97 eukaryotic protein kinase-like kinases (ELKs) were coded and numerous other proteins with capability as regulators as for e.g. transcriptional regulators, DNA methyltransferases or protein kinases, much more than in other bacteria (Goldman *et al.*, 2006; Perez *et al.*, 2008), for which iron-response has been investigated. The genome sequences of the myxobacteria reveal that they incorporate a complex network of regulatory functions, including enhancer binding proteins, two-component systems, and ELKs (Schneiker *et al.*, 2007). As *M. xanthus* contains almost 100 ELKs, phosphorylation is suggested to be a critical regulatory strategy in *M. xanthus*. Such modifications are not apparent from transcriptomic data, again motivating the use of proteome analysis in the case of *M. xanthus*, including the analysis of protein-phosphorylation patterns of iron-responsive proteins.

There was no evidence for up-regulation of the two Fur proteins themselves under iron-limitation, which seems likely to be observed in 2D-gels, but also no Fur protein was detected in similar experiments with *P. putida* (Heim *et al.*, 2002), *H. pylori* (Ernst *et al.*, 2005) or *S. oneidensis* (Thompson *et al.*, 2002; Wan *et al.*, 2004), which can be explained by marginal changes in expressions of Fur proteins, which are too small to be detected. Furthermore, it might be possible that other iron-responsive mechanisms can switch between an active and an inactive form of Fur proteins, hypothetically accomplished by posttranslational modifications. However, polypeptides with the size of Fur proteins (< 20 kDa) are known to be hard to detect on 2D-gels, reaching the limit of resolving power of polyacrylamide gels with generally used

Discussion

crosslinker levels (Rehm, 1997). In addition to this, the identification of such small proteins is difficult anyway, caused by the small number of generated peptides by proteolytic cleavage (Yates, 2004). The results from *M. xanthus* may be attributed to the non-auto-regulated Fur expression, because no indication was found for Fur boxes at both promoter regions of the Fur family genes in *M. xanthus* (MXAN_3702 and MXAN_6967). Continuative, this suggests the involvement of other regulatory mechanisms for Fur expression by alternative transcriptional regulators as discovered for *M. xanthus* by DNA pull-down assays, which were also known in other bacteria (Lee *et al.*, 2003). Also in cases of auto-regulation of Fur expression, the corresponding Fur proteins are typically not detected by proteome or transcriptome analysis (Wandersman *et al.*, 2004; Gaballa *et al.*, 2008).

In the particular case of *M. xanthus*, both Fur homologues did not show any indication for auto-regulation in both, bioinformatic searches or practical experiments (proteome and DNA pull down). This was found in accordance to the Fur model from *P. aeruginosa* (Vasil *et al.*, 1999), which was used in Virtual Footprint analysis.

Although this proteome analysis represents an incomplete picture of the *M. xanthus* iron response, the number and kind of up- or down-regulated proteins agrees well with the measured Fur regulons of other bacteria (Heim *et al.*, 2002; Wandersman *et al.*, 2004; Rudolph *et al.*, 2006).

From all posttranslational modifications, the **protein-phosphorylations** are mostly described and probably best understood (Reinders and Sickmann, 2005; D'Ambrosio *et al.*, 2007). Given this extensive kinase-based regulatory network in *M. xanthus* DK1622, cellular response to low iron might be mediated, at least in parts, by protein-phosphorylation of key proteins. To address this question directly, every differently regulated protein spot from proteome experiments was further examined by mass spectrometry (MALDI-ToF/ToF or LTQ-Orbitrap) for the presence of one or more phosphorylation(s), detected by specific induction of the neutral loss of the phosphate group (section 2.9.3.2).

Proteins, present as more than one spot in the 2D-DIGE analysis, were expected to carry different functional groups (such as posttranslational modifications like protein-phosphorylations), causing the variations in molecular weight and sometimes pI-value. If in such cases no difference in modifications was detectable, it can be explained by the general low abundance of modifications, which makes them difficult to detect anyway. Additionally,

Discussion

it is possible that one or more of the other protein-modifications had been accomplished (Walsh *et al.*, 2005), which were not detectable with the method used. Furthermore, it is known that some posttranslational modifications, such as protein-phosphorylations could be lost during the ionization processes (McLachlin and Chait, 2001; Kjellstrom *et al.*, 2004).

In comparison to the semi-automated data interpretation of MALDI-MS/MS, the analysis of phospho-peptides by LTQ-Orbitrap requires detailed manual control of composite spectra with overlapping mass ranges. This experimental set-up was found to perform highly precise measurements (error < 1 ppm) as reported before (Olsen *et al.*, 2005; Macek *et al.*, 2006; Chi *et al.*, 2007; Olsen *et al.*, 2007) but is on the other hand very time consuming.

As a result, from the 172 proteins from 2D-DIGE, 15 protein spots (12 proteins) were measured with one or more phosphorylation(s) (table 3.7). From these 15 protein spots, 10 were detected with one, 4 with two and 1 protein spot with three phosphorylations (table a2). For almost all detected phosphorylations, a trend of phosphorylation could be defined, if the respective modification was induced or reduced by iron-limitation. By correlation of mass spectrometric data to 2D-DIGE records, it was possible to determine that **MXAN_2440, 3571, 4863, 5401** and **6911** show an induction of protein-phosphorylation(s) under iron-limiting conditions, while it was found reduced in **MXAN_3079, 3307, 3326, 4137, 4467** and **7497** (table a2). For technical reasons, it was not possible to find out if the phosphorylated protein **MXAN_5055** was more present under iron-rich or iron-limiting conditions (table a2). The protein functions and details of the identified protein-phosphorylations are further explained in the following section.

This approach revealed that from 12 identified proteins (table 3.7/table a2) with one or more phosphorylation(s), six hypothetical proteins (MXAN_2440, MXAN_3079, MXAN_3571, MXAN_4137, MXAN_5055 and MXAN_5401) were among the phosphorylated species; two of which incorporated more than one phosphate group.

As an example, two spots, both identified as MXAN_2440, were found up-regulated in single- and double-phosphorylated form. Similar results were detected when analyzing MXAN_6911. The data from the analysis of MXAN_2440 and 6911 strongly suggests a trend for both proteins to become more important and to be more often phosphorylated under iron restriction as a consequence. For both proteins, the increase of the phosphorylated spot is higher than the increase of the un-phosphorylated protein spot. The opposite was detected for MXAN_3326 (RNA polymerase RpoA) and MXAN_4467 (GroEL1 chaperonin). Here,

Discussion

dephosphorylated and phosphorylated spots show reduced expression, so both proteins become less important under iron-limiting conditions.

In detail, the up-regulation of **MXAN_2440** could be confirmed for two spots, containing one (3.2fold up) or two phospho-residues (2.7fold up on iron starvation), respectively. The non-phosphorylated protein species was not detected to be differently regulated in 2D-DIGE. Hence, the tendency for MXAN_2440 can be clearly defined with a higher degree of phosphorylations under iron-limitation. More information about the function of this protein can be found in the discussion part of the generated knockout mutant (section 4.4).

Furthermore, the hypothetical protein **MXAN_3079** was found to be phosphorylated, but significantly reduced under iron-limitation. Unfortunately, the BLAST analysis showed no convincing homologies to known proteins with assigned function.

The detection of the down-regulation of a phosphorylated 50S ribosomal L29 protein (**MXAN_3307**) under iron-limiting conditions may be correlated to the general reduction of translational processes, which agrees to the results from this and other proteome experiments (Baichoo *et al.*, 2002b; Ernst *et al.*, 2005). In accordance to that, the RNA polymerase α -subunit (**MXAN_3326**, RpoA) was detected as 3 spots with one, two or three phosphorylations, respectively. All three spots showed a similar down-regulation (all between - 2 and - 2.3fold), indicating that not only the quantity of this protein was reduced, but also the level of phosphorylation was decreased under iron-poor conditions. Changes in RNA polymerase phosphorylation patterns are thought to orchestrate the association of different sets of factors with the transcriptase and strongly influence functional organization of the core domain (Phatnani and Greenleaf, 2006). The reduction of both proteins point to an undirected reduction of the complete transcription in *M. xanthus* under iron-limiting conditions, possibly to save resources and energy for more important processes. This characteristic reduction of the overall metabolism of bacteria during iron-starvation was also expected for *M. xanthus*, indicated by the data from growth.

In the proteome analysis, two spots with different expression profile were identified as **MXAN_3571** (hypothetical protein). One spot was - 2.1fold down-regulated (without any detectable modifications), while a second spot was 2.7fold up-regulated (containing one phosphorylation). While the intensity of the dephosphorylated spot of MXAN_3571 was reduced, the phosphorylated form was found with higher intensity. The protein BLAST indicates high similarity to members from the flotillin-band 7 protein family. These proteins cluster to form membrane microdomains and have been implicated in signal transduction and

Discussion

regulation of cation conductance (Langhorst *et al.*, 2005). The strong increase of the phosphorylated species of this protein suggests important differences in function, induced by the protein-phosphorylation, which was also reported from other bacteria (Zhang *et al.*, 2005a).

MXAN_4137 (hypothetical protein) was measured with a tendency to decrease phosphorylation levels during iron-starvation. Unfortunately, the BLAST analysis showed no convincing homologies to known proteins with assigned function.

Another protein, identified as 60 kDa chaperonin GroEL1 (**MXAN_4467**) was detected as 4 spots (all between - 2.1 and - 2.4fold down regulated), only one spot was found to contain one phospho-residue (- 2.1fold down), other modifications (which cause the occurrence as several spots) could not be detected. GroEL proteins are known to cooperate in their function as chaperones, which is drastically increasing after phosphorylation, partially required for this proteins to be active (Kumar *et al.*, 2009). The result may be correlated to the reduced transcription/translation and a general reduced metabolism of *M. xanthus* under iron-limiting conditions, accordingly a lower emerging of proteins per time need less chaperone-like folding helpers.

The protein **MXAN_4863** (adventurous gliding motility protein AgmK) was detected with a tendency to increase the phosphorylated protein species under iron-deprivation. An increased amount of the phosphorylated protein species may be a hint that polymerization-function was enhanced in order to amplify cell movement by adventurous motility. The motility of *M. xanthus* was already connected to protein-phosphorylation, as some proteins require to interact with specific protein tyrosine kinase (Youderian and Hartzell, 2007).

The trend of phosphorylation of **MXAN_5055** was inconsistent for this protein with unknown function, present in the proteome result as 3 individual spots (7.1fold up without, - 3.2fold down containing one, 2.8 for up containing two phosphorylations). A protein BLAST exhibits a methyltransferase type 11 domain, additionally to a SMC domain (structural maintenance of chromosomes). More information about the function of this protein can be found in the discussion part of the generated knockout mutant (section 4.4).

MXAN_5401 (hypothetical protein) was measured with a tendency to increase the level of phosphorylated protein during iron-starvation. Unfortunately, the BLAST analysis showed no convincing homologies to known proteins with assigned functions.

Furthermore, in this analysis **MXAN_6911** (TonB receptor) was detected with 0 and 3 phospho-residues, the corresponding two spots were both up-regulated (4.1fold and 2.7fold). Here, the protein was clearly induced and phosphorylation was amplified in the adaptational

Discussion

process to iron-limitation. This argues again for the activation of import of iron-siderophore complexes by *M. xanthus* TonB systems (Karlin *et al.*, 2006), as expected from measured iron-uptake rates and proteome response under iron-limiting conditions.

Analysis of the phosphorylation pattern of the metal-depending peptidase M16B (**MXAN_7497**) revealed that the degree of phosphorylation decreases under iron-limitation. This protein family of processing proteases is known to cleave signal sequences from larger proteins (Aleshin *et al.*, 2009), but because the exact substrate of MXAN_7497 is unknown, it is difficult to give a statement about correlation to iron metabolism.

Retrospectively, in proteome experiments two sensor kinases were down-regulated (MXAN_0720, - 2.7fold and MXAN_1892, - 2.5fold), while a FHA phospho-receiver domain protein (MXAN_2520, 2.6fold) was induced in *M. xanthus* under iron-limitation. That several (5 of 12) of the phosphorylated protein species were detected as induced, was found in contrast to the two down-regulated kinases from proteome responds. This apparently conflict may be explained by the up-regulation of other protein-kinases, which were below the threshold (factor 2), so the difference was too small to be discovered in the 2D-DIGE experiment, but may have strong cellular effects.

Nevertheless, the analysis supports a central role for kinase-mediated regulation in the ability of *M. xanthus* to respond to changed environmental conditions, such as iron availability. The detection of many variations in the phosphorylation pattern is consistent with the expectations of key roles of phosphorylation in regulation of myxobacterial metabolism (Perez *et al.*, 2008), not only development (Jain and Inouye, 1998). On the other hand, this finding is quite unusual, because bacteria typically restructure the quantitative and qualitative composition of the protein profile, rather than to modify it, which is more common in eukaryotes (Deutscher *et al.*, 2006a).

4.2.4 DNA binding proteins at promoter MXAN_3702 and MXAN_6967

For the identification of proteins interacting *in vitro* with high specificity to the promoter regions of MXAN_3702 (*fur*) or MXAN_6967 (*fur* homologue), the DNA pull-down strategy was used (see section 2.10). By this method, the interacting proteins from each promoter can be determined, using protein extracts from different growth conditions.

Discussion

For implementation, protein extracts from *M. xanthus*, grown in iron-rich (CTT) or iron-limiting (CTT-Fe^{MIN}) media, were analyzed for binding to streptavidin-coupled polynucleotide sequences (both ca. 440 bp), corresponding to the promoter regions of MXAN_3702 or MXAN_6967. Finally, SDS-PAGE and MALDI-ToF/ToF MS were used to identify proteins isolated by this DNA pull-down strategy (section 3.2.4).

The major difficulty when studying transcriptional mechanisms is the distinct identification of proteins caused by their low abundance. Isolated from DNA pull-down assays in sub-micromole quantities, the complexes can be dissociated; the proteins can be resolved by SDS-PAGE and revealed by staining. Proteins were then further analyzed by proteolytic cleavage (in-gel digestion), followed by mass spectrometry and protein database search. The current standards in MS have mostly overcome the quantitative problem (Drewett *et al.*, 2001).

In previous experiments, a more stable, non-oxidative environment with stringent protein-DNA binding conditions could be generated, when adding manganese instead of iron as potential cofactor, as recommended for the binding of bacterial Fur proteins and other iron-requiring transcriptional regulators (Hantke, 2001). By this method, it is ensured that enough metal ions were supplied, which might be necessary for some DNA binding proteins to be active.

The transcriptional regulation at both promoters of MXAN_3702 and MXAN_6967 is performed by highly dynamic aggregates of proteins, whose composition changes significant in face of different iron-concentrations (table 3.8). Many proteins were not correlated to iron-depended regulation of transcription, some not even to transcriptional control at all.

In detail, the SbcC nuclease MXAN_0959 was found to bind to the promoter of MXAN_3702 under iron-rich and iron-limiting conditions (iron-concentration-independent), but to the promoter of MXAN_6967 only during iron-starvation. Therefore, it can be concluded that the binding of MXAN_0959 is only partially linked to iron-availability. The SbcCD protein complexes cleave DNA hairpin structures and disaggregate certain DNA-protein complexes, which can inhibit DNA replication, DNA recombination and expression events (Connelly *et al.*, 1998).

On the other hand MXAN_1359 (putative DeoR-like regulator) binds only to the promoter of MXAN_3702 under both conditions (highly sequence-specific, iron-independent). The protein family of DeoR-like transcriptional regulators was expected to be involved in regulation of Fur expression as reported for several other bacteria as for e.g. *P. aeruginosa*

Discussion

(Vasil *et al.*, 1999), *B. japonicum* (Rudolph *et al.*, 2006) or *Campylobacter jejuni* (Holmes *et al.*, 2005).

Remarkably, MXAN_1562 (DPS/bactoferritin) was found to bind to both promoter regions under iron-limitation (Fur and Fur homologue promoter specific, iron-dependent), further target sequences are unknown. Thus, this protein may have regulatory, iron-correlated functions, additionally to the DNA protection under starvation conditions. Partially, MXAN_1562 was modified via phosphorylation, as detected at the promoter of MXAN_3702 (table 3.8). Such a modification is known to induce significant conformational changes (Hong *et al.*, 1991), hypothetically correlated to sequence-specificity in order to offer more individual control of expression. This might be also evident for the two Fur genes in *M. xanthus*. Functionally, the DPS subfamilies are very diverse, some exhibit a DNA-binding activity that is at least partially linked with iron complexation (Zeth *et al.*, 2004). This protein seems to play a central role in response to iron-limitation, shown by the binding of MXAN_1562 to both promoter regions under iron-limitation and the high up-regulation (27fold), detected in proteomic study of *M. xanthus*. In order to gain deeper insight into the cellular function of MXAN_1562, the gene was selected as target for a knockout. More details about the protein function and the respective knockout mutant can be found in section 4.4.

Interestingly, the DNA methyltransferase MXAN_1808 (putative restriction/modification enzyme) was detected to bind to the promoter of MXAN_6967 only during iron starvation, so expression may be silenced by DNA methylation. A discussion of the knockout mutant and the possible cellular function of MXAN_1808 can be found in section 4.4.

Another protein, identified as gene product of MXAN_5055 (hypothetical protein) binds to the promoter of MXAN_6967 under both conditions, but to the promoter of MXAN_3702 only under iron-rich conditions (partially iron depending). The BLAST analysis results in two domains with a SMC/methyltransferase function. Most likely, the combination of the SMC DNA binding domain and a methyltransferase domain indicates DNA as methylation target, which was not determinable more exactly from the methyltransferase sequence. DNA methyltransferases are used to silence expression of this gene, usually regulating a whole subset of genes (Jensen and Shapiro, 2003). These facts may indicate that the promoter of MXAN_6967 is poorly accessible under both conditions, but the promoter of MXAN_3703 only under iron-rich conditions via silencing the respective gene via methylation of distinct promoters. Since the protein MXAN_5055 was not detected to bind to the promoter of MXAN_3702 under iron-limitation, this may be a sign of de-repression under these

Discussion

conditions. The gene MXAN_5055 may be of special importance for *M. xanthus* iron-response, therefore the gene was targeted for a inactivation experiment (section 4.4).

Interestingly, under sufficient iron supply MXAN_3203 (FHA domain protein) was detectable at the promoter of MXAN_6967. This protein is typically correlated to eukaryotic nuclear signaling mechanisms and is required for some transcription factors (Durocher *et al.*, 1999; Durocher and Jackson, 2002). As the data from DNA pull-down assays were unsatisfying, the gene MXAN_3203 was selected for a knockout experiment, to find out more about the cellular role of the protein. More details about the protein function and the knockout strain can be found in section 4.4.

Several proteins are found to perform highly specific and iron-depended promoter interaction as for e.g. MXAN_2347 (a protamine P1 homologue) was only detected at the promoter of MXAN_3702 under iron-rich conditions. Protamines are small, arginine-rich proteins that are believed to be necessary in DNA stabilization (Takami *et al.*, 2004). Because this protein family is rarely detected in prokaryotes, knowledge is limited. No knockout mutant of the selected gene MXAN_2347 could be generated, indicating a central function in the regulation of metabolism in *M. xanthus*.

Several regulatory proteins were identified at the promoter of MXAN_6967 under iron-limitation (the adenine-specific DNA methylase MXAN_1808, and two transcriptional regulators (MXAN_5271 and MXAN_5872). Probably most importantly, transcriptional regulators were found to be involved in regulation of Fur expression, also found in several bacteria as for e.g. *P. aeruginosa* (Vasil *et al.*, 1999), *B. japonicum* (Rudolph *et al.*, 2006) or *Campylobacter jejuni* (Holmes *et al.*, 2005).

No methyltransferase was detected at the promoter of the probably iron-correlated *fur* homologue MXAN_3702 during iron starvation, arguing for a good accessibility under these conditions, in contrast to iron limitation.

No indication was found for the binding of one from both Fur homologue proteins in *M. xanthus*, neither at the promoter of the *fur* gene (MXAN_3702), nor of the *fur* homologue (MXAN_6967), despite the usage of different transition metals as binding co-factors (section 2.10). The absence of any evidence for binding activities of Fur (MXAN_3702) or the Fur homologue (MXAN_6967) is found in accordance to results from some other bacteria and it was consistent with the absence of Fur boxes in *M. xanthus*, analyzed by the virtual footprint

Discussion

software. However, Fur expression control by several regulators, more than solely Fur proteins was already described (Lee *et al.*, 2003) and could also be confirmed for *M. xanthus* by DNA pull-down assays (table 3.8).

Several protein-bands from the SDS-gel of the DNA pull-down assay (figure 3.8) could not be identified. The problem might be explained by the low amounts of proteins (bands can be a mixture of different proteins in quite low amounts) or by the used silver staining, which is known to complicate and sometimes disable a subsequent mass spectrometric analysis. Anyway, this staining method was used because of required low detection limits, which are known to be much lower than for example Coomassie staining of protein gels (Sinha *et al.*, 2001). Some of these unidentified bands were found in good agreement at both screened promoters when using protein samples from iron-limiting conditions (namely in the lanes 3 and 5); three highly similar bands occur in the low molecular weight regions (at ca. 10-15 kDa). These polypeptides may represent important key factors in regulation of Fur expression, but since those were not identified, it is impossible to give any final statement about function. As mentioned, the identification of such small proteins is complicated anyway, caused by the small number of generated peptides by proteolytic cleavage (Yates, 2004).

To conclude, the Fur model of transcriptional auto-regulation seems not to be applicable for *M. xanthus*, also described for other bacteria like for *B. japonicum* (Rudolph *et al.*, 2006), *Campylobacter jejuni* (Holmes *et al.*, 2005) or *P. aeruginosa* (Vasil *et al.*, 1999), which was used as model in the Virtual footprint analysis. In these organisms, different sets of transcriptional regulators accomplish the control of Fur protein expression in order to adapt to iron-concentrations, as demonstrated for *M. xanthus* by DNA pull-down assays.

4.2.5 The response of the *M. xanthus* secondary metabolome to iron-limitation

The quantitative measurement of natural products by HPLC-MS is based on the MS^2 peak area and provides a highly specific and quantitative method to compare secondary metabolites from different samples, stable over several orders of magnitude (see section 2.13). The correlation of peak area and metabolite concentration was generated with a dilution series from an independently grown wild type culture and showed R^2 values higher than 0.999 for all metabolites. The peak area of the major fragment (MS^2 peak area) is taken as a basis for

Discussion

quantitative calculations. The advantage of this method is the exclusion of false positive molecules, which can co-elute at the same time; in case metabolites show the same mass, fragmentation patterns will be different.

Inspection of the genome sequence of *M. xanthus* DK1622 revealed that the myxobacterium harbors 18 distinct gene clusters for the biosynthesis of polyketide and non-ribosomal peptide secondary metabolites (Goldman *et al.*, 2006). However, to date, only six compound classes (the myxochelins, DKxanthenes, myxalamids, myxovirescins, myxochromides and the ribosomally produced cittilins) have been discovered from the strain (Krug *et al.*, 2008a; Wenzel *et al.*, 2009a), even though 17 of the clusters have been shown to be transcriptionally or translationally active (Schley *et al.*, 2006; Bode *et al.*, 2009). In principle, proteins from natural product biosynthesis might provide a competitive advantage for *M. xanthus* against other bacteria, particularly under conditions of nutrient limitation.

In the first instance, the variations in yields of the monitored metabolites from cultures grown under iron-rich and iron-restricted conditions were analyzed (table 3.9). In iron-rich environment, production rates of the myxochelins, myxalamids and myxovirescins were stable during the later culture period (between 48 and 64 h).

As predicted from the observed increase in iron uptake efficiency under iron starvation, biosynthesis of both myxochelins A and B was significantly boosted (81 and 678fold, respectively). Furthermore, the ratio of the two myxochelin derivates changes from 17-19fold more B than A under iron rich to 142-157fold more B than A under iron-limiting conditions. This adaptation was expected because in 2D-DIGE, a strong up-regulation of MxcL was discovered (two spots; 10.6 and 19.7fold), which catalyzes the generation of the amino-derivate myxochelin B. Comparing the ratios of myxochelin A and B, the proportion of amino-derivative was significantly increased in CTT-Fe^{MIN}; therefore it can be speculated that the myxochelin B has the higher affinity and binding constant, which would allow a more efficient iron-binding and subsequent uptake in case of iron-competitors, which could cause the iron-limitation. Final determination of affinity and binding constants can be performed now after complete chemical synthesis (Prof. Dr. K. Hegetschweiler, S. Wilbrand; Universität des Saarlandes).

Analysis of regulation of siderophore biosynthesis is of special importance, since these compounds are used in clinical pharmacy to treat acute iron intoxications or

Discussion

hemochromatosis, as e.g. desferrioxamine (Desferal®), a siderophore which is produced by *Streptomyces pilosus* (Nielsen *et al.*, 1995; Vermylen, 2008). Furthermore, some siderophores are known to act as additional virulence factors in some pathogens (Lamont *et al.*, 2002; Bhatt and Denny, 2004; Kunkle and Schmitt, 2005; Vasil, 2007). Latest results show also promising approaches with siderophores as drug delivery agents (Möllmann *et al.*, 2009). To understand regulation of siderophore biosynthesis in *M. xanthus* will possibly help to elucidate regulation in other bacteria or regulation of secondary metabolites generally and might also facilitate to find new applications for this or other natural product families.

In addition to siderophore biosynthesis, the yield of the myxochromides was also increased (23fold for myxochromide A2) during iron-starvation. This increase may reflect a role of the myxochromides in gliding, enabling the *M. xanthus* swarm to move faster. As a hypothesis, the myxochromide fatty acid chain, which is variable in length, has a potential influence on surface tension. Indeed, an increase in swarming rate has been observed previously for a *M. xanthus* mutant strain, engineered to overproduce the myxochromides (R. Müller, S.C. Wenzel; unpublished data). There was no indication of a Fur box upstream of the myxochromide gene cluster, which would explain the up-regulation of this compound class during iron starvation. Interestingly, also 4 gliding-associated proteins were all found up-regulated in 2D-DIGE analysis. The enhancement of motility-associated proteins is a comprehensible consequence of *M. xanthus* during iron-limitation to move to a more promising environment.

Another observed fact was the significant reduction of citterlin under iron starvation (75fold), maybe to save amino acid resources (tyrosine and isoleucine for citterlin). Presumably, this drastic decrease in the production of citterlin must be an indirect effect of iron-limitation, because there is no indication for a Fur box upstream of the coding DNA sequence. The reduction of citterlin may be an unspecific, secondary effect; created by the general reduction of metabolism, mainly translational and transcriptional processes. Anyway, the function of citterlin is still unclear.

The levels of the three other metabolite families, the DKxanthenes, myxalamids and myxovirescins remain unchanged. The yields of the DKxanthenes might have been anticipated to increase under iron starvation, due to the demonstrated role of these yellow metabolites in the developmental process of *M. xanthus* (Meiser *et al.*, 2006a). Although, *M. xanthus* cells grown in liquid culture do not sporulate, and so there was no additional

Discussion

requirement for the DKxanthenes under these conditions, as no cell-cell contacts or exactly localized signals are available. Of course, cells in liquid culture do not glide or develop to fruiting bodies, but these genetically coded events have evolved to adapt to soil as preferred habitat, which is far away from nutrient-rich, well-controlled laboratory conditions.

Taking all the facts together, secondary metabolome response in *M. xanthus* consists of an increase of siderophore production to enhance iron uptake under iron-limiting conditions. Furthermore, the biological agents myxovirescin and myxalamid were still produced at high levels during iron-starvation, hypothetically to prevent growth of potential competitors (Rabsch *et al.*, 1991; Ambrozic *et al.*, 1998). No differences could be detected in the production levels of the development-associated metabolite family of DKxanthenes, while citilin production was almost disengaged completely. As mentioned before, the enhanced myxochromide production may be used to facilitate movement to find and solubilize new iron resources.

As a starting point for discovering unknown metabolites, all the promoter regions of the remaining secondary metabolite gene clusters were analyzed for the presence of Fur boxes. Promisingly, putative Fur binding sites were predicted upstream of a NRPS gene (MXAN_4532) and a cluster encoding a putative PKS (chalcone/stilbene synthase) with allied tailoring genes (MXAN_6635-MXAN_6640).

These findings support the hypothesis that these silent secondary metabolite genes might be awakened under iron poor conditions. As MXAN_4532 encodes two modules of a non-ribosomal peptide synthetase, the known correlation between the domain complement of NRPSs and their products was used (Fischbach and Walsh, 2006) for structure-prediction of the produced metabolite, in order to guide the search efforts. According to classical rules of NRPS biochemistry, a bimodular system should produce a dipeptide. However, the second module of enzymatic functions lacks an activity to catalyze release of the mature product (typically a thioesterase). This observation raises the possibility that the synthetase may collaborate with other multienzymes in *M. xanthus*, to give rise to a longer peptide. Promising, MXAN_4532 has a very close homologue (66 % I, 76 % S) in *Stigmatella aurantiaca* DW4/3-1 (MtaG); such interspecies conservation suggests that it serves a common function for the two myxobacteria. Alternatively, the NRPS may be a member of pathway in an ancestor common to both *M. xanthus* and *S. aurantiaca*, which has been degraded.

Discussion

However, the molecule which is produced by the coded RppA-like chalcone/stilbene synthase (MXAN_6639) is unknown, but the typical broad substrate specificity of these enzymes yields in a wide variety of products. For e.g. RppA is involved in the biosynthesis of melanin in *S. griseus* (Funai *et al.*, 2002). The pigment provides UV protection, as possibly in *M. xanthus*, which might be necessary in face of metal-mediated differences of the cellular redox status (Asad *et al.*, 1998). On the other hand, the RppA homologue of *S. cellulosum* Soce 56 (Sce2133) was heterologously expressed and the production was found to be limited to flaviolin (Gross *et al.*, 2006). In contrast to the high similarity of MXAN_6639 to the chalcone synthase STIAU_8629 from *S. aurantiaca*, the respective homologue of *S. cellulosum* was detected with much lower similarity to MXAN_6639 (34 % I, 51 % S). Therefore, no final conclusion can be made about the potential structures, produced by MXAN_6639 and also not about a possible iron-affinity or a further destiny in secondary metabolism of the produced molecule.

In any case, no product of MXAN_4532, MXAN_6639 or any other novel or modified metabolites in extracts of DK1622 could be discovered, despite scrutiny of both the UV/Vis and mass spectrometry data. Thus, manipulation of environmental iron does not appear to be a productive strategy for genome mining, at least not in *M. xanthus*.

Further explanations for the absence of new secondary metabolites are that products exist only as traces, because the conditions were not found yet for expression and/or activation of proteins in sufficient amounts or, on the other hand, to provide enough building blocks for product synthesis. An additional possibility is that the biosynthetic proteins could be inactive or the pathway might be degraded generally in *M. xanthus* or the metabolite was lost during pre-analysis sample treatment. Further environmental changes would perhaps support the generation of still unknown secondary metabolites of *M. xanthus*, as e.g. fruiting body development under iron-limiting conditions.

Carotenoid analysis was disregarded, GC-MS guided approaches have shown massive non-iron-responsive variations, which were rather growth phase correlated. At all, more than 60 carotenoid-derivates are published from *M. xanthus* (Dworkin and Kaiser, 1993; Chapter 7: Genetics of regulation and pathway of synthesis of carotenoids), so a detailed analysis would here far exceed the timeframe of the work. However, carotenoid biosynthesis in *M. xanthus* had been shown to be affected mainly by light and copper (Moraleda-Munoz *et al.*, 2005), in agreement with the results from other microorganisms (Tisch and Schmoll, 2010).

Discussion

The unusual regulatory mechanisms and secondary metabolite response of *M. xanthus* can prospectively contribute to understand and positively impact the siderophore production or regulation of secondary metabolites generally in microorganisms, not only in *M. xanthus*. However, elucidation of pathways and regulation of the biosynthesis of secondary metabolites from *M. xanthus* will also help to make this organism play a more important role in biotechnological processes in the future.

4.2.6 Importance of iron and Fur for *M. xanthus*

From the available proteome data it is not possible to distinguish between Fur-dependent and Fur-independent effects of iron-responsive proteins whose expression has changed in this experiment. Additional proteome analysis with a desirable inactivation mutant of the *fur* gene MXAN_3702 would allow to divide Fur-dependent from –independent effects in response to iron-limitation and generate by this way a much deeper insight into the regulatory networks of the respective strain (Thompson *et al.*, 2002; Wan *et al.*, 2004; Lee *et al.*, 2004). Such a desirable, engineered knockout-mutant in the putative Fur gene MXAN_3702 would help in comparative studies with the wild type to disentangle Fur-dependent and Fur-independent events in iron response (Lee *et al.*, 2004; Holmes *et al.*, 2005; Ernst *et al.*, 2005). As mentioned before, it was not possible to inactivate MXAN_3702, suggesting that the gene is essential in *M. xanthus* DK1622. That Fur proteins were apparently essential has been noted for a number of other bacteria, as for e.g. *Rhizobium leguminosarum* (de Luca *et al.*, 1998), *Synechococcus* sp. strain PCC7942 (Ghassemian and Straus, 1996), *Pseudomonas putida* (Venturi *et al.*, 1995a; Vasil *et al.*, 1999), *Neisseria gonorrhoeae* and *Neisseria meningitidis* (Berish *et al.*, 1993; Grifantini *et al.*, 2003), but it remains unclear why Fur is essential for some strains and not for others.

Anyway, Fur proteins are known to control siderophore production, adaptation of the cellular redox status, and movement in many microorganisms (Ochsner *et al.*, 2002; Baichoo *et al.*, 2002b; Ernst *et al.*, 2005). Several of these proteins, some in key positions, could be associated to low-iron response in *M. xanthus*. Anticipatory, in this study neither the Fur protein (MXAN_3702) nor the Fur protein homologue (MXAN_6967) were detected to be differently regulated in the proteome analysis or found in the DNA interaction studies to bind to the respective promoter regions. The fact that Fur seems to be essential and not auto-regulated in both, *M. xanthus* and *Pseudomonas*, argue for the correctness of the applied

Discussion

Pseudomonas-model in the virtual footprint software to generate a *M. xanthus* Fur box consensus sequence.

In *M. xanthus*, the importance of the Fur protein with “classical” iron-responsive structure (MXAN_3702) was clearly indicated by the fact that the gene could not be destroyed by deletion or single crossover gene disruption (as in *P. aeruginosa*; Vasil *et al.*, Vasil, 2007), in face of the usage of several homologue DNA regions, cloned into different plasmids, as pSWU41, pBJ113 and pBJ114 (Wu *et al.*, 1996; Black *et al.*, 2004). The generation of some single crossover clones of iron-responsive genes may be a result of adding 10 µM FeCl₂ to selection plates, to ensure that availability of iron is not part of selection pressure. The approach to provide sufficient iron supply for the initial growth of iron-uptake/-metabolism deficient mutants failed for the mutation of MXAN_3702.

In the model strain *E. coli*, Fur is the downstream gene in the bicistronic *fldA-fur* operon; the *fldA* gene is essential and encodes flavodoxin, a flavin-containing protein which may be essential for providing iron in the ferrous (Fe²⁺) form for Fur (Andrews *et al.*, 2003). In *M. xanthus*, MXAN_3702 seems very likely to be the upstream gene of a bicistronic operon, containing a gene for another redox enzyme, thioredoxin, which might be involved in the reduction-coupled release of ferrous iron from ferric-siderophore complexes. Anyway, inactivation of MXAN_3702 via in-frame deletion limits effects to the target gene, so polar effects from neighboring genes under the same promoter control are eliminated, in contrast to single crossover inactivation approaches.

In contrast, MXAN_6967 is likely to be regulated independently from either its up- or downstream neighbors.

Also the established strategy to generate spontaneous *fur* point mutations, induced by high concentrations of transition metals (usually manganese; between 10 and 200 µM MnCl₂) failed here. This method was applied successfully to other “difficult” Fur candidates (Hantke, 1987; Thomas and Sparling, 1996; Hickey and Cianciotto, 1997), but not in the case of *M. xanthus* DK1622. Mutants of *M. xanthus*, which were generated by this method were able to grow on high-metal selection-plates, but did not show any differences in DNA analysis of the Fur proteins or the related promoter sequences (data not shown).

Furthermore, no disruption mutant of the myxochelin gene cluster could be generated up to now, again arguing for the importance of iron for *M. xanthus* DK1622. It must be mentioned that all other gene clusters coding for secondary metabolites in *M. xanthus* could be inactivated by members of our group (R. Müller, D. Krug, Cortina, N.S.; unpublished results).

Discussion

In contrast, a mutant of *S. aurantiaca* could be generated after iron-supplementation, which did not produce detectable amounts of myxochelin (Silakowski *et al.*, 2000), again arguing for a very heterogeneous regulation of iron-metabolism in myxobacteria generally, perhaps correlated to predatory or scavenger life style of the respective strain. The compound class of siderophores was found to be essential, for example in *Agrobacterium tumefaciens* (Sonoda *et al.*, 2002) or *Aeromonas salmonicida* (Najimi *et al.*, 2008), but not in *V. cholerae* (Wyckoff *et al.*, 2006) or *Bordetella* strains (Brickman *et al.*, 2007). The essential requirement of iron-chelating metabolites potentially depends on the existence and efficiency of alternative iron uptake systems and the importance of iron for the respective strain. For many pathogenic strains, siderophore production is strictly linked to iron-limiting environments, like host tissues, where it acts sometimes as pathogenesis factor. Thus, in laboratory passages with sufficient iron supply, siderophore production can be inactivated, in which some of the strains lose thereby the ability of colonialization of iron-low surroundings (Hickey *et al.*, 1997; Wyckoff *et al.*, 2006).

This indicates an environmental-specific requirement of highly efficient iron uptake systems, but up to now, no conditions for *M. xanthus* could be found, where the conservation of siderophore production (including the potential main regulator Fur; MXAN_3702) was not essential. Furthermore, *M. xanthus* was found to be a constitutive myxochelin producer, also in the state of iron-overfeeding (data not shown). On the other hand, not one of the generated mutants exhibited a significant increase in myxochelin production or in iron uptake. *M. xanthus* allows only small and limited modifications of the iron-network, again arguing for the importance of uptake and metabolism of this trace metal in this organism, since modifications of iron-responsive proteins lead to strong impacts to primary and secondary metabolism.

In reflection of its central role in iron metabolism of *M. xanthus*, *fur* is an essential gene as in some other bacteria (Escolar *et al.*, 1999; Vasil *et al.*, 1999; Andrews *et al.*, 2003; Grifantini *et al.*, 2003). Iron can become easily the limiting factor in the natural environment, caused by low concentrations of uncomplexed iron in soil and the extreme low solubility at biological pH (Vasil *et al.*, 1999), so *M. xanthus* must have developed some highly specific iron-limiting response strategies.

It is very difficult to give a final comprehensive statement, how *M. xanthus* resists iron-limitation, some findings are characteristic strategies, typically known from other Gram-negative bacteria with Fur as key regulator or the up-regulation of siderophore metabolites and their pathways; some findings are quite unusual, such as the potential uptake and

Discussion

degradation of heme derivates, which had been connected only to pathogen microorganisms (Voyich *et al.*, 2004; Martinez *et al.*, 2005; Battisti *et al.*, 2007) or a few α -proteobacteria (Rudolph *et al.*, 2006).

Iron is probably the most important trace metal for *M. xanthus*, indicated by the high number of proteins involved in iron-transport and regulation in both approaches, applying bioinformatic forecast (table 3.1) and proteome analysis (table 3.5). Both results suggest that *M. xanthus* can use unknown, alternative strategies besides Fur proteins to control iron balance.

However, transcriptional control by Fur can occur indirectly through expression of small regulatory RNAs, AraC-like transcriptional regulators, alternative sigma-factors as for e.g. RipA (regulator of iron proteins A) and two-component systems (Vasil *et al.*, 1999; Hantke, 2001). Several AraC-like regulators were found in the genome of *M. xanthus* and some in 2D-DIGE, but from sequence analysis alone, it is not possible to produce a reliable prediction if the protein activity is somehow correlated to iron or iron-regulation. Three alternative sigma-factors of the Rrf2 protein family (transcriptional main regulators of cytochromes) were discovered in *M. xanthus* (MXAN_1152, MXAN_1643 and MXAN_6918), which were known to be involved in regulation of iron metabolism-correlated genes, but were neither found as differently regulated in 2D-DIGE, nor detected to bind to *fur* promoter sequences. In DNA pull-down (table 3.8) and proteome experiments (table 3.6), several alternative sigma-factors were detected, including some putative.

It can be concluded that *M. xanthus* can use some already known strategies of Gram-negative bacteria to overcome iron shortage in soil and to regulate iron metabolism with Fur as the key player.

Many bacteria can produce different heme derivates; mostly for long-term storage of iron (Panek *et al.*, 2002) or as protein co-factor (e.g. P450 cytochromes). On the other hand, only a few can take up and metabolize these molecules from foreign organisms. In addition to the unusual heme biosynthesis of *M. xanthus* (Dailey and Dailey, 1996; Shepherd *et al.*, 2006), here some first evidence was found that myxobacteria can import and use extracellular heme as iron resource, which was thought to be a niche of pathogens (Voyich *et al.*, 2004; Martinez *et al.*, 2005; Battisti *et al.*, 2007) and a few α -proteobacteria (Rudolph *et al.*, 2006). By follow-up experiments, it would be possible to clarify if *M. xanthus* can metabolize foreign heme structures.

Discussion

4.3 Probing the function of MXAN_6967 by gene inactivation

Many bacteria incorporate multiple members of the Fur family, usually an authentic, iron-responsive Fur and one or more homologues with a range of possible functions, including sensing of alternative metal ions (zinc, manganese and nickel; Zur, Mur and Nur), peroxide stress (PerR) or heme availability (Irr) (Lee *et al.*, 2007). Based on sequence and phylogenetic analysis (see results, figure 3.1 and figure 3.2), it was predicted that the Fur homologue MXAN_6967 would not be directly involved in sensing iron as characteristic iron-binding residues in the amino acid sequence were absent. A more detailed prediction of function is difficult, caused by inconclusive results from sequence and phylogenetic analysis.

The existence of the second Fur homologue (MXAN_6967) as an additional intracellular regulator allows *M. xanthus* the control of an additional, specific subset of genes, which could not be identified up to now. A more precise determination of function of MXAN_6967 is difficult, because of the very high sequence homology of Fur-like proteins (section 3.1.1), but different functions of these homologues (Hantke, 2001). Most probably, MXAN_6967 may be functional as heme-sensing Fur homologue Irr-like transcriptional regulator, as logical consequence in face of several heme-uptake and -degradation enzymes of *M. xanthus* (see table 3.2 and section 4.1) and the high homology in the sequence of MXAN_6967 to some characteristic amino acids of Irr proteins from other organisms (figure 3.1), in contrast to lower overall sequence similarity to hydrogen peroxide tolerance PerR proteins (figure 3.2). However, the exact heme-responsive motif in Irr proteins is unclear (Mense and Zhang, 2006).

Nonetheless, no putative Fur box within the MXAN_6967 promoter could be identified (table 3.1). Indeed, no Fur protein was found to interact to the promoter in the DNA pull-down assay, suggesting that the gene product might not be member of the Fur regulon. To probe its possible roles, the gene was aimed to be inactivated by in-frame deletion mutagenesis. Encouragingly, deletions of each type of Fur family member had been reported for various organisms as for e.g. Zur and Nur of *Streptomyces coelicolor* (Ahn *et al.*, 2006; Shin *et al.*, 2007), Mur of *Rhizobium leguminosarum* (Diaz-Mireles *et al.*, 2004), Irr of *Bradyrhizobium japonicum* (Yang *et al.*, 2006) and both PerR and Zur of *B. subtilis* (Bsat *et al.*, 1998). In contrast to MXAN_3702, the second *fur* homologue MXAN_6967 could be inactivated successfully (figure 3.10).

It is very complex to compare the results from other microorganisms with non-iron-responsive Fur mutations to the outcome of *M. xanthus* mutants, in which a different combination of partially Fur-controlled regulators is responsible for maintaining of iron

Discussion

homeostasis. Furthermore, in not one of the above mentioned approaches, a meaningful proteome or secondary metabolite analysis was performed, which complicates the finding to the similarities in results from the deletion mutant DEL6967. The phenotype of DEL6967 shared only some general similarities (as a delay in growth) to results obtained from other bacteria (*B. japonicum*, *B. subtilis*, *C. jejuni*, *R. leguminosarum*, *S. coelicolor*), in which a second non-iron-responsive Fur family member could be disrupted (Bsat *et al.*, 1998; van Vliet *et al.*, 1999; Diaz-Mireles *et al.*, 2004; Ahn *et al.*, 2006; Yang *et al.*, 2006; Shin *et al.*, 2007).

To compare the importance of Fur proteins in other microorganisms, in *Mycobacterium tuberculosis* two metal-dependent regulators (FurA and FurB) were described (Lucarelli *et al.*, 2008), where FurA acts as classical iron-responsive regulator, while FurB shares some homology with Zur proteins (Maciag *et al.*, 2007). Both Fur proteins of *M. tuberculosis* were declared as non-essential, in contrast to the results from this work. Furthermore in *M. tuberculosis*, no Fur auto-regulation was detectable (Pym *et al.*, 2001).

Similar to results from *M. xanthus*, for *V. vulnificus* (containing one “classical” Fur and a non-iron-responsive Fur protein) it was postulated that the gene cluster coding for the siderophore biosynthetic machinery could not be inactivated (Lee *et al.*, 2003). Nevertheless, the only iron-responsive Fur protein could be deleted (Litwin and Calderwood, 1993), leading to an iron-blind mutant with up-regulated iron import. Unfortunately, no inactivation of the second Fur protein, probably functional as Zur, was performed up to now in this organism.

Three Fur proteins could be clearly identified in *Anabaena* strains (Hernandez *et al.*, 2004), where also the iron-responsive homologue AazoDRAFT_4021 was found to be essential, in contrast to both other Fur homologues (AazoDRAFT_1189 and AazoDRAFT_6240), which miss the iron-binding residues (personal communication; Prof. Dr. M. F. Fillat, University of Zaragoza, Spain).

In fact, it was possible to inactivate the Fur homologue MXAN_6967 in *M. xanthus*, which probably does not have an iron-correlated function, in contrast to the possibly iron-responsive Fur protein MXAN_3702. Anyway, by inactivation of MXAN_3702 via in-frame deletion, polar effects (potential influence to neighboring genes) can be excluded, in contrast to single crossover inactivation approaches. The potential organization of MXAN_3702 with a second down-stream gene was not influenced in double crossover mutants.

Discussion

The MXAN_6967 mutant showed a drastically altered phenotype compared to the wild type strain. Growth was delayed for approximately 25 h in comparison to the wild type, but reached approximately the same cell density (92 %), before falling off again. The mutant strain shows almost 50 % ($15.9 \text{ nmol h}^{-1} \text{ O.D.}^{-1}$) of the iron-uptake of the wild type (table 3.11). It has been observed previously that mutations of iron-responsive *fur* genes lead to constitutive expression of siderophore biosynthetic pathways, iron transporters and other Fur-repressed genes, resulting in intracellular iron overload (Touati *et al.*, 1995; Abdul-Tehrani *et al.*, 1999). Contrarywise, in DEL6967 the siderophore production was significantly compromised. However, the finding that the rate of iron uptake was not seriously reduced in the mutant of MXAN_6967 is consistent with the hypothesis that the protein serves an alternative function than transcription-control of iron-responsive genes. Surprisingly, production rates of all metabolites were drastically reduced (all between 0.3 and 6 % of wild type production) with the exception of myxochromide (ca. 50 % reduced). This result implicates that MXAN_6967 operates in controlling secondary metabolism in *M. xanthus* DK1622, although the mechanism for this regulation remains unclear and might be indirect. Further examination, such as targeted mutagenesis of selective, important amino acids in the sequence of MXAN_6967, could exhibit residues involved in complexation of metal ions, dimerization or DNA-binding (Gonzalez de Peredo *et al.*, 1999) and so, finally allow a deeper insight into cellular function of MXAN_6967 in gene regulation.

Four metabolites are known to be common to *M. xanthus* DK1622 and *Stigmatella aurantiaca* DW4/3-1 (myxochromide, myxochelin, myxalamid and DKxanthene), which could account for the presence of a strong MXAN_6967 homologue in *S. aurantiaca*, to control production of these metabolites. Consequently, MXAN_6967 might represent a “super-regulator” of secondary metabolism in myxobacteria, an intriguing possibility which is currently being addressed by overexpression of the gene. These results may also point to a potential function of MXAN_6967 in heme-sensing. Hypothetically, extracellular heme molecules may be taken as a signal molecule for successful lysis of organic structures, so further production of biological agents is not necessary.

Indeed, a genetically engineered overexpression mutant of MXAN_6967 showed in first experiments an increase of several secondary metabolites, namely the myxalamids, myxochelin A and the myxochromides (R. Müller, T. Klefisch, unpublished results). Such a mutant could be used further for the purification of the protein MXAN_6967 and subsequently for the determination of the regulon of MXAN_6967 by the identification of the DNA binding sequence via DNA footprint analysis.

Discussion

The elimination of 324 bp from the core region of the Fur homologue gene MXAN_6967 did not result exactly in the phenotype expected from other strains with knockouts in homologue genes, as for e.g. Irr inactivation in *B. abortus* or Zur inactivation in *C. diphtheriae* (Martinez et al., 2005; Smith et al., 2009), which share both some important sequence-motifs with MXAN_6967. Typically, these mutants did not show a significant deregulation in production of their siderophores; none or only minor effects were measured here. In contrast, the inactivation of MXAN_6967 results in the significant decline of all secondary metabolites, including siderophore production (table 3.12).

On the other hand, findings were made in several bacteria that mutants of iron-responsive Fur genes show a strong deregulation of siderophore production, as in *Legionella pneumophila* (Hickey et al., 1997) or *Actinobacillus actinomycetemcomitans* (Haraszthy et al., 2002; Haraszthy et al., 2006). Anyway, the discrepancy between the low myxochelin production (ca. 0.5 % of the wild type level) and the efficient iron-uptake (ca. 50 % of the wild type level) of the mutant DEL6967 could be explained by the use of alternative ways to shuttle iron through the membrane.

All this indicates that the traditional Fur-model is a simplified guidepost, but bacterial cells behave more complex, addicted to the availability and importance of iron in the natural environment of the individual strain.

To provide a comprehensive statement about the deletion mutant MXAN_6967, the complete secondary metabolism was reduced, showing the global response of this protein at least by secondary effects (table 3.12). A similar effect was detected only in *P. aeruginosa*, where the mutation of a non-iron-responsive Fur homologue (Prince et al., 1991) leads to a mutant with reduced siderophore production (Barton et al., 1996).

Surprisingly, in the deletion mutant also secondary metabolites were found altered, which did not show any response in the wild type strain under iron-limiting conditions, such as DKxanthenes, myxalamids and myxovirescins. In detail, the deletion mutant of the Fur homologue (MXAN_6967) exhibits a strong reduced siderophore production (both derivates more than 200fold, see table 3.12), while the cells show almost 50 % of the iron uptake of the wild type (table 3.11), which can only be explained by a specific restructuring of the cell-surface and membrane, a known reaction of bacteria to modulate iron-influx (Ernst et al., 2005). As mentioned, the data suggests an efficient uptake of iron, perhaps connected to rather basic structures as postulated for dicitrato molecules (Marshall et al., 2009), cysteine

Discussion

(Jiang *et al.*, 1997) or myxochelin components, such as 2,3-dihydroxybenzoate (Screen *et al.*, 1995; Rowland *et al.*, 1996a; Rowland and Taber, 1996b). Such an alternative pathway is perhaps only expressed in the mutant, but not present or not functional in wild type. Another fact arguing for this hypothesis is the presence of various *tonB* genes of *M. xanthus* (table 3.2), which would be required for the uptake of iron bound to organic iron-chelating compounds besides myxochelin molecules.

Furthermore, some genetic rearrangement may occur, indicated by the Fur box control of an integrase/recombinase (table 3.1) and the 3.3fold induction of a SbcCD nuclease under iron-limitation (table 3.4). This protein may be required for a new genetic combination of iron-import genes, which are present as numerous templates in *M. xanthus*. The protein family of integrases/recombinases was already associated to promoter control by inverting small sequence parts, potentially to generate intact Fur box sequences (Segall *et al.*, 2005) or to genome integration of plasmids, coding for proteins from iron acquisition (Sonoda *et al.*, 2002).

In conclusion, the analysis of DEL6967 could not clarify the exact function of the Fur homologue MXAN_6967 in *M. xanthus*, it might be functional in heme sensing.

To get deeper insight into the function of MXAN_6967, it would be desirable to perform an additional proteome analysis with the wild type and the deletion mutant of MXAN_6967, also with heme as only iron resource. The synergistic use of proteomic techniques and knockout mutants of *Synechocystis* was found to be a powerful strategy to study metal homeostasis in microorganisms and get relevant information from comparative expression profiles and subproteomes (De la Cerda *et al.*, 2007).

Discussion

4.4 Probing the function of iron-responsive genes by site-directed mutagenesis

The analysis of *M. xanthus* was extended to investigate specific proteins with putative roles in the response to iron-limitation, implicated by proteome or DNA pull-down experiments.

The genes **MXAN_0142**, **MXAN_0144**, **MXAN_1562**, **MXAN_1619**, **MXAN_1808**, **MXAN_1864**, **MXAN_1893**, **MXAN_1988**, **MXAN_2094**, **MXAN_2347**, **MXAN_2440**, **MXAN_2520**, **MXAN_3203**, **MXAN_4189**, **MXAN_4535**, **MXAN_5055** and **MXAN_5484** were selected for inactivation via single crossover knockout (see section 2.12). The annotated gene function can be found in table 4.1.

Table 4.1: Annotated gene functions / BLAST results of single crossover targets

The table shows the single crossover target genes and potential functions of the encoded proteins. Hypothetical functions of uncharacterized proteins were obtained by BLAST analysis. Successful knockouts are indicated in the column “KO”. Gene numbers in bold indicate possible operon structures.

Gene number	Annotation	BLAST	KO
MXAN_0142	WD domain G-beta repeat/PBS lyase HEAT-like repeat protein		no
MXAN_0144	Uncharacterized conserved protein	WGR domain protein	yes
MXAN_1562	DPS/bactoferritin		yes
MXAN_1619	Putative uncharacterized protein	Helix-turn-helix type 11 domain protein	no
MXAN_1808	Putative restriction/modification enzyme		yes
MXAN_1864	N6-adenine DNA methyltransferase		yes
MXAN_1893	Putative uncharacterized protein	ClpX protease	yes
MXAN_1988	Putative uncharacterized protein	C5-cytosine methyltransferase	yes
MXAN_2094	Putative uncharacterized protein	TPR domain protein	no
MXAN_2347	Putative uncharacterized protein	Protamine P1 homologue	no
MXAN_2440	Putative uncharacterized protein	Transcription termination Rho factor	yes
MXAN_2520	FHA domain/tetratricopeptide repeat (TPR) protein		no
MXAN_3203	FHA domain protein		yes
MXAN_4189	TPR domain protein		yes
MXAN_4535	Putative RNA polymerase sigma factor		yes
MXAN_5055	Putative uncharacterized protein	Chromosome segregation SMC protein / type 11 methyltransferase	yes
MXAN_5484	Putative uncharacterized protein	HasB	yes

Some genes (**MXAN_0142**, **1619**, **2094**, **2347** and **2520**) could not be inactivated in spite of the addition of iron to growth media, suggesting the respective gene may be essential. Assuming that knockouts of these proteins with diverse functions entail significant deregulation of fundamental cellular processes, possibly an iron-concentration-decoupled

Discussion

uptake from CTT, which would finally result in the overload of intracellular iron-storage pools and induce lethal redox-stress. On the other hand, a complete disruption of iron-uptake is a further explanation, why some of these mutants were unable to grow. Also iron-correlated proteins may have very important functions in the accomplishment of redox-stress or play key roles in central metabolism, so inactivation of those could be lethal.

Knockouts of target genes, which were possibly part of a potential operon structures (hypothetical polycistronic mRNAs) are discussed at the end of this part, in section “Comparing of a subset of mutants”.

Growth rates, iron uptake and the secondary metabolome of the mutants generated were compared under iron-repleted conditions to the wild type (see section 3.3). Remarkably, the majority of mutations affected all three metabolic parameters.

Many mutations resulted in a delayed onset of exponential growth, lower overall cell density, or both. None of the mutants exhibited a higher O.D.₆₀₀ (figure 3.11), higher iron-uptake rates (table 3.11) or enhanced myxochelin production compared to the wild type. Unexpectedly, several other secondary metabolites showed a significant increase in some of the mutants (table 3.12). Additionally, some mutants are able to grow faster than the wild type, indicating that some parts of metabolism were not active or the cell-cycle was accelerated by deregulation of important switching points.

The secondary metabolite production of the generated knockout-mutants was also analyzed, as well as from the in-frame deletion mutant of the Fur family gene MXAN_6967. All generated clones show diverse phenotypes, different in each case from the wild type under standard conditions or under iron-limitation. Some of the growth profiles show similarities, but all secondary metabolite profiles show strong variations. All mutants showed a reduced siderophore production or reaches maximal wild type levels, none exhibited a significant enhanced biosynthesis of this class of compounds (table 3.12), which corresponds to the estimated iron-uptake rates of the mutants, reaching only wild type levels or less (table 3.11). Surprisingly, several mutants generated (MXAN_0144, MXAN_1562, MXAN_1893, MXAN_4535 and DEL6967) show a strong reduction of myxochelin production (all: more than 100fold decreased; table 3.12), but never a complete interruption. The myxochelins were only present as traces, but in some mutants iron-uptake was effected only a little, which again suggests an efficient import of iron, perhaps connected to basic structures, such as catechol-derivates like 2,3-dihydroxybenzoate, used by *B. subtilis* (Rowland *et al.*, 1996b) or as dicitrate molecules, used by *P. aeruginosa* (Marshall *et al.*, 2009). Both alternative iron-

Discussion

uptake mechanisms could be used only as survival support, but did not enable normal growth, which also may be evident for several of the mutants generated of *M. xanthus*, which show iron-uptake rates below 3 % of the wild type (table 3.11). Comparing the wild type iron-uptake rate to rates of these mutants (MXAN_1562, 4189 or 5484), the knockout strains exhibit an almost complete inhibition of iron import (table 3.11). Contrariwise, some mutants show efficient iron uptake, like the knockout mutants of the genes MXAN_1808, 1893, 1988, 2440 and 5055 or the deletion mutant of MXAN_6967, suggesting a non-iron-responsive role of those gene products.

As a follow-on experiment, it would be interesting to evaluate if the Fur box of the myxochelin gene cluster can be mutated, subsequently followed by determination of iron-uptake rates and secondary metabolite product profiling. Additionally, DNA pull-down assays with protein extracts from iron-rich and iron-poor conditions at the promoter of the myxochelin gene cluster would be ideal to monitor proteins involved in its transcriptional regulation, possibly MXAN_3702.

Phenotype of the single knockout mutants: The functions of the inactivated genes and the resulting phenotypes of the generated single crossover mutants are described in detail in the following section.

Targets for inactivation experiments were mainly selected from proteins, which exhibited an extraordinary strong difference in expression in the proteome comparison of iron-rich and iron-limiting conditions. It must be mentioned that proteins which occur as several differently regulated spots in 2D-DIGE may be of higher importance in contrast to single-spot-proteins, which is even more significant, if the different spots of the same protein are all constantly up- or down-regulated. Furthermore, destruction of genes encoding proteins which were detected to carry one of the bacterial-unusual phosphorylations may provide deeper insight into regulatory cascades of *M. xanthus*.

The disruption of **MXAN_0144** (encoding an uncharacterized conserved protein) was performed because of the up-regulation under iron-limiting conditions as two individual spots (2.9 and 3.2fold, for both no phosphorylation was detectable). A BLAST analysis proves a high homology (58 % I, 71 % S) to WGR proteins (named after the most conserved central motif of the domain). This domain is found in a variety of polyA polymerases, in the *E. coli*

Discussion

molybdate metabolism regulator yehH and other proteins of unknown functions for which it was suggested to contain a nucleic acid binding pocket (White *et al.*, 2009). Indeed, the protein was detected in the DNA pull-down assay to bind only to the promoter of MXAN_3702 under iron-rich conditions.

The knockout mutant shows in growth a longer lag-phase (ca. 30 h), but similar doubling times and maximum O.D.₆₀₀ (96 %) as the wild type. Quite unusually, the strain exhibited a kind of stationary phase at an O.D.₆₀₀ of approximately 2.4 for ca. 30 h. The mutant cells show an iron uptake rate of 8.2 nmol per h per O.D.₆₀₀, which accords to ca. 22 % of the wild type rate under same conditions. In secondary metabolite analysis, for the inactivation mutants of MXAN_0144 the strongest reduction in myxochelin A production of all generated mutant was discovered. While myxochelin B was reduced by the factor 276, myxochelin A was not detectable anymore. This was the only case of all mutants, where a secondary metabolite could not be detected. Furthermore, myxovirescin production was found reduced by the factor 186. The production of both, citterlin and myxalamid was lowered to only 26 % of the wild type production, while myxochromide and DKxanthene were not much affected. It must be mentioned that in this mutant the production of secondary metabolites was reduced or not influenced, no up-regulation was detectable. The significant reduction of myxochelins did not correlate to an only small reduction of iron-import. However, MXAN_0144 seems not only to be involved in transcriptional control of the myxochelin gene cluster, but must have also regulatory function correlated to the promoter of *mxcL*, indicated by the important fact that only the amino-derivate was present.

The gene product of **MXAN_1562** TpF1 (DPS/bactoferritin) was found to bind to both *fur* promoter regions under iron-limitation (Fur and Fur homologue promoter specific, iron-dependent binding). At this, MXAN_1562 was detected with a phosphorylation when interacting with the promoter regions of MXAN_3702; the phosphorylation may be necessary for precise adjustment of DNA interaction properties, contributing to sequence specificity. Furthermore, MXAN_1562 was selected for a knockout because of the extreme up-regulation found in proteome experiments (27.1fold). The function was annotated as DPS/bactoferritin (DNA binding, iron storage). DPS/bactoferritin proteins are one of the major reservoirs of intracellular iron in bacteria, but nothing is known about possible interactions to promoters. Members of the this protein family were originally discovered as stress proteins, which protect DNA against oxidative stress during nutrient starvation (DPS: DNA protection during starvation protein), but functionally the DPS subfamilies are much more diverse (Zeth *et al.*,

Discussion

2004). Bactoferritins build a broad superfamily of iron storage proteins, widespread in all domains of life. Ferritins, bacterioferritins and DPS/bactoferritins are very important non-heme iron storage proteins in animals, plants, and microorganisms and have essentially the same architecture, assembling in a 24mer cluster to form a hollow construction (Carrondo, 2003). DPS/bactoferritin consists of a mineral core of up to 500 iron atoms, which are enclosed by the multi-subunit protein shell, and consequently assures the solubility of the complex in aqueous environment.

Several members of this group exhibit a DNA-binding activity that is at least partially linked with iron availability, such as the DPS/bacterioferritin from *E. coli* or the homologue from *B. subtilis* (Zeth *et al.*, 2004). Anyway, the DNA target sequences of DPS proteins are unknown and the exact protein function is obscure (Abdul-Tehrani *et al.*, 1999). The function of DPS/bactoferritin did not explain the significant up-regulation during iron starvation, because the lower amount of extracellular iron would cause less redox stress. Thus, the lower availability of intracellular iron would entail a reduction of iron-storage proteins. Therefore, it can be concluded that the regulatory function of the DNA binding of DPS proteins might have been underestimated for this protein family.

The knockout mutant exhibited in growth a very long lag-phase (almost 50 h) and a lower maximum O.D.₆₀₀ (ca. 80 % of the wild type), but similar doubling times as the wild type under the same iron rich conditions. The cells showed an almost complete disruption of iron-import, with only 1.3 % the lowest uptake rate of all mutants. This can be explained by the drastic reduction of both myxochelin derivates, which were here only detectable in traces (myxochelin A reduced by the factor 209, B reduced by 2084.3; the strongest reduction of myxochelin B from all mutants). These cells produce 20.4fold less of DKxanthenes, myxovirescin production is reduced by the factor 47.6, compared to wild type under iron rich conditions. The production of citterlin was lower by the factor 23.9, myxalamid by the factor 27.7, myxochromide was lowered by the factor 3.4. It is mentionable that in this mutant the production of all secondary metabolites was significantly reduced, indicating an important function of MXAN_1562 in central metabolism or perhaps a more specific function in the regulation of secondary metabolism gene clusters.

In parts, the phenotype of the mutant behaves according to the expectations, namely the strong reduction of iron uptake caused by the loss of an important storage function. This was found in accordance to the strong decrease of siderophore synthesis, which needs to be reduced to restrict iron-import, thereby avoiding additional redox-stress by free intracellular iron ions. On the other hand, shielding by iron-encapsulation may not be the only effect of the

Discussion

DPS/bactoferritin protein MXAN_1562, but it may play a central role in response to iron-limitation, indicated by the extraordinary high up-regulation in the wild type during iron starvation and detection at both *fur* promoters. Thus, this protein may be more important under iron starvation than just protecting DNA, but rather have regulatory functions via interaction with distinct promoters.

The consequences of the loss of MXAN_1562 in the mutant are drastic, in face of the existence of a homologue gene (MXAN_0866; 42 % I, 51 % S), which codes a protein with obviously different DNA binding activity (table 3.8).

This multiplicity of effects is difficult to rationalize. Based on the putative function of MXAN_1562 in redox stress defense/iron-storage and its massive up-regulation in anticipation of iron influx under low-iron cultivation in the wild type, the central role of the encoded protein in binding DNA under iron-sufficient conditions is reflected.

In contrast, an inactivation mutant of a homologue protein in *E. coli* showed a slightly increased iron uptake rate and no growth deficits at all (Abdul-Tehrani *et al.*, 1999), the same results were obtained for an *E. coli* overproducer strain (Hudson *et al.*, 1993). The only hypothesis could be made for the bactoferritin domain, which might be used for long-term storage of iron in *M. xanthus*; the precise function of MXAN_1562 remains unclear.

The disruption of **MXAN_1808** (encoding a putative restriction/modification enzyme) was performed because of the strong up-regulation under iron-limiting conditions (3.9fold) and the detection in the DNA pull-down assay at the promoter of MXAN_6967 only under iron-limiting conditions.

A BLAST analysis proves two domains for MXAN_1808, exhibiting high homologies to DEAD box helicases and N6-adenine DNA methyltransferases, respectively. A number of eukaryotic and prokaryotic proteins involved in NTP-dependent, nucleic-acid unwinding have been characterised on the basis of their structural similarity. All these proteins share a number of conserved sequence motifs, such as the so-called DEAD box, also detected in the first domain of MXAN_1808. These proteins form the large DEAD box helicase superfamily and are conserved in all kingdoms of life. The DEAD box helicases show a high diversity of biological functions and are associated with processes of RNA metabolism, including transcription, pre-mRNA splicing, ribosome biogenesis, translation and RNA turnover (Wasserman and Steitz, 1991; Aubourg *et al.*, 1999).

Taking a look at the second domain, the major role of DNA methylation in prokaryotes is the protection of DNA against degradation by restriction enzymes, but also regulation of gene

Discussion

expression via silencing of distinct promoters (Timminkas *et al.*, 1995; Murphy *et al.*, 2008). The cofactor S-adenosyl methionine (SAM) is utilized as methyl donor. N6-adenine DNA methyltransferases are enzymes that recognize a specific sequence in DNA and methylate an adenine in that sequence (Timminkas *et al.*, 1995). Members of this class methylate exocyclic nitrogens and form N6-methyladenine (N6-methyltransferases).

Commonly, the protein family of DNA methyltransferases has three biological roles in prokaryotes: 1) distinction of self and foreign DNA as a defense against infection of bacteria by restriction of foreign DNA molecules as from bacteriophages, 2) direction of post-replicative mismatch repair, and 3) control of DNA replication and cell cycle by silencing of specific chromosomal regions (Jeltsch, 2002; Erova *et al.*, 2006; Jeltsch *et al.*, 2007; Seshasayee, 2007). Here, protein methyltransferase activity can be clearly limited to DNA silencing. Neither foreign DNA molecules make an additional digestion and subsequent protection of chromosomal DNA necessary, nor could an enhanced mismatching be connected to the iron-limiting environment. To the contrary, a lower O.D.₆₀₀ of *M. xanthus* under iron-limiting conditions proofs a reduced cell division per time, and so causing less cellular stress by DNA mismatching. Therefore, it can be concluded that in this case DNA methyltransferase activity is connected to silencing of expression of distinct genes in *M. xanthus*. This protein family usually regulates a whole subset of genes in other bacteria (Timminkas *et al.*, 1995; Seshasayee, 2007).

The knockout mutant shows the same lag-phase in growth and same maximum O.D.₆₀₀ as the wild type under iron rich conditions, but smaller doubling times. A kind of stationary phase (O.D.₆₀₀ of ca. 2.5; ca. 97 % of the wild type) was achieved after ca. 40 h, stable for approx. 24 h. The cells showed a reduced, but still efficient iron uptake compared to the wild type (42 %).

Myxochelin production was found to be only slightly reduced (myxochelin A reduction by the factor 5, B reduced by 4.3), which contributes to the insignificant reduction of iron uptake. This may argue that MXAN_1808 is not involved in regulation of genes from siderophore biosynthesis or from uptake of iron-siderophore complexes. The mutant cells produce 18.4fold more of DKxanthenes, myxovirescin production is also increased by the factor 11.5, compared to wild type under iron rich conditions. The enhanced production of myxalamid (factor 8.3) results in the highest overproduction of these metabolites of all generated mutants, which was also the case for the myxovirescin overproduction. The production of citterlin was not influenced, similar to the production of myxochromide. These non-uniform responses of secondary products as the insignificant changes in siderophore production, coupled to an only

Discussion

slight decrease of iron uptake rates argues for a role of MXAN_1808 rather in controlling central metabolism than regulation of iron- or secondary metabolism.

The disruption of **MXAN_1864** (encoding a N6-adenine DNA methyltransferase) was performed because of the up-regulation under iron-limiting conditions (3.3fold). A detailed explanation of the function of N6-adenine DNA methyltransferase proteins was provided earlier in this section (see knockout mutant MXAN_1808).

The knockout mutant shows a shorter lag-phase in growth, smaller doubling times, but a slightly lower maximum O.D.₆₀₀ as the wild type under iron rich conditions (94 %). The maximum O.D.₆₀₀ (approx. 2.4) is achieved 15 h earlier. Unexpectedly, the O.D.₆₀₀ arrested at a kind of stationary phase at an O.D.₆₀₀ of approx. 1.7 for around 20 h. The iron uptake was found significantly reduced in this mutant strain (7.1 % of the wild type iron uptake). This drastic decrease cannot be explained by the only moderate decrease of the two produced myxochelin derivates, which were detected by HPLC-MS in sufficient amounts (ca. 14 % of both derivates were present, compared to wild type under iron rich conditions). Obviously, *mxcL* was not regulated individually by MXAN_1864, indicated by the fact that the ratio of myxochelin A and B was identical to the wild type under the same conditions. Furthermore, DKxanthenes were found to be reduced (12.2fold), myxovirescin production was also decreased by the factor 35.6 and citterlin by the factor 20.6. Furthermore, myxalamid was reduced by the factor 6.4. The production of myxochromide shows the smallest alteration (reduced by the factor 1.8). All secondary metabolite synthesis rates of this mutant were reduced compared to the wild type.

Because iron-uptake rates in this mutant were found much more reduced than siderophore biosynthesis, it can be concluded that uptake or hydrolysis of iron-siderophore complexes was significantly affected, but still present. All secondary metabolite synthesis rates of this mutant were reduced compared to the wild type, which indicates a genome-wide activity of the DNA methyltransferase or at least of genes controlled by the DNA methyltransferase. Overall, strong effects were found in the mutant of MXAN_1864, where the loss of a single DNA methyltransferase activity leads to a partially extreme decrease of all examined secondary metabolites. This suggests the involvement of this protein in the regulation of diverse secondary metabolic gene clusters. Up to now, no mechanisms were described, in which DNA methyltransferases act globally as activators of expression of secondary metabolite gene clusters, which would be the case in the wild type. On the other hand, the results could be

Discussion

explained by the hypothesis that MXAN_1864 is responsible for silencing of one or more repressors of biosynthetic genes.

These interesting effects of the knockout mutant of MXAN_1864 lead to the inactivation of a homologue in *S. cellulosum* Soce 56 (Sce2777), which exhibited similar effects in secondary metabolism (seriously compromised production of ajudazols and etnangiens; R. Müller, S. Rachid, unpublished results).

The disruption of **MXAN_1893** (encoding a putative uncharacterized protein) was performed because of the strong up-regulation under iron-limiting conditions (12.2fold). A protein BLAST analysis exhibits high homology to ClpX proteases (E-value: $6 * 10^{-47}$). ClpX is a member of the heat-shock protein 100 family, which functions as an ATP-dependent molecular chaperone (Grimaud *et al.*, 1998). These proteins are involved in DNA damage repair, stationary-phase gene expression, and ssrA-mediated protein quality control. Some of these proteins bind zinc, but many interact with other metals such as iron or, rarely, no metal at all. To date more than 50 proteins including transcription factors, metabolic enzymes, and proteins involved in the starvation and oxidative stress responses have been identified as substrates (Flynn *et al.*, 2003). Mutants of the *clpX* genes in *Streptococcus pneumoniae* had been found to be less functional in metal ion transport (Robertson *et al.*, 2002).

The knockout mutant shows a much larger lag-phase in growth (39 h), but smaller doubling times, and did not reach the same maximum O.D.₆₀₀ as the wild type under iron rich conditions. The maximum O.D.₆₀₀ (approx. 2.1; ca. 84 %) was achieved after 64 h. The cells show almost the same iron uptake rate as the wild type (difference ca. 12 %), in contrast to the results from *S. pneumoniae* (Robertson *et al.*, 2002). The *M. xanthus* mutant cells exhibited almost wild type iron uptake rates, which was not found in accordance to the low amounts of myxochelins, here detectable only as traces. Myxochelin production was found to be reduced (myxochelin A reduced by the factor 632, B reduced by 652). The smaller doubling times and lower overall O.D.₆₀₀ compared to the wild type may indicate a bypass metabolism. Maybe these cells use an alternative way for iron uptake, which is probably only expressed in the mutant, but not functional in wild type, as some bacteria are known to import iron connected to more basic structures (Rowland *et al.*, 1996b; Jiang *et al.*, 1997; Marshall *et al.*, 2009). The mutant exhibits partially drastic reduction of secondary metabolite levels. The production of myxovirescin is also decreased by the factor 657 and cittilin by the factor 556, compared to the wild type under iron rich conditions. Also the production rate of myxochromide shows a decrease in this mutant (factor 104). Generally, all monitored secondary metabolites in this

Discussion

mutant were found to be strongly reduced. It must be mentioned that this mutant showed the most drastic decrease in myxochromide, myxovirescin and cittilin production. In comparison to the relatively small differences in growth and iron-uptake it can be concluded that MXAN_1893 takes action as gene regulator for some biosynthetic gene clusters from secondary metabolism.

The disruption of **MXAN_1988** (encoding a putative uncharacterized protein) was generated, because of 4.6fold up-regulation under iron-limiting conditions. In BLAST analysis, a high homology to C5-cytosine DNA methyltransferases was discovered, as to STIAU_4118 (E-value: 0.0; 81 % I, 88 % S; 97 % sequence coverage). C5-cytosine methyltransferases are enzymes, which utilize SAM to specifically methylate the C5 carbon of cytosines in defined DNA sequences to produce C5-methylcytosine. The function of DNA methyltransferases was described already in this section (see knockout mutant MXAN_1808).

The knockout mutant shows the same lag-phase as the wild type under iron rich conditions in growth, but larger doubling times, and reaches a first maximum (O.D.₆₀₀ of 1.1; corresponds to 45 % of the wild type level) after 40 h, a second maximum (O.D.₆₀₀ of 1.6; corresponds to 65 %) after 64 h. However, overall growth profile of the mutant strain varied significant to wild type profile. The cells show almost the same iron uptake rate than the wild type (ca. 78 %).

This mutant strain was the only one, in which the myxochelin production was found to be differential regulated (myxochelin A reduced by the factor 57.7, B increased by 1.8). These cells produce 22.4fold more of DKxanthenes, and 5.3fold more myxovirescin. Otherwise, the production of myxalamid was decreased by the factor 5.5, compared to wild type under iron rich conditions. The production rate of myxochromide was not influenced in the mutant, as well as for cittilin.

The focus of myxochelin production was significantly shifted to produce more of the amino-derivate B as end product, more than in any generated mutant or in the wild type under any tested conditions: in the wild type, the ratio of the two myxochelin derivates changes from 17-19fold more B than A under iron rich to 142-157fold more B than A under iron-limiting conditions, while the ratio in the mutant was determined with 1898fold more B than A. In the mutant, MxcL might be somehow over-activated because this result cannot be caused by the complete abolishment of the function of the NAD(P)H-dependent reduction domain of MxcG, which is required to yield the free myxochelin-aldehyde intermediate, the substrate, for which the reduction domain of MxcG competes with MxcL to generate a hydroxy-group or an

Discussion

amino-group instead of the aldehyde function, respectively (Li *et al.*, 2008). Therefore, it can be concluded that MXAN_1988 inhibits the functionality of MxcL in *M. xanthus* DK1622.

Furthermore, the highest DKxanthene up-regulation of all mutants was noticed in this strain, which may point to an induction of development, as this natural product family was detected to play a major role during this process (Meiser *et al.*, 2006a).

The disruption mutant of **MXAN_2440** (encoding a putative uncharacterized protein) was generated, because of the induction of the protein in iron-limiting environment in two individual spots (3.2fold up-regulated, carries one phosphorylation and 2.7fold, carries two). A protein BLAST analysis discovered two domains, whereof the first did not have convincing homologues in public databases, while the second showed as result high similarities to RNA/DNA helicases, more precisely to transcription termination Rho factors (E-value CDD: $3 * 10^{-25}$). This protein disengages newly transcribed RNA from its DNA template at certain, specific transcripts. In the *M. xanthus* genome, two further Rho factors (MXAN_2479 and MXAN_5636) had been annotated, probably each responsible for a specific subset of genes. Generally, there are two types of terminators for transcription in the bacterial genomes: 1) Intrinsic terminators characterized by a GC-rich inverted repeat followed by an oligo(dT) stretch that induces RNA polymerase to disengage RNA; and 2) the factor-dependent terminators, which depend on an essential protein factor, called Rho, for termination (Chalissery *et al.*, 2007). The protein is one of the few examples, where exogenous proteins regulate the termination of transcription in prokaryotes (Skordalakes and Berger, 2003). The unusual combination of a Rho factor domain to a second large domain with hypothetical function (ca. 420 amino acids) had not been reported before and might be correlated to regulatory processes, which motivates for the inactivation of this gene in *M. xanthus*.

The knockout mutant of MXAN_2440 shows the same lag-phase as the wild type, but strong differences in growth. The cells grow with much larger doubling times (stable value between 20 and 60 h) and reach only a maximum O.D.₆₀₀ of approx. 1.8 (ca. 75 % of the wild type level), which was achieved after 64 h. This significant lowering of overall growth and growth speed may be caused by intracellular iron-limitation, because the mutant strain shows 66 % of the wild type iron uptake, which agrees quite well with the reduced O.D.₆₀₀.

Correspondingly, the effects on myxochelin production were relatively small, more precisely myxochelin A was reduced by factor 8.5, B reduced by factor 5, compared to the wild type. The cells produce 12.4fold more of DKxanthenes (but high standard deviation), myxovirescin production is also increased by a factor of 4. The production of citterlin was reduced by the

Discussion

factor 36, compared to wild type under iron rich conditions. The production of myxalamid was not influenced, like the one of myxochromide.

Thus, MXAN_2440 does not seem to be an important regulatory protein, at least not for iron metabolism. Detectable influences on the regulatory network of iron in the knockout mutant are relatively small, the iron uptake and myxochelin production were quite close to wild type level, but growth was compromised. The higher production of DKxanthene may point to a role of MXAN_2440 in development. Hypothetically, MXAN_2440 operates in a more central position in primary metabolism, rather than to regulate the expression of secondary metabolite gene clusters or iron-acquisition associated genes. In comparison to the other mutants, here the secondary metabolite production was not influenced or underlies only minor changes. This non-uniform response maybe based on secondary effects.

The disruption of **MXAN_3203** (encoding a FHA domain-containing protein) was performed, because of the highly specific binding to the promoter region of MXAN_6967 under iron rich conditions.

The FHA (forkhead-associated domain) proteins act as recognition site for phospho-residues in protein sequences and are found to be connected to signaling domains of protein kinases and transcription factors (Hofmann and Bucher, 1995). Protein phosphorylation, which plays a key role in most cellular activities, is a reversible process mediated by protein kinases and phosphoprotein phosphatases (Hanks *et al.*, 1988). Phosphorylation of a protein substrate side chain results in a conformational change, which affects ultimately protein function, enzymatic activity or cellular location and has important functions in signal transfer (Manning *et al.*, 2002). It was already postulated that the phosphorylation status of some proteins is used as global regulator of gene expression in bacteria (Saskova *et al.*, 2007).

In *M. xanthus*, FHA domain proteins were already found in association to sigma-54 transcriptional regulator proteins (Jelsbak *et al.*, 2005).

The knockout mutant exhibited in growth the same lag-phase and the same doubling times, but did not reach the same maximum O.D.₆₀₀ as the wild type under iron rich conditions (69 %). The exponential phase ends at an O.D.₆₀₀ of 1.8, which passes into a stationary phase, stable for ca. 30 h. The cells show only 26 % of the iron uptake rate of the wild type.

This was found in contrast to the relative high amounts of both myxochelins, which reach almost wild type levels. Also, the production of myxochromide, myxalamid and citterlin showed no significant differences to wild type rates. To the contrary, DKxanthene production was increased 19fold, myxovirescin 5fold. It might be possible that for most of these

Discussion

metabolites, one of the numerous FHA domain proteins could compensate the inactivation of MXAN_3203 in face of 26 genes, coding for such proteins in *M. xanthus*. Generally, the influence on secondary metabolism in the mutant was very limited, the only notable effect was the strong up-regulation of the two families of DKxanthenes and myxovirescins. These facts, together with the finding that growth was seriously compromised, may argue for a more central function of MXAN_3203, possibly correlated to sporulation, because of the extraordinary high production level of DKxanthenes, a substance class which had already been connected to developmental processes (Meiser *et al.*, 2006a).

The disruption of **MXAN_4189** (encoding a tetratricopeptide repeat protein) was generated, because of 3.4fold up-regulation under iron-limiting conditions.

The tetratricopeptide repeat region (TPR) is a structural motif present in a wide range of proteins. It mediates protein-protein interactions and the assembly of multiprotein complexes (Das *et al.*, 1998). TPR motifs have been identified in various organisms, ranging from bacteria to humans. Proteins containing TPRs are involved in a wide range of biological processes, such as cell cycle regulation, transcriptional control and protein folding (Goebl and Yanagida, 1991; D'Andrea and Regan, 2003).

The knockout mutant shows in growth the same lag-phase as the wild type under iron rich conditions, and the same doubling times, but the overall growth profile varies significantly from the wild type. The first growth maximum was reached after ca. 38 h at an O.D.₆₀₀ of ca. 1.6 (65 % of the wild type O.D.₆₀₀), a second maximum at an O.D.₆₀₀ of ca. 1.8 (73 %) after ca. 62 h. Additionally, the cells show almost no iron uptake (2.2 % of the iron uptake rate of the wild type), but this reduction could not be further connected to a very drastic reduction of myxochelin production. The two myxochelin derivates were present in sufficient amounts, both with ca. 35 % of the wild type level. No significant change was detected in ratio of myxochelin A and B, suggesting that MxcL is not regulated individually by MXAN_4189. While myxovirescin, myxochromide and DKxanthene production was not altered, myxalamid and cittilin production was reduced to only 11 and 15 % of the wild type levels, respectively. Generally, secondary metabolites in the knockout mutant of MXAN_4189 were found to be not affected or were only slightly reduced.

Another mutant, carrying a knockout in **MXAN_4535** (encoding a putative RNA polymerase sigma factor) was generated, which showed a strong down-regulation (- 3.1fold) under iron-limitation. Additionally, the function as transcriptional regulator motivates for inactivation.

Discussion

The bacterial core RNA polymerase complex, which consists of five subunits, is sufficient for transcription elongation and termination but is unable to initiate transcription. Transcription initiation from promoter elements requires a sixth, dissociable subunit called sigma factor, which reversibly associates with the core RNA polymerase complex to form a holo-enzyme. Bacteria typically express a multiplicity of sigma factors which all act highly specific, so one cannot restore the action of another. Two of these factors, sigma-70 (the so-called major sigma factor) and sigma-54 direct the transcription of a wide variety of genes. Further sigma factors, known as alternative sigma factors, are required for the transcription of specific subsets of genes. RNA polymerase recruits alternative sigma factors as a means of switching on specific regulons (Helmann and Chamberlin, 1988). A BLAST analysis discovered that MXAN_4535 clearly belongs to the sigma-70 subfamily.

The knockout mutant shows a very short lag-phase (< 10 h) in growth and very small doubling times. The cells reach the maximum O.D.₆₀₀ (approx. 2.2) after 53 h, which is almost the same time, the wild type needs under iron rich conditions to reach the highest cell density. The strain exhibited a kind of stationary phase at an O.D.₆₀₀ of approx. 1.8 for 26 h. The cells show only 27 % of the iron uptake of the wild type.

The knockout mutant of MXAN_4535 was found to exhibit reduced production of myxochelin A by the factor 129.1, B was reduced by the factor 796.7. So, it can be concluded that MXAN_4535 might be a candidate to be involved in the specific regulation of transcription of *mxcL*, reflected by the strong shifting of the derivates of the myxochelins more towards the amino-derivate myxochelin B. Additionally, the mutant strain produces only 16 % myxovirescin, compared to production of the wild type. On the other hand, the levels of most secondary metabolites were not influenced (such as myxochromides, DKxanthenes, citilins and myxalamids). The response of secondary metabolism was found to be limited to a few pathways; most levels were not affected or only narrow, which could also be derived from natural variations in production rates. Thus, this sigma factor seems to be highly specific for expression of the myxochelin biosynthetic gene cluster among others, where the strongest effect from all secondary products was noted in this mutant.

As follow experiments, it would be desirable to discover protein-DNA binding via DNA pull-down assay on the promoter of MXAN_4535, possibly Fur protein interaction, also if the protein intensity was decreased during iron starvation. Additionally, the involvement of MXAN_4535 in the regulation of the myxochelin biosynthetic genes may be proven by a DNA pull-down assays on the promoter region of the cluster. Furthermore, to discover the

Discussion

regulon of MXAN_4535, overproduction and purification of this protein would be necessary, subsequently followed by *in vitro* DNA footprint analysis.

The disruption of **MXAN_5055** (encoding a putative uncharacterized protein) was generated, because of the different regulation of this protein as three individual protein spots (7.1fold without detectable phosphorylation, - 3.2fold with one and 2.8fold with two phosphorylations) in 2D-DIGE analysis and the binding to the promoter region of MXAN_6967 under both, but to the promoter of MXAN_3702 only under iron rich conditions.

A BLAST analysis exhibited two domains, each with high scores in the BLAST conserved domain database (CDD). The first domain of the protein shares some homology to chromosome segregation SMC proteins (E-value CDD: $2 * 10^{-12}$), the second domain to type 11 methyltransferases (E-value CDD: $3 * 10^{-14}$). However, the DNA binding of the first domain could be clearly correlated to chromosome segregation SMC (structural maintenance of chromosomes) proteins, which interact with specific DNA sequences and perform organizing and segregating of chromosomes for partition, here probably correlated to DNA methylation. SMC proteins are found in bacteria, archaea, and eukaryotes. These proteins function together with other proteins in a range of chromosomal transactions, including chromosome condensation, sister-chromatid cohesion, recombination, DNA repair and epigenetic silencing of gene expression (Jensen *et al.*, 2003). The protein family of type 11 methyltransferase utilizes S-adenosyl-L-methionine (SAM) and modifies DNA (Jeltsch *et al.*, 2007), RNA (Sergiev *et al.*, 2007), proteins and small molecules, such as catechol (Dhar and Rosazza, 2000). Most likely, the combination of the SMC DNA binding domain and a methyltransferase domain indicating DNA as methylation target, which could not be determined more exactly. SMC proteins are used to silence expression of this gene, usually regulating a whole subset of genes (Jensen *et al.*, 2003). These facts may indicate that the promoter of MXAN_6967 is only poorly accessible under both, but the promoter of MXAN_3703 only under iron-rich conditions via silencing the respective gene via methylation of distinct promoters. That the protein MXAN_5055 was not detected to bind to the promoter of MXAN_3702 under iron-limitation may be a sign of de-repression under these conditions.

In contrast to the DNA methyltransferases MXAN_1808, MXAN_1864 or MXAN_1988, which were already explained in detail before in this section, the substrate specificity of the methyltransferase domain of MXAN_5055 was unknown, to use DNA at least as binding

Discussion

substrate was hypothesized from BLAST results and proven by DNA pull-down assays. To interpret the role of MXAN_5055 as DNA methyltransferase with gene silencing function its reasonable, *fur* genes were typically inactive under iron sufficient conditions, which might be the case here, indicated by the binding of MXAN_5055 to the promoter of MXAN_3702 under iron-rich conditions. Anyway, the combination of SMC/methyltransferase type 11 domains was not described before in literature.

The knockout mutant shows a much larger lag-phase (35 h) in growth, the same doubling times and reaches almost the same maximum O.D.₆₀₀ (89 %) as the wild type under iron rich conditions. The maximum O.D.₆₀₀ (approx. 2.2) is achieved after 73 h. The cells show 62 % of the iron uptake of the wild type, explainable by the relatively small reduction of siderophore production (myxochelin A reduced by the factor 4.0, B reduced by 8.4). This mutant strain produces 2.3fold less of myxalamid, citterlin production was also decreased by the factor 16.8. Also the production of myxovirescin was reduced by the factor 8.9, compared to wild type under iron rich conditions. The production of myxochromide was not influenced, like the one of DKxanthenes.

The effects found in this mutant had obviously only marginal interference with iron regulation, because siderophore production and iron uptake were found relatively close to values from the wild type. All differences in secondary metabolite profile from this mutant were relatively small, compared to the wild type, while some other mutants show much stronger effects. This argues for a function of MXAN_5055 in more central position, rather than regulating expression of secondary metabolite gene clusters or genes from iron-acquisition.

In contrast to the results from the knockout of MXAN_5055, SMC homologues had been identified from various bacteria, such as *Bacillus subtilis*, *Caulobacter crescentus* or *E. coli*, but disruption of these results in wild type phenotypes, which exhibit no difference in growth, but temperature-sensitivity (Jensen *et al.*, 2003)

The disruption of **MXAN_5484** (encoding a putative uncharacterized protein) was performed, because of the differences in spot intensity for two spots in 2D-DIGE (one spot 8.5fold up-, the other - 2.1fold down-regulated). For both spots, no modification was detectable.

A BLAST analysis showed convincing sequence homologies to HasB (heme acquisition system) proteins from *Serratia marcescens* (Benevides-Matos *et al.*, 2008). This protein family is involved in heme uptake in analogy to iron-siderophore complex import by TonB-dependent systems (Letoffe *et al.*, 1994).

Discussion

The knockout mutant shows a long lag-phase (40 h) and slightly enlarged doubling times. The maximum O.D.₆₀₀ of 2.3 was reached after approx. 80 h and found to be quite similar to the wild type (92 %). In contrast, the cells show only 1.9 % of the wild type iron uptake.

Myxochelin A production was reduced by the factor 15.4, B reduced by the factor 88.2. Also the production of citterlin was reduced by the factor 31.4, compared to wild type under iron rich conditions, but myxalamid production has increased slightly by the factor 2.1, also measured for myxochromid (3.7fold more). The production of myxovirescin was not influenced significantly, as the one of DKxanthenes.

However, the overall growth profile looks very similar to the wild type; only somehow delayed, despite of obvious restriction of iron-import. Nevertheless, that very drastic effects were detected in iron uptake, the knockout of MXAN_5484 can compensate the lower availability of intracellular iron, as effects on both, growth profile and secondary metabolism were relatively small. Additionally, it must be mentioned that MXAN_5484 might be responsible for the regulation of *mxcL*, which was indicated by a significant difference in the ratio of the two myxochelin derivates in the mutant. These facts argue for a specific role of MXAN_5484 in regulation of iron-uptake and intracellular distribution, contributing to a potential function as member of iron-subordinated heme-catabolism.

Comparison of a subset of mutants

Some of the mutants generated share striking similarities, which will be highlighted in the following section. Such similarities might be explained by inactivation of proteins from the same reaction- or information transfer-cascade. Additionally, it is possible that the phenotypes of two mutants are almost identical, because both proteins were required for interaction or cooperate somehow or the events detected could be caused by random.

Generally, the results reinforce the idea that proteomics-guided engineering of regulatory pathways is a viable strategy for improving metabolite yields through fermentation. Most of the mutants show only reductions of secondary metabolism, but in some cases strong increases of one or more natural product families were detectable. This suggests that *M. xanthus* cells behave like well-optimized cellular factories, where a gene knockout mostly results in a significant slowing down of productivity. To understand the regulation of *M. xanthus* is the first step to rationally improve secondary metabolite yields.

Discussion

Many of the knockout targets code for proteins, which may have regulatory functions for further genes or proteins. Some of these might represent important key factors that increase strain competitiveness in the hostile environment of the soil. Here, the highlight overproducer was the knockout mutant of MXAN_1808, where the highest up-regulation of all mutants was detected for the myxalamids (8fold) and the myxovirescins (12fold). Additionally, the biosynthesis of the DKxanthenes was also enhanced (18fold). Furthermore, the mutant strain of MXAN_1988 was found to be the strongest DKxanthene overproducing strain (22fold), compared to the other mutants. Moreover, myxovirescin production in this mutant had also increased (5fold).

Not one of the mutants exhibited convincing similarities to the wild type under the same, iron-rich conditions or showed such strong restriction of growth as the wild type under iron-limiting conditions. It can be concluded that *M. xanthus* uses very diverse mechanisms to regulate metabolism in response to iron availability, some of the discussed, individual strategies are known and some are quite common for bacteria.

From growth and modulation of secondary metabolite profile, it is difficult to derive an exact function of the protein in the respective knockout mutant, complicated by the fact that mostly the combination of effects was very mutant-specific and the regulatory mechanisms of iron, central metabolism, secondary metabolite pathways, development and movement in *M. xanthus* are strongly cross-linked

Mostly, mutations resulted in a delayed exponential growth phase, lower overall cell density, or both (figure 3.11). All mutants exhibited only wild type levels or less in iron-uptake rates (table 3.11), also detected for myxochelin production, but several other secondary metabolites showed a significant increase in some of the mutants (table 3.12). Furthermore, some mutants are able to growth faster than the wild type, indicating that some parts of metabolism were not active or cell-cycle was accelerated by deregulation of important switching points. The available data of several of the mutated strains suggests important functions for the respective, inactivated protein in controlling general metabolism or iron-correlated reactions in *M. xanthus*.

Typically, mutations result in reduced secondary metabolite yields across multiple metabolite classes (table 3.12). In fact, in mutants of MXAN_1562 and MXAN_1893, production of all compounds was significantly reduced, while in mutant MXAN_0144, the production of all metabolites with the exception of the myxochromides, were lower. In some cases (mutants of

Discussion

MXAN_4189, MXAN_4535 and MXAN_5055), the effects were limited to a subset of metabolite classes (myxovirescin, myxalamid and the myxochelins). In contrast, in the mutants of MXAN_1808, MXAN_1988 and MXAN_2440 a drastic increase in production of specific compounds was detected, including the DKxanthenes and myxovirescin, and in the case of MXAN_1808 also myxalamids were up-regulated.

The two disruption mutants of MXAN_1562 (DPS/bactoferritin) and MXAN_1864 (N6-adenine DNA methyltransferase) show a global secondary metabolite response, precisely a reduction of all production rates. Both strains show also a strong decrease in iron uptake, compared to the wild type (below 10 %). Myxochelin production was found to be much lower in KO_1562, correspondingly to the lower iron-uptake rate of this strain. Furthermore, the secondary metabolite product profile was found to be highly similar to the deletion mutant DEL6967. In detail, all differences in production were below 2 %, compared to KO_1562, only the myxochromides exhibited a difference of ca. 20 %. Additionally, the growth profile was detected to be quite similar for both strains. In contrast, only the knockout strain of MXAN_1562 showed a significant reduction in iron uptake, which is explainable by the loss of an important bactoferritin iron-storage function in this mutant, which makes it necessary to restrict iron-import. However, the high conformity of both strains leads to the conclusion that MXAN_1562 might have a key role in regulation of MXAN_6967 or the other way round. This hypothesis could be corroborated by the detection of MXAN_1562 interacting with the promoter of MXAN_6967 under iron-limiting conditions. It might be possible that MXAN_1864 is also somehow involved in regulation of MXAN_1562 and/or MXAN_6967. In contrast, the in-frame deletion mutant of MXAN_6967 and the disruption mutant of MXAN_1893 (putative ClpX protease) show also such a global response in secondary metabolism, but in both the effects on iron uptake were not very prominent. Perhaps the regulatory process, in which MXAN_1893 is involved could be connected to the one of MXAN_6967, also if MXAN_1893 was not detected to bind to the promoter of MXAN_6967. Anyway, both mutants share several similarities in growth, iron uptake and effects to secondary metabolite production.

On the other hand, the mutations of MXAN_1808 (DEAD box helicase/N6-adenine DNA methyltransferase), MXAN_1988 (putative C5-cytosine DNA methyltransferase) and MXAN_2440 (putative transcription termination Rho factor) produced significant increases in

Discussion

the titers of selected metabolites, including the DKxanthenes, myxovirescin and the myxalamids. The effects on the DKxanthenes were most pronounced (18-, 22- and 12fold up-regulated, respectively), but myxovirescin biosynthesis was up-regulated by at least 4fold in each of the mutants, and an 8fold increase in myxalamid production was observed only for the MXAN_1808 mutant. However, as the number and kind of genes, controlled by the three proteins MXAN_1808, MXAN_1988 and MXAN_2440 is unclear, it is again difficult to explain these results. However, the phenotype of each mutant argues for a disruption of high-ranking switch-like mechanisms. Further biochemical tests would be necessary to identify the exact DNA target sequences of the proteins. Nonetheless, it is clear that exact elucidating of the roles of these proteins in regulating secondary metabolism might ultimately afford opportunities to rationally increase production levels. It makes sense that some iron responsive proteins were functional in regulation of secondary metabolism, at least coupled to some of these pathways by secondary effects. Iron-limitation typically induced the accumulation of some, specific metabolites, while others were discriminated (Heim *et al.*, 2002; Basler *et al.*, 2006; Vidakovics *et al.*, 2007). Proteome experiments, comparing the wild type and different mutant strains may clarify the function of some of the iron responsive proteins more precisely, including contributions to regulation of iron and secondary metabolism.

The mutant of MXAN_1988 (putative C5-cytosine DNA methyltransferase) shares additionally a high degree of similarities to the mutant of MXAN_4189 (tetra tricopeptide repeat protein), concerning the unusual growth profile, in contrast to results from secondary metabolite analysis, where MXAN_1988 exhibited some significant up-regulation of diverse natural product families, while MXAN_4189 showed only reductions. Furthermore, significant variations were detected in the amount of produced myxochelin, in addition to the strong differences in iron uptake. Both mutants produce still high amounts of myxochelin, but only the knockout mutant of MXAN_1988 can take up iron efficiently.

Similarly to the knockout mutant of MXAN_4189 findings were made for the mutant of MXAN_1808, concerning the loss of efficient iron uptake in combination with an only small reduction of myxochelin. Again, the mutants differ significantly in secondary metabolite product profile. The regulatory function of the three proteins MXAN_1808, 1988 and 4189 seems not to be connected very closely.

Discussion

Almost identical production profiles were detected for the single crossover-based gene disruption mutants of MXAN_2440 (putative transcription termination Rho factor) and MXAN_3203 (FHA domain protein), except for the compound class of chtilins. Additionally, both strains exhibited a reduced, but still efficient iron uptake in comparison to the wild type. Despite of variations between both growth curves, maximum O.D.₆₀₀ for both strains was significant lower (reach ca. 70 %) than estimated for the non-mutated strain. The similarities of both phenotypes suggest that both proteins MXAN_2440 and MXAN_3203 share several biochemical targets, are part of the same regulatory cascade or are somehow involved in similar or the same control processes.

However, the phenotype of knockout mutant of MXAN_2440 may derive from polar effects, for example by the loss or shortage of important polycistronic mRNAs, which carry the information of several genes. For simple, single crossover knockout mutants, it is possible to generate the respective phenotype as a result of the loss of several important proteins, coded by polycistronic mRNA, but not only the target.

If genes are part of an operon structure, ultimate elimination of polar effects could only be obtained when the target gene would be deleted in-frame from the genome sequence (Windgassen *et al.*, 2000).

In total, 4 genes which were inactivated show the structure of potential operons; in detail:
MXAN_0144-0143; containing a cupin-like storage protein,
MXAN_1562-1560; containing a putative lipoprotein and an aminotransferase,
MXAN_2440-2445; containing a hypothetical protein and 4 proteins of flagellum assembly and flagellar motor switch proteins,
MXAN_5484-5483; containing a sensory protein; a protein family which is already known to interact with protein-kinases.

Indeed, for the knockout strain of MXAN_2440 a significant up-regulation of DKxanthene was discovered, which might correlate to operon MXAN_2440-2445 for the enhancement of cellular movement, required for development. This process could be facilitated by the flagellum-correlated potential operon, additionally to the S- and A-motility mechanisms, so DKxanthenes were up-regulated to compensate the reduced mobility of the mutant. Anyway, effects in these mutants could be derived by polar effects, which cause unpredictable consequences for cellular metabolism.

Discussion

Analysis of the mutants suggests that regulation of secondary metabolism is depended on the exact interplay between many intra- and extra-cellular factors, regulatory proteins, such as protein-kinases or transcriptional regulators, so also strong influences were discovered, when disrupting the balance in the regulatory network of iron, at least by secondary effects. Some previously uncharacterized proteins/genes of *M. xanthus* with a response in expression under iron starvation had been identified to play central roles in fundamental cellular processes.

The unusual regulatory mechanisms of *M. xanthus* to iron-limitation were found to influence primary metabolism and secondary metabolite production, including the significant up-regulation of siderophore biosynthesis. However, elucidation of pathways and regulation of the biosynthesis of secondary metabolites from *M. xanthus* may also be a first step to understand iron regulation in myxobacteria generally.

The combination of 2D-DIGE proteome analysis, DNA-binding assays and HPLC-MS-based secondary metabolite quantification, paired with gene inactivation experiments has provided a further module in the understanding of the highly complex regulation networks in *M. xanthus* DK1622.

5. Conclusion and Outlook

As iron is essential for microbial life, bacteria have evolved complex mechanisms to balance metabolism and iron availability. In many Gram-negative and Gram-positive bacteria, this metabolic remodeling is mediated by the ferric uptake regulator (Fur), a transcriptional regulator with central function in iron-response. In this study, it was investigated how the myxobacterial model strain *Myxococcus xanthus* DK1622 responds to conditions of iron-limitation, concerning effects on growth, iron uptake rates, proteome pattern, and secondary metabolite production. In addition, DNA interaction studies (DNA pull-down assays) under iron-rich and iron-limiting conditions had been performed on both *fur* promoters (MXAN_3702 and MXAN_6967). In this process, no evidence was found for an auto-regulation of Fur expression.

The probably iron-responsive Fur protein (MXAN_3702) seems to be essential in *M. xanthus*. Therefore, it was not possible to inactivate the respective gene and to decouple Fur-dependent and Fur-independent effects in proteome analysis. Nonetheless, the growth limitation and the spectrum of changes in cellular protein composition, which had been observed during iron starvation agrees well with results of previously characterized iron-response from other bacteria.

On the other hand, an extraordinarily high percentage of these proteins exhibit regulatory functions, because many DNA interaction proteins (as transcriptional regulators or DNA methyltransferases) or proteins from other regulatory events (as protein kinases) could be detected with differences in expression under iron-limiting conditions.

Twelve different proteins were found to carry up to three phosphorylations. Phosphorylation-patterns of much more proteins were altered in *M. xanthus* during iron-limitation than expected for bacteria, which is more common in eukaryotes. This may be explained by the extraordinary large genome size, which encodes ca. 100 eukaryotic-like protein kinases and the complex life cycle of *M. xanthus*, generally. In contrast, *M. xanthus* possibly utilizes a more complex iron-regulation than expected from traditional bacterial models. Both Fur proteins from *M. xanthus* were not detected as differently regulated during iron starvation, but some other potential regulators which may contribute to intracellular iron balance. To have such additional players in the iron-regulatory network might be essential to survive in the typically iron-poor environment of soil bacteria, indicated by drastic altered phenotypes of the knockout mutants of some of these potential regulators.

Conclusion

Additionally, several proteins from A- and S-motility were found in the proteome experiment to be activated in the sub-optimal environment of iron-limitation.

In comparable experiments with other bacteria, a significant rearrangement of proteins with redox-functions was detected, which was also the case in *M. xanthus*. This is probably explained by the change of cellular iron influx, which is a very important factor in redox-balancing. Also the up-regulation of siderophore biosynthetic proteins was observed in *M. xanthus*, which is a typical effect in bacteria during iron starvation, resulting in *M. xanthus* in a 5fold increase of the relative iron uptake yield. In addition, several characteristic key points in central metabolism, which are known to be functional as iron-controlling element, were also detected in *M. xanthus* to be influenced by iron availability (e.g. several members from the TCA cycle).

A high percentage of the identified proteins has no annotated function yet. Several of these show no convincing homologies to characterized proteins from databases with already known activities; therefore no final conclusion can be regarding about their functions.

The disadvantage of the used 2D-DIGE-based proteome analysis is that most of the PKS and NRPS proteins are not detectable. An enormous amount of energy and precursors must be provided to keep the large-size gene clusters in the chromosome, express the corresponding biosynthetic proteins and finally synthesize the PKS- or NRPS-products. Several of these secondary metabolites have important physiological roles, as the siderophore myxochelin, whose gene cluster was found to be essential in *M. xanthus*.

The response of the *M. xanthus* secondary metabolome to iron-limitation exhibits a drastic increase of siderophore production (myxochelin A: 81fold; myxochelin B: 678fold). The substance family of myxochromides was also found enhanced (23fold), maybe used to facilitate movement to find and metabolize new iron resources. Furthermore, the biological agents myxovirescin and myxalamid were still produced at high levels during iron-starvation, hypothetically to prevent growth of potential competitors. No differences could be detected in the production levels of the development-associated metabolite family of DKXanthenes, while citterlin production was almost disengaged completely (75fold reduced).

There is a big interest in pharmaceutical chemistry/biology to identify new bioactive substances. A potential anti-cancer activity was postulated for myxochelin A (Miyanaga *et al.*, 2006). Today, siderophore structures from microorganisms are used also for the treatment of acute iron intoxication (Nielsen *et al.*, 1995; Vermeylen, 2008). For *M. xanthus*, a significant

Conclusion

amplification of the myxochelin production was discovered under iron-limitation, so the methods and results from the present work can be taken as instructions to produce significantly higher amounts of siderophores with the same resources.

Additional studies had been performed to generate myxochelin derivates by total chemical synthesis (Prof. K. Hegetschweiler, S. Wilbrand; Universität des Saarlandes). Subsequently, examination of the destiny of ferri-myxochelin molecules after re-import into the cell could be performed.

In spite of failure of the strategy to detect novel compounds from *M. xanthus* DK1622 under iron-limiting conditions, it might be successful in other myxobacteria such as *Sorangium cellulosum* So ce56 or *Stigmatella aurantiaca* DW4/3-1. The regulation of iron in each sub-order seems to be completely different, so it will be interesting to evaluate the effects of iron-limitation, Fur-inactivation or both in these organisms. In addition, myxobacterial development could be analyzed under iron starvation conditions, again motivated by the potential awaking of silent secondary metabolite gene clusters.

Further examinations of remodeling of the cellular surface structures could be a next research topic, using a combined approach of (perhaps fluorescent-based) microscopy and membrane sub-proteome analysis to elucidate iron-regulation and iron uptake more in detail.

Inactivation of selected, iron-correlated genes were generated, such as from the *fur* homologue MXAN_6967. The in-frame deletion of MXAN_6967 results in a mutant with a significant decrease in complete secondary metabolism, but only a slight reduction in iron uptake, which both argues for a function of MXAN_6967 apart from iron regulation.

An genetically engineered overexpression mutant of MXAN_6967 showed in first experiments an increase of several secondary metabolites, namely the myxalamids, myxochelin A and the myxochromides (R. Müller, T. Klefisch, unpublished results), which accounts for a function of MXAN_6967 in controlling expression of secondary metabolism gene clusters, as suggested by data from secondary metabolite analysis of the deletion mutant of MXAN_6967.

Unexpectedly, some indications were found that *M. xanthus* may be able to import and metabolize heme molecules, as the presence of some proteins from heme-import and heme-degradation or some important sequence motifs of Irr-like heme sensing Fur proteins in

Conclusion

MXAN_6967, which is the second, obviously not-iron-responsive Fur homologue in *M. xanthus*. For verification of the hypothesis, *M. xanthus* could be grown in iron-limiting media, supplemented with heme as only iron resource. Furthermore, this experiment could be repeated with the deletion mutant of MXAN_6967 instead of the wild type strain to evaluate a possible heme-sensing function of MXAN_6967, perhaps both approaches could be followed by proteome analysis.

A next consequent step would be the proteome analysis of the wild type grown on several, different iron concentration in comparison to the mutant, carrying the in-frame deletion in MXAN_6967 to find out more about the cellular role of this probably not-iron-correlated ferric uptake regulator.

Furthermore, homologues of the DNA methyltransferase MXAN_1864 were detected in other myxobacteria (*Sorangium cellulosum* Soce 56, *Stigmatella aurantiaca* DW4/3-1). A gene knockout of the homologoue gene in *S. cellulosum* Soce 56 (Sce2777) had been performed. The mutant strain exhibited similar effects to the *M. xanthus* mutant KO_1864, precicely a seriously compromised secondary metabolite production (R. Müller, S. Rachid, unpublished results).

This was the first time that a contribution of a DNA methyltransferase to regulation of secondary metabolite pathways in myxobacteria was suggested. In order to gain a deeper understanding of the regulation of secondary metabolite gene clusters, this gene could be inactivated in *S. aurantiaca* as well.

Surprisingly, it was found that inactivation of several iron-responsive genes with no obvious role in secondary metabolism significantly enhanced production of selected natural products, but not myxochelin. In contrast, the deletion mutant of the second, probably not-iron-responsive *fur* gene MXAN_6967 results in a significant reduction of all secondary metabolites, also detected for some other inactivation mutants of iron-responsive genes for *M. xanthus*.

The synergistic use of 2D-DIGE proteome techniques, HPLC-MS-based secondary metabolite quantification, DNA-binding assays and knockout mutants of *M. xanthus* had been found to be a powerful combination to study metal homeostasis and get some first information from comparative expression profiles about the highly complex regulation networks in *M. xanthus* DK1622.

6. Abstract

The myxobacterium *Myxococcus xanthus* DK1622 is a reliable producer of different secondary metabolites with partially unknown bioactivities. In the present work the response of iron availability were evaluated, concerning effects on growth, proteome profile and secondary metabolite production.

The production of the siderophore myxochelin A was increased by the factor 81, myxochelin B by the factor 678. Unexpectedly, several other secondary metabolite production rates were found influenced, as e.g. myxochromids und ctitilins.

In proteome analysis, 1979 protein spots were detected in average, whereof 172 exhibited an iron-induced change in expression. A subsequent analysis by tandem mass spectrometry identified 169 of these spots as 131 individual proteins, some with up to 3 protein-phosphorylations.

Furthermore, the functions of some, interesting proteins were investigated by knockout of the respective coding gene. At all, 12 *single crossover* mutants were generated and compared in iron-rich environment concerning effects on growth and rates of iron uptake or secondary metabolite production to the wild type strain. Typically, mutant strains show variations in all three parameters.

An in-frame deletion mutant in one of the two fur genes (MXAN_6967) exhibited reduced growth and a decrease in iron uptake (ca. 49 % of the wild type). Additionally, production of all seven monitored secondary metabolites cannot be explained with the traditional Fur model, which suggests a new, unexpected regulation in *M. xanthus*.

7. Zusammenfassung

Das Myxobakterium *Myxococcus xanthus* DK1622 ist ein verlässlicher Produzent verschiedenster Sekundärmetabolite mit teilweise unbekannten biologische Aktivitäten. In der vorliegenden Arbeit wurde der Einfluss der Verfügbarkeit von Eisen auf Wachstum, Proteom-Muster und Sekundärmetabolit-Produktion untersucht.

Die Produktion der Siderophore Myxochelin A wurde bei Eisenlimitierung um den Faktor 81 gesteigert, Myxochelin B um den Faktor 678. Unerwarteterweise wurden auch weitere Sekundärmetabolite-Produktionen stark beeinflusst, wie z.B. Myxochromid und Cittilin.

In Proteomexperimenten konnten von durchschnittlich 1979 detektierten Proteinspots für 172 eine eiseninduzierte Konzentrationsveränderung gezeigt werden. Hiervon wurden 169 Spots mittels Tandem-Massenspektrometrie identifiziert als 131 individuelle Proteine mit bis zu 3 Phosphorylierungen.

Des Weiteren wurde die Rolle von interessanten Proteinen durch Knockout entsprechender, codierender Genom-Bereiche untersucht. Insgesamt konnten 12 *single-crossover* Mutanten generiert werden, welche in eisenreicher Umgebung bezüglich Wachstum, Eisenaufnahmeraten und Sekundärmetabolit-Produktionsraten mit dem Wildtyp-Stamm verglichen wurden, wobei die Mehrzahl Abweichungen vom Wildtyp in allen drei Parametern zeigten.

Eine in-frame Deletionsmutante von einem der beiden *fur*-Gene (MXAN_6967) zeigte im Vergleich mit dem Wildtyp reduziertes Wachstum. Die Verminderung der Eisenaufnahmeraten (49 % des Wildtyps) und Abnahme der Produktionsraten aller sieben Sekundärmetabolite kann mit dem traditionellen Fur-Model nicht erklärt werden, was eine neue, unerwartete Regulation bei *M. xanthus* nahe legt.

8. Bibliography

REFERENCES

1. (2007). *Myxobacteria: multicellularity and differentiation*. ASM Press, Chicago.
2. Abdul-Tehrani H, Hudson AJ, Chang YS, Timms AR, Hawkins C, Williams JM, Harrison PM, Guest JR, and Andrews SC (1999) Ferritin mutants of *Escherichia coli* are iron deficient and growth impaired, and fur mutants are iron deficient. *J Bacteriol*, **181**, 1415-1428.
3. Abergel RJ, Warner JA, Shuh DK, and Raymond KN (2006) Enterobactin protonation and iron release: Structural characterization of the salicylate coordination shift in ferric enterobactin. *J Am Chem Soc*, **128**, 8920-8931.
4. Ahn BE, Cha J, Lee EJ, Han AR, Thompson CJ, and Roe JH (2006) Nur, a nickel-responsive regulator of the Fur family, regulates superoxide dismutases and nickel transport in *Streptomyces coelicolor*. *Mol Microbiol*, **59**, 1848-1858.
5. Alban A, David S, Bjorkesten L, Andersson C, Sloge E, Lewis S, and Currie I (2003) A novel experimental design for comparative two-dimensional gel analysis: two-dimensional difference gel electrophoresis incorporating a pooled internal standard. *Proteomics Proteomics*, **3**, 36-44.
6. Alberts B, Johnson A, Lewis J, Raff M, Roberts K, and Walter P (2002). *Molecular Biology of the Cell*. Garland Science.
7. Alechin AE, Gramatikova S, Hura GL, Bobkov A, Strongin AY, Stec B, Tainer JA, Liddington RC, and Smith JW (2009) Crystal and solution structures of a prokaryotic M16B peptidase: an open and shut case. *Structure*, **17**, 1465-1475.
8. Altschul SF, Gish W, Miller W, Myers EW, and Lipman DJ (1990) Basic local alignment search tool. *Journal of Molecular Biology*, **215**, 403-410.
9. Altschul SF, Madden TL, Schaffer AA, Zhang JH, Zhang Z, Miller W, and Lipman DJ (1997) Gapped BLAST and PSI-BLAST: a new generation of protein database search programs. *Nucleic Acids Res*, **25**, 3389-3402.
10. Ambrosi HD, Hartmann V, Pistorius D, Reissbrodt R, and Trowitzsch-Kienast W (1998) Myxochelins B, C, D, E and F: A new structural principle for powerful siderophores imitating nature. *Eur J Org Chem*, 541-551.
11. Ambrozic J, Ostroversnik A, Stracic M, Kuhar I, Grabnar M, and Zgur-Bertok D (1998) *Escherichia coli* CoIV plasmid pRK100: genetic organization, stability and conjugal transfer. *Microbiology*, **144**, 343-352.
12. An YJ, Ahn BE, Han AR, Kim HM, Chung KM, Shin JH, Cho YB, Roe JH, and Cha SS (2009) Structural basis for the specialization of Nur, a nickel-specific Fur homolog, in metal sensing and DNA recognition. *Nucleic Acids Res*, **37**, 3442-3451.
13. Anderson ES, Paulley JT, and Roop RM2 (2008) The AraC-Like Transcriptional Regulator DhbR Is Required for Maximum Expression of the 2,3-Dihydroxybenzoic

Acid Biosynthesis Genes in *Brucella abortus* 2308 in response to iron deprivation. *J Bacteriol*, **190**, 1838-1842.

14. Andrews SC, Robinson AK, and Rodriguez-Quinones F (2003) Bacterial iron homeostasis. *FEMS Microbiol Rev*, **27**, 215-237.
15. Aranda J, Cortes P, Garrido ME, Fittipaldi N, Llagostera M, Gottschalk M, and Barbe J (2009) Contribution of the FeoB transporter to *Streptococcus suis* virulence. *Int Microbiol*, **12**, 137-143.
16. Archambault M, Labrie J, Rioux CR, Dumas F, Thibault P, Elkins C, and Jacques M (2003) Identification and preliminary characterization of a 75-kDa hemin- and hemoglobin-binding outer membrane protein of *Actinobacillus pleuropneumoniae* serotype 1. *Can J Vet Res*, **67**, 271-277.
17. Archibald F (1983) *Lactobacillus plantarum*, an organism not requiring iron. *FEMS Microbiol Lett*, **19**, 29-32.
18. Arnott D, Shabanowitz J, and Hunt DF (1993) Mass spectrometry of proteins and peptides: sensitive and accurate mass measurement and sequence analysis. *Clin Chem*, **39**, 2005-2010.
19. Arosio P and Levi S (2002) Ferritin, Iron Homeostasis, and Oxidative Damage. *Free Radic Biol Med*, **33**, 457-463.
20. Asad NR, Asad LM, Silva AB, Felzenszwalb I, and Leitao AC (1998) Hydrogen peroxide effects in *Escherichia coli* cells. *Acta Biochim Pol*, **45**, 677-690.
21. Aubourg S, Kreis M, and Lecharny A (1999) The DEAD box RNA helicase family in *Arabidopsis thaliana*. *Nucleic Acids Res*, **27**, 628-636.
22. Bach S, Buchrieser C, Prentice M, Guiyoule A, Msadek T, and Carniel E (1999) The high-pathogenicity island of *Yersinia enterocolitica* Ye8081 undergoes low-frequency deletion but not precise excision, suggesting recent stabilization in the genome. *Infect Immun*, **67**, 5091-5099.
23. Baichoo N and Helmann JD (2002a) Recognition of DNA by Fur: a reinterpretation of the Fur box consensus sequence. *J Bacteriol*, **184**, 5826-5832.
24. Baichoo N, Wang T, Ye R, and Helmann JD (2002b) Global analysis of the *Bacillus subtilis* Fur regulon and the iron starvation stimulon. *Mol Microbiol*, **45**, 1613-1629.
25. Baltes N, Hennig-Pauka I, and Gerlach GF (2002) Both transferrin binding proteins are virulence factors in *Actinobacillus pleuropneumoniae* serotype 7 infection. *FEMS Microbiol Lett*, **209**, 283-287.
26. Barton HA, Johnson Z, Cox CD, Vasil AI, and Vasil ML (1996) Ferric uptake regulator mutants of *Pseudomonas aeruginosa* with distinct alterations in the iron-dependent repression of exotoxin A and siderophores in aerobic and microaerobic environments. *Mol Microbiol*, **21**, 1001-1007.

References

27. Basler M, Linhartova I, Halada P, Novotna J, Bezouskova S, Osicka R, Weiser J, Vohradsky J, and Sebo P (2006) The iron-regulated transcriptome and proteome of *Neisseria meningitidis* serogroup C. *Proteomics Proteomics*, **6**, 6194-6206.
28. Battisti JM, Smitherman LS, Sappington KN, Parrow NL, Raghavan R, and Minnick MF (2007) Transcriptional regulation of the heme binding protein gene family of *Bartonella quintana* is accomplished by a novel promoter element and iron response regulator. *Infect Immun*, **75**, 4373-4385.
29. Benevides-Matos N, Wandersman C, and Biville F (2008) HasB, the *Serratia marcescens* TonB Paralog, Is Specific to HasR. *J Bacteriol*, **190**, 21-27.
30. Berish SA, Subbarao S, Chen CY, Trees DL, and Morse SA (1993) Identification and cloning of a fur homolog from *Neisseria gonorrhoeae*. *Infect Immun*, **61**, 4599-4606.
31. Berleman JE, Chumley T, Cheung P, and Kirby JR (2006) Rippling is a predatory behavior in *Myxococcus xanthus*. *J Bacteriol*, **188**, 5888-5895.
32. Berleman JE and Kirby JR (2007) Multicellular development in *Myxococcus xanthus* is stimulated by predator-prey interactions. *J Bacteriol*, **189**, 5675-5682.
33. Bertani G (1951) Studies on lysogenesis. I. The mode of phage liberation by lysogenic *Escherichia coli*. *J Bacteriol*, **62**, 293-300.
34. Bhatt G and Denny TP (2004) *Ralstonia solanacearum*: Iron scavenging by the siderophore staphyloferrin B is controlled by PhcA, the global virulence regulator. *J Bacteriol*, **186**, 7896-7904.
35. Biemann K (1990) Sequencing of peptides by tandem mass-spectrometry and high-energy collision-induced dissociation. *Methods in Enzymology*, **193**, 455-479.
36. Birnboim HC and Doly J (1979) A rapid alkaline extraction procedure for screening recombinant plasmid DNA. *Nucleic Acids Res*, **7**, 1513-1523.
37. Black WP and Yang Z (2004) *Myxococcus xanthus* chemotaxis homologs DifD and DifG negatively regulate fibril polysaccharide production. *J Bacteriol*, **186**, 1001-1008.
38. Bode HB, Meiser P, Klefisch T, Socorro D.J.Cortina N, Krug D, Göhring A, Schwär G, Mahmud T, Elnakady YA, and Müller R (2007) Mutasynthesis-derived myxalamids and origin of the isobutyryl-CoA starter unit of myxalamid B. *ChemBioChem*, **8**, 2139-2144.
39. Bode HB, Ring MW, Kaiser D, David AC, Kroppenstedt RM, and Schwär G (2006a) Straight-chain fatty acids are dispensable in the myxobacterium *Myxococcus xanthus* for vegetative growth and fruiting body formation. *J Bacteriol*, **188**, 5632-5634.
40. Bode HB, Ring MW, Schwär G, Altmeyer MO, Kegler C, Jose IR, Singer M, and Müller R (2009) Identification of additional players in the alternative biosynthesis pathway to isovaleryl-CoA in the myxobacterium *Myxococcus xanthus*. *ChemBioChem*, **10**, 128-140.

41. Bode HB, Ring MW, Schwär G, Kroppenstedt RM, Kaiser D, and Müller R (2006b) 3-Hydroxy-3-methylglutaryl-coenzyme A (CoA) synthase is involved in the biosynthesis of isovaleryl-CoA in the myxobacterium *Myxococcus xanthus* during fruiting body formation. *J Bacteriol*, **188**, 6524-6528.
42. Bradford MM (1976) A rapid and sensitive method for the quantitation of microgram quantities of protein utilizing the principle of protein-dye binding. *Analytical Biochemistry*, **72**, 248-254.
43. Braun JE and Neusser HJ (2002) Threshold photoionization in time-of-flight mass spectrometry. *Mass Spectrom Rev*, **21**, 16-36.
44. Bretscher AP and Kaiser D (1978) Nutrition of *Myxococcus xanthus*, a fruiting myxobacterium. *J Bacteriol*, **133**, 763-768.
45. Brickman TJ, Anderson MT, and Armstrong SK (2007) Bordetella iron transport and virulence. *Biometals*, **20**, 303-322.
46. Brock TD and Madigan MT (1991). *Biology of Microorganisms*. Prentice Hall.
47. Bsat N, Herbig A, Casillas-Martinez L, Setlow P, and Helmann JD (1998) *Bacillus subtilis* contains multiple Fur homologues: identification of the iron uptake (Fur) and peroxide regulon (PerR) repressors. *Mol Microbiol*, **29**, 189-198.
48. Buchanan SK, Smith BS, Venkatramani L, Xia D, Esser L, Palnitkar M, Chakraborty R, van der Helm D, and Deisenhofer J (1999) Crystal structure of the outer membrane active transporter FepA from *Escherichia coli*. *Nat Struct Biol*, **6**, 56-63.
49. Carrondo MA (2003) Ferritins, iron uptake and storage from the bacterioferritin viewpoint. *EMBO J*, **22**, 1959-1968.
50. Carter P (1971) Spectrophotometric determination of serum iron at the submicrogram level with a new reagent (ferrozine). *Anal Biochem*, **40**, 450-458.
51. Cartron ML, Maddocks S, Gillingham P, Craven CJ, and Andrews SC (2006) Feo--transport of ferrous iron into bacteria. *Biometals*, **19**, 143-157.
52. Cavet JS, Borrelly GP, and Robinson NJ (2003) Zn, Cu and Co in cyanobacteria: selective control of metal availability. *FEMS Microbiol Rev*, **27**, 165-181.
53. Chalissery J, Banerjee S, Bandey I, and Sen R (2007) Transcription termination defective mutants of Rho: role of different functions of Rho in releasing RNA from the elongation complex. *J Mol Biol*, **371**, 855-872.
54. Chamrad DC, Körting G, Stühler K, Meyer HE, Klose J, and Blüggel M (2004) Evaluation of algorithms for protein identification from sequence databases using mass spectrometry data. *Proteomics Proteomics*, **4**, 619-628.
55. Chao TC, Buhrmester J, Hansmeier N, Pühler A, and Weidner S (2005) Role of the regulatory gene rirA in the transcriptional response of *Sinorhizobium meliloti* to iron limitation. *Appl Environ Microbiol*, **71**, 5969-5982.

References

56. Chaurand P, Luetzenkirchen F, and Spengler B (1999) Peptide and protein identification by matrix-assisted laser desorption ionization (MALDI) and MALDI-post-source decay time-of-flight mass spectrometry. *J Am Soc Mass Spectrom*, **10**, 91-103.
57. Chenna R, Sugawara H, Koike T, Lopez R, Gibson TJ, Higgins DG, and Thompson JD (2003) Multiple sequence alignment with the Clustal series of programs. *Nucleic Acids Res*, **31**, 3497-3500.
58. Chi A, Huttenhower C, Geer LY, Coon JJ, Syka JEP, Bai DL, Shabanowitz J, Burke DJ, Troyanskaya OG, and Hunt DF (2007) Analysis of phosphorylation sites on proteins from *Saccharomyces cerevisiae* by electron transfer dissociation (ETD) mass spectrometry. *P Natl Acad Sci USA*, **104**, 2193-2198.
59. Cinkaya I. Substrat induzierte Radikalbildung in dem Eisen-Schwefel-Flavoenzym 4-Hydroxybutyryl-CoA-Dehydratase aus *Clostridium aminobutyricum*. 2002. Marburg, Philipps-Universität.
Ref Type: Thesis/Dissertation
60. Clemans DL, Chance CM, and Dworkin M (1991) A development-specific protein in *Myxococcus xanthus* is associated with the extracellular fibrils. *J Bacteriol*, **173**, 6749-6759.
61. Connelly JC, Kirkham LA, and Leach DR (1998) The SbcCD nuclease of *Escherichia coli* is a structural maintenance of chromosomes (SMC) family protein that cleaves hairpin DNA. *Proc Natl Acad Sci U S A*, **95**, 7969-7974.
62. Cornelissen CN and Sparling PF (1994) Iron piracy: acquisition of transferrin-bound iron by bacterial pathogens. *Mol Microbiol*, **14**, 843-850.
63. Cornish AS and Page WJ (1998) The catecholate siderophores of *Azotobacter vinelandii*: their affinity for iron and role in oxygen stress management. *Microbiology*, **144**, 1747-1754.
64. Cortes J, Velasco J, Foster G, Blackaby AP, Rudd BA, and Wilkinson B (2002) Identification and cloning of a type III polyketide synthase required for diffusible pigment biosynthesis in *Saccharopolyspora erythraea*. *Mol Microbiol*, **44**, 1213-1224.
65. Cotter RJ, Griffith W, and Jelinek C (2007) Tandem time-of-flight (TOF/TOF) mass spectrometry and the curved-field reflectron. *J Chromatogr B Analyt Technol Biomed Life Sci*, **855**, 2-13.
66. Coulton JW, Mason P, Cameron DR, Carmel G, Jean R, and Rode HN (1986) Protein fusions of beta-galactosidase to the ferrichrome-iron receptor of *Escherichia coli* K-12. *J Bacteriol*, **165**, 181-192.
67. Crosa JH (1997) Signal transduction and transcriptional and posttranscriptional control of iron-regulated genes in bacteria. *Microbiol Mol Biol Rev*, **61**, 319-336.
68. Crosa JH and Walsh CT (2002) Genetics and assembly line enzymology of siderophore biosynthesis in bacteria. *Microbiol Mol Biol Rev*, **66**, 223-249.

69. Curtis PD, Atwood J, Orlando R, and Shimkets LJ (2007) Proteins associated with the *Myxococcus xanthus* extracellular matrix. *J Bacteriol*, **189**, 7634-7642.
70. D'Andrea LD and Regan L (2003) TPR proteins: the versatile helix. *Trends Biochem Sci*, **28**, 655-662.
71. Dahl JL, Tengra FK, Dutton D, Yan J, Andacht TM, Coyne L, Windell V, and Garza AG. Identification of major sporulation proteins of *Myxococcus xanthus* using a proteomic approach. *Journal of Bacteriology* 189[8], 3187-3197. 2007.
Ref Type: Thesis/Dissertation
72. Dailey HA and Dailey TA (1996) Protoporphyrinogen oxidase of *Myxococcus xanthus*. Expression, purification, and characterization of the cloned enzyme. *J Biol Chem*, **271**, 8714-8718.
73. Dancik V, Addona TA, Clauser KR, Vath JE, and Pevzner PA (1999) De novo peptide sequencing via tandem mass spectrometry. *J Comput Biol*, **6**, 327-342.
74. Das AK, Cohen PW, and Barford D (1998) The structure of the tetratricopeptide repeats of protein phosphatase 5: implications for TPR-mediated protein-protein interactions. *EMBO J*, **17**, 1192-1199.
75. Dawid W (2000) Biology and global distribution of myxobacteria in soils. *FEMS Microbiol Rev*, **24**, 403-427.
76. De la Cerda B, Castielli O, Duran RV, Navarro JA, Hervas M, and De la Rosa MA (2007) A proteomic approach to iron and copper homeostasis in cyanobacteria. *Brief Funct Genomic Proteomic*, **6**, 322-329.
77. de Luca NG, Wexler M, Pereira MJ, Yeoman KH, and Johnston AW (1998) Is the fur gene of *Rhizobium leguminosarum* essential? *FEMS Microbiol Lett*, **168**, 289-295.
78. De Zoysa A, Efstratiou A, and Hawkey PM (2005) Molecular characterization of diphtheria toxin repressor (dtxR) genes present in nontoxigenic *Corynebacterium diphtheriae* strains isolated in the United Kingdom. *J clin Microbiol*, **43**, 223-228.
79. Deutscher J, Francke C, and Postma PW (2006a) How phosphotransferase system-related protein phosphorylation regulates carbohydrate metabolism in bacteria. *Microbiol Mol Biol Rev*, **70**, 939-1031.
80. Deutscher J and Saier MH, Jr. (2006b) Ser/Thr/Tyr protein phosphorylation in bacteria - for long time neglected, now well established. *J Mol Microbiol Biotechnol*, **9**, 125-131.
81. Dhar K and Rosazza JPN (2000) Purification and characterization of *Streptomyces griseus* catechol O- methyltransferase. *Appl Environ Microbiol*, **66**, 4877-4882.
82. Diaz-Mireles E, Wexler M, Sawers G, Bellini D, Todd JD, and Johnston AW (2004) The Fur-like protein Mur of *Rhizobium leguminosarum* is a Mn(2+)-responsive transcriptional regulator. *Microbiology*, **150**, 1447-1456.

References

83. Downard J and Kroos L (1993). Transcriptional regulation of developmental gene expression in *Myxococcus xanthus*. In Dworkin,M. and Kaiser,D. (Eds.), *Myxobacteria II*, . ASM Press, Washington, D.C., pp. 183-199.
84. Drewett V, Molina H, Millar A, Muller S, von Hesler F, and Shaw PE (2001) DNA-bound transcription factor complexes analysed by mass-spectrometry: binding of novel proteins to the human c-fos SRE and related sequences. *Nucleic Acids Res*, **29**, 479-487.
85. Du L and Shen B (2001) Biosynthesis of hybrid peptide-polyketide natural products. *Curr Opin Drug Discov Devel*, **4**, 215-228.
86. Duan Y, Zhou L, Hall DH, Li W, Doddapaneni H, Lin H, Liu L, Vahling CM, Gabriel DW, Williams KP, Dickerman A, Sun Y, and Gottwald T (2009) Complete genome sequence of citrus huanglongbing bacterium, 'Candidatus Liberibacter asiaticus' obtained through metagenomics. *Mol Plant Microbe Interact*, **22**, 1011-1020.
87. Durocher D, Henckel J, Fersht AR, and Jackson SP (1999) The FHA domain is a modular phosphopeptide recognition motif. *Mol Cell*, **4**, 387-394.
88. Durocher D and Jackson SP (2002) The FHA domain. *FEBS Lett*, **513**, 58-66.
89. Dussurget O, Timm J, Gomez M, Gold B, Yu S, Sabol SZ, Holmes RK, Jacobs WR, Jr., and Smith I (1999) Transcriptional control of the iron-responsive fxbA gene by the mycobacterial regulator IdeR. *J Bacteriol*, **181**, 3402-3408.
90. Dworkin M (1996) Recent advances in the social and developmental biology of the myxobacteria. *Microbiol Rev*, **60**, 70-102.
91. Dworkin M (1962) Nutritional requirements for vegetative growth of *Myxococcus xanthus*. *J Bacteriol*, **84**, 250-257.
92. Dworkin M and Kaiser D (1993). *Myxobacteria II*. American Society for Microbiology, Washington DC.
93. D'Ambrosio C, Salzano AM, Arena S, Renzone G, and Scaloni A (2007) Analytical methodologies for the detection and structural characterization of phosphorylated proteins. *J Chromatogr B Analyt Technol Biomed Life Sci*, **849**, 163-180.
94. Elnakady YA, Rohde M, Sasse F, Backes C, Keller A, Lenhof H-P, Weissman KJ, and Müller R (2007) Evidence for the mode of action of the highly cytotoxic *Streptomyces* polyketide kendomycin. *ChemBioChem*, **8**, 1261-1272.
95. Ernst FD, Bereswill S, Waidner B, Stoof J, Mäder U, Kusters JG, Kuipers EJ, Kist M, van Vliet AH, and Homuth G (2005) Transcriptional profiling of *Helicobacter pylori* Fur- and iron-regulated gene expression. *Microbiology*, **151**, 533-546.
96. Erova TE, Pillai L, Fadl AA, Sha J, Wang S, Galindo CL, and Chopra AK (2006) DNA adenine methyltransferase influences the virulence of *Aeromonas hydrophila*. *Infect Immun*, **74**, 410-424.
97. Escolar L, Perez-Martin J, and de Lorenzo V (1999) Opening the iron box: Transcriptional metalloregulation by the Fur protein. *J Bacteriol*, **181**, 6223-6229.

98. Fenyö D (2000) Identifying the proteome: software tools. *Curr Opin Biotechnol*, **11**, 391-395.
99. Ferguson AD, Hofmann E, Coulton JW, Diederichs K, and Welte W (1998) Siderophore-Mediated Iron Transport: Crystal Structure of FhuA with Bound Lipopolysaccharide. *Science*, **282**, 2215-2220.
100. Finking R and Marahiel MA (2004) Biosynthesis of nonribosomal peptides. *Annu Rev Microbiol*, **58**, 453-488.
101. Fischbach MA and Walsh CT (2006) Assembly-line enzymology for polyketide and nonribosomal Peptide antibiotics: logic, machinery, and mechanisms. *Chem Rev*, **106**, 3468-3496.
102. Floss HG (2006) Combinatorial biosynthesis - Potential and problems. *J Biotechnol*, **124**, 242-257.
103. Flynn JM, Neher SB, Kim YI, Sauer RT, and Baker TA (2003) Proteomic discovery of cellular substrates of the ClpXP protease reveals five classes of ClpX-recognition signals. *Mol Cell*, **11**, 671-683.
104. Frost GE and Rosenberg H (1975) Relationship between the tonB locus and iron transport in Escherichia coli. *J Bacteriol*, **124**, 704-712.
105. Fuangthong M and Helmann JD (2003) Recognition of DNA by three ferric uptake regulator (Fur) homologs in Bacillus subtilis. *J Bacteriol*, **185**, 6348-6357.
106. Funai N, Ohnishi Y, Ebizuka Y, and Horinouchi S (2002) Properties and substrate specificity of RppA, a chalcone synthase-related polyketide synthase in Streptomyces griseus. *J Biol Chem*, **277**, 4628-4635.
107. Gaballa A, Antelmann H, Aguilar C, Khakh SK, Song KB, Smaldone GT, and Helmann JD (2008) The *Bacillus subtilis* iron-sparing response is mediated by a Fur-regulated small RNA and three small, basic proteins. *Proc Natl Acad Sci U S A*, **105**, 11927-11932.
108. Gaitatzis N, Kunze B, and Müller R (2001) In vitro reconstitution of the myxochelin biosynthetic machinery of *Stigmatella aurantiaca* Sg a15: Biochemical characterization of a reductive release mechanism from nonribosomal peptide synthetases. *P Natl Acad Sci USA*, **98**, 11136-11141.
109. Gaitatzis N, Kunze B, and Müller R (2005) Novel insights into siderophore formation in myxobacteria. *ChemBioChem*, **6**, 365-374.
110. Gao H, Zhou D, Li Y, Guo Z, Han Y, Song Y, Zhai J, Du Z, Wang X, Lu J, and Yang R (2008) The iron-responsive Fur regulon in Yersinia pestis. *J Bacteriol*, **190**, 3063-3075.
111. GE Healthcare Bio-Sciences (2005). *Ettan DIGE System User Manual*. GE Healthcare Bio-Sciences AB, a General Electric company.
112. Gershon D (2003) Proteomics technologies: probing the proteome. *Nature*, **424**, 581-587.

References

113. Gerth K, Bedorf N, Höfle G, Irschik H, and Reichenbach H (1996) Epothilons A and B: antifungal and cytotoxic compounds from *Sorangium cellulosum* (Myxobacteria). Production, physico-chemical and biological properties. *J Antibiot*, **49**, 560-563.
114. Gerth K, Irschik H, Reichenbach H, and Trowitsch W (1982) The myxovirescins, a family of antibiotics from *Myxococcus virescens* (Myxobacterales). *J Antibiot*, **35**, 1454-1459.
115. Gerth K, Jansen R, Reifenstahl G, Höfle G, Irschik H, Kunze B, Reichenbach H, and Thierbach G (1983) The myxalamids, new antibiotics from *Myxococcus xanthus* (Myxobacterales). I. Production, physico-chemical and biological properties, and mechanism of action. *J Antibiot*, **36**, 1150-1156.
116. Gerth K, Pradella S, Perlova O, Beyer S, and Müller R (2003) Myxobacteria: proficient producers of novel natural products with various biological activities - past and future biotechnological aspects with the focus on the genus *Sorangium*. *J Biotechnol*, **106**, 233-253.
117. Gerth K, Schummer D, Höfle G, Irschik H, and Reichenbach H (1995) Ratjadon: a new antifungal compound from *Sorangium cellulosum* (myxobacteria) production, physio-chemical and biological properties. *J Antibiot*, **48**, 973-976.
118. Gevaert K, Demol H, Martens L, Hoorelbeke B, Puype M, Goethals M, Van Damme J, DeBoeck S, and Vandekerckhove J (2001) Protein identification based on matrix assisted laser desorption/ionization-post source decay-mass spectrometry. *Electrophoresis*, **22**, 1645-1651.
119. Ghassemian M and Straus NA (1996) Fur regulates the expression of iron-stress genes in the cyanobacterium *Synechococcus* sp. strain PCC 7942. *Microbiology*, **142**, 1469-1476.
120. Goebel M and Yanagida M (1991) The TPR snap helix: a novel protein repeat motif from mitosis to transcription. *Trends Biochem Sci*, **16**, 173-177.
121. Goldman BS, Nierman WC, Kaiser D, Slater SC, Durkin AS, Eisen J, Ronning CM, Barbazuk WB, Blanchard M, Field C, Halling C, Hinkle G, Iartchuk O, Kim HS, Mackenzie C, Madupu R, Miller N, Shvartsbeyn A, Sullivan SA, Vaudin M, Wiegand R, and Kaplan HB (2006) Evolution of sensory complexity recorded in a myxobacterial genome. *P Natl Acad Sci USA*, **103**, 15200-15205.
122. Goldstein S, Meyerstein D, and Czapski G (1993) The Fenton reagents. *Free Radic Biol Med*, **15**, 435-445.
123. Gonzalez de Peredo A, Saint-Pierre C, Adrait A, Jacquemet L, Latour JM, Michaud-Soret I, and Forest E (1999) Identification of the two zinc-bound cysteines in the ferric uptake regulation protein from *Escherichia coli*: chemical modification and mass spectrometry analysis. *38*, **26**, 8589.
124. Görg A (1999) IPG-Dalt of very alkaline proteins. *Methods Mol Biol*, **112**, 209.
125. Görg A, Obermaier C, Boguth G, Harder A, Scheibe B, Wildgruber R, and Weiss W (2000) The current state of two-dimensional electrophoresis with immobilized pH gradients. *Electrophoresis*, **21**, 1037-1053.

126. Görg A, Weiss W, and Dunn MJ (2004) Current two-dimensional electrophoresis technology for proteomics. *Proteomics Proteomics*, **4**, 3665-3685.
127. Grabley S and Thiericke R (1999). *Drug Discovery from Nature*. Springer, Berlin.
128. Grant SG, Jessee J, Bloom FR, and Hanahan D (1990) Differential plasmid rescue from transgenic mouse DNAs into Escherichia coli methylation-restriction mutants. *P Natl Acad Sci USA*, **87**, 4645-4649.
129. Granvogl B, Ploscher M, and Eichacker LA (2007) Sample preparation by in-gel digestion for mass spectrometry-based proteomics. *Analytical and Bioanalytical Chemistry*, **389**, 991-1002.
130. Greenwald J, Hoegy F, Nader M, Journet L, Mislin GL, Graumann PL, and Schalk IJ (2008) Real time fluorescent resonance energy transfer visualization of ferric pyoverdine uptake in *Pseudomonas aeruginosa*. A role for ferrous iron. *J Biol Chem*, **282**, 2987-2995.
131. Grifantini R, Sebastian S, Frigimelica E, Draghi M, Bartolini E, Muzzi A, Rappuoli R, Grandi G, and Genco CA (2003) Identification of iron-activated and -repressed Fur-dependent genes by transcriptome analysis of *Neisseria meningitidis* group B. *Proc Natl Acad Sci U S A*, **100**, 9542-9547.
132. Griffiths E (1990) Iron-regulated membrane proteins and bacterial virulence. *J Biosci*, **15**, 173-177.
133. Grimaud R, Kessel M, Beuron F, Steven A.C., and Maurizi MR (1998) Enzymatic and structural similarities between the *Escherichia coli* ATP-dependent proteases, ClpXP and ClpAP. *J Biol Chem*, **273**, 12476-12481.
134. Gross F, Luniak N, Perlova O, Gaitatzis N, Jenke-Kodama H, Gerth K, Gottschalk D, Dittmann E, and Müller R (2006) Bacterial type III polyketide synthases: Phylogenetic analysis and potential for the production of novel secondary metabolites by heterologous expression in pseudomonads. *Arch Microbiol*, **185**, 28-38.
135. Haferburg G, Groth I, Möllmann U, Kothe E, and Sattler I (2009) Arousing sleeping genes: shifts in secondary metabolism of metal tolerant actinobacteria under conditions of heavy metal stress. *Biometals*, **22**, 225-234.
136. Hall RM and Collis CM (1995) Mobile gene cassettes and integrons: capture and spread of genes by site-specific recombination. *Mol Microbiol*, **15**, 593-600.
137. Hamann N. Identifizierung und Charakterisierung der katalytischen Untereinheit von Heterodisulfid-Reduktase aus methanogenen Archaea. 2007. Marburg, Philipps-Universität.
Ref Type: Thesis/Dissertation
138. Hanks SK, Quinn AM, and Hunter T (1988) The protein kinase family: conserved features and deduced phylogeny of the catalytic domains. *Science*, **241**, 42-52.
139. Hantke K (1987) Selection procedure for deregulated iron transport mutants (fur) in *Escherichia coli* K 12: fur not only affects iron metabolism. *Mol Gen Genet*, **210**, 135-139.

References

140. Hantke K (2001) Iron and metal regulation in bacteria. *Curr Opin Microbiol*, **4**, 172-177.
141. Hantke K (2002) Members of the Fur protein family regulate iron and zinc transport in *E. coli* and characteristics of the Fur-regulated *fhuF* protein. *J Mol Microbiol Biotechnol*, **4**, 217-222.
142. Haraszthy VI, Jordan SF, and Zambon JJ (2006) Identification of Fur-regulated genes in *Actinobacillus actinomycetemcomitans*. *Microbiology*, **152**, 787-796.
143. Haraszthy VI, Lally ET, Haraszthy GG, and Zambon JJ (2002) Molecular cloning of the fur gene from *Actinobacillus actinomycetemcomitans*. *Infect Immun*, **70**, 3170-3179.
144. Hardy KG (1993). *Plasmids - a practical approach*. IRL Press, Oxford.
145. Heim S, Heuer H, Nimtz M, and Timmis KN (2002) Proteome reference map of *Pseudomonas putida* strain KT2440 for genome expression profiling: distinct responses of KT2440 and *P. aeruginosa* strain PAO1 to iron-deprivation and a new form of superoxide dismutase. *Env Microbiol, special issue: Pseudomonas Genomics*.
146. Helmann JD and Chamberlin MJ (1988) Structure and function of bacterial sigma factors. *Annu Rev Biochem*, **57**, 839-872.
147. Hernandez JA, Lopez-Gomollon S, Bes MT, Fillat MF, and Peleato ML (2004) Three *fur* homologues from *Anabaena* sp. PCC7120: exploring reciprocal protein-promoter recognition. *FEMS Microbiol Lett*, **236**, 275-282.
148. Hernandez P, Müller M, and Appel RD (2006) Automated protein identification by tandem mass spectrometry: issues and strategies. *Mass Spectrom Rev*, **25**, 235-254.
149. Hickey EK and Cianciotto NP (1997) An iron- and fur-repressed *Legionella pneumophila* gene that promotes intracellular infection and encodes a protein with similarity to the *Escherichia coli* aerobactin synthetases. *Infect Immun*, **65**, 133-143.
150. Hill PJ, Cockayne A, Landers P, Morrissey JA, Sims CM, and Williams P (1998) SirR, a novel iron-dependent repressor in *Staphylococcus epidermidis*. *Infect Immun*, **66**, 4123-4129.
151. Hoffmann T, Schütz A, Brosius M, Völker A, Völker U, and Bremer E (2002) High-salinity-induced iron limitation in *Bacillus subtilis*. *J Bacteriol*, **184**, 718-727.
152. Hofmann K and Bucher P (1995) The FHA domain: a putative nuclear signalling domain found in protein kinases and transcription factors. *Trends Biochem Sci*, **20**, 347-349.
153. Holmes K, Mulholland F, Pearson BM, Pin C, McNicholl-Kennedy J, Ketley JM, and Wells JM (2005) *Campylobacter jejuni* gene expression in response to iron limitation and the role of Fur. *Microbiology*, **151**, 243-257.
154. Hong SK, Kito M, Beppu T, and Horinouchi S (1991) Phosphorylation of the AfsR product, a global regulatory protein for secondary-metabolite formation in *Streptomyces coelicolor* A3(2). *J Bacteriol*, **173**, 2311-2318.

155. Horiuchi T, Taoka M, Isobe T, Komano T, and Inouye S (2002) Role of fruA and csgA genes in gene expression during development of *Myxococcus xanthus*. Analysis by two-dimensional gel electrophoresis. *J Biol Chem*, **277**, 26753-26760.
156. Hubbard JA, Lewandowska KB, Hughes MN, and Poole RK (1986) Effects of iron-limitation of *Escherichia coli* on growth, the respiratory chains and gallium uptake. *Arch Microbiol*, **146**, 80-86.
157. Hudson AJ, Andrews SC, Hawkins C, Williams JM, Izuohara M, Meldrum FC, Mann S, Harrison PM, and Guest JR (1993) Overproduction, purification and characterization of the *Escherichia coli* ferritin. *Eur J Biochem*, **218**, 985-995.
158. Hunt DF, Yates JR, III, Shabanowitz J, Winston S, and Hauer CR (1986) Protein sequencing by tandem mass spectrometry. *Proc Natl Acad Sci U S A*, **83**, 6233-6237.
159. Ilg K. Mobilization and Mobility of Colloidal Phosphorus in Sandy Soils. 2007. Berlin, Technische Universität.
Ref Type: Thesis/Dissertation
160. Ishihama Y, Rappaport J, and Mann M (2006) Modular stop and go extraction tips with stacked disks for parallel and multidimensional peptide fractionation in proteomics. *J Proteome Res J Proteome Res*, **5**, 988-994.
161. Ishikawa J and Hotta K (1999) FramePlot: a new implementation of the frame analysis for predicting protein-coding regions in bacterial DNA with a high G + C content. *FEMS Microbiol Lett*, **174**, 251-253.
162. Jacquament L, Traoré DA, Ferrer JL, Proux O, Testemale D, Hazemann JL, Nazarenko E, El Ghazouani A, Caux-Thang C, Duarte V, and Latour JM (2009) Structural characterization of the active form of PerR: insights into the metal-induced activation of PerR and Fur proteins for DNA binding. *Mol Microbiol*, **73**, 20-31.
163. Jain R and Inouye S (1998) Inhibition of development of *Myxococcus xanthus* by eukaryotic protein kinase inhibitors. *J Bacteriol*, **180**, 6544-6550.
164. Jelsbak L, Givskov M, and Kaiser D (2005) Enhancer-binding proteins with a forkhead-associated domain and the sigma54 regulon in *Myxococcus xanthus* fruiting body development. *P Natl Acad Sci USA*, **102**, 3010-3015.
165. Jeltsch A (2002) Beyond Watson and Crick: DNA methylation and molecular enzymology of DNA methyltransferases. *ChemBioChem*, **3**, 274-293.
166. Jeltsch A, Jurkowska RZ, Jurkowski TP, Liebert K, Rathert P, and Schlicker M (2007) Application of DNA methyltransferases in targeted DNA methylation. *Appl Microbiol Biotechnol*, **75**, 1233-1240.
167. Jensen RB and Shapiro L (2003) Cell-cycle-regulated expression and subcellular localization of the *Caulobacter crescentus* SMC chromosome structural protein. *J Bacteriol*, **185**, 3068-3075.
168. Jeong JY, Kim YJ, Cho N, Shin D, Nam TW, Ryu S, and Seok YJ (2004) Expression of ptsG encoding the major glucose transporter is regulated by ArcA in *Escherichia coli*. *J Biol Chem*, **279**, 38513-38518.

References

169. Jiang X, Payne MA, Cao Z, Foster SB, Feix JB, Newton SM, and Klebba PE (1997) Ligand-specific opening of a gated-porin channel in the outer membrane of living bacteria. *Science*, **276**, 1261-1264.
170. Johnson AW, Todd JD, Curson AR, Lei S, Nikolaïdou-Katsaridou N, Gelfand MS, and Rodionov DA (2007) Living without Fur: the subtlety and complexity of iron-responsive gene regulation in the symbiotic bacterium Rhizobium and other alpha-proteobacteria. *Biometals*, **20**, 501-511.
171. Jones AM, Boucher PE, Williams CL, Stibitz S, and Cotter PA (2005) Role of BvgA phosphorylation and DNA binding affinity in control of Bvg-mediated phenotypic phase transition in *Bordetella pertussis*. *Mol Microbiol*, **58**, 700-713.
172. Jung YS and Kwon YM (2008) Small RNA ArrF regulates the expression of sodB and feSII genes in *Azotobacter vinelandii*. *Curr Microbiol*, **57**, 593-597.
173. Kaiser D (2003) Coupling cell movement to multicellular development in myxobacteria. *Nat Rev Microbiol*, **1**, 45-54.
174. Kaiser D (1979) Social gliding is correlated with the presence of pili in *Myxococcus xanthus*. *P Natl Acad Sci USA*, **76**, 5952-5956.
175. Kalume DE, Molina H, and Pandey A (2003) Tackling the phosphoproteome: tools and strategies. *Curr Opin Chem Biol*, **7**, 64-69.
176. Karas M, Bachmann D, and Hillenkamp F (1985) Influence of the Wavelength in High-Irradiance Ultraviolet Laser Desorption Mass Spectrometry of Organic Molecules. *Anal Chem*, **57**, 2935-2939.
177. Karlin S, Brocchieri L, Mrazek J, and Kaiser D (2006) Distinguishing features of delta-proteobacterial genomes. *Proc Natl Acad Sci U S A*, **103**, 11352-11357.
178. Kearns DB, Bonner PJ, Smith DR, and Shimkets LJ (2002) An extracellular matrix-associated zinc metalloprotease is required for dilauroyl phosphatidylethanolamine chemotactic excitation in *Myxococcus xanthus*. *J Bacteriol*, **184**, 1678-1684.
179. Kearns DB, Venot A, Bonner PJ, Stevens B, Boons GJ, and Shimkets LJ (2001) Identification of a developmental chemoattractant in *Myxococcus xanthus* through metabolic engineering. *P Natl Acad Sci USA*, **98**, 13990-13994.
180. Kellner R, Lottspeich F, and Meyer HE (1999) Microcharacterization of Proteins. *Wiley-VCH Verlag, Weinheim, second edition*.
181. Kerbarh O, Bulloch EM, Payne RJ, Sahr T, Rebeille F, and Abell C (2005) Mechanistic and inhibition studies of chorismate-utilizing enzymes. *Biochem Soc Trans*, **33**, 763-766.
182. Khosla C, Gokhale RS, Jacobsen JR, and Cane DE (1999) Tolerance and specificity of polyketide synthases. *Annu Rev Biochem*, **68**, 219-253.
183. Kim J, Choi JN, Kim P, Sok DE, Nam SW, and Lee CH (2009) LC-MS/MS Profiling-Based Secondary Metabolite Screening of *Myxococcus xanthus*. *J Microbiol Biotechnol*, **19**, 51-54.

184. Kirby AE, Metzger DJ, Murphy ER, and Connell TD (2001) Heme utilization in *Bordetella avium* is regulated by RhulI, a heme-responsive extracytoplasmic function sigma factor. *Infect Immun*, **69**, 6951-6961.
185. Kjellstrom S and Jensen ON (2004) Phosphoric acid as a matrix additive for MALDI MS analysis of phosphopeptides and phosphoproteins. *Anal Chem*, **76**, 5109-5117.
186. Klausner RD and Rouault TA (1993) A double life: cytosolic aconitase as a regulatory RNA binding protein. *Mol Biol Cell*, **4**, 1-5.
187. Klein J, Leupold S, Münch R, Pommerenke C, Johl T, Kärst U, Jänsch D, and Retter I (2008) ProdoNet: identification and visualization of prokaryotic gene regulatory and metabolic networks. *Nucleic Acids Res*, **36**, W460-W464.
188. Koebnik R (2005) TonB-dependent trans-envelope signalling: the exception or the rule? *Trends Microbiol*, **13**, 343-347.
189. Koenig JE, Boucher Y, Charlebois RL, Nesbo C, Zhaxybayeva O, Baptiste E, Spencer M, Joss MJ, Stokes HW, and Doolittle WF (2008) Integron-associated gene cassettes in Halifax Harbour: assessment of a mobile gene pool in marine sediments. *Environ Microbiol*, **10**, 1024-1038.
190. Kosman DJ (2003) Molecular mechanisms of iron uptake in fungi. *Mol Microbiol*, **47**, 1185-1197.
191. Krewulak KD and Vogel HJ (2008) Structural biology of bacterial iron uptake. *Biochim Biophys Acta*, **1778**, 1781-1804.
192. Kroos L (2007) The *Bacillus* and *Myxococcus* developmental networks and their transcriptional regulators. *Annu Rev Genet*, **41**, 13-39.
193. Kroos L, Kuspa A, and Kaiser D (1986) A global analysis of developmentally regulated genes in *Myxococcus xanthus*. *Dev Biol*, **117**, 252-266.
194. Krug D, Zurek G, Revermann O, Vos M, Velicer GJ, and Müller R (2008a) Discovering the hidden secondary metabolome of *Myxococcus xanthus*: a study of intraspecific diversity. *Appl Environ Microbiol*, **74**, 3058-3068.
195. Krug D, Zurek G, Schneider B, Garcia R, and Müller R (2008b) Efficient mining of myxobacterial metabolite profiles enabled by liquid chromatography-electrospray ionization-time-of-flight mass spectrometry and compound-based principal component analysis. *Anal Chim Acta*, **624**, 97-106.
196. Kumar CM, Khare G, Srikanth CV, Tyagi AK, Sardesai AA, and Mande SC (2009) Facilitated oligomerization of mycobacterial GroEL: evidence for phosphorylation-mediated oligomerization. *J Bacteriol*, **191**, 6525-6538.
197. Kuner JM and Kaiser D (1982) Fruiting Body Morphogenesis in Submerged Cultures of *Myxococcus-Xanthus*. *J Bacteriol*, **151**, 458-461.
198. Kunkle CA and Schmitt MP (2005) Analysis of a DtxR-regulated iron transport and siderophore biosynthesis gene cluster in *Corynebacterium diphtheriae*. *J Bacteriol*, **187**, 422-433.

References

199. Kunze B, Bedorf N, Kohl W, Höfle G, and Reichenbach H (1989) Myxochelin A, a new iron-chelating compound from *Angiococcus disciformis* (Myxobacterales). Production, isolation, physico-chemical and biological properties. *J Antibiot*, **42**, 14-17.
200. Kwon YD, Lee SY, and Kim P (2008) A Physiology Study of Escherichia coli Overexpressing Phosphoenolpyruvate Carboxykinase. *Biosci Biotechnol Biochem*, **72**, 1138-1141.
201. Lamont IL, Beare PA, Ochsner U, Vasil AI, and Vasil ML (2002) Siderophore-mediated signaling regulates virulence factor production in *Pseudomonas aeruginosa*. *P Natl Acad Sci USA*, **99**, 7072-7077.
202. Langhorst MF, Reuter A, and Stuermer CA (2005) Scaffolding microdomains and beyond: the function of reggie/flotillin proteins. *Cell Mol Life Sci*, **62**, 2228-2240.
203. Lau J, Frykman S, Regentin R, Ou S, Tsuruta H, and Licari P (2002) Optimizing the heterologous production of epothilone D in *Myxococcus xanthus*. *Biotechnol Bioeng*, **78**, 280-288.
204. Laue BE and Gill RE (1995) Using a phase-locked mutant of *Myxococcus xanthus* to study the role of phase variation in development. *J Bacteriol*, **177**, 4089-4096.
205. Lee HJ, Park KJ, Lee AY, Park SG, Park BC, Lee KH, and Park SJ (2003) Regulation of *fur* Expression by RpoS and Fur in *Vibrio vulnificus*. *J Bacteriol*, **185**, 5891-5896.
206. Lee HW, Choe YH, Kim DK, Jung SY, and Lee NG (2004) Proteomic analysis of a ferric uptake regulator mutant of *Helicobacter pylori*: Regulation of *Helicobacter pylori* gene expression by ferric uptake regulator and iron. *Proteomics Proteomics*, **4**, 2014-2027.
207. Lee JW and Helmann JD (2007) Functional specialization within the Fur family of metalloregulators. *Biometals*, **20**, 485-499.
208. Letoffe S, Ghigo JM, and Wandersman C (1994) Iron acquisition from heme and hemoglobin by a *Serratia marcescens* extracellular protein. *Proc Natl Acad Sci U S A*, **91**, 9876-9880.
209. Li Y, Florova G, and Reynolds KA (2005) Alteration of the fatty acid profile of *Streptomyces coelicolor* by replacement of the initiation enzyme 3-ketoacyl acyl carrier protein synthase III (FabH). *J Bacteriol*, **187**, 3795-3799.
210. Li Y, Weissman KJ, and Müller R (2008) Myxochelin biosynthesis: direct evidence for two- and four-electron reduction of a carrier protein-bound thioester. *J Am Chem Soc*, **130**, 7554-7555.
211. Litwin CM and Calderwood SB (1993) Cloning and genetic analysis of the *Vibrio vulnificus* fur gene and construction of a fur mutant by in vivo marker exchange. *J Bacteriol*, **175**, 706-715.
212. Lodge JM, Williams P, and Brown MR (1986) Influence of growth rate and iron limitation on the expression of outer membrane proteins and enterobactin by *Klebsiella pneumoniae* grown in continuous culture. *J Bacteriol*, **165**, 353-356.

213. Lottspeich F and Engels JW (2006). *Bioanalytik*. Spektrum, Elsevier, München.
214. Lu A, Waanders LF, Almeida R, Li GQ, Allen M, Cox R, Olsen JV, Bonaldi T, and Mann M (2007) Nanoelectrospray peptide mapping revisited: Composite survey spectra allow high dynamic range protein characterization without LCMS on an orbitrap mass spectrometer. *International Journal of Mass Spectrometry*, **268**, 158-167.
215. Lucarelli D, Russo S, Garman E, Milano A, Meyer-Klaucke W, and Pohl E (2007) Crystal structure and function of the zinc uptake regulator FurB from *Mycobacterium tuberculosis*. *J Biol Chem*, **282**, 9914-9922.
216. Lucarelli D, Vasil ML, Meyer-Klaucke W, and Pohl E (2008) The Metal-Dependent Regulators FurA and FurB from *Mycobacterium Tuberculosis*. *Int J Mol Sci*, **9**, 1548-1560.
217. Macek B, Waanders LF, Olsen JV, and Mann M (2006) Top-down protein sequencing and MS3 on a hybrid linear quadrupole ion trap-orbitrap mass spectrometer. *Molecular & Cellular Proteomics*, **5**, 949-958.
218. Maciag A, Dainese E, Rodriguez GM, Milano A, Provvedi R, Pasca MR, Smith I, Palu G, Riccardi G, and Manganelli R (2007) Global analysis of the *Mycobacterium tuberculosis* Zur (FurB) regulon. *J Bacteriol*, **189**, 730-740.
219. Mahadevan R, Bond DR, Butler JE, Esteve-Nunez A, Coppi MV, Palsson BO, Schilling CH, and Lovley DR (2006) Characterization of metabolism in the Fe(III)-reducing organism *Geobacter sulfurreducens* by constraint-based modeling. *Appl Environ Microbiol*, **72**, 1558-1568.
220. Mahé B, Masclaux C, Rauscher L, Enard C, and Expert D (1995) Differential expression of two siderophore-dependent iron-acquisition pathways in *Erwinia chrysanthemi* 3937: characterization of a novel ferrisiderophore permease of the ABC transporter family. *Mol Microbiol*, **18**, 33-43.
221. Makarov A, Denisov E, Kholomeev A, Balschun W, Lange O, Strupat K, and Horning S (2006) Performance evaluation of a hybrid linear ion trap/orbitrap mass spectrometer. *Anal Chem*, **78**, 2113-2120.
222. Manning G, Plowman GD, Hunter T, and Sudarsanam S (2002) Evolution of protein kinase signaling from yeast to man. *Trends Biochem Sci*, **27**, 514-520.
223. Marouga R, David S, and Hawkins E (2005) The development of the DIGE system: 2D fluorescence difference gel analysis technology. *Anal Bioanal Chem*, **382**, 669-678.
224. Marshall B, Stintzi A, Gilmour C, Meyer JM, and Poole K (2009) Citrate-mediated iron uptake in *Pseudomonas aeruginosa*: involvement of the citrate-inducible FecA receptor and the FeoB ferrous iron transporter. *Microbiology*, **155**, 305-315.
225. Martinez M, Ugalde RA, and Almiron M (2005) Dimeric *Brucella abortus* Irr protein controls its own expression and binds haem. *Microbiology*, **151**, 3427-3433.

References

226. Massé E and Arguin M (2005) Ironing out the problem: new mechanisms of iron homeostasis. *Trends Biochem Sci*, **30**, 462-468.
227. Massé E and Gottesman S (2002) A small RNA regulates the expression of genes involved in iron metabolism in *Escherichia coli*. *Proc Natl Acad Sci U S A*, **99**, 4620-4625.
228. Massé E, Salvail H, Desnoyers G, and Arguin M (2007) Small RNAs controlling iron metabolism. *Curr Opin Microbiol*, **10**, 140-145.
229. Mauriello EM and Zusman DR (2007) Polarity of motility systems in *Myxococcus xanthus*. *Curr Opin Microbiol*, **10**, 624-629.
230. McAdams HH and Shapiro L (2003) A bacterial cell-cycle regulatory network operating in time and space. *Science*, **301**, 1874-1877.
231. McHugh JP, Rodríguez-Quinones F, Abdul-Tehrani H, Svistunenko DA, Poole RK, Cooper CE, and Andrews SC (2003) Global iron-dependent gene regulation in *Escherichia coli*. A new mechanism for iron homeostasis. *J Biol Chem*, **278**, 29478-29486.
232. McLachlin DT and Chait BT (2001) Analysis of phosphorylated proteins and peptides by mass spectrometry. *Curr Opin Chem Biol*, **5**, 591-602.
233. Meiser P, Bode HB, and Müller R (2006b) DKxanthenes: Novel secondary metabolites from the myxobacterium *Myxococcus xanthus* essential for sporulation. *P Natl Acad Sci USA*, **103**, 19128-19133.
234. Meiser P, Bode HB, and Müller R (2006a) The unique DKxanthene secondary metabolite family from the myxobacterium *Myxococcus xanthus* is required for developmental sporulation. *Proc Natl Acad Sci U S A*, **103**, 19128-19133.
235. Meiser P, Weissman KJ, Bode HB, Krug D, Dickschat JS, Sandmann A, and Müller R (2008) DKxanthene biosynthesis -- understanding the basis for diversity-oriented synthesis in myxobacterial secondary metabolism. *Chem Biol*, **15**, 771-781.
236. Mense SM and Zhang L (2006) Heme: a versatile signaling molecule controlling the activities of diverse regulators ranging from transcription factors to MAP kinases. *Cell Res*, **16**, 681-692.
237. Miethke M and Marahiel MA (2007) Siderophore-based iron acquisition and pathogen control. *Microbiol Mol Biol Rev*, **71**, 413-+.
238. Miethke M, Westers H, Blom EJ, Kuipers OP, and Marahiel MA (2006) Iron Starvation Triggers the Stringent Response and Induces Amino Acid Biosynthesis for Bacillibactin Production in *Bacillus subtilis*. *J Bacteriol*, **188**, 8655-8657.
239. Mignot T and Kirby JR (2008) Genetic circuitry controlling motility behaviors of *Myxococcus xanthus*. *Bioessays Bioessays*, **30**, 733-743.
240. Mignot T, Merlie JP, Jr., and Zusman DR (2005) Regulated pole-to-pole oscillations of a bacterial gliding motility protein. *Science*, **310**, 855-857.

241. Mills SA and Marletta MA (2005) Metal binding characteristics and role of iron oxidation in the ferric uptake regulator from Escherichia coli. *Biochemistry-US*, **44**, 13553-13559.
242. Minden J (2007) Comparative Proteomics and Difference Gel Electrophoresis. *Biotechniques*, **43**, 739-743.
243. Miyanaga S, Obata T, Onaka H, Fujita T, Saito N, Sakurai H, Saiki I, Furumai T, and Igarashi Y (2006) Absolute configuration and antitumor activity of myxochelin A produced by *Nomonuraea pusilla* TP-A0861. *J Antibiot*, **59**, 698-703.
244. Moeck GS and Coulton JW (1998) TonB-dependent iron acquisition: mechanisms of siderophore-mediated active transport. *Mol Microbiol*, **28**, 675-681.
245. Möllmann U, Heinisch L, Bauernfeind A, Köhler T, and Ankel-Fuchs D (2009) Siderophores as drug delivery agents: application of the "Trojan Horse" strategy. *Biometals*, **22**, 615-624.
246. Moore BS, Hertweck C, Hopke JN, Izumikawa M, Kalaitzis JA, Nilsen G, O'Hare T, Piel J, Shipley PR, Xiang L, Austin MB, and Noel JP (2002) Plant-like biosynthetic pathways in bacteria: from benzoic acid to chalcone. *J Nat Prod*, **65**, 1956-1962.
247. Moore CM and Helmann JD (2005) Metal ion homeostasis in *Bacillus subtilis*. *Curr Opin Microbiol*, **8**, 188-195.
248. Moraleda-Munoz A, Perez J, Fontes M, Murillo FJ, and Munoz-Dorado J (2005) Copper induction of carotenoid synthesis in the bacterium *Myxococcus xanthus*. *Mol Microbiol*, **56**, 1159-1168.
249. Mulzer J (2009). *The Epothilones - An Outstanding Family of Anti-Tumour Agents: From Soil to the Clinic*. Springer, New York.
250. Münch R, Hiller K, Grote A, Scheer M, Klein J, and Jahn D (2005) Virtual Footprint and PRODORIC: an integrative framework for regulon prediction in prokaryotes. *Bioinformatics*, **21**, 4187-4189.
251. Murphy KC, Ritchie JM, Waldor MK, Lobner-Olesen A, and Marinus MG (2008) Dam methyltransferase is required for stable lysogeny of the Shiga toxin (Stx2)-encoding bacteriophage 933W of enterohemorrhagic *Escherichia coli* O157:H7. *J Bacteriol*, **190**, 438-441.
252. Najimi M, Lemos ML, and Osorio CR (2008) Identification of siderophore biosynthesis genes essential for growth of *Aeromonas salmonicida* under iron limitation conditions. *Appl Environ Microbiol*, **74**, 2341-2348.
253. Neilands JB (1995) Siderophores: structure and function of microbial iron transport compounds. *J Biol Chem*, **270**, 26723-26726.
254. Nielsen P, Fischer R, Engelhardt R, Tondüry P, Gabbe EE, and Janka GE (1995) Liver iron stores in patients with secondary haemosiderosis under iron chelation therapy with deferoxamine or deferiprone. *Br J Haematol*, **91**, 827-833.

References

255. Nies DH (2003) Efflux-mediated heavy metal resistance in prokaryotes. *FEMS Microbiol Rev*, **27**, 313-339.
256. Nilsson MT, Mossing MC, and Widersten M (2000) Functional expression and affinity selection of single-chain cro by phage display: isolation of novel DNA-binding proteins. *Protein Eng*, **13**, 519-526.
257. Noya F, Arias A, and Fabiano E (1997) Heme compounds as iron sources for nonpathogenic Rhizobium bacteria. *J Bacteriol*, **179**, 3076-3078.
258. O'Farrell PH (1975) High resolution two-dimensional electrophoresis of proteins. *J Biol Chem*, **250**, 4007-4021.
259. Ochsner UA, Wilderman PJ, Vasil AI, and Vasil ML (2002) GeneChip((R)) expression analysis of the iron starvation response in *Pseudomonas aeruginosa*: identification of novel pyoverdine biosynthesis genes. *Mol Microbiol*, **45**, 1277-1287.
260. Olczak T, Sroka A, Potempa J, and Olczak M (2008) *Porphyromonas gingivalis* HmuY and HmuR: further characterization of a novel mechanism of heme utilization. *Arch Microbiol*, **189**, 197-210.
261. Ollinger J, Song KB, Antelmann H, Hecker M, and Helmann JD (2006) Role of the Fur regulon in iron transport in *Bacillus subtilis*. *J Bacteriol*, **188**, 3664-3673.
262. Olsen JV, de Godoy LMF, Li GQ, Macek B, Mortensen P, Pesch R, Makarov A, Lange O, Horning S, and Mann M (2005) Parts per million mass accuracy on an orbitrap mass spectrometer via lock mass injection into a C-trap. *Molecular & Cellular Proteomics*, **4**, 2010-2021.
263. Olsen JV, Macek B, Lange O, Makarov A, Horning S, and Mann M (2007) Higher-energy C-trap dissociation for peptide modification analysis. *Nature Methods*, **4**, 709-712.
264. Otani M, Inouye M, and Inouye S (1995) Germination of myxospores from the fruiting bodies of *Myxococcus xanthus*. *J Bacteriol*, **177**, 4261-4265.
265. Panek H and O'Brian MR (2002) A whole genome view of prokaryotic haem biosynthesis. *Microbiology*, **148**, 2273-2282.
266. Pappin DJC, Hojrup P, and Bleasby AJ (1993) Rapid identification of proteins by peptide-mass fingerprinting. *Curr Biol*, **3**, 327-332.
267. Patton WF (2002) Detection technologies in proteome analysis. *J Chromatogr B Analyt Technol Biomed Life Sci*, **771**, 3-31.
268. Pecquer L, D'Autréaux B, Dupuy J, Nicolet Y, Jacquemet L, Brutscher B, Michaud-Soret I, and Bersch B (2006) Structural changes of *Escherichia coli* ferric uptake regulator during metal-dependent dimerization and activation explored by NMR and X-ray crystallography. *J Biol Chem*, **281**, 21286-21295.
269. Pelling AE, Li Y, Shi W, and Gimzewski JK (2005) Nanoscale visualization and characterization of *Myxococcus xanthus* cells with atomic force microscopy. *P Natl Acad Sci USA*, **102**, 6484-6489.

270. Pereira-Medrano AG, Sterling A, Snijders AP, Reardon KF, and Wright PC (2007) A systematic evaluation of chip-based nanoelectrospray parameters for rapid identification of proteins from a complex mixture. *J Am Soc Mass Spectrom*, **18**, 1714-1725.
271. Perez J, Castaneda-Garcia A, Jenke-Kodama H, Müller R, and Munoz-Dorado J (2008) Eukaryotic-like protein kinases in the prokaryotes and the myxobacterial kinase. *Proceedings of National Academy of Sciences USA*, **105**, 15950-15955.
272. Peters EC, Brock A, and Ficarro SB (2004) Exploring the phosphoproteome with mass spectrometry. *Mini-Reviews in Medicinal Chemistry*, **4**, 313-324.
273. Phatnani HP and Greenleaf AL (2006) Phosphorylation and functions of the RNA polymerase II CTD. *Genes & Development*, **20**, 2922-2936.
274. Plaga W and Ulrich SH (1999) Intercellular signalling in *Stigmatella aurantiaca*. *Curr Opin Microbiol*, **2**, 593-597.
275. Pohl E, Haller JC, Mijovilovich A, Meyer-Klaucke W, Garman E, and Vasil ML (2003) Architecture of a protein central to iron homeostasis: crystal structure and spectroscopic analysis of the ferric uptake regulator. *Mol Microbiol*, **47**, 903-915.
276. Pressler U, Staudenmaier H, Zimmermann L, and Braun V (1988) Genetics of the iron dicitrate transport system of *Escherichia coli*. *J Bacteriol*, **170**, 2716-2724.
277. Prince RW, Storey DG, Vasil AI, and Vasil ML (1991) Regulation of *toxA* and *regA* by the *Escherichia coli* *fur* gene and identification of a Fur homologue in *Pseudomonas aeruginosa* PA103 and PA01. *Mol Microbiol*, **5**, 2823-2831.
278. Pym AS, Domenech P, Honoré N, Song J, Deretic V, and Cole ST (2001) Regulation of catalase-peroxidase (KatG) expression, isoniazid sensitivity and virulence by *furA* of *Mycobacterium tuberculosis*. *Mol Microbiol*, **40**, 879-889.
279. Quatrini R, Lefimil C, Veloso FA, Pedroso I, Holmes DS, and Jedlicki E (2007) Bioinformatic prediction and experimental verification of Fur-regulated genes in the extreme acidophile *Acidithiobacillus ferrooxidans*. *Nucleic Acids Res*, **35**, 2153-2166.
280. Rabilloud T (2000) Detecting proteins separated by 2-D gel electrophoresis. *Anal Chem*, **72**, 48A-55A.
281. Rabsch W, Höfle G, Reichenbach H, and Reissbrodt R (1991) Iron Supply of *E. coli* - and *Salmonella* strains by siderophores from Myxobacteria. *Bioforum*, **14**, 42.
282. Rappaport J, Ishihama Y, and Mann M (2003) Stop and go extraction tips for matrix-assisted laser desorption/ionization, nanoelectrospray, and LC/MS sample pretreatment in proteomics. *Anal Chem*, **75**, 663-670.
283. Rappaport J, Mann M, and Ishihama Y (2007) Protocol for micro-purification, enrichment, pre-fractionation and storage of peptides for proteomics using StageTips. *Nature Protocols*, **2**, 1896-1906.
284. Raymond KN, Dertz EA, and Kim SS (2003) Enterobactin: an archetype for microbial iron transport. *P Natl Acad Sci USA*, **100**, 3584-3588.

References

285. Rehm H (1997). *Der Experimentator: Proteinbiochemie*. Gustav Fischer, Stuttgart. Jena. Lübeck. Ulm.
286. Reichenbach H (1988) Gliding Bacteria in Biotechnology. *Biotechnology*, **6b**, 674-696.
287. Reichenbach H (2001) Myxobacteria, producers of novel bioactive substances. *J Ind Microbiol Biotechnol*, **27**, 149-156.
288. Reinders J and Sickmann A (2005) State-of-the-art in phosphoproteomics. *Proteomics Proteomics*, **5**, 4052-4061.
289. Ridley CP, Lee HY, and Khosla C (2008) Evolution of polyketide synthases in bacteria. *Proc Natl Acad Sci U S A*, **105**, 4595-4600.
290. Rix U, Fischer C, Remsing LL, and Rohr J (2002) Modification of post-PKS tailoring steps through combinatorial biosynthesis. *Nat Prod Rep*, **19**, 542-580.
291. Robertson GT, Ng WL, Foley J, Gilmour R, and Winkler ME (2002) Global transcriptional analysis of clpP mutations of type 2 *Streptococcus pneumoniae* and their effects on physiology and virulence. *J Bacteriol*, **184**, 3508-3520.
292. Rosenberg E, Fytlovitch S, Carmeli S, and Kashman Y (1982) Chemical properties of *Myxococcus xanthus* antibiotic TA. *J Antibiot*, **35**, 788-793.
293. Rowland BM, Grossman TH, Osburne MS, and Taber HW (1996a) Sequence and genetic organization of a *Bacillus subtilis* operon encoding 2,3-dihydroxybenzoate biosynthetic enzymes. *Gene*, **178**, 119-123.
294. Rowland BM and Taber HW (1996b) Duplicate isochorismate synthase genes of *Bacillus subtilis*: regulation and involvement in the biosyntheses of menaquinone and 2,3-dihydroxybenzoate. *J Bacteriol*, **178**, 854-861.
295. Rudolph G, Hennecke H, and Fischer HM (2006) Beyond the Fur paradigm: iron-controlled gene expression in rhizobia. *FEMS Microbiol Rev*, **30**, 631-648.
296. Sanchez JC, Rouge V, Pisteur M, Ravier F, Tonella L, Moosmayer M, Wilkins MR, and Hochstrasser DF (1997) Improved and simplified in-gel sample application using reswelling of dry immobilized pH gradients. *Electrophoresis*, **18**, 324-327.
297. Sangwan I, Small SK, and O'Brian MR (2008) The *Bradyrhizobium japonicum* Irr protein is a transcriptional repressor with high-affinity DNA-binding activity. *J Bacteriol*, **190**, 5172-5177.
298. Saskova L, Novakova L, Basler M, and Branny P (2007) Eukaryotic-type serine/threonine protein kinase StkP is a global regulator of gene expression in *Streptococcus pneumoniae*. *J Bacteriol*, **189**, 4168-4179.
299. Sayyed RZ and Chincholkar SB (2006) Purification of siderophores of *Alcaligenes faecalis* on amberlite XAD. *Bioresour Technol*, **97**, 1026-1029.
300. Scheler C, Lamer S, Pan Z, Li XP, Salnikow J, and Jungblut P (1998) Peptide mass fingerprint sequence coverage from differently stained proteins on two-dimensional

electrophoresis patterns by matrix assisted laser desorption/ionization-mass spectrometry (MALDI-MS). *Electrophoresis*, **19**, 918-927.

301. Schley C, Altmeyer MO, Swart R, Müller R, and Huber CG (2006) Proteome analysis of *Myxococcus xanthus* by off-line two-dimensional chromatographic separation using monolithic poly-(styrene-divinylbenzene) columns combined with ion-trap tandem mass spectrometry. *J Proteome Res J Proteome Res*, **5**, 2760-2768.
302. Schneider S, Sharp KH, Barker PD, and Paoli M (2006) An induced fit conformational change underlies the binding mechanism of the heme transport proteobacteria-protein HemS. *J Biol Chem*, **281**, 32606-32610.
303. Schneider TD and Stephens RM (1990) Sequence logos: a new way to display consensus sequences. *Nucleic Acids Res*, **18**, 6097-6100.
304. Schneiker S, Perlova O, Kaiser O, Gerth K, Alici A, Altmeyer MO, Bartels D, Bekel T, Beyer S, Bode E, Bode HB, Bolten CJ, Choudhuri JV, Doss S, Elnakady YA, Frank B, Gaigalat L, Goesmann A, Groeger C, Gross F, Jelsbak L, Jelsbak L, Kalinowski J, Kegler C, Knauber T, Konietzny S, Kopp M, Krause L, Krug D, Linke B, Mahmud T, Martinez-Arias R, McHardy AC, Merai M, Meyer F, Mormann S, Munoz-Dorado J, Perez J, Pradella S, Rachid S, Raddatz G, Rosenau F, Ruckert C, Sasse F, Scharfe M, Schuster SC, Suen G, Treuner-Lange A, Velicer GJ, Vorholter FJ, Weissman KJ, Welch RD, Wenzel SC, Whitworth DE, Wilhelm S, Wittmann C, Blöcker H, Pühler A, and Müller R (2007) Complete genome sequence of the myxobacterium *Sorangium cellulosum*. *Nat Biotechnol*, **25**, 1281-1289.
305. Schwarzer D, Finking R, and Marahiel MA (2003) Nonribosomal peptides: From genes to products. *Nat Prod Rep*, **20**, 275-287.
306. Screen J, Moya E, Blagbrough IS, and Smith AW (1995) Iron uptake in *Pseudomonas aeruginosa* mediated by N-(2,3-dihydroxybenzoyl)-L-serine and 2,3-dihydroxybenzoic acid. *FEMS Microbiol Lett*, **127**, 145-149.
307. Segall AM and Craig NL (2005) New wrinkles and folds in site-specific recombination. *Mol Cell*, **19**, 433-435.
308. Sergiev PV, Bogdanov AA, and Dontsova OA (2007) Ribosomal RNA guanine-(N2)-methyltransferases and their targets. *Nucleic Acids Res*, **35**, 2295-2301.
309. Seshasayee AS (2007) An assessment of the role of DNA adenine methyltransferase on gene expression regulation in *E coli*. *PLoS ONE*, **2**, e273-e276.
310. Shapiro JA (1998) Thinking about bacterial populations as multicellular organisms. *Annu Rev Microbiol*, **52**, 81-104.
311. Sheikh MA and Taylor GL (2009) Crystal structure of the *Vibrio cholerae* ferric uptake regulator (Fur) reveals insights into metal co-ordination. *Mol Microbiol*, **72**, 1208-1220.
312. Shenar N, Sommerer N, Martinez J, and Enjalbal C (2009) Comparison of LID versus CID activation modes in tandem mass spectrometry of peptides. *J Mass Spectrom*, **44**, 621-632.

References

313. Shepherd M, Dailey TA, and Dailey HA (2006) A new class of [2Fe-2S]-cluster-containing protoporphyrin (IX) ferrochelatases. *Biochem J*, **397**, 47-52.
314. Shevchenko A, Tomas H, Havlis J, Olsen JV, and Mann M (2006) In-gel digestion for mass spectrometric characterization of proteins and proteomes. *Nature Protocols*, **1**, 2856-2860.
315. Shevchenko A, Wilms M, Vorm O, and Mann M (1996) Mass spectrometric sequencing of proteins silver-stained polyacrylamide gels. *Anal Chem*, **68**, 850-858.
316. Shimkets L, Dworkin M, and Reichenbach H (2006). The Myxobacteria. In Dworkin,M. (Ed.), *The Prokaryotes*, . Springer, Berlin, pp. 31-115.
317. Shin JH, Oh SY, Kim SJ, and Roe JH (2007) The zinc-responsive regulator Zur controls a zinc uptake system and some ribosomal proteins in Streptomyces coelicolor A3(2). *J Bacteriol*, **189**, 4070-4077.
318. Sieber SA and Marahiel MA (2005) Molecular mechanisms underlying nonribosomal peptide synthesis: approaches to new antibiotics. *Chem Rev*, **105**, 715-738.
319. Silakowski B, Kunze B, and Müller R (2001a) Multiple hybrid polyketide synthase/non-ribosomal peptide synthetase gene clusters in the myxobacterium *Stigmatella aurantiaca*. *Gene*, **275**, 233-240.
320. Silakowski B, Kunze B, Nordsiek G, Blöcker H, Höfle G, and Müller R (2000) The myxochelin iron transport regulon of the myxobacterium *Stigmatella aurantiaca* Sg a15. *Eur J Biochem*, **267**, 6476-6485.
321. Silakowski B, Nordsiek G, Kunze B, Blöcker H, and Müller R (2001b) Novel features in a combined polyketide synthase/non-ribosomal peptide synthetase: The myxalamid biosynthetic gene cluster of the myxobacterium *Stigmatella aurantiaca* Sga15. *Chem Biol*, **8**, 59-69.
322. Silver S and Walderhaug M (1992) Gene regulation of plasmid- and chromosome-determined inorganic ion transport in bacteria. *Microbiol Rev*, **56**, 195-228.
323. Simunovic V. Biosynthesis and regulation of production of the antibiotic myxovirescin A in *Myxococcus xanthus* DK1622. 2007. Naturwissenschaftlich-Technische Fakultät III der Universität des Saarlandes.
Ref Type: Thesis/Dissertation
324. Simunovic V and Müller R (2007b) 3-Hydroxy-3-methylglutaryl-CoA-like synthases direct the formation of methyl and ethyl side groups in the biosynthesis of the antibiotic myxovirescin A. *ChemBioChem*, **8**, 497-500.
325. Simunovic V and Müller R (2007a) Mutational analysis of the myxovirescin biosynthetic gene cluster reveals novel insights into the functional elaboration of polyketide backbones. *ChemBioChem*, **8**, 1273-1280.
326. Simunovic V, Zapp J, Rachid S, Krug D, Meiser P, and Müller R (2006) Myxovirescin biosynthesis is directed by hybrid polyketide synthases/ nonribosomal peptide synthetase, 3-hydroxy-3-methylglutaryl CoA synthases and trans-acting acyltransferases. *ChemBioChem*, **7**, 1206-1220.

327. Sinha P, Poland J, Schnölzer M, and Rabilloud T (2001) A new silver staining apparatus and procedure for matrix-assisted laser desorption/ionization-time of flight analysis of proteins after two-dimensional electrophoresis. *Proteomics Proteomics*, **1**, 835-840.
328. Skordalakes E and Berger J (2003) Structure of the Rho Transcription TerminatorMechanism of mRNA Recognition and Helicase Loading. *Cell*, **114**, 135-146.
329. Smith KF, Bibb LA, Schmitt MP, and Oram DM (2009) Regulation and activity of a zinc uptake regulator, Zur, in *Corynebacterium diphtheriae*. *J Bacteriol*, **191**, 1595-1603.
330. Smith MJ, Sheehan PE, Perry LL, O'Connor K, Csonka LN, Applegate BM, and Whitman LJ (2006) Quantifying the magnetic advantage in magnetotaxis. *Biophys J*, **91**, 1098-1107.
331. Sonoda H, Suzuki K, and Yoshida K (2002) Gene cluster for ferric iron uptake in *Agrobacterium tumefaciens* MAFF301001. *Genes Genet Syst*, **77**, 137-146.
332. Spormann AM (1999) Gliding motility in bacteria: insights from studies of *Myxococcus xanthus*. *Microbiol Mol Biol Rev*, **63**, 621-641.
333. Stintzi A, Barnes C, Xu J, and Raymond KN (2000) Microbial iron transport via a siderophore shuttle: a membrane ion transport paradigm. *P Natl Acad Sci USA*, **97**, 10691-10696.
334. Stojiljkovic I and Hantke K (1994) Transport of haemin across the cytoplasmic membrane through a haemin-specific periplasmic binding-protein-dependent transport system in *Yersinia enterocolitica*. *Mol Microbiol*, **13**, 719-732.
335. Stookey LL (1970) Ferrozine - A New Spectrophotometric Reagent for Iron. *Anal Chem*, **42**, 779-781.
336. Tabb DL, Friedman DB, and Ham AJL (2006) Verification of automated peptide identifications from proteomic tandem mass spectra. *Nature Protocols*, **1**, 2213-2222.
337. Takami H, Takaki Y, Chee GJ, Nishi S, Shimamura S, Suzuki H, Matsui S, and Uchiyama I (2004) Thermoadaptation trait revealed by the genome sequence of thermophilic *Geobacillus kaustophilus*. *Nucleic Acids Res*, **32**, 6292-6303.
338. Takayama S, Yamanaka S, Miyashiro S, Yokokawa Y, and Shibai H (1988) Novel macrocyclic antibiotics: megavalicins A, B, C, D, G and H. II. Isolation and chemical structures of megavalicins. *J Antibiot*, **41**, 439-445.
339. Thomas CE and Sparling PF (1996) Isolation and analysis of a fur mutant of *Neisseria gonorrhoeae*. *J Bacteriol*, **178**, 4224-4232.
340. Thompson DK, Beliaev AS, Giometti CS, Tollaksen SK, Khare T, Lies DP, Nealson KH, Lim H, Yates JR, III, Brandt CC, Tiedje JM, and Zhou J (2002) Transcriptional and proteomic analysis of a ferric uptake regulator (fur) mutant of *Shewanella oneidensis*: possible involvement of fur in energy metabolism, transcriptional regulation, and oxidative stress. *Appl Environ Microbiol*, **68**, 881-892.

References

341. Thompson JD, Higgins DG, and Gibson TJ (1994) CLUSTAL W: Improving the sensitivity of progressive multiple sequence alignment through sequence weighting, position-specific gap penalties and weight matrix choice. *Nucleic Acids Res*, **22**, 4673-4680.
342. Timminska A, Butkus V, and Janulaitis A (1995) Sequence motifs characteristic for DNA [cytosine-N4] and DNA [adenine-N6] methyltransferases. Classification of all DNA methyltransferases. *Gene*, **157**, 3-11.
343. Tisch D and Schmoll M (2010) Light regulation of metabolic pathways in fungi. *Appl Microbiol Biotechnol*, **85**, 1259-1277.
344. Todd JD, Sawers G, and Johnston AW (2005) Proteomic analysis reveals the wide-ranging effects of the novel, iron-responsive regulator RirA in Rhizobium leguminosarum bv. viciae. *Mol Gen Genomics*, **273**, 197-206.
345. Touati D, Jacques M, Tardat B, Bouchard L, and Despied S (1995) Lethal oxidative damage and mutagenesis are generated by iron in delta fur mutants of Escherichia coli: protective role of superoxide dismutase. *J Bacteriol*, **177**, 2305-2314.
346. Traoré DA, Ghazouani EL, Ilango S, Dupuy J, Jacquament L, Ferrer JL, Caux-Thang C, Duarte V, and Latour JM (2006) Crystal structure of the apo-PerR-Zn protein from Bacillus subtilis. *Mol Microbiol*, **61**, 1211-1219.
347. Trowitzsch W, Wray V, Gerth K, and Höfle G (1982) Structure of Myxovirescin A, a new macrocyclic antibiotic from gliding bacteria. *J Chem Soc , Chem Commun*, 1340-1341.
348. Trowitzsch-Kienast W. Cittilins: Bicyclic Isotryptyrosines from *Myxococcus xanthus*. German Chemists' Society, 24th General meeting, Sep 5-11, 1993. 496-497. 1993.
1993.
Ref Type: Conference Proceeding
349. Trowitzsch-Kienast W, Gerth K, Reichenbach H, and Höfle G (1993) Myxochromid A: Ein hochungesättigtes Lipopeptidlacton aus *Myxococcus virescens*. *Liebigs Ann Chem*, 1233-1237.
350. Ünlü M, Morgan ME, and Minden JS (1997) Difference gel electrophoresis: A single gel method for detecting changes in protein extracts. *Electrophoresis*, **18**, 2071-2077.
351. Van den Bergh G, Clerens S, Cnops L, Vandesande F, and Arckens L (2003) Fluorescent two-dimensional difference gel electrophoresis and mass spectrometry identify age-related protein expression differences for the primary visual cortex of kitten and adult cat. *J Neurochem*, **85**, 193-205.
352. van Vliet AH, Baillon ML, Penn CW, and Ketley JM (1999) *Campylobacter jejuni* contains two fur homologs: characterization of iron-responsive regulation of peroxide stress defense genes by the PerR repressor. *J Bacteriol*, **181**, 6371-6376.
353. Vartivarian SE and Cowart RE (1999) Extracellular Iron Reductases: Identification of a New Class of Enzymes by Siderophore-Producing Microorganisms. *Arch Biochem Biophys*, **364**, 75-82.

354. Vasil ML (2007) How we learnt about iron acquisition in *Pseudomonas aeruginosa*: a series of very fortunate events. *Biometals*, **20**, 587-601.
355. Vasil ML and Ochsner U (1999) The response of *Pseudomonas aeruginosa* to iron: genetics, biochemistry and virulence. *Mol Microbiol*, **34**, 399-413.
356. Vecerek B, Moll I, and Bläsi U (2007) Control of Fur synthesis by the non-coding RNA RyhB and iron-responsive decoding. *EMBO J*, **26**, 965-975.
357. Velayudhan J, Hughes NL, McColm AA, Bagshaw J, Clayton CL, Andrews SC, and Kelly DJ (2000) Iron acquisition and virulence in *Helicobacter pylori*: a major role for FeoB, a high-affinity ferrous iron transporter. *Mol Microbiol*, **37**, 274-286.
358. Venturi V, Ottevanger C, Bracke M, and Weisbeek P (1995a) Iron regulation of siderophore biosynthesis and transport in *Pseudomonas putida* WCS358: involvement of a transcriptional activator and of the Fur protein. *Mol Microbiol*, **15**, 1081-1093.
359. Venturi V, Weisbeek P, and Koster M (1995b) Gene regulation of siderophore-mediated iron acquisition in *Pseudomonas*: not only the Fur repressor. *Mol Microbiol*, **17**, 603-610.
360. Vermylen C (2008) What is new in iron overload? *Eur J Pediatr*, **167**, 377-381.
361. Vidakovics ML, Paba J, Lamberti Y, Ricart CA, de Sousa MV, and Rodriguez ME (2007) Profiling the *Bordetella pertussis* proteome during iron starvation. *J Proteome Res J Proteome Res*, **6**, 2518-2528.
362. Vokes SA, Reeves SA, Torres AG, and Payne SM (1999) The aerobactin iron transport system genes in *Shigella flexneri* are present within a pathogenicity island. *Mol Microbiol*, **33**, 63-73.
363. Voyich JM, Braughton KR, Sturdevant DE, Vuong C, Kobayashi SD, Porcella SF, Otto M, Musser JM, and DeLeo FR (2004) Engagement of the pathogen survival response used by group A *Streptococcus* to avert destruction by innate host defense. *J Immunol*, **173**, 1194-1201.
364. Wackett LT, Orme-Johnson WH, and Walsh CT (1989). Transition metal enzymes in bacterial metabolism. In Beveridge,T.J. and Doyle,R.J. (Eds.), *Metal ions and bacteria*, . John Wiley & Sons, Inc., New York, N.Y., pp. 165-206.
365. Walsh CT, Garneau-Tsodikova S, and Gatto GJ, Jr. (2005) Protein posttranslational modifications: The chemistry of proteome diversifications. *Angew Chem Int Ed*, **44**, 7342-7372.
366. Walsh CT, Gehring AM, Weinreb PH, Quadri LE, and Flugel RS (1997) Post-translational modification of polyketide and nonribosomal peptide synthases. *Curr Opin Chem Biol*, **1**, 309-315.
367. Wan XF, Verberkmoes NC, McCue LA, Stanek D, Connelly H, Hauser LJ, Wu L, Liu X, Yan T, Leaphart A, Hettich RL, Zhou J, and Thompson DK (2004) Transcriptomic and proteomic characterization of the fur modulon in the metal-reducing bacterium *Shewanella oneidensis*. *J Bacteriol*, **186**, 8385-8400.

References

368. Wandersman C and Delepelaire P (2004) Bacterial iron sources: from siderophores to hemophores. *Annual Review of Microbiology*, **58**, 647.
369. Wasinger VC, Cordwell SJ, Cerpa-Poljak A, Yan JX, Gooley AA, Wilkins MR, Duncan MW, Harris R, Williams KL, and Humphrey-Smith I (1995) Progress with gene-product mapping of the Mollicutes: *Mycoplasma genitalium*. *Electrophoresis*, **16**, 1090-1094.
370. Wasserman DA and Steitz JA (1991) RNA splicing. Alive with DEAD proteins. *Nature*, **349**, 463-464.
371. Weinig S, Mahmud T, and Müller R (2003) Markerless mutations in the myxothiazol biosynthetic gene cluster: A delicate megasynthetase with a superfluous nonribosomal peptide synthetase domain. *Chem Biol*, **10**, 953-960.
372. Weissman KJ (2008) Taking a closer look at fatty acid biosynthesis. *ChemBioChem*, **9**, 2929-2931.
373. Weissman KJ (2009) Introduction to Polyketide Biosynthesis. *Meth Enzymol*, **459**, 3-16.
374. Weissman KJ and Müller R (2008) A brief tour of myxobacterial secondary metabolism. *Bioorg Med Chem*, **In press**.
375. Wennerhold J, Krug A, and Bott M (2005) The AraC-type regulator RipA represses aconitase and other iron proteins from *Corynebacterium* under iron limitation and is itself repressed by DtxR. *J Biol Chem*, **280**, 40500-40508.
376. Wenzel SC, Kunze B, Höfle G, Silakowski B, Scharfe M, Blöcker H, and Müller R (2005a) Structure and biosynthesis of myxochromides S1-3 in *Stigmatella aurantiaca*: Evidence for an iterative bacterial type I polyketide synthase and for module skipping in nonribosomal peptide biosynthesis. *ChemBioChem*, **6**, 375-385.
377. Wenzel SC, Meiser P, Binz T, Mahmud T, and Müller R (2006) Nonribosomal peptide biosynthesis: Point mutations and module skipping lead to chemical diversity. *Angew Chem Int Ed*, **45**, 2296-2301.
378. Wenzel SC and Müller R (2005b) Formation of novel secondary metabolites by bacterial multimodular assembly lines: deviations from text book biosynthetic logic. *Curr Opin Chem Biol*, **9**, 447-458.
379. Wenzel SC and Müller R (2009a) The impact of genomics on the exploitation of the myxobacterial secondary metabolome. *Nat Prod Rep*, **26**, 1385-1407.
380. Wenzel SC and Müller R (2009b) Myxobacteria--'microbial factories' for the production of bioactive secondary metabolites. *Mol Biosyst*, **5**, 567-574.
381. Wenzel SC and Müller R (2009b) The biosynthetic potential of myxobacteria and their impact on drug discovery. *Current Opinion in Drug Discovery & Development*, **12**, 220-230.
382. Wessel D and Flügge UI (1984) A method for the quantitative recovery of protein in dilute solution in the presence of detergents and lipids. *Anal Biochem*, **138**, 141-143.

383. Westermeier R (2006) Sensitive, quantitative, and fast modifications for coomassie blue staining of polyacrylamide gels. *Proteomics Proteomics*, 61-64.
384. White C, Gagnon SN, St-Laurent JF, Gravel P, Proulx LI, and Desnoyers S (2009) The DNA damage-inducible *C. elegans* tankyrase is a nuclear protein closely linked to chromosomes. *Mol Cell Biochem*, **324**, 73-83.
385. Wilderman PJ, Sowa NA, FitzGerald DJ, FitzGerald PC, Gottesman S, Ochsner UA, and Vasil ML (2004) Identification of tandem duplicate regulatory small RNAs in *Pseudomonas aeruginosa* involved in iron homeostasis. *P Natl Acad Sci USA*, **101**, 9792-9797.
386. Windgassen M, Urban A, and Jaeger KE (2000) Rapid gene inactivation in *Pseudomonas aeruginosa*. *FEMS Microbiol Lett*, **193**, 201-205.
387. Winkelmann G (2002) Microbial siderophore-mediated transport. *Biochem Soc Trans*, **30**, 691-696.
388. Winkelmann G, van der Helm D, and Neilands JB (1987). *Iron transport in microbes, plants and animals*. VCH, Weinheim.
389. Wooldridge K.G. and Williams PH (1993) Iron uptake mechanisms of pathogenic bacteria. *FEMS Microbiol Rev*, **12**, 325-348.
390. Wu SS and Kaiser D (1996) Markerless deletions of pil genes in *Myxococcus xanthus* generated by counterselection with the *Bacillus subtilis* *sacB* gene. *J Bacteriol*, **178**, 5817-5821.
391. Wu WW, Wang G, Baek SJ, and Shen RF (2006) Comparative study of three proteomic quantitative methods, DIGE, cICAT, and iTRAQ, using 2D gel- or LC-MALDI TOF/TOF. *J Proteome Res*, **5**, 651-658.
392. Wyckoff EE, Mey AR, Leimbach A, Fisher CF, and Payne SM (2006) Characterization of ferric and ferrous iron transport systems in *Vibrio cholerae*. *J Bacteriol*, **188**, 6515-6523.
393. Yan JX, Devenish AT, Wait R, Stone T, Lewis S, and Fowler S (2001) Fluorescence two-dimensional difference gel electrophoresis and mass spectrometry based proteomic analysis of *Escherichia coli*. *Proteomics Proteomics*, **2**, 1682-1698.
394. Yang J, Ishimori K, and O'Brian MR (2005) Two heme binding sites are involved in the regulated degradation of the bacterial iron response regulator (Irr) protein. *J Biol Chem*, **280**, 7671-7676.
395. Yang J, Sangwan I, Lindemann A, Hauser F, Hennecke H, Fischer HM, and O'Brian MR (2006) *Bradyrhizobium japonicum* senses iron through the status of haem to regulate iron homeostasis and metabolism. *Mol Microbiol*, **60**, 427-437.
396. Yates J, Aroyo M, Sherratt DJ, and Barre FX (2003) Species specificity in the activation of Xer recombination at dif by FtsK. *Mol Microbiol*, **49**, 241-249.
397. Yates JRI (1998a) Database searching using mass spectrometry data. *Electrophoresis*, **19**, 893-900.

References

398. Yates JRI (2004) MASS SPECTRAL ANALYSIS IN PROTEOMICS. *Annu Rev Biophys Biomol Struct*, **33**, 297-316.
399. Yates JRI (1998b) Mass spectrometry and the age of the proteome. *J Mass Spectrom*, **33**, 1-19.
400. Yates JRI, Cociorva D, Liao LJ, and Zabrouskov V (2006) Performance of a linear ion trap-orbitrap hybrid for peptide analysis. *Anal Chem*, **78**, 493-500.
401. Yates JRI, Speicher S, Griffin PR, and Hunkapiller T (1993) Peptide mass maps: a highly informative approach to protein identification. *Anal Biochem*, **314**, 397-408.
402. Youderian P and Hartzell PL (2007) Triple mutants uncover three new genes required for social motility in *Myxococcus xanthus*. *Genetics*, **177**, 557-566.
403. Yu F, Anaya C, and Lewis JP (2007) Outer membrane proteome of *Prevotella intermedia* 17: Identification of thioredoxin and iron-repressible hemin uptake loci. *Proteomics Proteomics*, **7**, 403-412.
404. Yu R and Kaiser D (2007) Gliding motility and polarized slime secretion. *Mol Microbiol*, **63**, 454-467.
405. Yuhara S, Komatsu H, Goto H, Ohtsubo Y, Nagata Y, and Tsuda M (2008) Pleiotropic roles of iron-responsive transcriptional regulator Fur in *Burkholderia multivorans*. *Microbiology*, **154**, 1763-1774.
406. Zafirri D, Rosenberg E, and Mirelman D (1981) Mode of action of *Myxococcus xanthus* antibiotic TA. *Antimicrob Agents Chemother*, **19**, 349-351.
407. Zeth K, Offermann S, Essen LO, and Oesterhelt D (2004) Iron-oxo clusters biomineralizing on protein surfaces: structural analysis of *Halobacterium salinarum* DpsA in its low- and high-iron states. *Proc Natl Acad Sci U S A*, **101**, 13780-13785.
408. Zhang HM, Li Z, Tsudome M, Ito S, Takama H, and Horikoshi K (2005a) An alkali-inducible flotillin-like protein from *Bacillus halodurans* C-125. *Protein J*, **24**, 125-131.
409. Zhang Z, Gosset G, Barabote R, Gonzalez CS, Cuevas WA, and Saier MHJ (2005b) Functional interactions between the carbon and iron utilization regulators, Crp and Fur, in *Escherichia coli*. *J Bacteriol*, **187**, 980-990.
410. Zhao G, Ceci P, Ilari A, Giangiacomo L, Laue TM, Chiancone E, and Chasteen ND (2002) Iron and hydrogen peroxide detoxification properties of DNA-binding protein from starved cells. A ferritin-like DNA-binding protein of *Escherichia coli*. *J Biol Chem*, **277**, 27689-27696.
411. Zhu H, Xie G, Liu M, Olson JS, Fabian M, Dooley DM, and Lei B (2008) Pathway for heme uptake from human methemoglobin by the iron-regulated surface determinants system of *Staphylococcus aureus*. *J Biol Chem*, **283**, 18450-18460.

9. Appendix

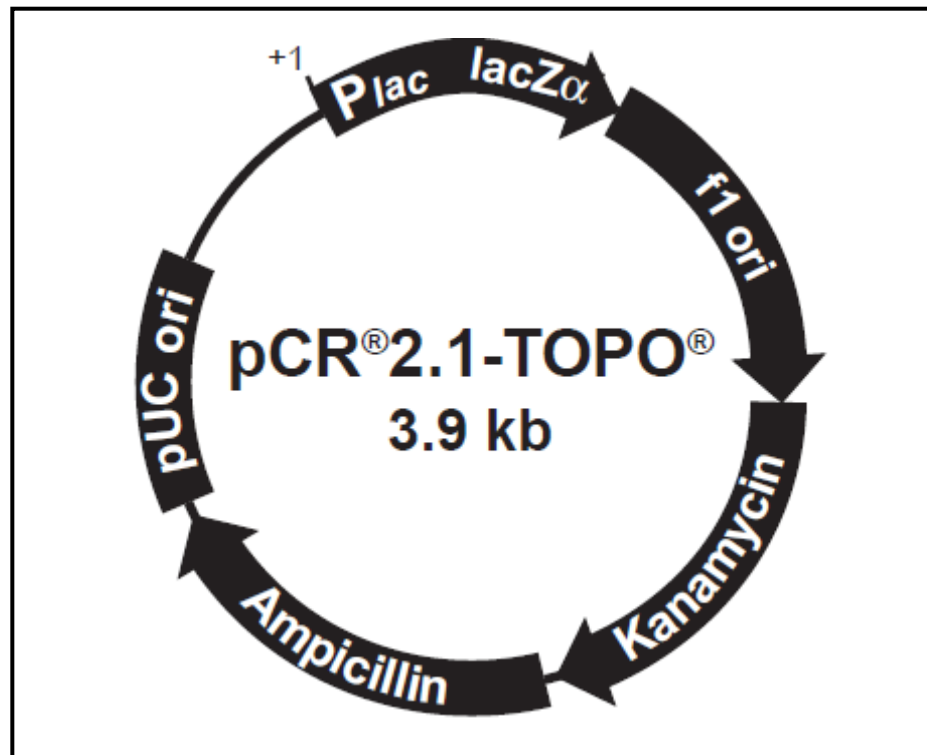


Figure A1: Vector map of pCR2.1-Topo (Invitrogen)

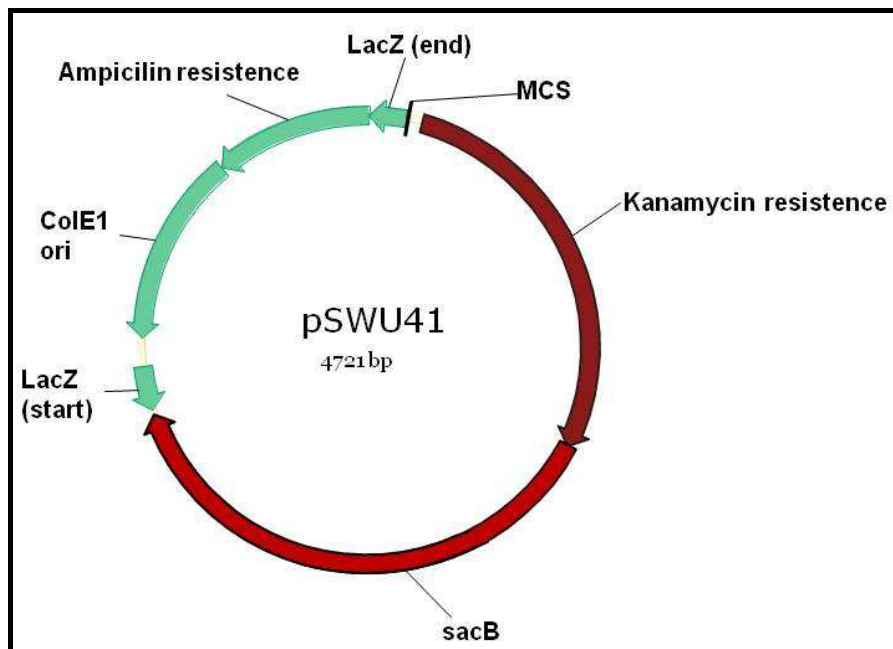


Figure A2: Vector map of pSWU41 (Wu et al., 1996)

Appendix

Table A1: Classification of 131 identified proteins from 2D-DIGE.

The 172 spots from 2D-DIGE experiment in response of iron-limitation of *M. xanthus* (table 3.4) were identified as 131 different proteins. These were categorized by their biochemical context. The corresponding spot-number from the 2D-DIGE result (table 3.4) is shown in column 2.

No.	DIGE-Spot no.	Gene-no.	Protein function
Central metabolism			
1	94	MXAN_1264	PckG (GTP-phosphoenolpyruvate carboxykinase)
2	126	MXAN_3388	CarB (carbamoyl-phosphate synthetase)
3	32	MXAN_3537	Icd (isocitrate dehydrogenase, NADP-dependent)
4	33	MXAN_3540	SdhB (succinate dehydrogenase, iron-sulfur protein)
5	34	MXAN_3542	SucD (succinyl-CoA synthetase)
6	143	MXAN_5070	Htp (hypoxanthine phosphoribosyltransferase)
7	144	MXAN_5108	ArgG (argininosuccinate synthase)
8	149	MXAN_5597	FtsZ (cell division protein)
9	159	MXAN_6450	Beta-lactamase
10	163	MXAN_6524	CobW/P47K family protein (essential for V _{B12} (cobalamin) biosynthesis, methionin synthase associated)
11	168	MXAN_7028	AtpA (ATP synthase F1)
12	170	MXAN_7380	CBS domain protein (sensors of cellular energy status)
Protein regulation; kinases, peptidases and protein metabolism			
1	75	MXAN_0142	WD domain G-beta repeat protein (mediation of protein-protein interaction)
2	5	MXAN_0463	PepP (Xaa-Pro aminopeptidase)
3	83	MXAN_0543	Peptidase M20 (glutamate carboxypeptidase) family
4	9	MXAN_0720	Sensor histidine kinase
5	87	MXAN_0791	Peptidase M16 (pitryllysine) family
6	88	MXAN_0831	Saccharopine dehydrogenase Lys1
7	93	MXAN_1141	Peptidase M16 (pitryllysine) family
8	14	MXAN_1892	Serine/threonine protein kinase
9	15	MXAN_2016	Prolyl endopeptidase Pep
10	116	MXAN_2520	FHA domain/tetratricopeptide repeat protein
11	138	MXAN_4189	TRP (tetratricopeptide repeat) protein
12	155	MXAN_5806	Glutamate-cysteine ligase
13	158	MXAN_6438	ClpP2 (ATP-dependent Clp protease)
14	72	MXAN_7497	Processing peptidase beta-subunit, M16B
Chaperone and GST domain proteins			
1	84	MXAN_0548	Glutathione-S-transferase domain protein
2	10	MXAN_1073	Hsp33 family protein
3	16	MXAN_2318	Glutathione-disulfide reductase Gor
4	43-47	MXAN_4467	60 kDa chaperonin GroEL1
5	50-58	MXAN_4895	60 kDa chaperonin GroEL2
Membrane-associated			
1	2	MXAN_0350	Putative membrane protein
2	7	MXAN_0559	ABC transporter, ATP-binding protein Mac1

Appendix

No.	DIGE-Spot no.	Gene-no.	Protein function
Membrane-associated			
3	60	MXAN_5168	ABC transporter, ATP-binding domain, unknown permase
4	68	MXAN_7040	Outer membrane protein P1
Iron acquisition			
1	95	MXAN_1318	HemS (heme binding protein)
2	129, 130	MXAN_3640	MxcL (myxochelin biosynthesis, aminotransferase)
3	131	MXAN_3644	MxcF (myxochelin biosynthesis, isochorismatase)
4	132	MXAN_3647	MxcC (myxochelin biosynthesis, 2,3-Dihydro-2,3-DHB dehydrogenase)
5	140	MXAN_5023	TonB-dependent receptor; outer membrane receptor
6	166, 167	MXAN_6911 ^b	TonB-dependent receptor
Redox stress resistance			
1	80	MXAN_0303	Oxidoreductase aldo/keto reductase family
2	81	MXAN_0351	Thioredoxin domain protein
3	89	MXAN_0866	Ferritin/ DPS (<u>DNA</u> protection during <u>starvation</u> protein) family protein (TpF2)
4	96	MXAN_1562	Ferritin/ DPS (<u>DNA</u> protection during <u>starvation</u> protein) family protein (TpF1)
5	97, 98	MXAN_1563	AhpD (Alkyl hydroperoxide reductase D)
6	99-101	MXAN_1564	AhpC (Alkyl hydroperoxide reductase C)
7	107	MXAN_1954	TrxB1 (Thioredoxin disulfide reductase)
8	120	MXAN_2729	NADH dehydrogenase I, D subunit
9	134, 135	MXAN_4003	Oxidoreductase
10	136	MXAN_4067	ThiS (ferredoxin-like protein)
11	151, 152	MXAN_5670	TrxB2 (Thioredoxin)
12	160, 161	MXAN_6482	Oxidoreductase
13	66	MXAN_6496	Tpx (thioredoxin peroxidase)
14	164, 165	MXAN_6536	Antioxidant, AhpC/Tsa family
15	169	MXAN_7090	Glutathione peroxidase family protein
Motility/chemotaxis			
1	115	MXAN_2513	GspE (secretory pathway protein E, type IV pilus biogenesis)
2	119	MXAN_2685	CheW (Chemotaxis protein)
3	137	MXAN_4149	FrzS (Response regulator)
4	139	MXAN_4863 ^b	AgmK (Adventerous gliding motility)
DNA metabolism/transcription			
1	78	MXAN_0236	DnaN (DNA polymerase III, beta subunit)
2	1	MXAN_0264	GyrB (DNA topoisomerase activity)
3	90	MXAN_0959	Nuclease SbcCD, C subunit
4	103	MXAN_1808	Restriction/modification enzyme (N6-adenine DNA methylase)
5	105	MXAN_1864	N6-adenine DNA methyltransferase
6	19	MXAN_2609	UvrA (Exonuclease ABC, A subunit)
7	29-31	MXAN_3326	RpoA (RNA polymerase subunit A)

Appendix

No.	DIGE-Spot no.	Gene-no.	Protein function
DNA metabolism/transcription			
8	39	MXAN_3777	Inosine-5'-monophosphate dehydrogenase GuaB
9	42	MXAN_4242	Transcriptional regulator
10	48	MXAN_4535	ECF sigma factor
11	154	MXAN_5795	Exonuclease
12	65	MXAN_6032	CheW domain (chemotaxis signal transduction response regulator)
13	67	MXAN_7020	Cas3 (CRISPR-associated helicase)
Translation			
1	4	MXAN_0405	YchF (GTP-binding protein)
2	109	MXAN_2073	PnpA (polyribonucleotide nucleotidyltransferase)
3	17, 18	MXAN_2408	FusA (Translation elongation factor G1)
4	118	MXAN_2675	GltX (glutamyl-tRNA synthetase)
5	22, 23, 123	MXAN_3068	Tu1 (Translation elongation factor)
6	26	MXAN_3297	FusA (Translation elongation factor G2)
7	27	MXAN_3298	Tu2 (Translation elongation factor)
8	28, 124	MXAN_3307 ^b	RpmC (50S ribosomal protein L29)
9	125	MXAN_3379	TypA (GTP-binding protein)
10	40	MXAN_3793	RpsA (Ribosomal protein S1)
Hypothetical proteins or unknown function			
1	76, 77	MXAN_0144	Hypothetical protein [WGR domain protein]
2	79	MXAN_0237	Hypothetical protein
3	3	MXAN_0365	Hypothetical protein [DUF 82]
4	6, 82	MXAN_0498	Lipoprotein
5	8, 85	MXAN_0599	Hypothetical protein [DUF 262/1524]
6	86	MXAN_0790	Hypothetical protein
7	91	MXAN_1024	Hypothetical protein
8	92	MXAN_1069	Hypothetical protein
9	11	MXAN_1158	Hypothetical protein [Fe-S assembly protein SufT]
10	12	MXAN_1539	Lipoprotein
11	102	MXAN_1591	Hypothetical protein [Sigma-54 factor/ AAA ATPase]
12	13	MXAN_1619	Hypothetical protein [Helix-turn-helix type 11 domain protein]
13	104	MXAN_1815	Hypothetical protein [DUF 2169]
14	106	MXAN_1893	Hypothetical protein [ClpX protease]
15	108	MXAN_1988	Hypothetical protein [SAM-dependent methyltransferase]
16	110	MXAN_2094	Hypothetical protein [TPR-domain protein]
17	111	MXAN_2347	Hypothetical protein [Protamine P1 homologue]
18	112	MXAN_2410	Hypothetical protein
19	113, 114	MXAN_2440	Hypothetical protein [Provisional transcription termination Rho domain]
20	117	MXAN_2539	Hypothetical protein
21	20	MXAN_2640	Hypothetical protein
22	21	MXAN_2822	Hypothetical protein
23	121	MXAN_2940	Hypothetical protein

Appendix

No.	DIGE-Spot no.	Gene-no.	Protein function
Hypothetical proteins or unknown function			
24	122	MXAN_2952	Hypothetical protein
25	24	MXAN_3079	Hypothetical protein
26	25	MXAN_3080	Hypothetical protein
27	35	MXAN_3556	Hypothetical protein [M18 bacteriocin protein]
28	36, 127	MXAN_3571	Hypothetical protein [flotillin-band 7 protein]
29	37, 128	MXAN_3617	Hypothetical protein
30	38	MXAN_3633	Hypothetical protein [DUF407]
31	133	MXAN_3679	Hypothetical protein [ArsR-like regulator]
32	41	MXAN_4137	Hypothetical protein
33	49	MXAN_4802	Hypothetical protein [DUF876]
34	59, 141, 142	MXAN_5055	Hypothetical protein [methyltransferase/SMC domain]
35	145	MXAN_5180	Hypothetical protein
36	146	MXAN_5401	Hypothetical protein
37	61, 147	MXAN_5484	Hypothetical protein [putative serine/threonine protein kinase]
38	62	MXAN_5511	Hypothetical protein
39	63, 148	MXAN_5588	Hypothetical protein
40	150	MXAN_5650	Hypothetical protein
41	153	MXAN_5743	Hypothetical protein [PEGA domain protein]
42	64	MXAN_5846	Hypothetical protein [M14-like metallocarboxypeptidase]
43	156	MXAN_5855	Hypothetical protein [Phosphate-selective porin superfamily]
44	157	MXAN_6434	Hypothetical protein
45	162	MXAN_6502	Hypothetical protein [SGNH-hydrolase]
46	69	MXAN_7393	Hypothetical protein [sigma-54 transcriptional regulator, Fis family]
47	70	MXAN_7446	Hypothetical protein
48	71, 171	MXAN_7492	Hypothetical protein

Appendix

Table A2: Peptides with detected phosphorylations.

By 2D-DIGE 172 proteins were analyzed as differently regulated, thereof 169 (98.3 %) identified by MS as 131 individual proteins. If the protein was detected as several spot (also without phosphorylation), it is also shown (marked by peptide sequence: “-”).

In the DNA pull-down assay, MXAN_1562 at promoter MXAN_3702 under iron-poor conditions was found to carry a phosphorylation (peptide: LADGLDLhpSQIK)

Phosphorylated protein-no.	Av. ratio (> 2 or < -2)	Identified MXAN- Nr.	Protein function	Peptide sequence with detected modification(s) Sequence; Modification* (Mod-Site)
1	2,69	MXAN_2440	Hypothetical protein [Provisional Rho domain protein]	RVHANVPDERSRV; P (S)
2	3,2	MXAN_2440	Hypothetical protein [Provisional Rho domain protein]	RVQSGAPDERS; P (S) RELLTMCDR; CAM (C); P (T)
3	-2,14	MXAN_3079	Hypothetical protein	RVDAAGTELKRK; P (T)
	5,95	MXAN_3307	50S ribosomal protein L29 RpmC	-
4	-2,67	MXAN_3307	50S ribosomal protein L29 RpmC	RETLFQDQLKRR; P (T)
	-2,25	MXAN_3326	RNA polymerase RpoA	-
5	-2,04	MXAN_3326	RNA polymerase RpoA	RMHTNETKTLRI; P (T) RGFGTTLGNSLRR; P (ST)
6	-2,03	MXAN_3326	RNA polymerase RpoA	RGFGTTLGNSLRRV; P (ST) KTLRIEAEGPKE; P (T)
7	-2,07	MXAN_3571	Hypothetical protein [Flotillin/band 7 protein]	-
	2,72	MXAN_3571	Hypothetical protein [Flotillin/band 7 protein]	RGDIKVTFVVRV; P (T)
8	-2,58	MXAN_4137	Hypothetical protein	MGMFMFDIPHSPLKE; P (S)
	-2,32	MXAN_4467	60 kDa chaperonin GroEL1	-
	-2,3	MXAN_4467	60 kDa chaperonin GroEL1	-
	-2,22	MXAN_4467	60 kDa chaperonin GroEL1	-
	-2,13	MXAN_4467	60 kDa chaperonin GroEL1	-
9	-2,12	MXAN_4467	60 kDa chaperonin GroEL1	KVGKEGVITVEEAKG; P (T)
10	7,18	MXAN_4863	Adventurous gliding motility protein AgmK	RACDLYRTHNDWRA; P (TY) KYFAEQGQKE; P (Y)
	7,06	MXAN_5055	Hypothetical protein [methyltransferase/SMC domain protein]	-
11	-3,23	MXAN_5055	Hypothetical protein [methyltransferase/SMC domain protein]	RSALESEQQGRA; P (S)
12	2,82	MXAN_5055	Hypothetical protein [methyltransferase/SMC domain protein]	RAVEQSEDERRR; P (S) RDALASSEEERR; P (S)

Appendix

Phosphorylated protein-no.	Av. ratio (> 2 or < -2)	Identified MXAN- Nr.	Protein function	Peptide sequence with detected modification(s) Sequence; Modification* (Mod-Site)
13	3,26	MXAN_5401	Hypothetical protein	RGRVIHTEAHGRL; P (T)
14	4,09	MXAN_6911	TonB-dependent receptor	-
	2,68	MXAN_6911	TonB-dependent receptor	RGISIRGMDSSYTLILVDGKR; P (STY) KGKWDWGNSEVRG; P (S) RGRTLYAGVNARF; P (TY)
15	-2.41	MXAN_7497	Signal-peptide processing peptidase (M16B)	KANAYYMAGQSLKL; P (Y)

*Modifications:
 CAM: Carbamidomethylation
 P: Phosphorylation

8 protein spots with one detectable phospho-residue

5 protein spots (4 proteins) with two detectable phospho-residue

1 protein spots with three detectable phospho-residue

Appendix

Table A3: List of potential Fur regulated proteins from proteome experiments.

Back analysis of promoter regions from differently expressed proteins (2D-DIGE), screened for the presence of potential Fur boxes, guided by the generated sequence key of Fur boxes in *M. xanthus* (GANAATSNNTCAWTNNNC; figure 3.3). 8 of 19 nucleotides (whereas only 12 are really defined) had to be identical for match. Sequence-hits in coding regions are marked by “Plus”. Hypothetical proteins were further checked by BLAST; result shown in squared brackets.

No.	Identified MXAN-Nr.	Sequence	Start distance	Protein function
1	MXAN_0365	GACGATGCGCTTCCATGGC	4	Hypothetical protein [DUF82]
2	MXAN_0463	CAGAATGCTGCTCCCTTCC	4	Xaa-Pro aminopeptidase pepP
3	MXAN_0548	GACGATGAAACTCTATTTC	4	Glutathione S-transferase domain protein
4	MXAN_0599	GAAACGCCTTTCAACTCC	28	Hypothetical protein [DUF262/1524]
5	MXAN_0831	GAAAATATAGGTCAATCGA	21	Saccharopine dehydrogenase lys1
6	MXAN_0866	GATGATGTTCTTCACCGGCC	116	DPS protein tpF2
7	MXAN_1892	GAGGATTACACAGCCATGAC	13	Putative serine/threonine protein kinase
8	MXAN_2318	GAGAGTCAAAACGCATGGC	13	Glutathione-disulfide reductase gor
9	MXAN_2539	GAGAGTCGCGCTGAACCCC	plus 9	Hypothetical protein
10	MXAN_3068	GCAGATCCAGAACAAATTTC	plus 4	Elongation factor Tu 1
11	MXAN_3080	GCACATGCCGTCGTTCCC	85	Hypothetical protein
12	MXAN_3571	GGCCATGGACCCCATTACC	2	Hypothetical protein [band 7 protein]
13	MXAN_3633	GAAAATGCCACACGTCAAC	4	Hypothetical protein
14	MXAN_3640	GTGAATCGCAGTCTCCGTC	2	Siderophore biosynthesis aminotransferase
15	MXAN_3647	GATAATGAAAATCATTCTC	57	Siderophore biosynthesis 2,3-dihydro-2,3-dihydroxybenzoate dehydrogenase
16	MXAN_3777	GGGAACGGCGTCAAAATC	plus 21	Inosine-5'-monophosphate dehydrogenase, guaB
17	MXAN_3793	GAGGACGAACGTCACTGCC	75	Ribosomal protein S1 rpsA
18	MXAN_4137	AATGATGAAGTTCGATATC	4	Hypothetical protein
19	MXAN_4149	GAAAATCCTGATCGTCGAA	plus 8	Response regulator frzS
20	MXAN_4189	GGTCATGGTTTCATGCGC	61	Tetratricopeptide repeat protein
21	MXAN_5023-24	GTTAATGACAATCAACTTC	32	TonB dependent receptor; outer membrane receptor
22	MXAN_5484	AAGGATGCGACGCATTGCG	16	Hypothetical protein
23	MXAN_5743	AGGACTCCTTCTCACTTGC	50	Hypothetical protein [PEGA domain surface layer protein]
24	MXAN_5795	GATGATTCCGGCGTTTC	68	Exonuclease
25	MXAN_5855	GAACGTCACCTCGGTAAC	30	Hypothetical protein [phosphate-selective porin superfamily]
26	MXAN_6032	GAAACGGTCCGTCAGTTCC	18	Putative response regulator/chemotaxis protein cheW
27	MXAN_6911	GCAAATCAATATCAATTGA	14	TonB-dependent receptor
28	MXAN_7040	GACACTCTCCCTCATCACG	plus 8	Putative outer membrane protein P1
29	MXAN_7090	GAACCTCTACGACATTCCC	plus 7	Glutathione peroxidase family protein

10. Erklärung

Hiermit erkläre ich, dass ich die vorliegende Arbeit selbstständig und ohne Benutzung anderer als der angegebenen Hilfsmittel angefertigt habe. Die aus anderen Quellen oder indirekt übernommenen Daten und Konzepte sind unter Angabe der Quelle gekennzeichnet.
Die Arbeit wurde bisher weder im In- noch im Ausland in gleicher oder ähnlicher Form in anderen Prüfungsverfahren vorgelegt.

Saarbrücken, November 2010

Appendix

DANKSAGUNG

Ich möchte mich zuerst bei Prof. Dr. Rolf Müller für das Überlassen dieses sehr interessanten und herausfordernden Themas bedanken. Des Weiteren bedanke ich mich für die wissenschaftlichen Freiheiten bei der Projektgestaltung und das Bereitstellen einer beeindruckenden Laborausstattung.

Prof. Dr. Claus Jacob hat freundlicherweise das Zweitgutachten dieser Arbeit übernommen. Prof. Dr. Alexandra Kiemer danke ich für die Übernahme des Prüfungskommissionsvorsitzes.

Für Ihre Unterstützung in Theorie und Praxis gilt mein Dank Prof. Dr. Helge Bode, Dr. Yasser Elnakady, Prof. Dr. Andreas Tholey und Dr. Kira Weissman. Für Ihre konstruktive Kritik und Hilfe beim Korrekturlesen der Arbeit danke ich Jennifer Herrmann, Dr. Nora Luniak und Dr. Carsten Kegler.

Der Arbeitsgruppe Pharmazeutische Biotechnologie danke ich für die schöne Zeit, die gute Zusammenarbeit und das freundschaftliche Betriebsklima.

Mein letzter Dank geht an meine Eltern und meine Freundin Sarah Jungmann, auf deren Unterstützung ich mich immer verlassen konnte und kann. Danke!